UNIVERSITY OF LONDON

IMPERIAL COLLEGE OF SCIENCE AND TECHNOLOGY
DEPARTMENT OF ELECTRICAL ENGINEERING

ON-LINE COMPUTER CONTROL OF TURBINE GENERATORS USING STATE ESTIMATION AND OPTIMAL FEEDBACK

by

Andrew David Noble

Thesis submitted for the Degree of
Doctor of Philosophy and the Diploma of
Imperial College in the Faculty of Engineering

NOVEMBER 1984

ABSTRACT

The objective here has been a theoretical and practical investigation into how turbine-generator stability might be improved by modifying voltage regulator or turbine governor action using supplementary signals added to one or both of these control loops by a microcomputer.

The approach was to simulate the machine with the controller, estimating the model state-variables on the basis of measurements taken from the real plant, and optimally feed the states back to the plant to give the supplementary signals. Practically, this scheme is superior to direct state-feedback since noise rejection is better, unmeasurable states may be estimated and any convenient inputs may be chosen.

A controller measuring generator rotor angle to the system busbar and field voltage to estimate twelve states was tested on computer simulations and implemented in real-time on a microcomputer controlling a scaled-down laboratory physical model of a typical modern large turbine-generator. Steady-state and dynamic stability were substantially improved.

A new method of optimal linear model order reduction is described. Experimental results showed that in this way the number of states could be reduced from twelve to four with very little degradation to the control, equivalent in efficacy to a conventionally reduced ninth order controller. This has the potential of making an industrial implementation much more cost-effective due to relaxation of time and storage demands on the on-line control computer.

Practical tests also showed that the controllers are effective for a wide range of operating points without alteration of gains, and that control was good even with noisy measurements.

Estimators/controllers giving a supplementary signal only to the voltage regulator seem particularly suited to older plant with slower governors. They give almost as good damping but less first rotor angle swing reduction following a transient disturbance as compared with control to both loops.

Power, terminal voltage and speed were considered as alternatives to load angle as an input to the estimator. Speed gave comparable results but power and terminal voltage, although more desirable from many viewpoints, did not give the same high degree of stability improvement.

Brief preliminary practical investigations of torsional shaft oscillations showed that for the conditions considered, they are not worsened by the controller. This seems to be the main area for continuing study.

ACKNOWLEDGEMENTS

This thesis presents work carried out under the supervision of **D.C. Macdonald, Ph.D., B.Sc., ACGI, C.Eng., MIEE,** Lecturer in the Electrical Engineering Department, Imperial College. I wish to thank Dr. Macdonald for his invaluable assistance and the great interest he has taken throughout this project.

Special thanks are also due to **Dr. D.J. Limebeer** for his extremely helpful advice, particularly that concerning Optimal Hankel - Norm Model Reduction.

In addition I wish to thank:

NEI Parsons Limited and the **Science and Engineering Research Council** for financial support. SERC also provided a grant for purchasing the on-line computer;

Dr. B.J. Cory for valuable discussions and guidance;

Dr. A. Walton and **Dr. P. Rush,** both of NEI Parsons Limited, for providing assistance, technical information and feedback from the industrial world;

Mr. P. Cheung who, with his experience in the world of microcomputers, was a most competent adviser on all aspects of the DEC LSI 11/23 on-line computer;

Finally, my colleagues in the **Power Systems Laboratory** who assisted me in many ways, and provided a friendly working environment.

CONTENTS

Page

CHAPTER 4: APPLICATION OF DISCRETE-TIME OPTIMAL CONTROL AND STATE ESTIMATION THEORY TO TURBINE GENERATOR SIMULATIONS

Page

Chapter 6 Continued..

Page

Appendices continued..

LIST OF SYMBOLS AND ABBREVIATIONS

A	state-space system matrix [general]
A_D	linearised discrete-time state-space system matrix [transition matrix]
A_L	linearised continuous-time state-space system matrix
A_N	state-space system matrix containing linear terms, for non-linear model
A_P	valve position
AVR	automatic voltage regulator
a,b	digital filter coefficients
B, B_D, B_L, B_N	state-space input matrices, subscripts as above
(B)	susceptance matrix
$\mathbb{C}$	the set of all complex numbers
C	state-space output matrix
Cos ϕ	power factor
CPU	Central Processing Unit
D	state-space direct transmission matrix
DEC	Digital Equipment Corporation [trademark]
du_1 du_2	supplementary control signals to generator
F	optimal feedback regulator gain matrix
f_o	power system reference frequency (Hz)
F_n	expression containing nonlinearities in nonlinear generator model
F.F.T.	fast Fourier transform
G(s)	general transfer function expression
G_a, G_e, G_g	AVR, exciter and governor gains
$\hat{G}_k(s)$	optimal reduced k^{th} order transfer function
H	inertia constant
$\|\cdot\|_H$	Hankel-norm of expression

$H(t)$	impulse response vector
h	integration time step
$[I]$, $[I_d]$, $[I_q]$	axis current vectors
i_d, i_q	d and q-axis stator currents
i_f	field current
i_{kd}, i_{kq}	d and q-axis damper currents
I_{mt}	peak terminal current
J	moment of inertia [$= 2H/\omega_o$]
K	estimator gain matrix
k	damping coefficient
k	sampling instant
$[L]$	inductance matrix
L_d, L_q	d and q-axis self inductance
L_{ffd}, L_{kkd}, etc.	defined in Appendix C
$\|\cdot\|_{L\infty}$	L - infinity norm of expression .
LQG	Linear-Quadratic-Gaussian
M_e	electrical torque
M_t	prime-mover torque
P	solution to matrix Riccati equation
p	Heaviside operator $\frac{d}{dt}$
PDP	Programmable Data Processor [DEC trademark]
P, P_t, P_b	power, terminal power, busbar power
P	controllability Gramian
p.u.	per unit
Q	observability Gramian
Q, Q_t, Q_B	reactive power [VAr], terminal VAr, busbar VAr
Q_R, Q_F	regulator and filter weighting matrices
$[R]$	machine resistance matrix

RAM	Random-Access-Memory
R_a, R_f, R_e, R_t	resistances of armature, field, tie-line and transformer
R_R, R_F	regulator and filter weighting matrices
[Rgd, Rgq]	machine d and q-axis resistance matrices
s	Laplace operator $\frac{d}{dt}$
$\sup_{\omega} \bar{\sigma}\left(G(j\omega)\right)$	supremum over all ω of largest singular value of $G(j\omega)$
T.C.R.	time constant regulator
T	transformation matrix
$[\ ]^T$	transpose of matrix
T_d', T_q'	d and q-axis transient time constants
T_d'', T_q''	d and q-axis subtransient time constants
T_{do}', T_{qo}' T_{do}'', T_{qo}''	d and q-axis transient and subtransient open-circuit time constants
T_a, T_e, T_v, T_s	time constants of AVR amplifier, exciter, valves and entrained steam
U	control vector
U_d, U_q	d and q-axis induced voltage components
[V]	machine voltage vector
v	measurement noise vector
V_b, V_{mb}	infinite busbar rms and peak voltage
V_t, V_{mt}	terminal rms and peak voltage
V_{bd}, V_{bq}	d and q-axis components of infinite busbar voltage
V_{td}, T_{tq} V_d, V_q	d and q-axis components of terminal voltage
V_f, V_e	field and exciter voltage
V_r	reference voltage
V.D.U.	Visual Display Unit

w	excitation noise vector or digital filter variable
x, $\bar{x}$	state vector, state estimate
$\bar{x}$, x_{ss}	nominal steady-state operating point
$\dot{x}$	$\frac{dx}{dt}$
X_a	armature leakage reactance
$X_{d'}$ X_q	d and q-axis self reactance
$X_{md'}$ X_{mq}	d and q-axis magnetising reactance
$X_{kd'}$ X_{kq}	d and q-axis damper winding leakage reactance
X_e	tie-line reactance
X_t	transformer reactance
X_d', X_q'	d and q-axis transient reactance
X_d'', X_q''	d and q-axis subtransient reactance
$[X_{gd}]$, $[X_{gq}]$	d and q-axis reactance matrices
y	output vector
$[Y_{gd}]$, $[Y_{gq}]$	d and q-axis admittance matrices
Y_o	speed reference level
z	transformed state variable [= Tx] vector
$\frac{\partial(F)}{\partial x_i}$	partial derivative of F with respect to x_i, the i^{th} state variable
δ, δ_∞, δb	load angle - rotor to infinite busbar
δ_t	load angle - rotor to terminals
Δ	small changes
$\sigma_i\left(G(s)\right)$	the i^{th} Hankel singular value of G(s)
$\lambda_i(A)$	the i^{th} eigenvalue of A
$\bar{\sigma}$, $\bar{\lambda}$	largest Hankel singular value, largest eigenvalue
$\Psi_{d'}$ Ψ_q	d and q-axis flux linkage
Ψ_f	field flux linkage
$\Psi_{kd'}$ Ψ_{kq}	d and q-axis damper winding flux linkages
ω	angular velocity of machine rotor (= $\omega_o + \dot{\delta}$)

ERRATA

page	line	correction
41	6	... gain at the output strongly affects it.
43	8	... magnitudes relating past inputs to future outputs.
46	2 & 3	for "casual" read "causal"
47	19	RHS of Equation 3.42 should be ">0"
115	7	Equation 6.5 should be "$\omega_{ac} = \tan(\omega_{dc} T/2)$"
120	3	... greater than predicted.
129	25	... dead-beat response.

ω_o	system angular frequency (= $2\pi fo$)
ϵ	is an element of
$\mathbb{R}$	the set of all real numbers

CHAPTER 1

INTRODUCTION

1.1 GENERAL

All turbine generators synchronised to electric power systems have their possible range of operation constrained by stability limits[1,2]. Higher generating unit output-to-inertia ratios and the tendency for power stations to be remotely sited from load centres have both tended to worsen stability problems recently. The situation may be ameliorated, however, by improving the generator control system.

Stability limits are usually encountered in under-excited generator operation; with long transmission lines the maximum power transfer may be limited. If at all possible, in most networks operators run the machines well away from steady-state stability limits due to the possibility of a fault such as a short circuit occurring. Disturbances of this type, called "transient disturbances", disrupt the equilibrium between input and output power of the generator, resulting in oscillations decaying to zero if the machine remains stable. If, however, the fault is not cleared quickly enough or there is insufficient margin of safety between the steady-state operating point and the stability limit, the machine loses synchronism and pole slips. Pole slipping is detrimental in many ways since high mechanical stresses occur in the turbine generator shaft and windings, large rotor currents flow and disruption may spread to the rest of the system, so if the machine does not re-synchronise quickly it has to be disconnected from the grid. Ensuring that the rest of the system is not overloaded in this eventuality necessitates extra, usually less economic, plant to be kept running to take up the lost capacity.

In addition to the importance of maintaining synchronism, it is also desirable to damp out any oscillations and return to steady-state operation as quickly as possible. In this way, disturbances are less likely to propogate to other machines in the system, and recent studies have shown that reduced mechanical fatiguing of the shaft caused by oscillations in torque is likely to prolong its life[3-6].

Turbine generators conventionally have two regulating loops: the governor and the automatic voltage regulator (AVR) compare speed and voltage respectively with reference values to regulate steam input and field voltage. Early governors such as the flyball or Watt type were too slow in response to have much effect on transient stability, but the stability improvement given by AVRs has long been recognised[1]. Modern electro-hydraulic governors enable valves to close at 6-7 pu/sec[7] and static thyristor excitation systems are also very fast[8].

The combination of fast response and high gain has led to inadequate damping in voltage regulators in many systems. Lead-lag compensators[10] are fitted which mean that, while the steady-state gain can be as high as 200, the transient gain during disturbances is usually about 25-30, improving the damping. Compensators of a similar type are also fitted to governors for similar reasons. The current practice is to tune compensation networks on site to meet specified responses, for example the voltage response following an AVR step change must meet certain overshoot and damping criteria.

Manufacturers have recognised the scope of micro-computers in the control of turboalternators[9] since they offer improvements in speed of response, flexibility and integration with [i] other plant [e.g., boiler] control schemes,

and [ii] centralised power system controllers. The logical first step is to build digital versions of conventional analogue regulators. However, numerous studies over the past twenty years, which will be reviewed later, have revealed that the "classical" generator control system described above can be improved upon to give a higher transient stability margin and better damping. On-line computers provide an ideal opportunity to implement an improved control scheme. Alternatively, electronic conventional governors and AVRs can easily be adapted to take computer-generated supplementary signals modifying their operation when necessary to improve transient performance.

Work has been done since 1977 at Imperial College on a controller which generates supplementary signals to add to the governor and voltage regulator loop reference points. Theoretical studies by Vaahedi and Macdonald[11,12] revealed that a promising way of doing this is by modelling the machine and estimating its state variables on-line, continually updating the estimates by taking measurements from the machine. The estimates are then fed back through an optimal feedback regulator to generate the supplementary signals. Subsequently practical studies by Menelaou and Macdonald[13-15] used a micromachine power system model, but the scope of this work was limited by the slow processing speed. Here the objective is to develop the work further using more advanced computer hardware, to perform theoretical and practical studies establishing which model and signals are best used as a basis for estimation and control, and to consider other appropriate factors relevant to the industrial implementation of such a control scheme.

1.2 TURBINE GENERATOR STABILITY

1.2.1 Classifications of stability

For convenience in power system analysis, turbine generator stability is generally subdivided into three main classifications:

a. Steady-state stability is understood to mean the ability of the machine to remain synchronised to the power system following a very small disturbance. It is well known[1,2] how a continuously acting voltage regulator extends stability beyond the theoretical unregulated steady-state limit [given by the short circuit ratio V_b^2/X_q] if the machine is under load. When operating in this mode, somewhat misleadingly the machine is said to be in the "dynamic stability" region.

b. Dynamic stability is concerned with the damping of electro-mechanical oscillations in the machine and the power system following small disturbances. They can occur anywhere in the generator operating region. Included in this classification are resonances between the turbo-generator shaft either [i] considered as a single mass system, or [ii] considered as a flexible distributed mass system, and the rest of the power system [sub-synchronous resonance] and oscillations caused by linking two or more interconnected systems [inter-area oscillations].

c. Transient stability is the ability of the machine to withstand large disturbances. It covers any sudden event which gives rise to such disturbances, such as three-phase faults, unbalanced line-line, or line-neutral faults, line switching, sudden application of load or transformer tap-changing. Of

these, the most severe - yet usually the least common - is the three-phase fault close to the generator, usually followed by disconnection of the faulted line. This worst-case situation is frequently the basis of transient stability studies.

There is no clear-cut distinction between each of the above classifications but different methods of analysis are used: For steady-state or dynamic stability studies disturbances are small and therefore the nonlinear generator equations may be linearised. In transient stability problems nonlinearities are important and a step-by-step solution of the machine equations is required, evaluating and taking account of non-linear effects at each time step. Transient stability analyses normally consider a single machine linked by a tieline to the rest of the system represented by an infinite busbar, whereas dynamic stability studies often require a detailed multimachine model of the entire system under investigation.

1.2.2 Stability improvement

Steady-state stability problems are frequently encountered in systems with long transmission lines, where there is a reactive power absorbtion problem. A reduced short circuit ratio[16], series capacitors, shunt capacitors or higher transmission voltages are all ways of improving the maximum power transfer capability in this situation.

Series capacitor compensation or high gain AVRs lead to dynamic instability problems, which power system stabilisers are intended to alleviate. Power system stabilisers[17] involve the feedback of an extra signal through suitable compensation into the voltage regulator. Power system stabilisers and series capacitor compensation

have both been causes of shaft torsional oscillations, which will be discussed in the next Section. In this country, power system stabilisers have been used to tackle England-Scotland inter-area oscillation difficulties[18,19].

Improvement of transient stability is the main objective in this work. However, a controller which improves system damping after a transient disturbance is also likely to make positive contributions to steady-state and dynamic stability. Motives for attempting to improve transient stability are the following:-

a. At any given operating point the generator is able to withstand a more severe fault; subsequent oscillations die out rapidly giving a generally well-behaved machine;

b. Generators may therefore be safely operated closer to their steady-state stability limits;

c. More power may be transmitted along existing transmission lines;

d. Better local controllers improve the chances of system recovery from an emergency state[20];

e. Since transient stability margins are higher, less spinning reserve plant is needed as machines are less likely to be lost.

1.3 REVIEW OF PREVIOUS WORK

1.3.1 Improving stability by modifying the plant and/or external system

Switched series capacitors[21,22] or shunt reactors[24,25] can be used to help maintain generator stability during a transient. Braking resistors[23] also improve stability by absorbing excess energy from

the machine to limit the first swing of the rotor angle. Autoreclosing circuit breakers[26] to reclose the faulted line as soon as possible after clearing are another method. However, U.K. utilities have not adopted this method due to the possibility of aggravating fault-induced shaft torsional oscillations [and exceeding peak design torques] before they have decayed[27].

The divided-winding rotor [DWR] generator has two independently-controllable field windings on both the direct and quadrature rotor axes[28]. This arrangement offers considerable stability improvements over conventionally wound machines[16,28,29]. However, major design modifications are necessary for this type of machine, including an extra excitation system, resulting in greater expense. It is for financial reasons that DWR machines, switched capacitors and reactors and braking resistors have not been more widely adopted, since all the methods require expensive hardware.

1.3.2 Improving stability by modifying the turbine generator control system

1.3.2.1 EXCITATION CONTROL

A scheme for the "artificial stabilisation" of a synchronous machine to improve long distance power transmission was proposed in 1946 by Wanger[30]. It involved feeding frequency deviation and rotor angle as additional signals into the excitation system. Another early supplementary controller in reference (31) fed rotor angle through a nonlinear "limiter" circuit which boosted the field when the angle became very high. The scheme was tested on site with a 60 MW turboalternator. High speed rectifier excitation systems introduced a few years later[10] were found to help limit the first load angle swing following a disturbance, but with high AVR gains damping was

sometimes poor. Output power[32], speed deviation[33], and frequency deviation[10] were all suggested as stabilising signals to feed into the AVR and improve damping. DeMello and Concordia[34] published a small perturbation analysis of synchronous machine stability, giving useful guidelines on designing AVR lead-lag compensators, also on designing a supplementary signal AVR stabilising network and when it is likely to be needed. In the discussion, it was argued that for major disturbances the supplementary signal should be switched off, but the authors thought that simply limiting the signal would still improve damping following the transient.

A few years later, torsional oscillations gave problems on an Ontario Hydro machine[35]. The cause was traced to be feedback of speed through a stabiliser to the AVR exciting natural shaft modes of oscillation. More seriously, torsional oscillations led to complete shaft failure at Mohave in the U.S.[36,37], although there they were caused by resonance between shaft modes of oscillation and series capacitor compensated transmission lines. Methods proposed to avoid speed based stabilisers exciting shaft oscillations were:

[i] Siting the speed transducer at the physical node of the oscillation[35];

[ii] Notch filters tuned to filter out resonant shaft frequencies[35,38]; and

[iii] An observer and controller designed using a pole assignment technique[39] to ensure torsional vibrations are not aggravated.

Alternatively, one can avoid using speed as a stabilising signal altogether replacing it with frequency[10], accelerating power[40,41], output power[32], or even air-gap flux[42]. Criteria to be considered

when choosing stabilising signals are:-

[i] Ease and accuracy of measurement;

[ii] Contribution to controllability [hence stability] of the system; and

[iii] Avoidance of undesirable torsional modes of oscillation.

1.3.2.2 GOVERNOR CONTROL

In 1868 Maxwell published an analysis of different types of governors[43] and suggested a compound governor which effectively controlled speed by feeding back velocity and acceleration. Dineley and Kennedy[44] used an analogue computer simulation to show that improved generator stability was possible with proportional-plus-derivative feedback of speed. A frequency-response analysis[45] showed that damping could be improved by proportional-plus-integral velocity feedback. Compensators are now commonplace in governors but there has been a general reluctance to provide supplementary stabilising signals to governors rather than voltage regulators, despite the existence of electro-hydraulic systems and the direct control of input power that can be achieved. This may be because utilities with a mixture of modern and older plant do not want steady-state governing and load sharing between machines to be interfered with. There are also problems in turbines of thermal stresses and steam condensation associated with sudden changes in load setting.

1.3.2.3 FAST VALVING

Fast valving[46,47] is a means of improving transient stability by rapidly shutting off the intercept valves and re-opening them within approximately 10 [ten] seconds. Intercept valves control the steam

input to the intermediate [and thence low] pressure cylinders of the turbine after it has been reheated following its passage through the high pressure stage. Fast valving is initiated upon detection of an unacceptable difference between input and output power of the turboalternator and seems especially effective at preventing over-speed following load rejection. For other transient disturbances, however, there are several problems:-

a. No post-fault contribution is made to system damping;

b. There is the danger of a minor disturbance [e.g. tap changing] triggering off the process;

c. Generation capacity is partially lost for several seconds;

d. Reheater steam pressure can build up to dangerously high levels if re-opening is delayed;

e. Re-opening could possibly have a destabilising effect if too rapid and badly timed;

f. With frequent rapid closure, valve life may be shortened.

1.3.2.4 BANG-BANG CONTROL

Bang-bang control schemes are so-called because system inputs are switched from one extreme to the other. Early work used rotor angle and frequency deviation to determine the critical switching times[48]. A time-optimal control approach for nonlinear systems has been used in other studies to determine switching times for a given disturbance for excitation control[49,50] and for both prime mover and excitation control[51]. The difficulty with bang-bang schemes is that optimal switching times have to be pre-determined for any fault considered. Unless the controller is specifically given information as to clearing time and type of fault [whether three-phase or

unbalanced], and has a look-up table of contingency actions for all possible faults, the control will not be optimal except for the design type of fault. In some circumstances the action could even be detrimental to stability. Another difficulty with time-optimal nonlinear control theory is in its application to multiple input/ multiple output systems.

1.3.2.5 OPTIMAL AIMING STRATEGIES

Optimal Aiming Strategies [OAS] are also applicable to nonlinear systems and were developed by Barnard[52]. Whereas general optimal control theory involves infinite-dimensional function space optimisations, OAS reduce the problem to finite-dimensional optimisations. The objective of OAS is to drive the system towards a stable equilibrium state when disturbed, and it involves defining:

[i] the present state;

[ii] the desired or "aim" state and a neighbourhood thereabouts of acceptable natural system stability, and

[iii] a set of state velocity vectors that can be achieved by the controls at any instant in time.

One process chooses the controls such that the angle between the possible trajectory, given the control inputs, and the desired trajectory is minimised [minimum-angle OAS] but there are different optimality criteria.

OAS algorithms have been tried out experimentally controlling braking resistors and switched series capacitors on the New England Test System[53], with reasonable success. Work has also been done on an OAS scheme for providing supplementary signals to turbine generators[54], but comprehensive test results have yet to be published.

1.3.2.6 OPTIMAL CONTROL

The process of optimally feeding back several machine variables to provide excitation or prime-mover control began receiving attention about twenty years ago. In reference[55], with only very limited computers then available for control, Nicholson suggested a set of "preprogrammed optimal linear control settings" on an on-line computer, the settings derived from off-line tests to minimise a performance index. The performance index, penalising deviations of system states from desired values and taking account of control effort, is fundamental to optimal regulators. Differential dynamic programming[56] requires advance knowledge of the machine post-fault trajectory to perform the optimisation, and consumes a large amount of computer time, hence it is not suitable for direct on-line application but it can be used as a basis for designing a controller for a general nonlinear system. Quasilinearisation[57] also presents a heavy computational burden in calculating optimal controls for nonlinear plant.

Other theoretical studies on generator optimal control used Pontryagin's maximum principle[58] to minimise the performance index leading to a Riccati equation, which yields the optimal feedback gains upon solution[59,60]. A linearised system representation is needed so the controller is only truly optimal close to the design operating conditions; even so, the studies showed a good transient performance was possible. Another drawback of these controllers is that all the states must be available for measurement. This can be overcome by approximating the model used in the controller design or by using optimal output controllers[61-63]. A third problem is in the arbitrary choice of weighting matrices for the performance index, which

quantify how much the deviations of each individual state-variable from the steady-state are penalised. A criterion for choosing the weighting matrices suggested by Yu and Moussa[64] is to shift dominant eigenvalues to the left of the complex plane so far as the available controls permit. Saturation of the controls can render this method ineffective, and the more usual method is design by trial-and-error, looking at simulated responses and modifying the weighting matrices until the desired performance is reached.

Experimental tests on the optimal control of micromachines were made using a computer[65,66,70] or preset amplifier gains[67]. They were based on very simple linearised models, the states being fed into the field system[65,67] or both exciter and prime-mover control systems[66,70]. Discrete-time system modelling was used in the computer control scheme of Newton and Hogg[70]. Results showed improvements in both steady-state and dynamic stability over conventional controls. Another practical micromachine study by Daniels, Davis and Pal[68] compared linear optimal control with an optimal controller designed by a nonlinear function minimisation technique, finding the nonlinear-designed controller marginally better. Dynamic programming as a method of calculating the optimal feedback gains also proved successful[69] in a scheme giving optimal prime-mover and excitation control using a 7^{th} order machine model.

Nonlinear function minimisation methods applied in designing generator optimal feedback systems[68,109,105] have generally been unconstrained quasi-Newton methods[110]. Although these methods handle general nonlinearities in systems, hard constraints due to

limits on controls and state-variables are not directly taken account of during the performance index minimisation. Mayne and Sahba[106] have developed an algorithm to design a nonlinear optimal state-feedback controller taking account of both hard and soft constraints, and showed in a theoretical paper[107] that the generator transient response was improved more than with fixed gain linear optimal or quasi-Newton designed nonlinear controllers.

1.3.2.7 LOOK-UP TABLES

A practical method of solving the problem of different gains needed to give optimal control at different operating points was suggested by Evans et al[65] and implemented experimentally by Bartlett, Gibbard and Woodward[71]. It involved the use of a look-up table of third order feedback gains for each node of a grid covering the entire operating region, stored in the on-line computer. However, the authors encountered limit cycle type oscillations in the dynamic stability [leading power factor] region due to the system hunting with repeated switching between adjacent feedback gains. Limebeer et al[72] significantly improved this type of scheme by using a discrete time system model, also linearised at several operating points, but with gains ramping at a predetermined rate to new values when the operating point changed. This inhibited the hunting encountered previously. Phung and Gibbard[73] achieved similar results by introducing the concept of "pseudo steady state" operating points. These were practically determined by digitally low-pass filtering instantaneous power and VAr values, and were used as a basis for selecting gains from the look-up table.

In work by Glavitsch et al[74,75] consideration is taken not only of the

generator operating condition but also its tie-line impedance to the rest of the system. This resulted in a three-dimensional look-up table with different power and voltage feedback gains for different values of power, reactive power and external impedance. The identification of the tie-line reactance required remote and local measurements of voltage, phase angle between sending and receiving end voltages and power.

Practical implementations of schemes involving look-up tables have so far been limited to simple low-order feedback controllers. Higher order algorithms with a large number of gains are likely to run into storage problems and the time taken to replace one set of gains with another will increase.

1.3.2.8 THE USE OF OBSERVERS OR STATE ESTIMATORS

All the optimal control techniques discussed so far suffer from degradation by system noise, and in the case of state-feedback controllers, the order of system model that can be used is constrained by states that are not easily measurable or are wholly fictitious. An approach overcoming these problems, adopted by Vaahedi, Menelaou and Macdonald in references [11-15] and used as a basis for this work is to estimate the machine state variables from measured outputs, then feed them back through a conventional optimal regulator. The process, based on theory developed by Kalman and Bucy[76], gives best estimates of the system states in the presence of white noise. Alternatively, a pole-placement technique may be used to design the estimator[77,39] resulting in a Luenberger[78] observer. A problem with designing an observer of this type is in deciding where to place the observer poles[39].

A drawback of state estimators [Kalman filters] and observers is that to design them requires a linearised system model, as with optimal regulators. Also the estimator needs to model the system on-line, resulting in a considerably greater on-line computation requirements than for a straightforward optimal regulator.

1.3.2.9 SELF-TUNING REGULATORS

Self-tuning regulators[79,80] were devised to control systems with unknown constant or continuously varying parameters. The principle has been applied to turbogenerator control, where there is some degree of uncertainty in the parameter determination and model validity, in references [81-83]. Ghosh et al[83] detail the different approaches to adaptive control, which may be divided into those with implicit and those with explicit system identification. Those with implicit identification require a predetermined model of the system, the regulator gains being determined by the difference between the model and the real system [model reference adaptive control]. Those with explicit identification require random or pseudorandom noise to be injected into the system inputs to perform the identification process.

Drawbacks of adaptive control approaches are firstly the time taken to identify the system and compute the regulator gains. Secondly, it may be undesirable to inject noise into the system inputs, and thirdly, the accuracy of identification may be influenced by the presence of feedback or of correlation in external disturbances. An approach of Hogg[84] on overcoming the first two of these drawbacks is to use a grid of controllers based on a priori system identification performed at several operating points.

Dual-rate sampling self-tuning regulators[108] are those which sample plant information [for identification] at a different rate to that used for outputting control signals. A scheme of Kanniah, Hope and Malik[108] sampled plant information at a rate several times faster than that for control outputs to overcome difficulties of the long computation time taken for identification as compared to control calculations. Practical tests demonstrated better small and large signal performance than with a standard self-tuning excitation regulator.

1.3.2.10 MULTIVARIABLE FREQUENCY-RESPONSE METHODS

These are an extension of classical single variable control design techniques, such as Bode's and Nyquist's methods, to multivariable systems. Multivariable frequency-response methods include direct Nyquist array [DNA] and inverse Nyquist array [INA] methods[85] and characteristic loci methods[86]. Hughes and Hamdan[87] used the DNA method to design a speed stabiliser for the excitation system considering both phase lead and phase lag type compensators. They found lag compensators to be more sensitive to changes in operating point, whereas lead compensators were more affected by noise. Ahson, Hogg and Pullman[88] considered an integrated micromachine prime-mover and excitation controller based on INA design techniques. Speed was fed into the AVR loop and acceleration into the governor loop, the compensation networks obtained by a computer-aided design package. Good rotor angle damping and voltage recovery were obtained over a wide range of operating conditions in response to a short circuit. The problem of such compensators possibly exciting shaft torsional oscillations is considered by Chan and Athans[89], for both single and multimachine systems, where

robustness margins are evaluated close to the critical frequencies. If the margins are sufficient the designer has confidence that torsional shaft oscillations will be avoided, and furthermore he has a tool for comparing the robustness of different controller designs.

1.3.3 Conclusion of review

Although this is by no means an exhaustive review, nonetheless the vast amount of work and number of different approaches to power system stability improvement will now be apparent. Each method has its own peculiar advantages and disadvantages over other methods, for example multivariable frequency response methods can result in easily implementable controllers without needing on-line control computers, but difficulties have been their adaptability to operating point changes and performance in a noisy environment. Self-tuning controllers adapt to changes in the system but accuracy and speed of identification are problems. Anderson summarises the situation well in his discussion on reference [88]: "Whether indeed any given method is generally superior will become apparent only over a period of time when a number of individuals has each obtained experience with all methods on a variety of practical problems."

However, the method adopted here of estimating states and optimally feeding them back overcomes objections to optimal control based on lack of practical availability of all the state variables. Moreover, the advanced on-line computers now available make it possible to try more detailed models than the maximum of seven states found to date in the literature. These, together with numerous other refinements detailed later, have enabled a more thorough

practical exploration of a Kalman filter-optimal regulator based turbine generator control scheme than has previously been documented. Eventually it is hoped that a direct comparison using the same hardware may be made between this and alternative control schemes.

1.4 OBJECTIVES

This work aims to develop and extensively test optimal control based on state estimation in an experimental application to a turboalternator model, working towards a feasible scheme for use in a real power system.

The approach is to obtain a nonlinear set of differential equations representing the machine as well as possible under transient conditions. This model is used for two things: firstly as a basis for designing the controller and, secondly, for simulating on a digital computer how the controller affects the behaviour of the machine under transient conditions.

To design the controller the nonlinear equations are linearised about the operating point of interest. This is necessary because optimal control and Kalman filtering theory are based on linear systems. The order of the linearised mathematical plant model can be reduced by a recently developed linear system model order reduction method[90,91]. The linear system is then transformed into the discrete-time domain, which is more suited to on-line computers which sample data at discrete instants[92].

Discrete-time state estimators and optimal controllers are then derived from the linearised discrete-time system equations by solving Riccati equations for the estimator and regulator respectively.

Once designed by this process, the controllers can be tested with nonlinear simulations. Experimentally the scheme may be tested with a micro-computer giving supplementary control to the standard voltage and speed feedback loops of a physical small-scale model of a large turbine-generator. Points of interest to industry which it is hoped will be clarified are:

a. What improvements in transient stability margins can be expected from such an advanced digital generator control scheme?

b. What is the contribution to system damping?

c. How much processing power is needed in the on-line computer?

d. Which measurements are needed for the controller to give best results?

e. What is the robustness of the controller with respect to changes in local operating conditions and in the system itself?

f. What modifications are required to the plant?

g. Do noise and parameter errors significantly degrade the controller?

h. What are the effects on steady-state operation of the turbine-generator?

i. Is the micromachine a valid representation of large machines for testing the controller; may it be improved?

j. What other problems may be expected when applying the controller to a real machine in a power system?

Other areas hoped to be of more general interest to control as well as

power engineers are:

a. The practical application of Kalman filtering for estimating the state-variables and optimally regulating a synchronous generator.

b. The use of a recently-developed model order reduction method in the above, thus experimentally verifying the validity of the technique which potentially has a much wider application.

1.5 ORIGINAL CONTRIBUTIONS

The original contributions of this thesis are thought to be the following:

a. The design and practical application by microcomputer of a state estimator and optimal regulator, derived from discrete-time theory, to a laboratory turbine-generator physical model with a view to improving transient stability.

b. The use of accurate models [up to twelve states] in the above scheme, and practical comparison between these and approximate models.

c. The first practical use in any control scheme of an optimal Hankel-norm reduced order model. A twelve-state generator model is reduced by this method to fourth order, and the controller performance is degraded less than when conventionally reduced models are used.

d. Achievement of an on-line calculation time for a generator state estimator/optimal controller of less than 11 ms with the microcomputer control system.

e. Comparison of generator controllers of the above type based on

different measurements: load angle to infinite busbar and field voltage; slip speed and field voltage; power and field voltage; power and terminal voltage.

f. Practical demonstration of the immunity of a state estimator/ optimal controller to severe noise.

g. Tests proving the adaptability of the above controllers to changes in generator operating condition.

h. A brief examination of the contribution of state estimation and optimal control to the turbine-generator dynamic stability.

i. A practical assessment of the controller performance when torsional vibrations occur on the machine shaft.

CHAPTER 2

MATHEMATICALLY MODELLING THE POWER SYSTEM

2.1 INTRODUCTION

The ability of large digital computers to handle complex power system models has meant that the use of grossly approximate generator representations in simulations is seldom necessary. Developments in finite-element analysis indicate the trend towards more and more complicated generator models, and the need to take account of anomalous effects due to changes in operating conditions and during transients.

Different approaches to modelling are necessary for different requirements; principal types of generator model and their applications are:-

a. Nonlinear models for transient stability analysis:

Used by manufacturers to predict whether machines will meet specified transient stability requirements, and by utilities to predict stability margins during system operation. Here nonlinear models are used to examine the effectiveness of a digital controller design before implementing it on a micromachine power system physical model. The usual representation, and that used here, is a single machine connected to the rest of the system [considered as an infinite busbar] by a double circuit transmission line, Fig. 2.1.

b. Linearised models:

When deviations from the steady-state operating point are small, a linear approximation of the system nonlinearities is justified.

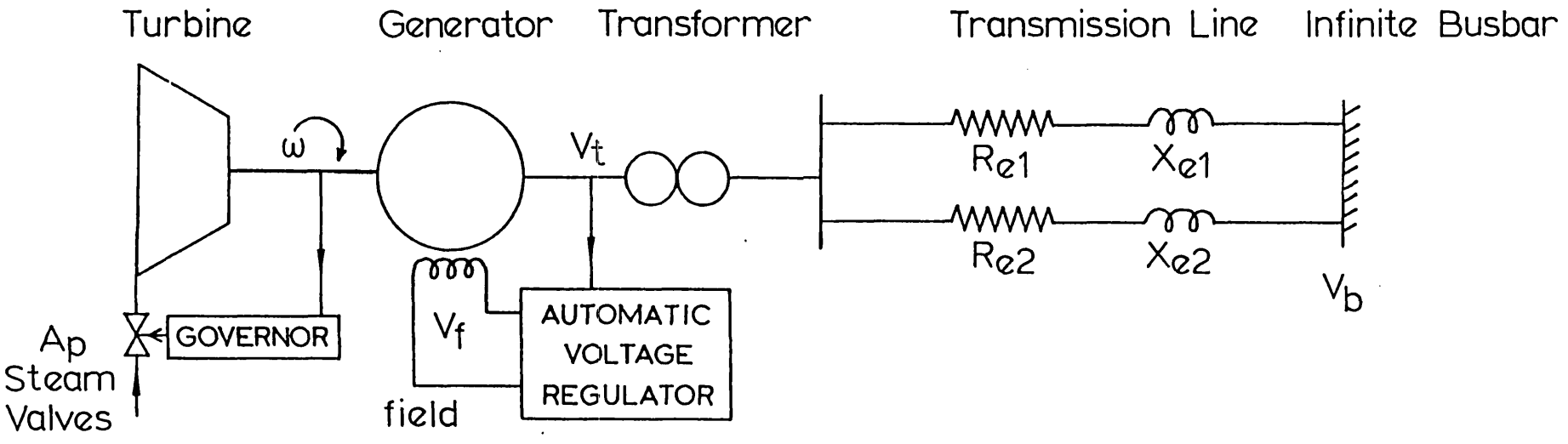

Fig. 2.1: General single-machine-infinite-busbar system.

Eigenvalue analysis may be applied to linear single- or multi-machine system models to give useful dynamic stability information. Linear models of varying degrees of approximation may also be used to design AVRs, governors, power system stabilisers and advanced integrated controllers. These are often applied even during large disturbances, although the initial assumptions are then contradicted.

c. Linearised discrete-time models:

More suited to on-line computer control, where data is sampled and output at finite intervals in time, are discrete-time equivalent models of the continuous-time models in (b). The two are related by a straightforward transformation between the continuous-time and discrete-time domains.

Simplification of linear models is often desirable for the following reasons:

[i] Reducing a large multi-machine problem to manageable proportions;

[ii] Reducing to an acceptable value the computation time taken by an on-line controller[11-15];

[iii] Deriving an optimal regulator based on conveniently measurable input signals[65-67,96].

Note that with a state estimator, however, a model with some difficult-to-measure or even fictitious state-variables may be used.

All the models in this work are derived using the two-axis theory. Fundamental to the two-axis theory is Park's transformation[94,16] replacing the

three actual phase coils by two fictitious axis coils that would set up the same mmf wave. The two-axis representation of the machine is shown in Fig. 2.2. As well as the two axis coils representing the stator winding (d, q) there is one field coil (f), and damping circuits are represented by one d-axis (kd) and either one or two q-axis short-circuited coils (kq1, kq2). Position and velocity are measured relative to a reference frame rotating at constant angular frequency ω_o [the synchronous frequency].

Assumptions made here are that saturation effects may be neglected and harmonic winding factors are zero. An infinite bus representation of the "stiff" external power system is used throughout. In addition, the turbogenerator shaft is considered as a single-mass system with no flexible couplings. Capacitance in the generator windings and transmission system is neglected. Finally, the system angular frequency at the infinite busbar is assumed to be constant at the nominal value of ω_o.

2.2 NONLINEAR MODELS OF THE GENERATOR AND ITS CONTROL LOOPS

A state-space model of the synchronous machine-infinite busbar system of the following form is set up:

$$\dot{x} = A_n x + F_n(x) + B_n u \qquad [2.1]$$

where A_n is the state matrix, B_n the control matrix [both containing only linear terms], and $F_n(x)$ accounts for system nonlinearities. x is the state variable vector and u the control variable vector. The machine model includes states to represent the generator itself, supplemented by states to model the dynamics of the governor and voltage regulator. Control inputs u are the reference signals to the speed and voltage feedback

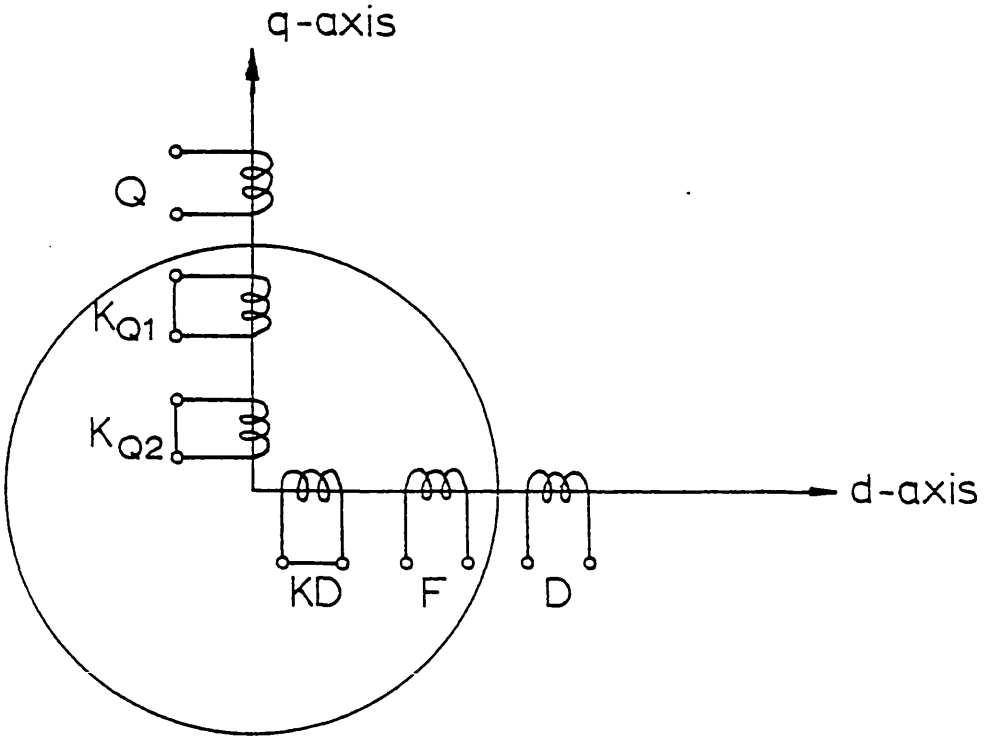

Fig. 2.2: Two-axis representation of the machine

loops. Outputs calculated when solving the state equations are voltages, fluxes or currents, torques and speed. The per-unit system and motoring sign convention of Adkins[16] have been adopted.

2.2.1 Voltage Regulator Modelling

Models for the many different excitation systems in use are described in a recent IEEE report[101]. To represent fully one of the more complex systems, including a lead-lag compensator, would require a large number of state variables. Here the AVR and excitation system model is based on an a.c. exciter supplying a static controlled rectifier feeding the field [IEEE Type AC4[101]]. This arrangement has a very fast response with a time constant of typically 5 msec, and is simple to model. Two time delays represent the system, one for the AVR and one for the exciter, and to simplify the simulation the lead-lag network is not fully modelled. This is because only transient performance is of interest, and accordingly the steady-state gain K_a of typically 200 has been reduced to a transient value of about 30[34]. The transfer function of the AVR-exciter model is shown in Fig. 2.3.

It is assumed that negative as well as positive field forcing is possible[101], but only positive field current is allowed. In state-space form the excitation system is represented as follows:

$$\dot{V}_e = (V_r + u_1 - V_t)G_a/T_a - V_e/T_a \qquad [2.2]$$

$$\dot{V}_f = -(V_e G_e + V_f)/T_e \qquad [2.3]$$

$$V_{emin} \leqq V_e \leqq V_{emax},\ V_{fmin} \leqq V_f \leqq V_{fmax} \qquad [2.4]$$

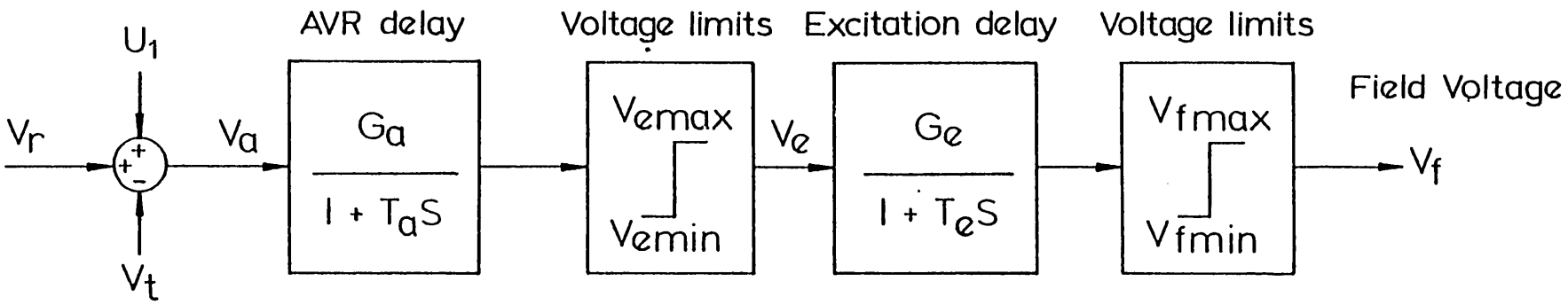

Fig. 2.3: The AVR system model

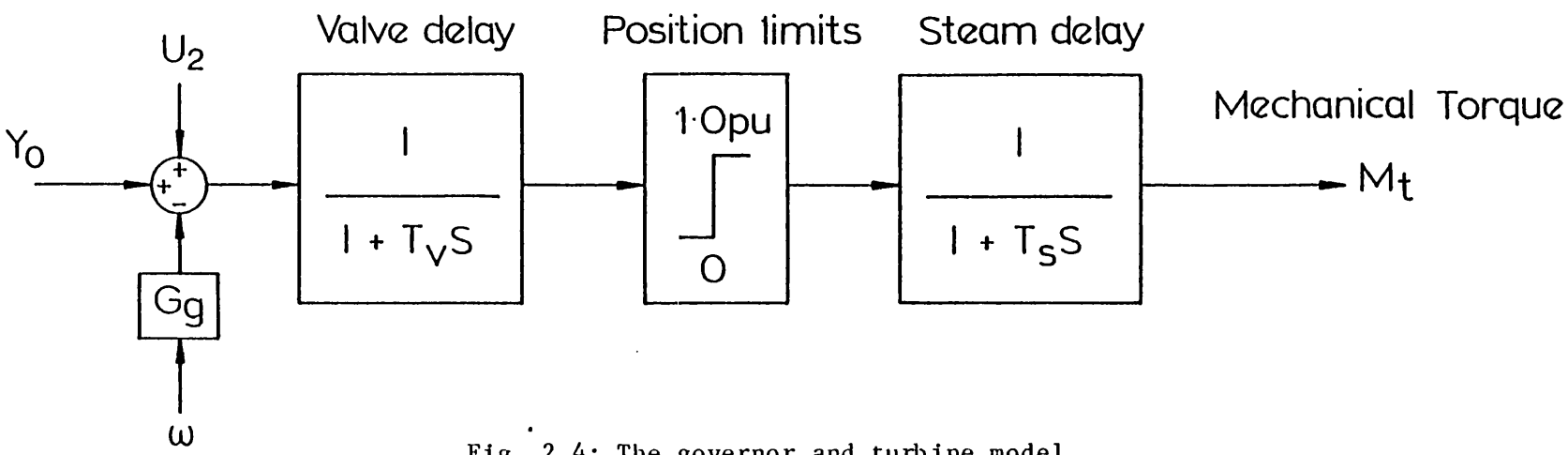

Fig. 2.4: The governor and turbine model

Manufacturers talk about an overall steady-state AVR gain K_a[104]:

$$V_t = K_a(V_r + u_1 - V_t) \qquad [2.5]$$

The relationship between K_a, G_a and G_e is derived in Appendix A.

Ceiling values for the excitation voltage V_e and the field voltage V_f are chosen to be ±3 times the rated load value.

2.2.2 Governor and Turbine Modelling

To model accurately the time lags associated with pilot and main hydraulic systems to open and close the valves, and those associated with entrained steam in the pipework and each individual turbine stage would require a large number of state-variables. A method of simplifying the governor/turbine model is to represent all the delays by two time constants[102], as in Fig. 2.4. A paper by Limebeer and Lahoud[93] shows how balanced model realisations may be used to calculate the simplified governor/turbine time constants [see also Chapter 3]. The valves are assumed to be high-pressure hydraulically activated with a maximum closing rate of 6-7 pu/sec. The differential equations are:

$$\dot{A}_p = -\frac{A_p}{T_v} - \frac{G_g\omega}{T_v} + \frac{[Y_o + u_2]}{T_v} \qquad [2.6]$$

$$\dot{M}_t = \frac{A_p}{T_s} - \frac{M_t}{T_s} \qquad [2.7]$$

$$0 \leq Y_o \leq 1 \qquad [2.8]$$

$$0 \leq A_p \leq 1 \qquad [2.9]$$

More accurate models of the governor and turbine are considered in the practical application [Chapters 5 and 6] which take account

of different valve opening and closing rates and the turbine and reheater entrained steam delays.

2.2.3 Modelling the generator as a whole

A state-space generator model using fluxes as state-variables is derived in Adkins and Harley[16], but one could just as well derive an equally accurate model using winding currents as state-variables[95]. Humpage et al[96] suggest that winding currents are better as state-variables since they are more accessible generator quantities; however, damper currents are not usually considered to be easily measurable. Simplification, and possibly a transformation of the original equations is necessary to obtain a state-space model consisting entirely of readily measurable states; This is not necessary here since unmeasurable states may be estimated.

Models using flux linkages, and models using currents as state-variables, have both been employed in this work. It has been found that deriving output matrices, which relate measurements taken from the plant to the state-variables, is generally more straightforward when currents are used in the formulation.

2.2.3.1 GENERATOR DIFFERENTIAL EQUATIONS IN TERMS OF FLUXES

The machine equations relating generator fluxes, currents and voltages [16, Eqn. [5.19] p.107] can be arranged in the form:

$$[\dot{\Psi}_d] = \begin{bmatrix} V_d - \omega_o \Psi_q + \Psi_q \omega \\ V_f \\ 0 \end{bmatrix} - [R_{gd}]\,[I_d] \qquad [2.10]$$

$$[\dot{\Psi}_q] = \begin{bmatrix} V_q + \omega_o \Psi_d - \Psi_d \omega \\ 0 \end{bmatrix} - [R_{gq}] [I_q] \qquad [2.11]$$

where the matrices and vectors are explained in Appendix B.

The currents are related to the fluxes by the following linear equations [neglecting saturation]:

$$[I_d] = [Y_{gd}] \ \omega_o [\Psi_d] \qquad [2.12]$$

$$[I_q] = [Y_{gq}] \ \omega_o [\Psi_q] \qquad [2.13]$$

By substituting [2.13] and [2.12] in [2.11] and [2.10] respectively, a state-space model of the generator in terms of fluxes can be derived:

$$[\dot{\Psi}_d] = \begin{bmatrix} V_d - \omega_o \Psi_q + \Psi_q \omega \\ V_f \\ 0 \end{bmatrix} - [R_{gd}] [Y_{gd}] \omega_o [\Psi_d] \qquad [2.14]$$

$$[\dot{\Psi}_q] = \begin{bmatrix} V_q + \omega_o \Psi_d - \Psi_d \omega \\ 0 \end{bmatrix} - [R_{gq}] [Y_{gq}] \omega_o [\Psi_q] \qquad [2.15]$$

The total torque is given by the electrical torque minus mechanical components:

$$M_t = M_e - J \ddot{\delta} - k\ddot{\delta} \qquad [2.16]$$

Where:

$$M_e = \frac{1}{2} \omega_o (\Psi_d i_q - \Psi_q i_d) \qquad [2.17]$$

Note that the constant frictional torque loss $k\omega_o$ is omitted from the mechanical torque expression for simplicity.

Using this derivation, a generator model in terms of 11 state variables [including AVR and governor] can be obtained:

$$[x] = [\delta, \dot{\delta}, \omega_o \Psi_d, \omega_o \Psi_f, \omega_o \Psi_{kd}, \omega_o \Psi_q, \omega_o \Psi_{kq}, V_e, V_f, A_p, M_t]^T \quad [2.18]$$

Full details of the nonlinear 11^{th} order model are in Appendix B.3.

2.2.3.2 SIMPLIFICATIONS

The eleventh order representation can be simplified without excessive error by neglecting stator transients ($\omega_o \dot{\Psi}_d$ and $\omega_o \dot{\Psi}_q$); also removal of these high-frequency terms allows an increase in the integration time step. The simplification does mean, however, that oscillating currents, and hence oscillating torque components following a severe fault are not simulated. Consequently, the back-swing effect does not appear in transient simulations[97].

The states of the 9^{th} order generator model are:

$$[x] = [\delta, \dot{\delta}, \omega_o \Psi_f, \omega_o \Psi_{kd}, \omega_o \Psi_{kq}, V_e, V_f, A_p, M_t]^T \quad [2.19]$$

Although the rate of change of fluxes Ψ_d and Ψ_q is assumed to be zero during integration, at the end of each time step the values are re-calculated by the approximations given in Appendix B.4

2.2.3.3 GENERATOR DIFFERENTIAL EQUATIONS IN TERMS OF CURRENTS

The generator equations as found in Adkins and Harley (16, Eqn. [4.27]) can be represented by the following matrix equation:

$$[V] = \{[R] + [G].\omega + [L].s\} [I] \quad [2.20]$$

where ω represents the rotor angular velocity and s is the Laplace operator. This can easily be rearranged into the following state-space form:

$$[\dot{I}] = [B]. \{[V] - ([R] + [G].\omega).[I]\} \quad [2.21]$$

where

$$[B] = [L]^{-1} \qquad [2.22]$$

Details of the matrices and vectors in Equations [2.20 - 21] are explained in Appendix C.

With two quadrature-axis damper coils, the resulting generator model has twelve states:

$$[x] = [\delta, \dot{\delta}, i_d, i_f, i_{kd}, i_q, i_{kq1}, i_{kq2}, M_T, V_f, V_e, A_p]^T \qquad [2.23]$$

2.2.3.4 SIMPLIFICATIONS

A much simplified 7-state generator model has been used as a basis for controller design. The states are:

$$[x] = [\delta, \dot{\delta}, i_f, V_f, V_e, A_p, M_t]^T \qquad [2.24]$$

In this model stator transients have been neglected as in the 9^{th} order model. An additional simplification has been to omit electrical damping terms, allowing for them instead by modifying the mechanical damping coefficient k, using a formula suggested by Crary[2,15]. The derivation of k is shown in Appendix C, together with the simplified model equations.

To simulate the transient performance of the generator in off-line studies, an eleventh order nonlinear model based on flux equations is used throughout. The other orders of model are linearised to design controllers for the machine. The process of linearisation is described in Section 2.4.

2.3 TRANSMISSION LINE AND TRANSFORMER MODEL

Here an uncompensated transmission line is assumed, and capacitors may be neglected, so that the transmission line and generator transformer may be represented by series resistance and inducance [Fig. 2.5].

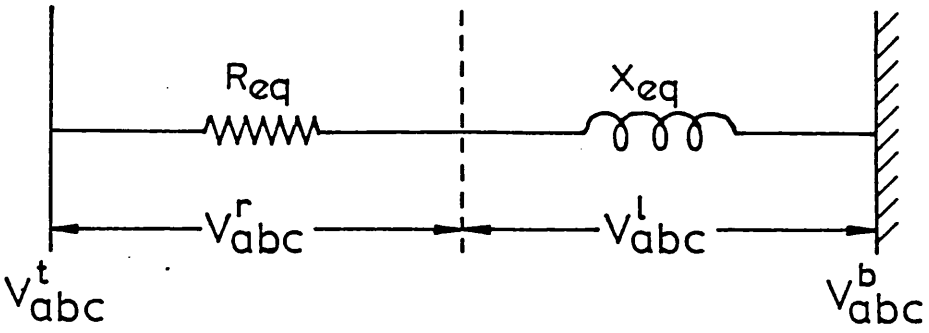

Fig. 2.5: Transformer and transmission line model.

Where R_{eq} and X_{eq} are the summed line and transformer resistances. The phase voltages are related by:

$$[V^t_{abc}] = [V^b_{abc}] - [V^l_{abc}] - [V^r_{abc}] \qquad [2.25]$$

Park's transformation[16] is used to obtain the above relationship in terms of axis quantities, resulting in:

$$V_{td} = V_{bd} - R_{eq}\, i_d - (X_{eq}\, \dot{i}_d + (\omega_o - \dot{\delta})\, i_q\, X_{eq})/\omega_o \qquad [2.26]$$

$$V_{tq} = V_{bq} - R_{eq}\, i_q - (X_{eq}\, \dot{i}_q - (\omega_o - \dot{\delta})\, i_d\, X_{eq})/\omega_o \qquad [2.27]$$

The "modified machine" representation is used throughout, where the external resistances and reactances between the generator and the infinite busbar [or fault point during a short circuit] are added to the generator resistances and reactances to give a modified machine model.

2.4 LINEARISED SYSTEM REPRESENTATION

All the state-space models of the machine discussed so far contain nonlinearities. To design controllers using linear optimal control theory and state estimation theory, a linear model is needed. Linear models can also be used in dynamic stability analysis of single or multimachine systems and in the design of conventional controllers.

The nonlinearities in Eqn. [2.1] are contained within $F_n(x)$, where x is the vector $[x_1, x_2 \ldots x_n]^T$. To obtain a linear approximation for $F_n(x)$, it is expanded in a Taylor series about a nominal operating point $\bar{x}$:

$$F_n(x) = F_n(\bar{x}) + \left\{\frac{\partial F}{\partial x_1}\Delta x_1 + \frac{\partial F}{\partial x_2}\Delta x_2 + \ldots + \frac{\partial F}{\partial x_n}\Delta x_n\right\} + \text{Higher terms} \qquad [2.28]$$

where the partial derivatives are evaluated at the nominal operating point. Higher terms are usually small compared to first order terms and can be neglected.

Using this technique the different orders of generator model may be linearised and represented in the following state-space form:

$$\Delta\dot{x} = A_L \Delta x + B_L \Delta u \qquad [2.29]$$

where A_L and B_L are the matrices of Eqn. [2.1], with linearised terms, the $\partial F/\partial x_i$, (i = 1...n) from Eqn. [2.28] for each state variable, added.

Equation [2.29] determines the deviations $\Delta x(t)$ from the nominal operating point, given changes $\Delta u(t)$ to the inputs to the system. The complex eigenvalues of the matrix $[A_L]$ can easily be found, and give information on the dynamic stability of the system at the nominal operating point.

Appendix D gives linearised models of the 12^{th}, 9^{th} and 7^{th} order models used in the controller design. A steady-state phasor diagram calculation is used to find the nominal operating point $\bar{x}$, given in Appendix E.

A useful check on the accuracy of a linearised representation is to compare responses for small disturbances with a nonlinear model. As an example, with small step changes in the governor or AVR reference level there should be very little difference between the responses of a model and its linear equivalent.

2.5 INTEGRATION METHOD

When the differential equations, whether linear or nonlinear, have been formed they may be solved to simulate the plant in time. A suitable method of integration for digital simulations used here is the Kutta-Merson fifth-order method. If there are nonlinearities, they have to be calculated at the end of each step of the integration before proceeding to the next step. As well as evaluating the algebraic nonlinearity expression $F_n(x)$, the inequalities in equations [2.4, 2.8 and 2.9] have to be tested and the variables constrained if limits are hit. The Kutta-Merson integration routine is described in Appendix F.

2.6 LINEARISED DISCRETE-TIME MODELS

With any computer-based control system sampling data at discrete instants in time, it is appropriate to replace continuous-time linear models [Eqn. 2.29] with their discrete-time equivalents[58,98,103] as follows:

$$\Delta x(kT + T) = A_D \Delta x(kT) + B_D \Delta u(kT) \qquad [2.30]$$

or:

$$\Delta x(k+1) = A_D \Delta x(k) + B_D \Delta u(k) \qquad [2.31]$$

where T is the sampling interval, k refers to the k^{th} sampling instant and A_D and B_D are the state and control transition matrices respectively, given by:

$$A_D = e^{A_L T} \qquad [2.32]$$

$$B_D = \int_o^T e^{A_L (T-\tau)} B_L \, d\tau \qquad [2.33]$$

The transition matrices A_D and B_D relate the states at the $(k+1)^{th}$ sampling instant to the states and controls at the k^{th} sampling instant. They model in discrete-time linearised form the continuous-time real system, and can be calculated as follows:

$$A_D = e^{A_L T} = I + A_L T + \frac{A_L{}^2 T^2}{2!} + \ldots + \frac{A_L{}^n T^n}{n!} + \ldots \qquad [2.34]$$

$$B_o = \int_o^T e^{A_L (T-\tau)} B_L \, d\tau = TB_L + \frac{A_L T^2 B_L}{2!} + \frac{A_L{}^2 T^3 B_L}{3!} + \ldots + \frac{A_L{}^n T^{n+1} B_L}{(n+1)!} + \ldots \qquad [2.35]$$

For stable systems, the above infinite series (Eqns. [2.34-2.35]) usually converge quickly.

The stability criterion of a discrete-time linear system matrix $[A_D]$ is that its eigenvalues be within a unit radius circle, centre the origin.

Linearised discrete-time models are used here to design the turbo-generator digital control scheme, described in Chapter 4.

CHAPTER 3

OPTIMAL LINEAR MODEL ORDER REDUCTION

3.1 INTRODUCTION

Standard methods of reducing the number of state-variables required to model a synchronous machine have been described in the previous Chapter. In eliminating state-variables in a nonlinear model, certain simplifying assumptions are made, and the eliminated variables are accounted for by modifying the remaining state equations. For example, in reducing a twelve-state model to seven variables, stator transients are neglected [eliminating states i_d and i_q], and damper currents [i_{kd}, i_{kq1} i_{kq2}] are removed from the model, and they are accounted for by modifying the damping coefficient k [Section 2.2.3.3-4]. For nonlinear models this remains a good method of approximation. However, new developments in linear systems theory indicate that there are better methods than these for reducing linearised models.

Alternatives to the above method for linear model reduction recently proposed include modal analysis, frequency domain methods and separation of fast from slow time constant subsystems. In power systems theory a method known as coherency is used to analyse when groups of machines swing together and may be replaced by a single equivalent unit in the system model. A reduction method proposed in 1981 by Moore[90] based on measures of controllability and observability has been applied to linearised turbogenerator models by Limebeer[93] and, because of its ability to retain system input-output characteristics with very little error even in much reduced form, it deserves attention here. Fundamental to this

approach to model reduction is the concept of system balancing.

3.2 SYSTEM BALANCING

The original model for the linear system in continuous time is a set of state equations of the form:

$$\dot{x}(t) = Ax(t) + Bu(t),\ x(t_o) = x_o \qquad [3.1]$$

$$y(t) = Cx(t) \qquad [3.2]$$

For a system of n states, r inputs and m outputs x(t) is dimension n, u(t) is dimension r and y(t) is dimension m. For convenience the model is referred to as $(A,B,C)_n$. Throughout the following discussion it will be assumed that $(A,B,C)_n$ is controllable, observable and asymptotically stable.

A simple example by Silverman[99] illustrates the concept of balanced systems. Consider the model:

$$\begin{bmatrix}\dot{x}_1\\ \dot{x}_2\end{bmatrix} = \begin{bmatrix}-1 & 0\\ 0 & -2\end{bmatrix}\begin{bmatrix}x_1\\ x_2\end{bmatrix} + \begin{bmatrix}\varepsilon\\ 1/\varepsilon\end{bmatrix} u \qquad [3.3]$$

$$y = \begin{bmatrix}\frac{1}{\varepsilon} & \varepsilon\end{bmatrix}\begin{bmatrix}x_1\\ x_2\end{bmatrix},\ \varepsilon \ll 1 \qquad [3.4]$$

The system transfer function, $\frac{y(s)}{u(s)}$, is given by:

$$G(s) = C(sI-A)^{-1}B \qquad [3.5]$$

for this system:

$$G(S) = \begin{bmatrix}\frac{1}{\varepsilon} & \varepsilon\end{bmatrix}\begin{bmatrix}s+1 & 0\\ 0 & s+2\end{bmatrix}^{-1}\begin{bmatrix}\varepsilon\\ 1/\varepsilon\end{bmatrix} = \frac{1}{s+1} + \frac{1}{s+2} \qquad [3.6]$$

so that from an input-output point of view, both system state-variables are

equally weighted. It would appear from just looking at the input or B-matrix that the first state is hardly affected by the input, and therefore could be discarded. This would be a mistake, however, since the same state is heavily weighted by $\frac{1}{\varepsilon}$ in the output. Similarly it would be a mistake to discard the x_2 variable due to its apparently small contribution to the input, since the $\frac{1}{\varepsilon}$ gain at the input strongly affects it.

This example is called a badly scaled model. An equivalent model, having the same input-output response with good scaling properties, is:

$$\begin{bmatrix} \dot{z}_1 \\ \dot{z}_2 \end{bmatrix} = \begin{bmatrix} -1 & 0 \\ 0 & -2 \end{bmatrix} \begin{bmatrix} z_1 \\ z_2 \end{bmatrix} + \begin{bmatrix} 1 \\ 1 \end{bmatrix} u \qquad [3.7]$$

$$y = [1 \quad 1] \begin{bmatrix} z_1 \\ z_2 \end{bmatrix} \qquad [3.8]$$

This model is said to be balanced in the sense that inputs and outputs are equally weighted with respect to each state variable.

The model

$$\begin{bmatrix} \dot{x}_1 \\ \dot{x}_2 \end{bmatrix} = \begin{bmatrix} -1 & 0 \\ 0 & -2 \end{bmatrix} \begin{bmatrix} x_1 \\ x_2 \end{bmatrix} + \begin{bmatrix} 1 \\ \varepsilon \end{bmatrix} u \qquad [3.9]$$

$$y = [1 \quad \varepsilon] \begin{bmatrix} x_1 \\ x_2 \end{bmatrix}, \quad \varepsilon \ll 1 \qquad [3.10]$$

is also balanced, and has the transfer function:

$$G(s) = [1 \quad \varepsilon] \begin{bmatrix} s+1 & 0 \\ 0 & s+2 \end{bmatrix}^{-1} \begin{bmatrix} 1 \\ \varepsilon \end{bmatrix} \qquad [3.11]$$

$$= \frac{1}{s+1} + \frac{\varepsilon^2}{s+2} \qquad [3.12]$$

Since it has little effect on input-output properties, the state variable x_2 may be discarded, since it is weakly weighted in the output and weakly

influenced by the input. The model order may thus be reduced to 1, and the balanced representation has given guidance in making the reduction.

3.3 MODEL REDUCTION

3.3.1 Balancing Transformation

Controllability and observability properties of general asymptotically stable linear systems $(A,B,C)_n$ are indicated by the following:

$$P = \int_0^\infty e^{At} BB^T e^{A^T t} dt \qquad [3.13]$$

$$Q = \int_0^\infty e^{A^T t} C^T C e^{At} dt \qquad [3.14]$$

where P is called the controllability Gramian and Q the observability Gramian. They can easily be shown to be the unique positive definite solutions to the following Lyapunov equations:

$$AP + PA^T + BB^T = 0 \qquad [3.15]$$

$$A^T Q + QA + C^T C = 0 \qquad [3.16]$$

The system is said to be "balanced" over the interval $[o,\infty]$ if the controllability and observability Gramians are equal and diagonal. However, for the general asymptotically stable system $(A,B,C)_n$ it is always possible to find a co-ordinate transformation T, which is orthogonal (i.e., $T^T = T^{-1}$] and such that the Gramians become diagonal and equal[99]. Thus:

$$z(t) = T\,x(t), \text{ det. } T \neq 0 \qquad [3.17]$$

$$\text{hence: } \dot{z} = T\dot{x} = TAx + TBu \qquad [3.18]$$

$$= TAT^{-1}z + TBu \qquad [3.19]$$

$$y = Cx = CT^{-1}z \qquad [3.20]$$

The balancing transformation is arranged to give the Gramians the form:

$$\tilde{P} = \tilde{Q} = \Sigma = \text{diag.}\,[\sigma_1, \sigma_2, \sigma_3, \ldots \sigma_n] \qquad [3.21]$$

where: $\sigma_1 \gg \sigma_2 \gg \sigma_3 \gg \ldots \gg \sigma_n \gg 0$ [3.22]

3.3.2 Effect of Balancing on input/output properties

It has been shown[100] that the σ's in equation [3.21] can be regarded as magnitudes relating past inputs to future outputs. For the original system $(A,B,C)_n$, with transfer function G(s) [Eqn. 3.5], input/output properties may be determined from the Hankel-singular-values of G(s), defined as:

$$\sigma_i \left(G(s)\right) := \left(\lambda_i(PQ)\right)^{\frac{1}{2}} \qquad [3.23]$$

where $\lambda_i(\cdot)$ is the i^{th} eigenvalue of the matrix within the brackets.

By substituting the system $(\tilde{A},\tilde{B},\tilde{C})_n$ [Eqns. 3.17-20] into the Lyapunov equations [3.15-16], where:

$$\tilde{A} = TAT^{-1} \quad \tilde{B} = TB \quad \tilde{C} = CT^{-1} \qquad [3.24]$$

It can be verified that:

$$\tilde{P} = TPT^{-1} \qquad [3.25]$$

and:
$$\tilde{Q} = T^{-T}QT^{-1} \qquad [3.26]$$

thus:
$$\tilde{P}\tilde{Q} = TPQT^{-1} \qquad [3.27]$$

but since T is an orthogonal transformation, the eigenvalues of $\tilde{P}\tilde{Q}$ are the same as those of PQ, hence the Hankel-singular-values and input/output properties are unaffected by the balancing transformation.

3.3.3 Truncating balanced realisations

If Σ [Eqn. 3.21] is partitioned as:

$$\Sigma = \left[\begin{array}{c|c} \Sigma_1 & O \\ \hline O & \Sigma_2 \end{array}\right] \qquad [3.28]$$

where Σ_1 is k x k and Σ_2 is (n-k) x (n-k) then the system $(A,B,C)_n$ can be partitioned conformally as follows:

$$A = \left[\begin{array}{c|c} A_{11} & A_{12} \\ \hline A_{21} & A_{22} \end{array}\right] \quad B = \left[\begin{array}{c} B_1 \\ \hline B_2 \end{array}\right] \quad C = \left[C_1 \,|\, C_2\right] \qquad [3.29]$$

If $\sigma_k >> \sigma_{k+1}$ then the truncated system $(A_{11}, B_1, C_1)_k$ represents a "robustly" controllable and observable part of the original system, and input/output properties remain largely unchanged. It can be proved, for example from results on the theory of the inertia of matrices[100], that both the $(A_{11}, B_1, C_1)_k$ and $(A_{22}, B_2, C_2)_{(n-k)}$ subsystems are stable, provided $\sigma_k \neq \sigma_{k+1}$.

3.4 OPTIMALITY OF REDUCED-ORDER BALANCED MODEL REALISATIONS

Early work[90,91,99] on this method of model order reduction did not consider in detail the quality of the approximations in the last section. Glover[100] defined the optimal reduction problem as that of minimising some norm of the error between the full model G(s) and the approximate model $\hat{G}(s)$:

$$E_k(s) = \left\| G(s) - \hat{G}_k(s) \right\| \qquad [3.30]$$

The Hankel-norm was shown to be an appropriate norm to choose for minimisation, giving a good measure of modelling error without excessive computation requirements. The Hankel-norm of G(s) is defined as:

$$\|G(s)\|_H := \bar{\sigma}(\Gamma_G) \qquad [3.31]$$

i.e., it is the largest singular value of the Hankel operator Γ_G [defined in ref. 100] which provides a mapping for continuous-time systems between past inputs and future outputs. It can be shown to be equivalent to:

$$\|G(s)\|_H = \left(\lambda_{max}(PQ)\right)^{\frac{1}{2}} \qquad [3.32]$$

In other words, the Hankel-norm is the largest Hankel-singular-value [Eqn. 3.23].

Another norm, useful for characterising the frequency-response error bounds of an approximate system, is the L∞-norm, defined as:

$$\|G(j\omega)\|_{L^\infty} = \sup_{\omega \in \mathbb{R}} \bar{\sigma}\left(G(j\omega)\right) \qquad]3.33]$$

where $\sup_{\omega \in \mathbb{R}} (\cdot)$ is the supremum [largest magnitude] for all real ω of the largest singular-value of the given function.

The Hankel-norm error of any stable k-state approximate system $\hat{G}_k(s)$ to the full system G(s) has a lower bound given by:

$$\|G(s) - \hat{G}_k(s)\|_H \geq \sigma_{k+1}\left(G(s)\right) \qquad [3.34]$$

Reduced-order models that minimise this error [i.e., are optimal with respect to the Hankel-norm criterion] may be found by considering optimal anti-causal approximations to causal transfer functions. A result of Adamjan, Arov and Krein[134] showed a surprising relationship between the Hankel-singular-values and the transfer function:

$$\sigma_1\left(G(s)\right) := \|G(s)\|_H \leq \|G(j\omega) - F(j\omega)\|_{L^\infty} \qquad [3.36]$$

where: $F \in H^\infty$ [3.36]

In other words, if it is desired to approximate a transfer function $G(j\omega)$ with poles in the left half-plane (casual) by $F(j\omega)$ with its poles in the right half-plane (anti-casual), then the smallest achievable error is the Hankel-norm of G(s). Glover[100] shows how $F(j\omega)$ may be chosen to achieve equality in [3.35]. Thus, by combining [3.34] and [3.35]

$$\left\| G(j\omega) - \hat{G}_k(j\omega) - F(j\omega) \right\|_{L^\infty} \geq \left\| G(s) - \hat{G}_k(s) \right\|_H \geq \sigma_{k+1}\left(G(s)\right) \qquad [3.37]$$

By choosing $\hat{G}_k(s)$ to be a truncated balanced realisation of G(s), and making F(s) an optimal anticausal approximation of $\left(G(s) - \hat{G}_k(s)\right)$, the inequalities of Eqn. [3.37] become equalities [Glover[100], Sections 7-8]. Thus truncated balanced realisations $(\hat{A},\hat{B},\hat{C})_k$ of the system $(A,B,C)_n$ are one class of optimal Hankel-norm approximations to the full order system.

Frequency-response error bounds of the truncated balanced realisations may be found by reducing the order one variable at a time from the full model. Using the theory of all-pass functions [i.e., those where $G(s)\,G^*(s) = I$], the error is shown to be:

$$\left\| G(s) - \hat{G}_k(s) \right\| \leq 2(\sigma_{k+1} + \sigma_{k+2} + \ldots + \sigma_n) \qquad [3.38]$$

where $\hat{G}_k(s)$ is a k^{th} order truncated balanced realisation.

The frequency-response error bound may be reduced by half by constructing an appropriate direct transmission of D-matrix which gives directly coupled input/output components. The Hankel-norm does not depend on D, but it does affect the L^∞- norm of the error since it alters the steady-state component. The D-matrix is not used in model reductions here, however, since it makes solutions of Riccati equations to obtain estimator and controller parameters more complicated.

An optimal reduced-order model of a continuous-time system can be transformed into the discrete-time domain by equations [2.34-5] since the Hankel-singular values of equivalent discrete and continuous time systems are identical[100].

3.5 ALGORITHM TO FIND BALANCED SYSTEM REALISATIONS

Given the original linear system A, B and C matrices, and assuming it is fully controllable, observable and asymptotically stable, a balanced realisation is obtained as follows[111]:

1. The Lyapunov equations [3.15-16] are solved to find P and Q, the controllability and observability Gramians:

$$AP + PA^T + BB^T = 0 \qquad [3.15]$$

$$A^TQ + QA + C^TC = 0 \qquad [3.16]$$

2. A Cholesky factorisation of Q is found:

$$Q = R^TR \qquad [3.39]$$

3. RPR^T is evaluated which will be a positive definite matrix that can be diagonalised as:

$$RPR^T = U\Sigma^2U^T \text{ with } U^TU = I \qquad]3.40]$$

and:

$$\Sigma = \text{diag.}\ (\sigma_1, \sigma_2, \ldots\ldots, \sigma_n) \qquad [3.41]$$

$$\sigma_1 \geqslant \sigma_2 \geqslant \sigma_3 \ldots\ldots \geqslant \sigma_n > \sigma \qquad [3.42]$$

4. Let: $T = \Sigma^{-\frac{1}{2}}U^TR$ [3.43]

The new Gramians are:

$$\tilde{P} = TPT^T = \Sigma^{-\frac{1}{2}} U^T R P R^T U \Sigma^{-\frac{1}{2}} = \Sigma \qquad [3.44]$$

$$\tilde{Q} = T^{-T} Q T^{-1} = \Sigma^{\frac{1}{2}} U^T R^{-T} R^T R R^{-1} U \Sigma^{\frac{1}{2}} = \Sigma \qquad [3.45]$$

5. The co-ordinate transformation on the original A, B and C matrices is performed to obtain the balanced realisation:

$$\left.\begin{aligned} \tilde{A} &= TAT^{-1} \\ \tilde{B} &= TB \\ \tilde{C} &= CT^{-1} \\ Z &= Tx \end{aligned}\right\} \qquad [3.46]$$

The above algorithm has been in use at Cambridge University since 1979, and is now also in use at Imperial College. The following example of the balancing and reduction process applied to a turbine-generator model used the "Cambridge Linear Analysis and Design Programs" software package.

3.6 BALANCING AND REDUCTION PROCESS APPLIED TO A 12-STATE LINEAR GENERATOR MODEL

The twelfth order generator model linearised A and B matrices were obtained by substituting the micromachine parameters [Appendix H.1] into the matrices of Appendix D.2. The model was linearised about the standard operating point in Appendix H.2.1. With rotor angle and field voltage as measurements, the C-matrix is:

$$C = \begin{bmatrix} 1 & 0 & 0 & 0 & 0 & 0 & 0 & 0 & 0 & 0 & 0 & 0 \\ 0 & 0 & 0 & 0 & 0 & 0 & 0 & 0 & 0 & 10 & 0 & 0 \end{bmatrix} \qquad [3.47]$$

It will be noted that the field voltage was multiplied by 10 to give it similar weighting to the rotor angle measurement. This was necessary

because otherwise, as a consequence of the per-unit system adopted, changes in the field voltage would be weakly weighted in the output and input/output information pertaining to it would be lost during the reduction.

The balancing transformation described in [3.5] was carried out, resulting in Hankel-singular-values [diagonal elements of Σ]:

$$\left.\begin{aligned} &\sigma_1 \ldots., \sigma_{12} = 1.96, 0.71, 0.67, 0.14, \\ &0.48.10^{-2}, 0.31.10^{-2}, 0.57.10^{-3}, 0.16.10^{-3}, \\ &0.51.10^{-4}, 0.22.10^{-7}, 0.16.10^{-7}, 0.14.10^{-8} \end{aligned}\right\} \quad [3.48]$$

It can be seen that $\sigma_5 \rightarrow \sigma_{12}$ are small compared to $\sigma_1 \rightarrow \sigma_4$. Therefore an optimal four-state approximate model would have a frequency-response error bound given by [Eqn. 3.38]:

$$\left.\begin{aligned} &\left\| G(j\omega) - \hat{G}_4(j\omega) \right\| \leqslant 2(0.48.10^{-2} + 0.31.10^{-2} + 0.57.10^{-3} \\ &+ 0.16.10^{-3} + 0.16.10^{-3} + 0.51.10^{-4} + 0.22.10^{-7} + 0.16.10^{-7} \\ &+ 0.14.10^{-8} \qquad \leqslant 1.74.10^{-2} \end{aligned}\right\} \quad [3.49]$$

Thus a four-state optimal reduced generator model retaining nearly identical input/output characteristics to the original twelve-state model can be obtained by truncating the balanced realisation to four states. A discrete-time equivalent model for designing the controller can be obtained using Equations [2.34 - 35].

3.7 CONCLUSIONS

A new method of reducing the order of linear system models has been presented. By making a balancing transformation on the original model which does not affect input/output properties, states which only weakly influence controllability and observability may be discarded. Although the states of the reduced model have no physical interpretation, input/output characteristics are optimally retained. An example shows that a twelve-state generator model may be reduced to four states with little frequency-response error. This model is used to design a state estimator and optimal regulator which is theoretically and practically tested in Chapters 4 and 6.

Limebeer[93] has shown in another example of the reduction method applied to linear turbine-generator models that the frequency-response error is an order of magnitude less than in a model reduced to the same order by traditional methods.

Optimally reduced models used to design state estimators and optimal controllers offer considerable savings in on-line computer time and storage requirements, making implementations more cost-effective. Another area of power systems where optimal Hankel-norm reduction methods may be applied is in reducing the dimension of linear multimachine power system models.

CHAPTER 4

APPLICATION OF DISCRETE-TIME OPTIMAL CONTROL AND STATE ESTIMATION THEORY TO TURBINE GENERATOR SIMULATIONS

4.1 INTRODUCTION

Turbine generator optimal control and state estimation theory as presented by Vaahedi, Menelaou and Macdonald[11-15] considers the controller as acting continuously in time. A practical digital control scheme receives and transmits information at discrete instants in time, and only very high sampling rates enable good control when the algorithm has been derived in the continuous time domain. Past practical experience[13-15] has shown that computation speed limits the sampling rate to a level where a discrete-time based controller would be more suitable. The control scheme considered here is shown in Fig. 4.1, with the digital controller interfaced to the plant by sample-and-hold devices.

Here a brief summary of discrete-time optimal control and state estimation theory is presented, together with the application of such a state estimator / optimal controller to computer simulations of turbine generators. Important design considerations are discussed, such as the choice of variables to be sampled from the machine, the order of the model to be used and the selection of weighting matrices.

Discrete-time optimal control and state estimation theory is based on the linearised system equations in discrete time:

$$\left.\begin{aligned} x(k+1) &= Ax(k) + Bu(k) \\ y(k) &= Cx(k) \end{aligned}\right\} \qquad [4.1]$$

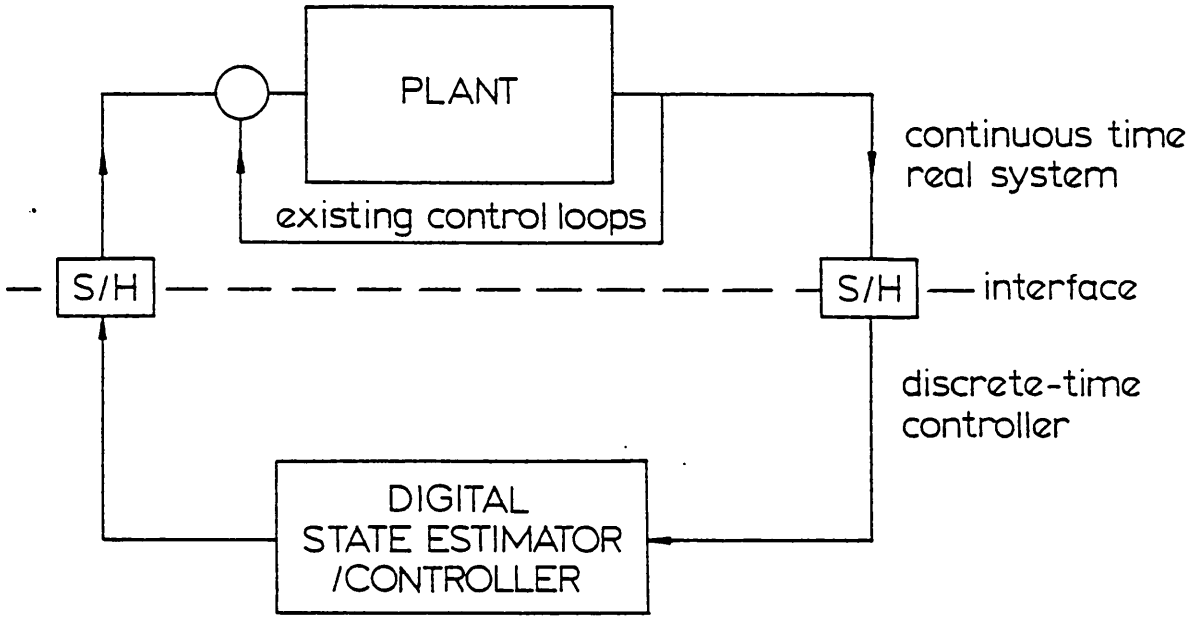

Fig. 4.1: Plant and digital controller

where A(n x n) and B(n x m) are the transition matrices derived from the continuous-time linear system by equations [2.32-33], and C(r x n) is the output matrix, for an n^{th} order system with m inputs and r outputs.

4.2 DISCRETE-TIME OPTIMAL CONTROL

Optimal control theory is concerned with the derivation of control inputs to a system such that its behaviour is optimal with respect to given criteria. In the discrete-time case, the problem may be stated as follows[92]:

Given the system of equations [4.1], find the optimal control $u^{\circ}(k)$ that minimises the quadratic performance index:

$$J_o = \sum_{k=o}^{\infty} \frac{1}{2} \left[x^T(k)\, Q_R\, x(k) + u^T(k) R_R\, u(k)\right] \qquad [4.2]$$

where Q_R is an n x n symmetric positive semi-definite state variable weighting matrix, and R_R is an m x m symmetric positive definite input weighting matrix.

Extension of Pontryagin's minimum principle to the discrete-time case leads to a solution of the form:

$$u^{\circ}(k) = Fx(k) \qquad [4.3]$$

where:

$$F = -[R_R + B^T P_R B]^{-1} B^T P_R A \qquad [4.4]$$

and P_R is the unique positive definite solution to the regulator algebraic discrete-time Riccati equation:

$$A^T P_R A - A^T P_R B[R_R + B^T P_R B]^{-1}\, B^T P_R A + Q_R - P_R = 0 \qquad [4.5]$$

Three methods of solving the Riccati equations have been considered:

a: A recursive method[58,72,92]

b: An eigenvalue-eigenvector method[12,113,114]

c: A method involving real Schur decomposition[115].

Recursive or dynamic programming methods of solution involve an initial positive definite guess of P_R, then repeated back substitution in a recursive form of the Riccati equation until P_R converges to a final value. Methods b: and c: involve the formation of a Simplectic matrix [the discrete-time equivalent of the Hamiltonian], then finding the eigenvalues and eigenvectors [method b:] or making a real Schur decomposition [method c:]. Method c: is the most recent and numerically sound method, but all three were found to give nearly identical results. Full details of the three methods are given in Appendix G.

The class of optimal regulator here is the infinite-time regulator, since the performance index to be optimised extends over an indefinite period [Eqn. 4.2]. This means it is necessary that the system in Eqn. 4.1 be controllable by the application of state feedback. Another requirement is that the pair [A,D] must be completely observable [see 4.4], where D is any n x n matrix satisfying $DD^T = Q_R$. If we choose a positive definite Q_R, we can always find a D which is a square matrix and [A,D] is completely observable for any A.

Vaahedi[12] showed that both governor and/or AVR action give complete controllability of all the system modes in a turbine-generator model and that some modes are better controlled than others by the two control inputs. For example, the stator transient fluxes Ψ_d and Ψ_q have relatively low controllability, but rotor angle and its rate of change were shown to be

more strongly controllable. Some variables are better controlled by one loop than the other; an obvious example is that field quantities are better controlled by inputs to the voltage regulator loop than the governor loop. Thus the best overall control is achieved by the use of both feedback loops.

4.3 CHOICE OF REGULATOR WEIGHTING MATRICES

The objectives when attempting to improve the response following a fault in the power system are firstly a reduction in the first load angle excursion and improving the damping of subsequent rotor swings. Secondly, it is desirable for the terminal voltage to recover quickly to near its pre-fault value without a large overshoot or excessive oscillations.

The optimal regulator state-variable weighting matrix Q_R is a diagonal matrix whose elements reflect the relative importance of reducing fluctuations of individual state variables from the steady-state. Its choice is completely arbitrary, although as noted in Chapter 1, Yu and Moussa[64] suggested a method which involves selecting elements of Q_R such that the dominant eigenvalues of the system with state feedback applied are shifted as far to the left as possible. However, since limits on controls are not accounted for, this method often results in excessive gains.

The control variable weighting matrix R_R reflects the penalty on the variations in the control inputs. The ratio of Q_R/R_R is important, as it determines the gain of the controller. It must be high enough for the controller to give a useful improvement in stability, but not so high that inordinately large control input variations are demanded for small disturbances. In practical terms the latter case could mean the operational life

of valves etc., is shortened due to excessive fluctuations in setting.

A trial-and-error method of performing nonlinear simulations and making adjustments in the weighting matrices to give the best response was used here with the following guidelines taken into account:

(a) Starting with both Q_R and R_R as matrices with equal elements, the ratio Q_R/R_R is adjusted until the most satisfactory response is obtained.

(b) Individual weights in Q_R are then adjusted. Weighting of speed gives an overdamped angle and poor voltage recovery, so generally this element has to be kept small. Increased weighting of load angle improves the response; the other state variables seem to give best results when approximately equally weighted.

(c) The control weighting matrix Q_R elements are individually adjusted to ensure best results without an excessive degree of saturation or control variable fluctuation in either feedback loop.

For the optimal Hankel-norm reduced order models, the state variables are not directly related to individual physical generator quantities. With these models, starting as in (a) above and making trial-and-error adjustments to their state-variables was found to give very good results.

4.4 DISCRETE-TIME STATE ESTIMATION

A discrete-time optimal regulator as described in the previous two sections

requires values of all the system state variables at each sampling instant. Even if direct measurement of all of them were feasible from a cost point of view, inaccuracy, time lags and the noise picked up in the transducers and their interconnections would all degrade such a controller in a practical environment. It would not be possible to use a regulator derived from an optimal Hankel-norm reduced order model in this way since the states would not be physically measurable at all. Output controllers[61,63] using transformations to relate measurements to the states overcome these problems to some extent but sensitivity to noise remains a problem, and theoretically output controllers are always inferior to those with all states available, particularly if important states are weakly observable in the outputs.

The dynamic state estimator, or Kalman-Bucy filter[76], appears to be a successful way of overcoming the above drawbacks, and has been studied theoretically in continuous-time application to generator control by Vaahedi[11 12]. By measuring a small number of convenient signals, the filter makes estimates of all the system state variables. The state estimator is designed to give good estimates in the presence of noise.

In the discrete-time derivation of the state estimator the system equations [4.1] are rewritten to include white noise w(k) [dimension n]:

$$x(k + 1) = A\,x\,(k) + Bu(k) + w(k) \qquad [4.6]$$

The filter has to extract the system information from a noisy measurement vector y:

$$y(k) = Cx(k) + v(k) \qquad [4.7]$$

where v(k) is the measurement noise vector of order r, and is assumed to be

uncorrelated with w(k) [i.e., the two noise processes are assumed to be independent]. Further, it is assumed that all the noise is white Gaussian. The problem[112] is how to obtain $\bar{x}(k)$, the "best" linear estimate of x(k). By "best", it is meant that estimators which minimise the mean-square error of each signal component simultaneously are required. Thus, in the filtering process, each mean-square error:

$$E[x_\alpha(k) - \bar{x}_\alpha(k)]^2 \; \alpha = 1, 2, \ldots n \qquad [4.8]$$

is to be minimised.

Equation [4.8] leads to what is defined as the error covariance matrix P(k):

$$P(k) = E[e(k)e^T(k)] \qquad [4.9]$$

where:

$$e(k) = x(k) - \bar{x}(k) \qquad [4.10]$$

Kalman's work[76] led to a solution of the optimal estimation problem, in the discrete-time case a recursive digital filter:

$$\bar{x}(k) = A\bar{x}(k-1) + Bu(k-1) + K(k)\left(y(k-1) - C\bar{x}(k-1)\right) \qquad [4.11]$$

where K(k) may be calculated by the discrete-time filter recursive Riccati equation.

$$K(k) = AP_1(k)C^T[CP_1(k)C^T + R_F]^{-1} \qquad [4.12]$$

where:

$$P_1(k) = AP(k-1)A^T + Q_F(k-1) \qquad [4.13]$$

The error covariance matrix is given by:

$$P(k) = P_1(k) - K(k)CP_1(k) \qquad [4.14]$$

$Q_F(k)$ is the positive semidefinite system noise covariance matrix, order

n x n:

$$Q_F(k) = E[w(k)w^T(k)] \qquad [4.15]$$

$R_F(k)$ is the positive semidefinite measurement noise covariance matrix, dimension r x r:

$$R_F(k) = E[v(k)\ v^T(k)] \qquad [4.16]$$

If, as has been assumed, there is no correlation between noise processes, off-diagonal terms of Q_F and R_F are zero.

For time-invariant systems, substitution of $P_1(k) = P_1(k+1) = P_F$ as $k \to \infty$ in Equations [4.12-14] gives the algebraic Riccati equation:

$$AP_FA^T - AP_FC^T[R_F + CP_FC^T]^{-1}CP_FA^T + Q_F - P_F = 0 \qquad [4.17]$$

and the filter gain K [also called the Kalman gain] is:

$$K = AP_FC^T[R_F + CP_FC^T]^{-1} \qquad [4.18]$$

The filter equation with constant gain K becomes:

$$\bar{x}(k) = A\bar{x}(k-1) + Bu(k-1) + K\Big(y(k-1) - C\bar{x}(k-1)\Big) \qquad [4.19]$$

Note that the equation contains a mathematical model of the plant and a tracking term $K\Big(y(k-1) - C\bar{x}(k-1)\Big)$. In practical applications the model is always, to a greater or lesser extent, an approximation of the actual situation in the plant; here there are linearised, discrete-time models in several different degrees of approximation to the real system. However, the tracking term ensures that even with these and other errors an acceptable estimate may be obtained, as has been shown by Vaahedi[11,12] for the continuous time case and is later shown here for the discrete-time case.

Also note that the filter estimates the states at time k, given system information at time k-1. Thus, as well as filtering the measurements, it is predicting the system states at the next time step. For this reason the type of filter used here is sometimes called a Kalman predictor, to distinguish it from filters obtaining $\bar{x}(k)$ from measurements $y(k)$.

The success of applying a Kalman filter depends on whether or not the system is completely observable, that is whether it is possible to determine from the measured outputs what the behaviour of the states is. This can be checked by verifying that the rank of the matrix:

$$\begin{bmatrix} C \\ CA \\ CA^2 \\ \cdot \\ \cdot \\ \cdot \\ CA^{n-1} \end{bmatrix} \qquad [4.20]$$

equals the system order n. Alternatively the eigenvalue-eigenvector method appearing in Vaahedi[11] gives a quantitative evaluation of the observability of states through various outputs.

4.5 CHOICE OF FILTER COVARIANCE MATRICES

The Kalman filter noise covariance matrices Q_F and R_F are chosen so as to provide a compromise between speed of reconstructing a good estimate and immunity to noise. At the design stage there is often little idea in advance of the noise variances associated with individual states and measurements. The procedure is therefore similar to the choice of optimal regulator weighting matrices, starting with arbitrary choices of Q_F and R_F, then tuning so as to give best results both in nonlinear simulations and on-line.

4.6 DESCRIPTION OF THE CONTROL ALGORITHM

Closing the loop, so that the state estimates are fed back into the plant inputs via the optimal feedback matrix, results in a system shown schematically in Fig. 4.2. The on-line controller predicts the estimated plant state vector $\bar{x}(k+1)$, gives the inputs $y(k)$ at time k, then uses these estimates to determine the inputs to control the plant. Since:

$$u(k) = F\bar{x}(k) \qquad [4.21]$$

a reduced equivalent form of the system in Fig. 4.2 may be found, shown in Fig. 4.3, with the following equations for the controller:

$$\begin{aligned} \bar{x}(k+1) &= (A - BF - KC)\,\bar{x}(k) + Ky(k) \\ u(k+1) &= F\bar{x}(k+1) \end{aligned} \qquad [4.22]$$

For simplicity the state and measurement noise processes are not shown in Figs. 4.2 and 4.3, but may be considered as implicit in the plant. In control systems parlance this type of controller based on feedback of state estimates is called a Linear-Quadratic-Gaussian [LQG] controller.

The control algorithm based on this method that may be programmed on a micro-computer is as follows:

At time $t = kT$

1. Read in $y(k)$ from plant;
2. Calculate:

$$\bar{x}(k+1) = z(k) + Ky(k) \qquad [4.23]$$

3. Calculate:

$$u(k+1) = F\bar{x}(k+1) \qquad [4.24]$$

4. Feed back $u(k+1)$ to the plant
5. Calculate $z(k+1) = (A - BF - KC)\,\bar{x}(k+1)$ [4.25]

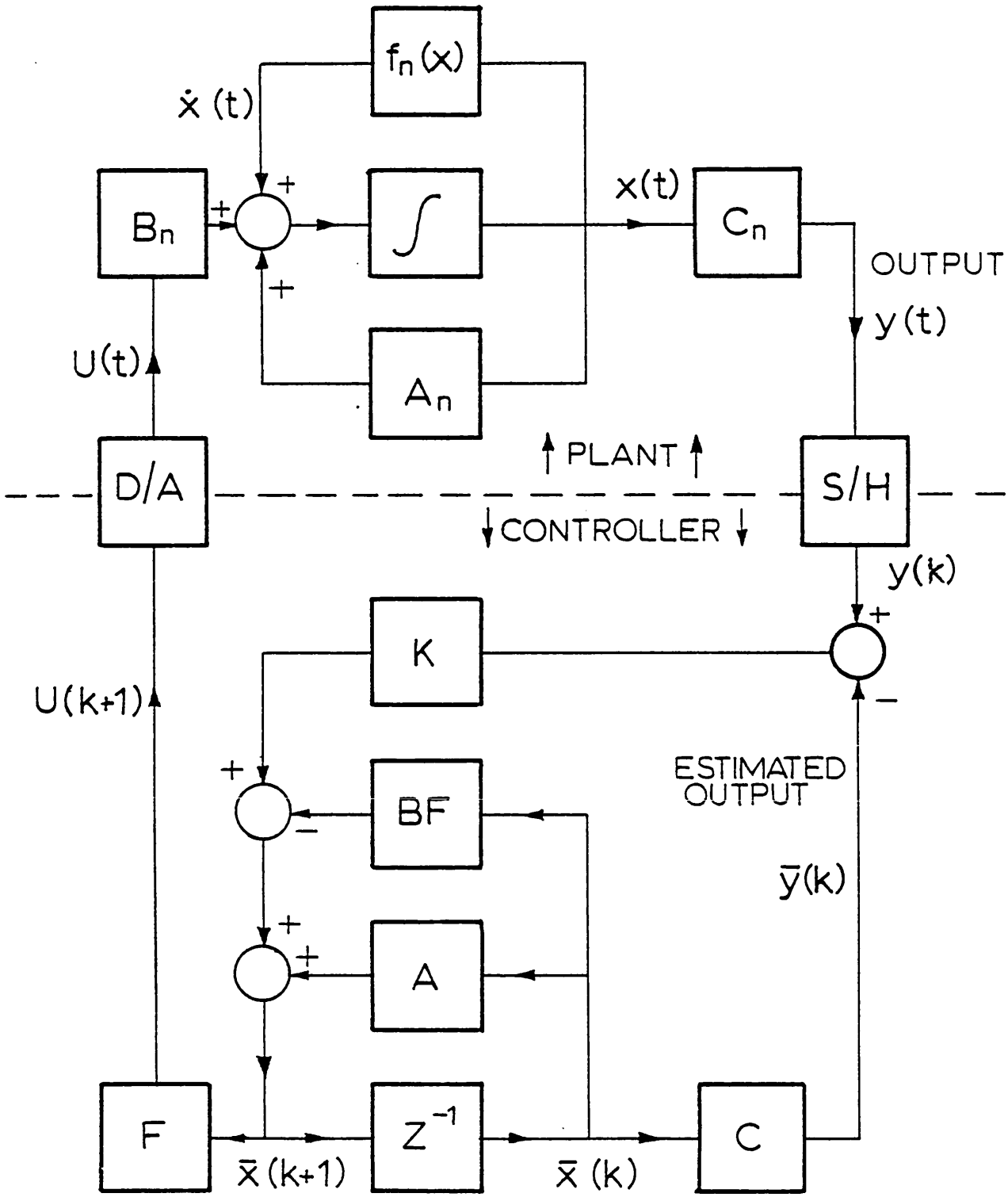

Fig. 4.2: Schematic of the control algorithm

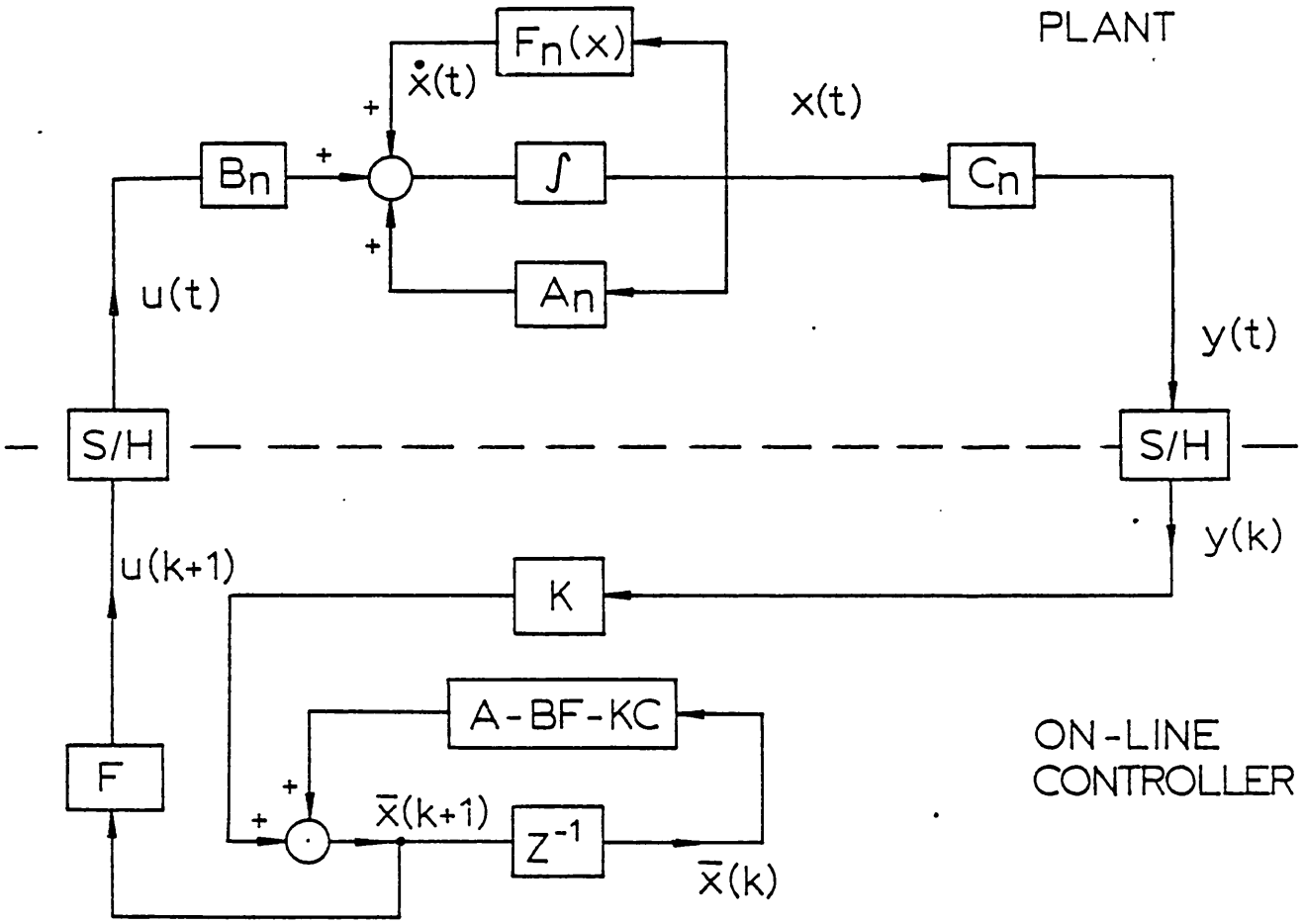

Fig. 4.3: Reduced equivalent of Fig. 4.2

At time t = (k+1)T 6. Repeat process from Step 1, with k = k+1.

This arrangement of the algorithm makes the control input u(k+1) available as rapidly as possible following the measurements taken at time kT, thus minimising delays in response. z(k+1) is then calculated in readiness for the next time step.

4.7 CONTROLLER DESIGN PROCEDURE

4.7.1 Parameters

The state estimator-optimal controller described in the preceding sections is based on the implicit assumption that a model of the system is known. This is an alternative philosophy to that of self-tuning controllers which mostly make no assumptions about the system model and perform on-line system identification. Therefore the first step in designing a generator LQG controller is to obtain the machine and system parameters. Turbine generator manufacturers perform calculations at the machine design stage, and practical tests are carried out in the factory and on site from which the relevant parameters may be determined. Using the techniques described in Chapter 2, linearised discrete-time A and B matrices may then be obtained to model the system.

4.7.2 Choice of measurements from the generator

A very important design decision is in the choice of output measurements to sample from the generator for the controller, which determine the output or C matrix. The number of measurements to be taken is also significant: Using a small number of signals

means the reliability of individual transducers matters more than with many samples, but the latter case will prove more expensive. The method of triplex redundancy[7], whereby three independent transducers and controllers perform the same task and are then "majority-voted" to check that they are all acting in the same way would improve the reliability of this type of control system.

Below is a list of the possible generator quantities which may be used [in any combination] as a basis for the state estimation and control, giving the advantages and disadvantages of each with this application in mind.

a] Load angle to the infinite busbar δ:

Advantages:- a state-variable shown to give a good contribution to optimal control[12].

Disadvantages:- it is a difficult variable to measure in a real system. Shaft position and remote busbar information is needed and there is the problem of deciding which part of the system may be considered as infinite.

b] Load angle to the machine terminals δ_t:

Advantages:- more easily measured than the above since no remote system information is needed.

Disadvantages:- only local information on the generator is given in δ_t. It is not a state-variable, therefore a linearised output or C matrix is needed, resulting in greater estimation errors. During the fault the terminal voltage of the machine collapses to nearly zero, so the terminal load angle may be indeterminate until the fault is removed.

c] Rate of change of load angle $\dot{\delta}$:

Advantages:- a state-variable shown by Vaahedi[12] to have very high modal observability indices, and giving the greatest contribution to optimal control of all the state-variables.

Disadvantages:- small changes in speed with reference to rated speed need to be measured, so high accuracy is needed. When used as a feedback signal for power system stabilisers, speed has led to torsional oscillations[35], so a method of overcoming these difficulties must be found if speed is to be used.

d] Terminal voltage V_t, current i_t, power P_t and reactive power Q_t:

Advantages:- all these quantities are easily measured using fast analogue or digital transducers near the machine terminals. Power feedback has not led to any shaft torsional oscillations in the operational experience of power system stabilisers so far, and so it is particularly favoured by utilities seeking advanced supplementary controllers.

Disadvantages:- none of them can be used as state-variables except in models which are linearised transformations of the models in Chapter 2. Here a linearised C-matrix will be needed and, ideally during transient disturbances, a new C-matrix is desirable for every change in the external system. This may lead to far greater errors in estimation than if original state-variables are used as measurements.

e] Field voltage V_f, current i_f and exciter voltage V_e:

Advantages:- practical measurement is straightforward except in rotating diode systems. They are all state-variables giving good observability of the electrical behaviour of the generator.

Disadvantages:- they do not give good information on the machine's

mechanical behaviour. A rapid transducer response is necessary to follow changes in field or exciter voltage during transients. When ceiling voltage levels are reached, state estimation errors may occur since the theory does not take account of limit-type nonlinearities [hard constraints].

f] Valve position A_p:

Advantages:- information on input power to the machine is obtained. Valve position transducers are already installed in many power stations for monitoring purposes and hence it is a readily available state-variable.

Disadvantages:- the valve position-steam flow characteristic is highly nonlinear and, again, there are position limits, both of which will degrade the estimation and control process.

g] Terminal frequency:

Advantages:- a recently suggested potentially useful input signal when transmission lines are long, as it reflects the influence of both machine and busbar effects.

Disadvantages:- accurate measurement of small deviations from the nominal frequency is difficult with standard zero-crossing detection methods due to noise. A linearised transformation is also necessary to relate terminal frequency to the system model state-variables.

h] Other variables - fluxes and mechanical torque:

Advantages:- State-variables used in the original model so no linearised output matrices are needed.

Disadvantages:- impractical to measure, and not the best variables to measure for controllability and observability of the system[12].

For the initial theoretical and practical tests it was decided to use load angle to the infinite busbar and field voltage as measurements. Load angle is a variable frequently used in results to indicate how effectively a controller is working, and since it is to be measured for this purpose it may also be used as an input to the controller. Field voltage supplements this with electrical information on the behaviour of the machine.

Other variables considered for the controller here are rate of change of load angle, terminal power, terminal voltage and valve position.

4.7.3 Estimator and Controller Design

The system A, B and C matrices determined in 4.7.1 and 4.7.2 are combined with initial choices of the regulator and filter weighting matrices P_R, Q_R, P_F and Q_F. The Riccati equations [4.5 and 4.17] are solved and the regulator and filter gain matrices F and K can be determined from Eqns. [4.4 and 4.18]. The estimator and controller may be tested separately with nonlinear simulations to ensure good estimation and control, the weighting matrices being altered as described in Sections 4.3 and 4.5 to give best results. With initial choices of weighting matrices similar to those of Vaahedi[15], good results were obtained with minor alterations.

Finally, the complete state estimator-optimal control algorithm is derived as described in Section 4.6, with A-BF-KC precalculated.

4.8 SIMULATIONS OF THE GENERATOR PERFORMANCE WITH AND WITHOUT SUPPLEMENTARY CONTROL

4.8.1 Comparison of micromachine and 660 MW generator simulations

An illustration of how faithful a model of 660 MW machine performance may be expected from the micromachine system can be made by comparing simulations using both sets of parameters from Appendix H for the same prefault power, reactive power, external conditions and fault duration. Fig. 4.4 shows the responses of both simulations for the prefault steady-state conditions [also in Appendix H] corresponding to

$P = -0.8$, $Q = 0.0$ and $V_t = 1.0$ pu.

The three-phase fault duration is 100 ms and the post-fault impedance is the same as before the fault [i.e., the faulted line is reclosed successfully after fault removal]. Hereafter we shall refer to this type and duration of fault under the above conditions as "standard".

Since the mutual reactances X_{md} and X_{mq} are different in the two sets of parameters, the steady-state load angles are about two degrees apart. After subtracting the steady-state difference in angle, the first swing is about two degrees more for the micromachine simulation, and subsequent damping is better for the 660 MW machine simultation. The natural oscillation frequency is very similar in both cases, as are the terminal and field voltage responses. Thus it would appear that, if the parameters are approximately correct, the micromachine should give a reasonably good, possibly slightly pessimistic, prediction of the transient performance of the full size machine.

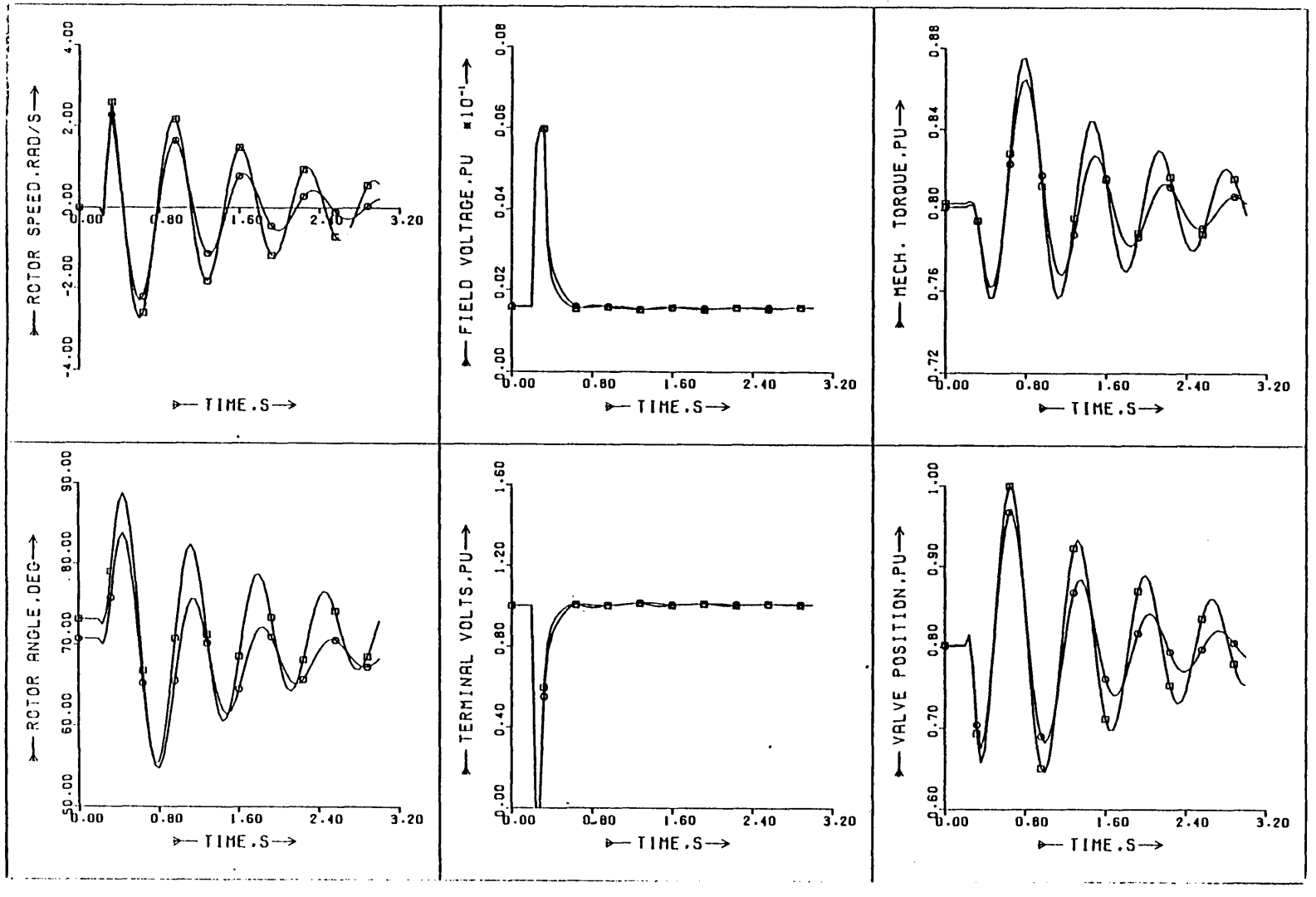

Fig. 4.4: Comparison of responses of o - 660 MW generator and □ - micromachine computer simulations.

4.8.2 Simulated response with a 12^{th} order controller measuring load angle to the busbar and field voltage

An estimator and controller were designed, as described in 4.7.3, using a 12^{th} order linearised model and a transition matrix time step of 10 ms. Sampled quantities from the simulated plant are load angle to the infinite busbar and field voltage. With the same pre-fault steady-state conditions and fault duration as in the previous Section, the response of the micromachine computer simulation with and without supplementary control is shown in Fig. 4.5. Calculation time delay is accounted for by not making the supplementary governor and AVR control signals available until just before the next sample is taken, i.e., after 10 ms of simulation time. A further 10 ms delay has been added to account for the expected time delay of the transducers themselves. This is shown to be a realistic figure in Chapter 5.

The response is well damped, the machine settling back to steady-state within 1.5 seconds of the fault. Voltage recovery does not suffer either, and it can be seen that almost immediately the fault is detected via the two measured signals, the supplementary signals help to limit the first swing by reducing the governor setting and increasing the AVR setting, reducing the 17° swing by about 1°. It is easily verified that state estimation gives almost as good a response as with direct state feedback, as has been done by Vaahedi[12].

4.8.3 Effect of varying the controller calculation time

Simulations were carried out to find a maximum limit to the controller time step, beyond which no improvement in machine

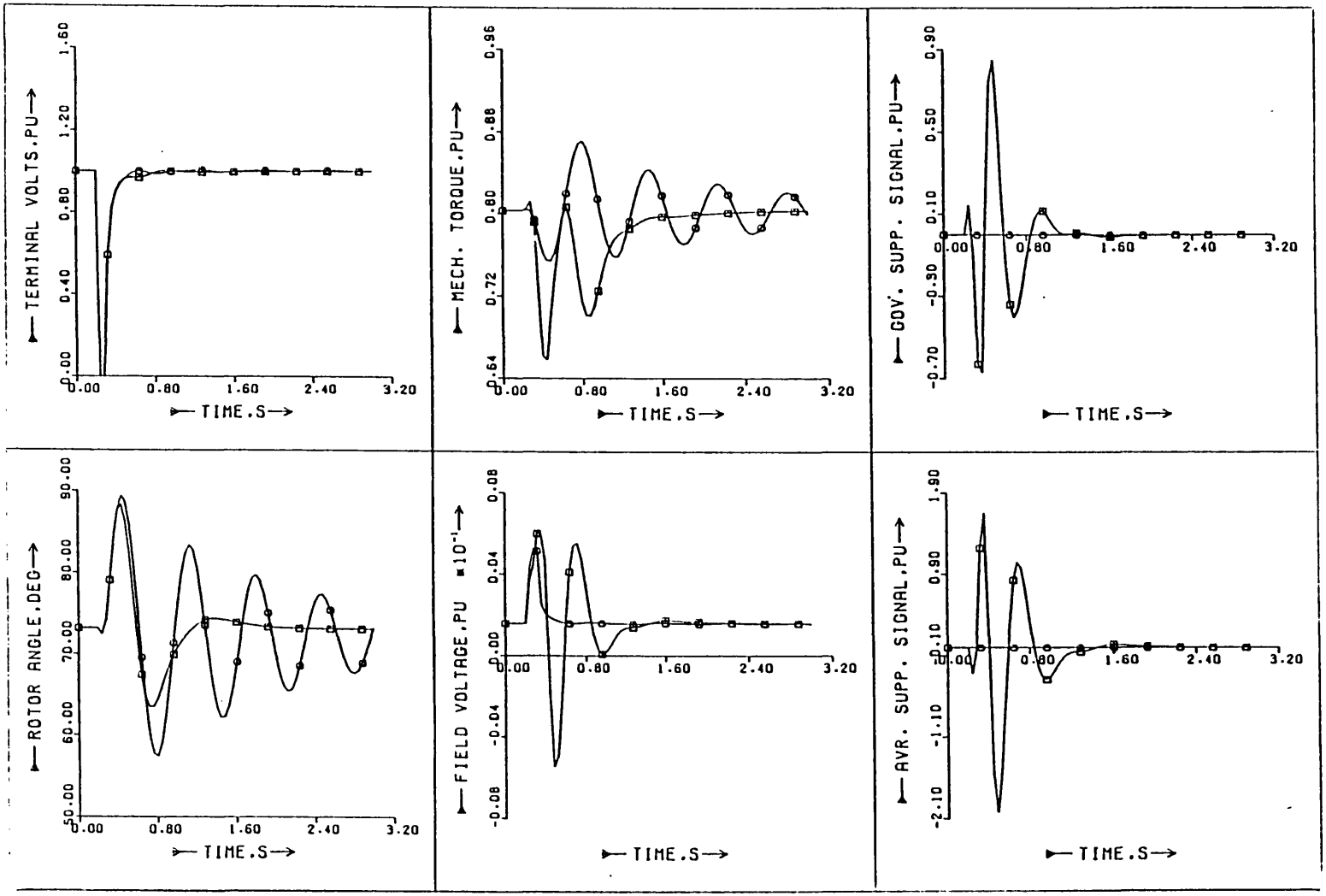

Fig. 4.5: Response of micromachine simulation to a 100 ms 3-phase short-circuit □ - with a 12th order controller measuring load angle and field voltage o - without supplementary control

performance can be expected, and also whether very small time steps improve the response even more than in the previous Section. Figure 4.6 shows the rotor angle responses of the micromachine simulation with a varying time step in the controller, for the standard 100 ms fault and operating conditions. As the time step is increased up to 85 ms, damping is slightly reduced and the first swing reduction is lost, but the response is still significantly improved. Above this threshold, the controller starts to adversely affect stability. In the 95 ms example, the system conditions change so much between taking samples and applying controls that the inputs have a detrimental effect on the system stability.

It will also be observed by comparing Fig. 4.6b with Fig. 4.5 that very little further improvement in response is gained by reducing the transition matrix time step from 10 ms to 2 ms.

4.8.4 Major and Minor System Disturbances

It is important that the controller does not just perform well for one type of disturbance, but that it also improves the response for less severe and much more severe faults. Figure 4.7 shows the predicted micromachine performance following the loss of one transmission line, reconnected after 50 milliseconds. The first rotor swing is reduced and oscillations are much better damped in load angle and terminal voltage when a 12^{th} order controller is applied. The gains and controller used are identical to those in Section 4.8.2.

A 270 ms three-phase fault was found to nearly drive the system

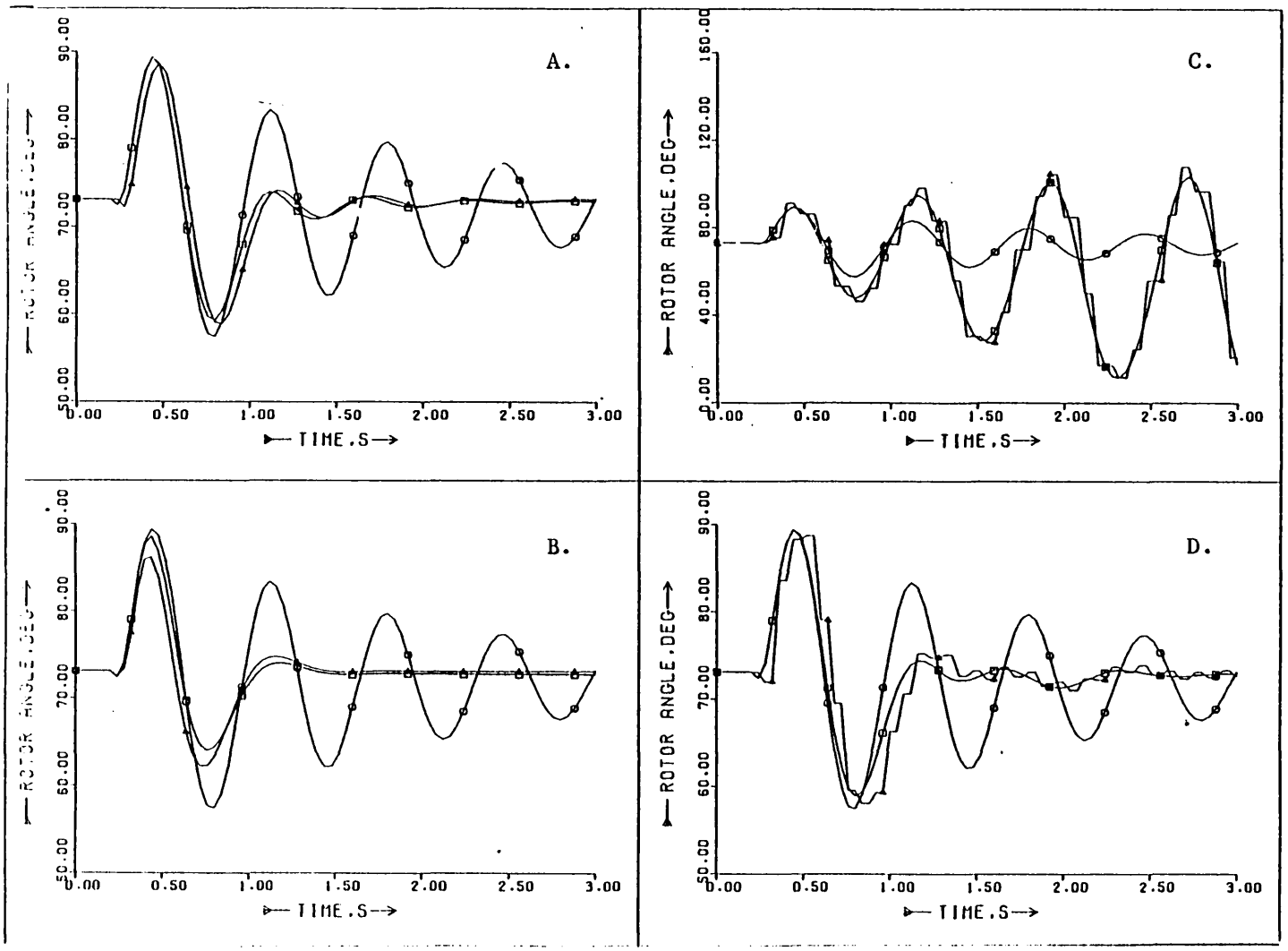

Fig. 4.6: Effect of varying the controller calculation time for a 100 ms short-circuit. Controller time step A: 20 ms, B: 2 ms; C: 95 ms; D: 85 ms. □ - with supplementary control; o - without supplementary control; Δ - estimated angle.

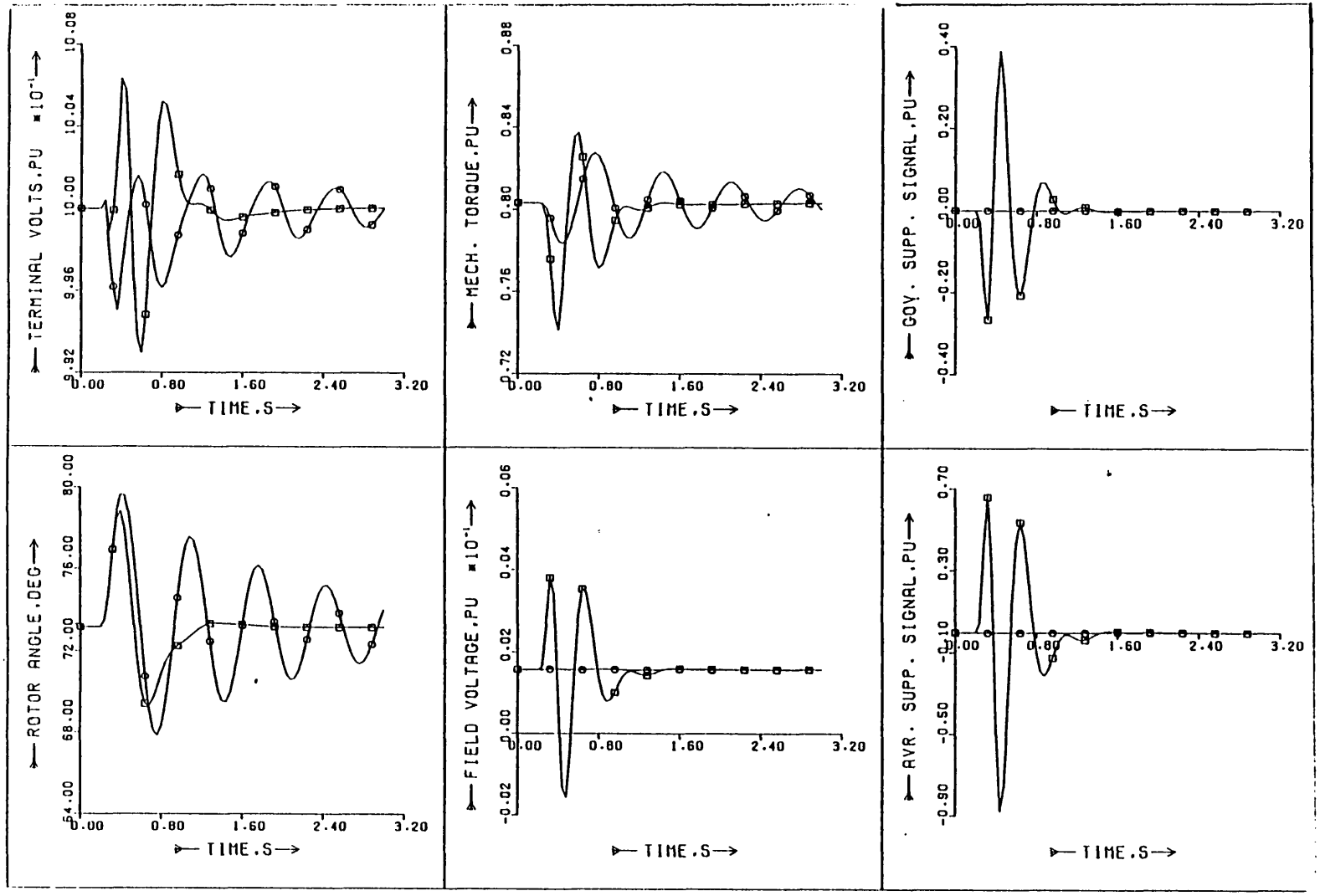

Fig. 4.7: Controller as in Fig. 4.5. Response to the loss of one transmission line for 50 ms □ - with and o - without supplementary control.

unstable in simulations [Fig. 4.8]. Application of the same 12th order controller as in the previous tests gives a much better voltage recovery and a first-swing reduction of about 20°. Application of a 275 ms fault caused the system without supplementary control to pole-slip, whereas with control the machine remained stable.

A three-phase fault followed by the loss of one transmission line is more likely to be encountered in this country, where fast reclosing circuit-breakers are not used. A 100 ms fault of this type is simulated in Fig. 4.9, and once again the controller clearly gives a much improved response. Note that the controller attempts to restore the angle to its pre-fault value; with washout filtering of the input signals [see Chapter 6] the controller will enable smooth settling to any required post-fault operating point as determined by the governor and AVR settings.

4.8.5 Comparison of controllers based on different order models

Fig. 4.10 shows a comparison of four different order controllers acting on the micromachine simulation, all designed with load angle and field voltage as measurements, and all with the same sampling time interval of 10 ms. The fault is 100 ms duration with full reclosure and the standard operating conditions of Section 4.8.1.

From the figure it can be seen that the twelfth order state estimator/optimal controller gives the best response. The ninth and optimally reduced fourth order controllers give very similar responses, both better than that of the seventh order controller where the angle is less well-damped. This confirms that the

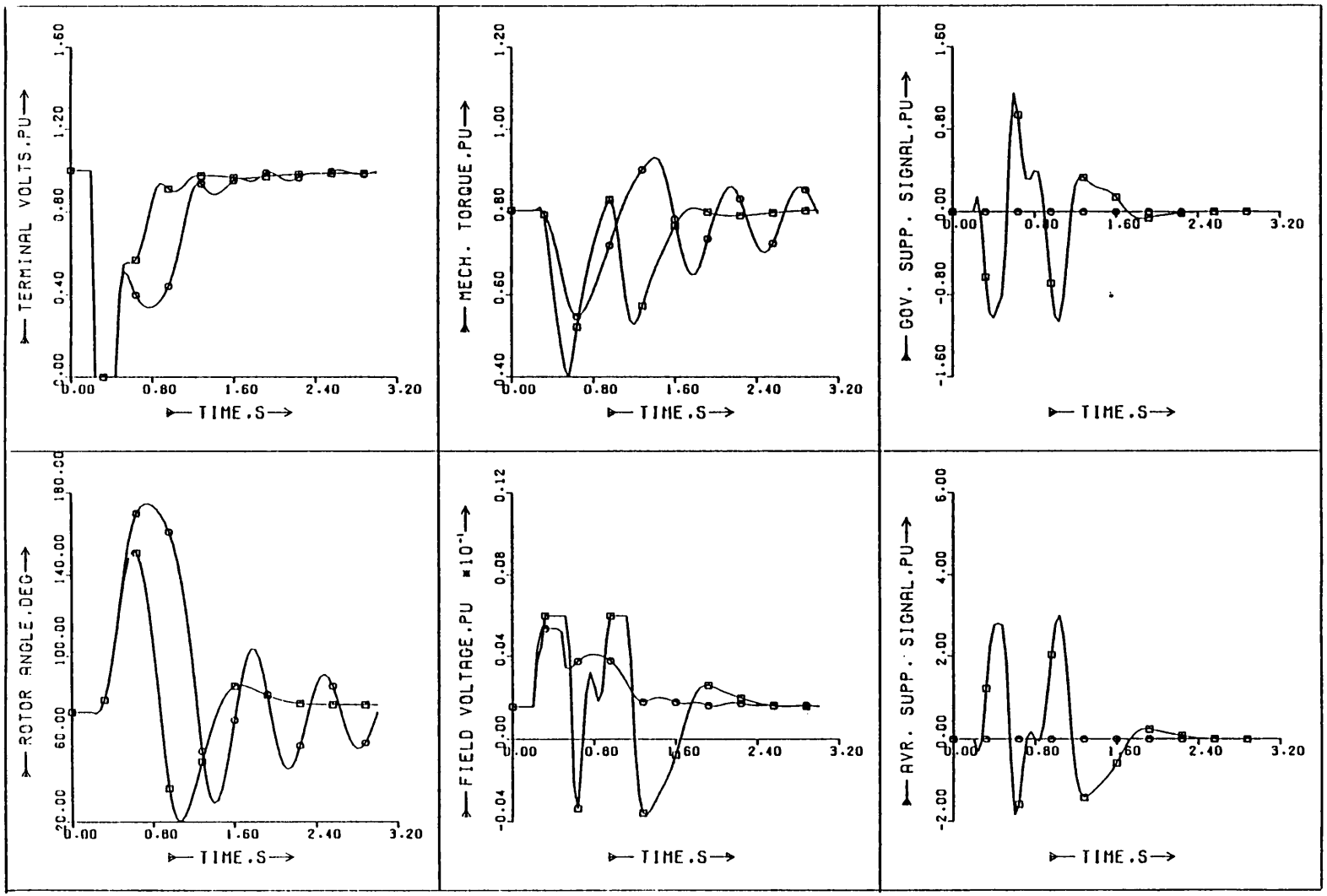

Fig. 4.8: 12th order controller as in Fig. 4.5. Response to a 270 ms 3-phase fault □ - with o - without supplementary control.

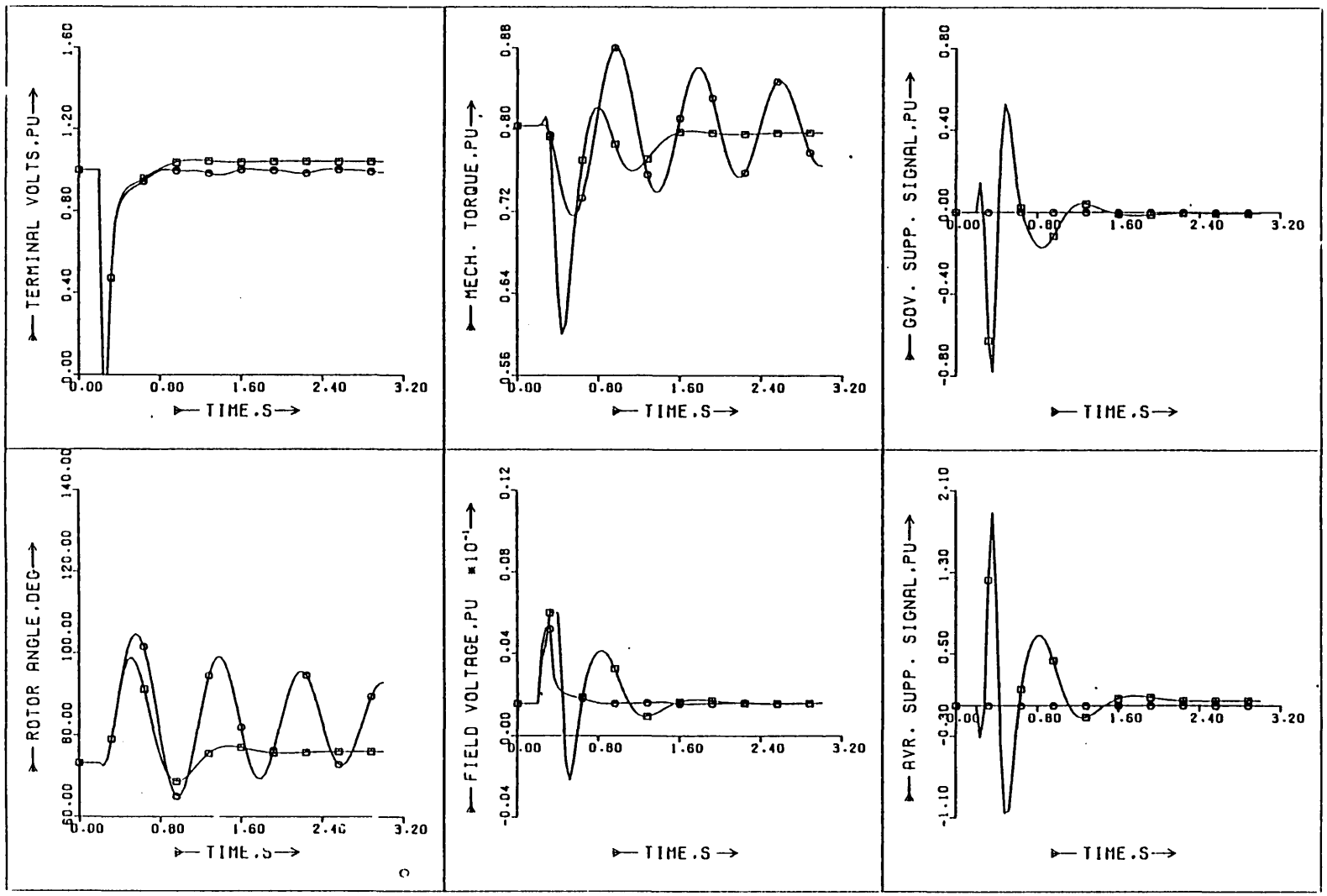

Fig. 4.9: 12th order controller as in Fig. 4.5. Response to a 100 ms 3-phase fault followed by the loss of one transmission line □ - with o - without supplementary control

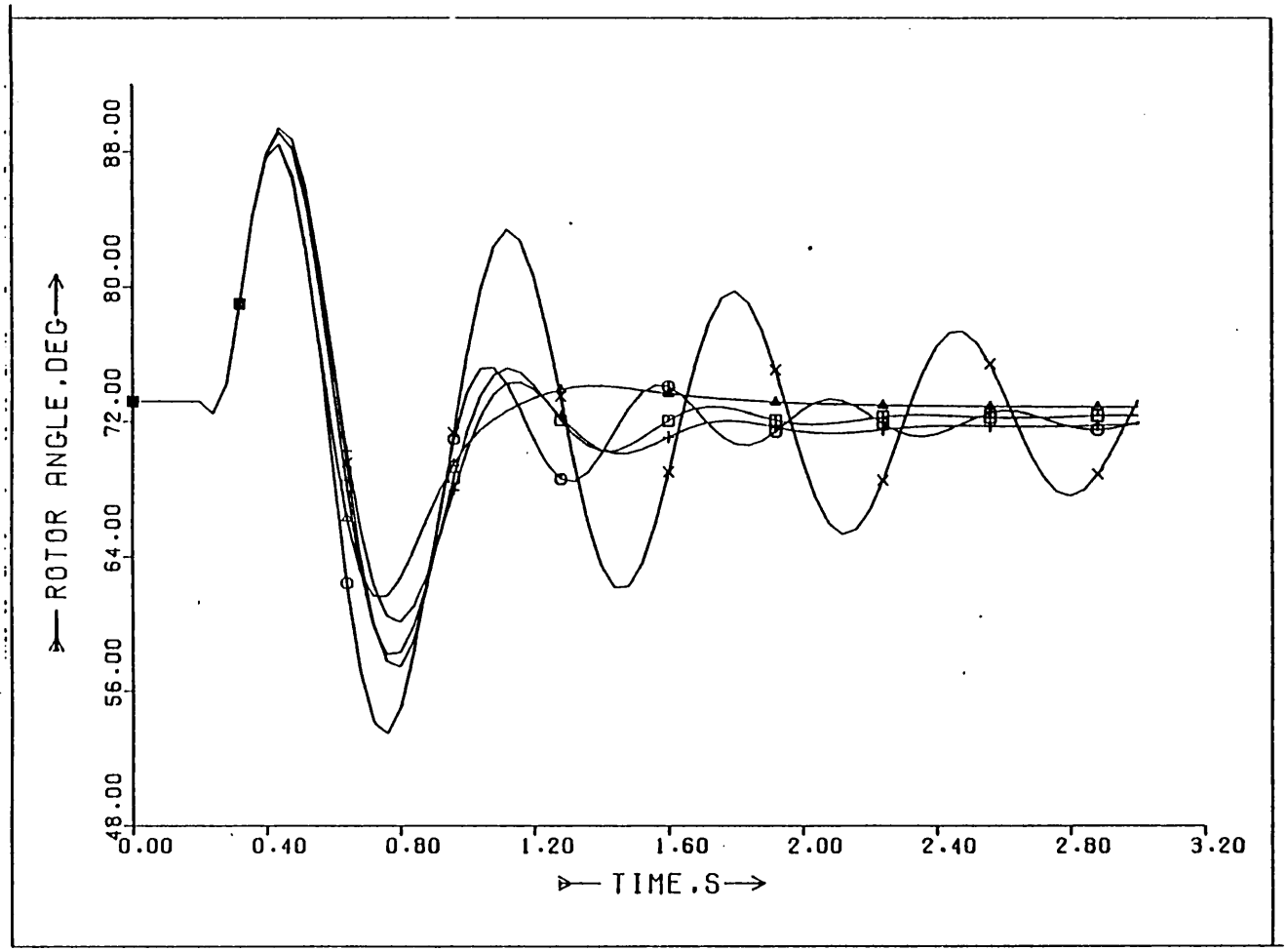

Fig.4.10: Comparison of simulated angle responses to a standard 100 ms fault for controllers measuring load angle and field voltage. △ - 12th order; □ - 9th order; o - 7th order; + - optimally reduced 4th order; X - no supplementary control.

optimal Hankel-norm reduction method has retained more essential information in the linear generator model than conventional methods of reduction.

4.8.6 Controllers designed for different mesurements

So far only controllers measuring load angle to the infinite busbar and field voltage have been considered in the simulations. However, controllers measuring other state variables may easily be designed simply by changing the unity elements in the output or C matrix to match the state-variable which is to be measured. If the controller is to measure quantities which are not state variables then the C matrix needs to contain linearised terms to express the measurement in terms of the state-variables. Measurements which require this are voltage, current, power, VAr and load angle at the machine terminals. Linearised terms for the terminal voltage which may be used in the output matrix are the same as those derived in Appendix D. Output matrices when other variables are measured are derived in Appendix I.

4.8.6.1 RATE OF CHANGE OF LOAD ANGLE AND FIELD VOLTAGE

The simulated results of replacing load angle to the infinite busbar with its rate of change as a measurement for a 12^{th} order controller are shown in Fig. 4.11, where a standard 100 ms fault [see 4.8.1] is applied. Control is even better than when load angle itself is measured, with better first swing reduction and virtually no second backswing. This agrees with Vaahedi's results which indicated that speed gives good system modal observability and makes a major contribution to optimal control[12]. However, as outlined in 4.7.2a, speed is considered to be an undesirable feedback signal

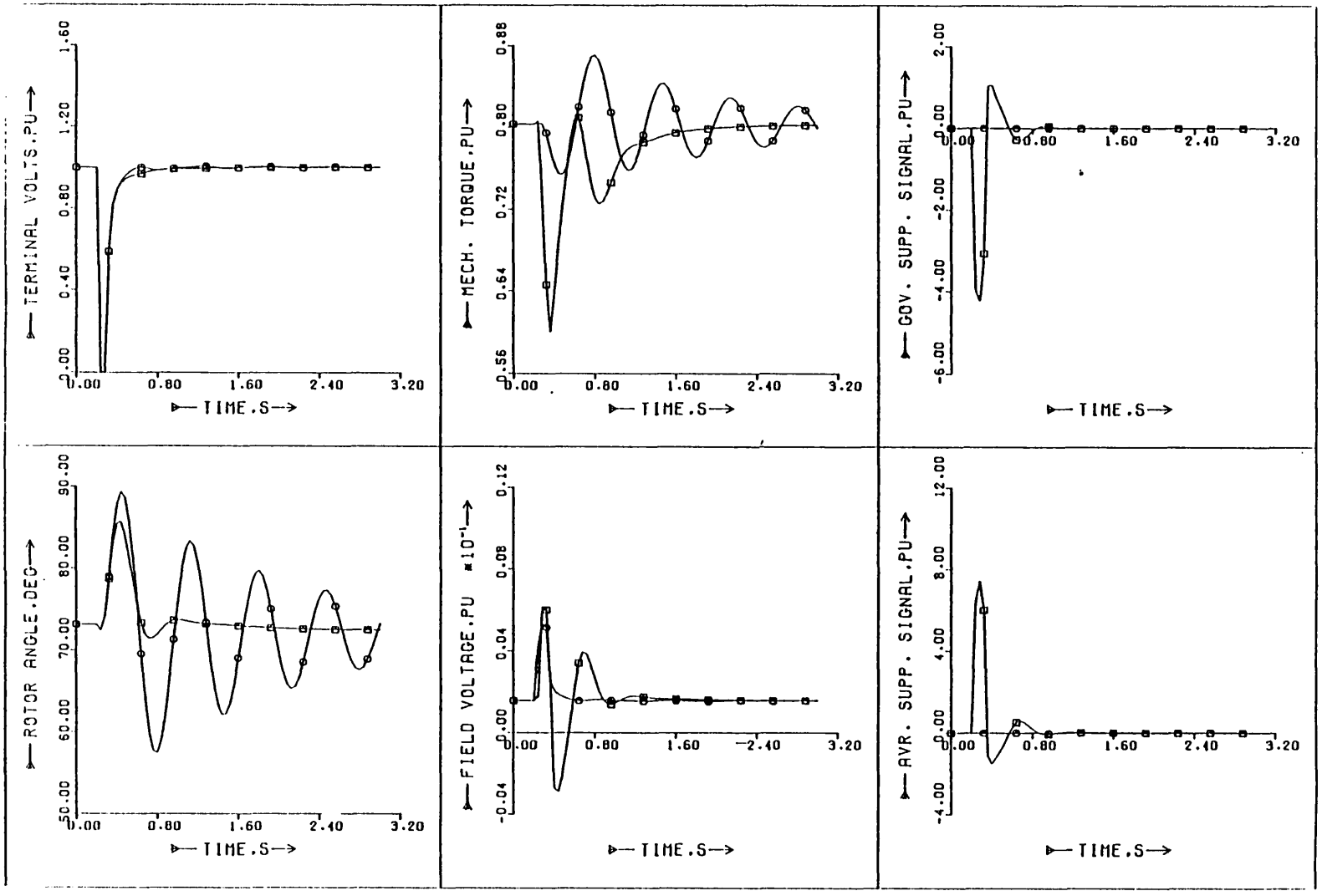

Fig. 4.11: Response of micromachine simulation to a standard 100 ms three-phase fault □ - with o - without a 12th order controller measuring rate of change of load angle and field voltage.

because of the torsional oscillations it has caused in the past. The good theoretical results obtained here suggest that it would be worthwhile using speed as a measurement for the estimator and controller if a satisfactory method of overcoming the drawbacks can be found.

4.8.6.2 TERMINAL POWER AND FIELD VOLTAGE

Fig. 4.12 shows the response to a standard 100 ms fault when terminal power and field voltage are used as input signals to a 7^{th} order controller. The first load angle swing is considerably reduced, but damping is not as good as with the measurements considered previously. The linearised terms in the output matrix mean greater errors in estimation when the machine is away from the design operating point, especially during the fault itself when the terminal power temporarily falls to nearly zero. This has the beneficial result of reducing the first swing but very little improvement is made to the subsequent backswing. However, the machine settles to steady conditions 2 secs. after the fault, which is a considerable improvement over conventional control loops only.

4.8.6.3 TERMINAL POWER AND TERMINAL VOLTAGE

These signals, both readily measurable in a real system, give the response in Fig. 4.13 when used as inputs to a 12^{th} order controller, with 100 ms fault duration and the standard conditions (P = -0.8, Q = 0.0). A good reduction in first swing amplitude is obtained, although the following negative swing is not reduced. This is probably due to similar reasons as in the previous simulation. Damping is not as good as with the previous controller, although still resulting in substantially better performance than with conventional control loops.

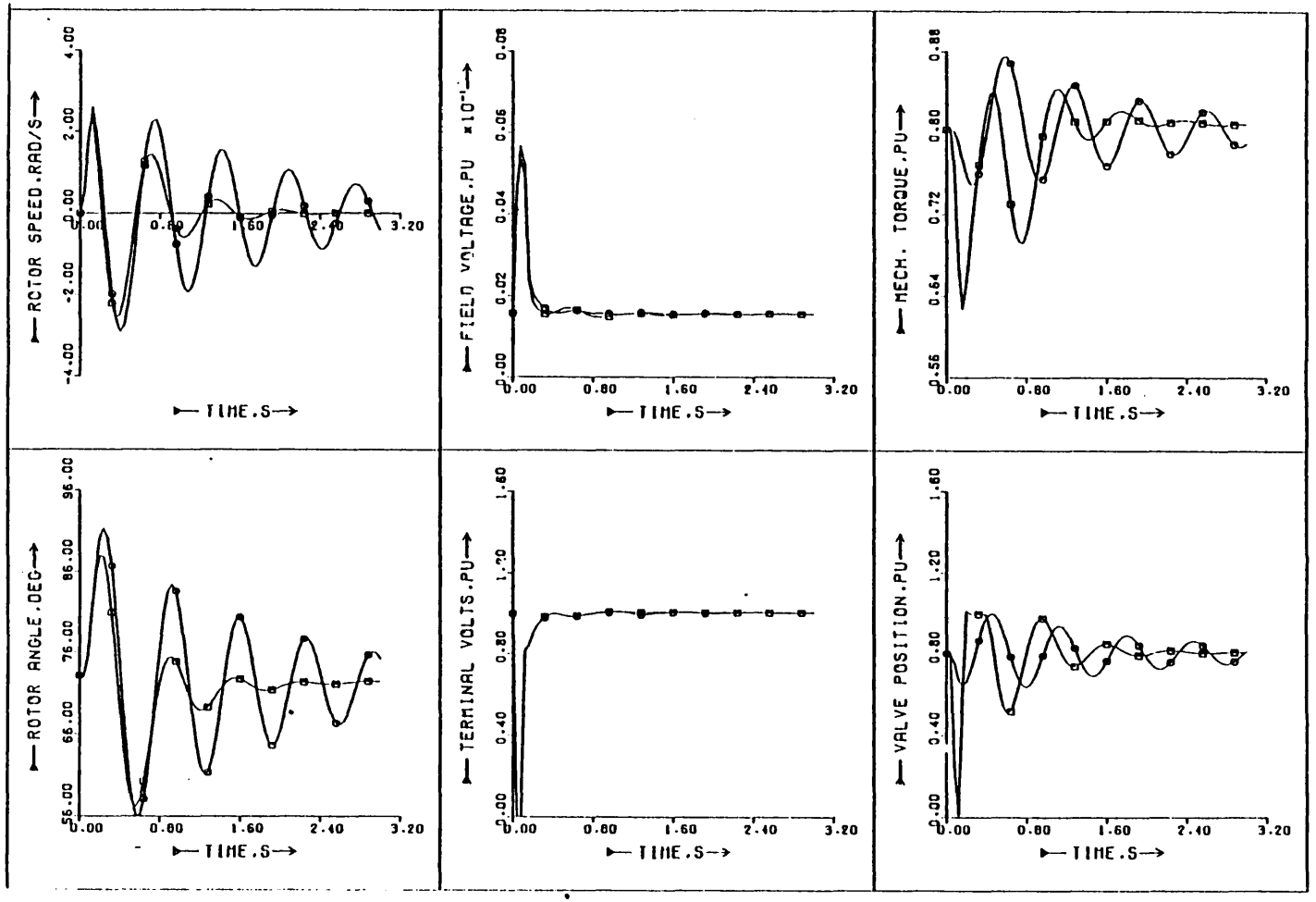

Fig. 4.12: Response to a standard 100 ms fault □ - with a 7th order controller measuring terminal power and field voltage; o - without supplementary control.

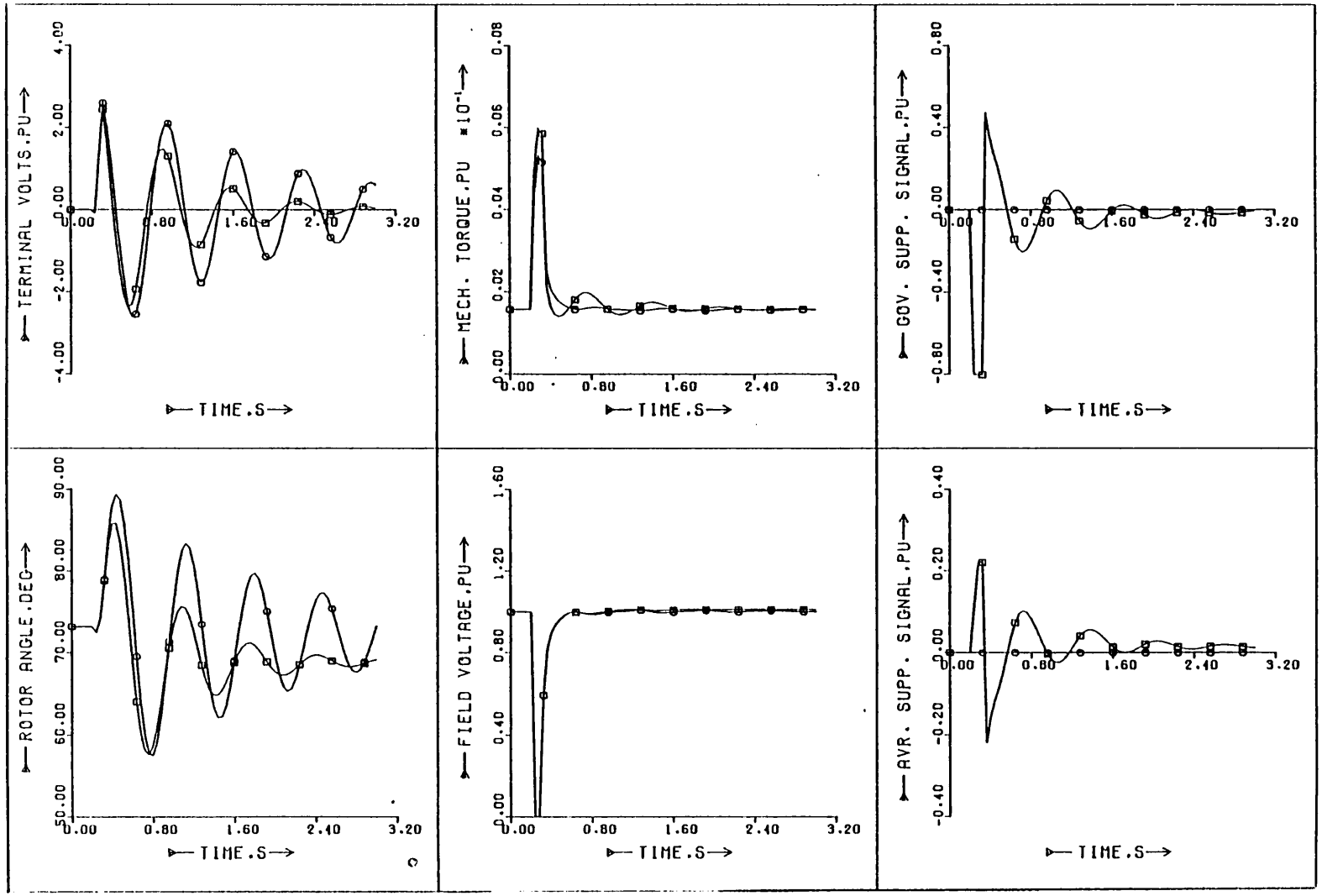

Fig. 4.13: Response to a standard 100 ms fault □ - with a 12th order controller measuring terminal power and terminal voltage; o - without supplementary control.

4.8.6.4 VALVE POSITION AND FIELD VOLTAGE

Fig. 4.14 shows the response of the system with a 9^{th} order controller to a standard fault, with valve position and field voltage as the measurements. A similar response to the previous two controllers is obtained despite both measurements being state-variables. Thus it appears that these are not the best state-variables to use, agreeing with Vaahedi's results indicating that valve position does not give particularly good contribution to optimal control compared with other states.

4.8.6.5 LOAD ANGLE AND FIELD VOLTAGE - SUPPLEMENTARY SIGNAL TO THE AVR ONLY

As stated in Chapter 1, many older machines have rather slow-responding mechanical-hydraulic governors to which supplementary signals may not readily be added. Thus in some cases it is desirable to have controllers providing a supplementary signal to the voltage regulator only.

The behaviour of such a controller acting on the machine subjected to a standard 100 ms fault is shown in Fig. 4.15, with load angle and field voltage the sampled variables. Although the reduction in the first swing is very small [as would be expected without prime-mover control], damping is almost as good as with both supplementary signals, and better than that obtained with the controllers in Sections 4.8.6.2 - 4.8.6.4.

4.8.6.6 TERMINAL POWER AND TERMINAL VOLTAGE - SUPPLEMENTARY SIGNAL TO THE AVR ONLY

In Fig. 4.16 the response of the machine to a standard fault is shown, the controller, measuring power and terminal voltage, giving a

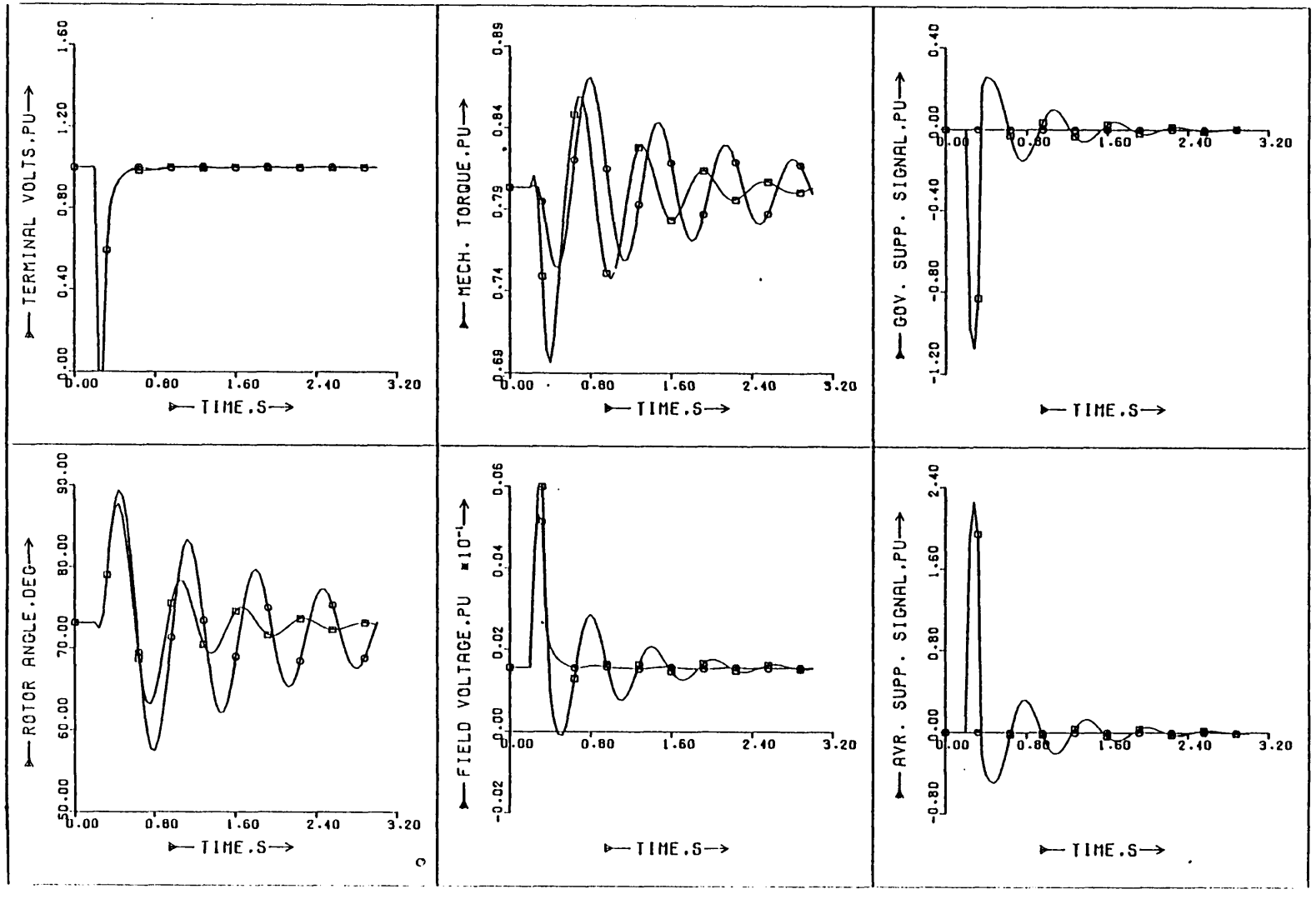

Fig. 4.14: Response to a standard 100 ms fault □ - with a 9th order controller measuring valve position and field voltage; o - without supplementary control.

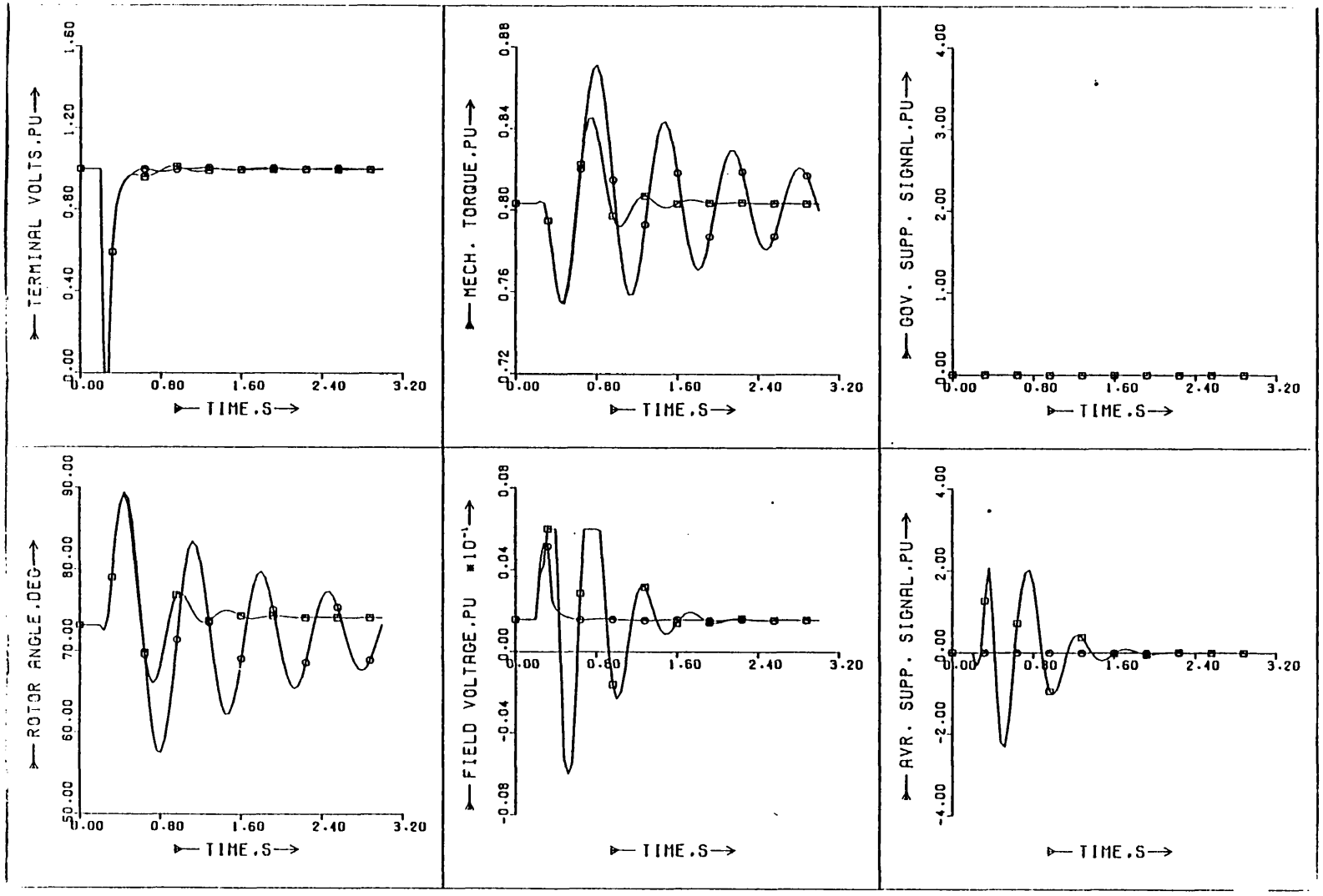

Fig. 4.15: Response to a standard 100 ms fault □ - with a 12th order controller measuring load angle and field voltage giving a supplementary signal to the AVR only o - without supplementary control.

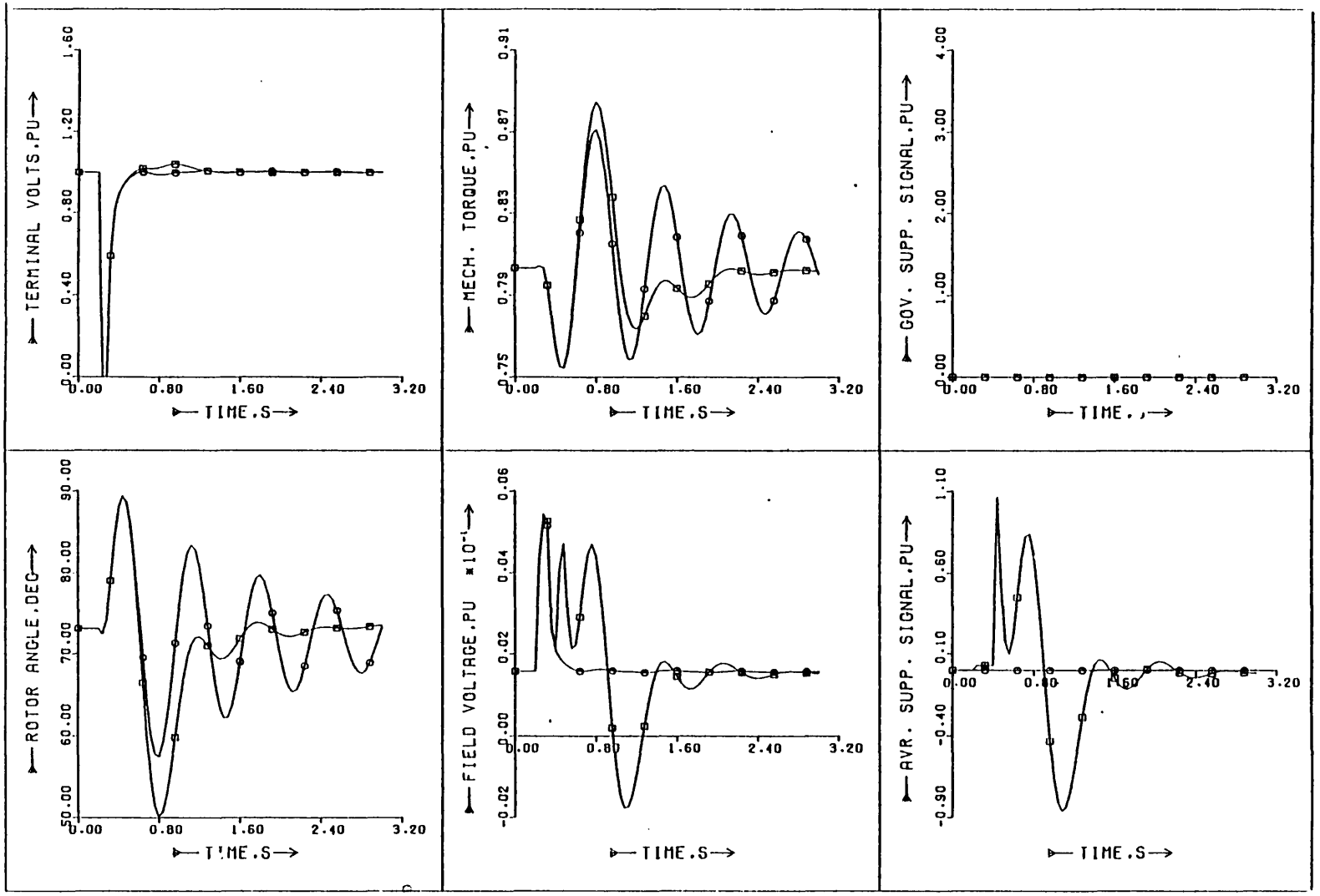

Fig. 4.16: Response to a standard 100 ms fault □ - with a 12th order AVR-only controller measuring terminal power and terminal voltage, o - without supplementary control.

supplementary signal to the AVR only. Estimation errors during and after the fault lead to a worsened second backswing, but subsequently damping is quite good, indicating the controller may work well for small-signal disturbances.

4.8.7 Robustness of the controller at different operating points

To test the effectiveness of a controller designed from a system linearised at one operating point under different operating conditions, studies were carried out using a 12^{th} order controller, as in 4.8.2, designed for the operating point P = -0.8, Q = 0.0 at six other operating points, as shown in Fig. 4.17.

For five of the six other operating points, plots A-D and F, the response is improved considerably. For plot E, however, corresponding to P = -0.3, Q = -0.7 the response is not improved. The initial large backswing [occurring due to the low power and high reactive power] is unchanged and the subsequent forward swing is increased by the controller. Thus it may be concluded that fixed-gain controllers of this type are effective over a range of leading and lagging power factors, provided the machine is not operating at considerably different real power outputs from the design operating point.

4.9 CONCLUSIONS

Discrete-time optimal control and state estimation theory is more suited to practical on-line computer controllers for generators than its continuous-time equivalent, due to the time steps involved. The optimal regulator

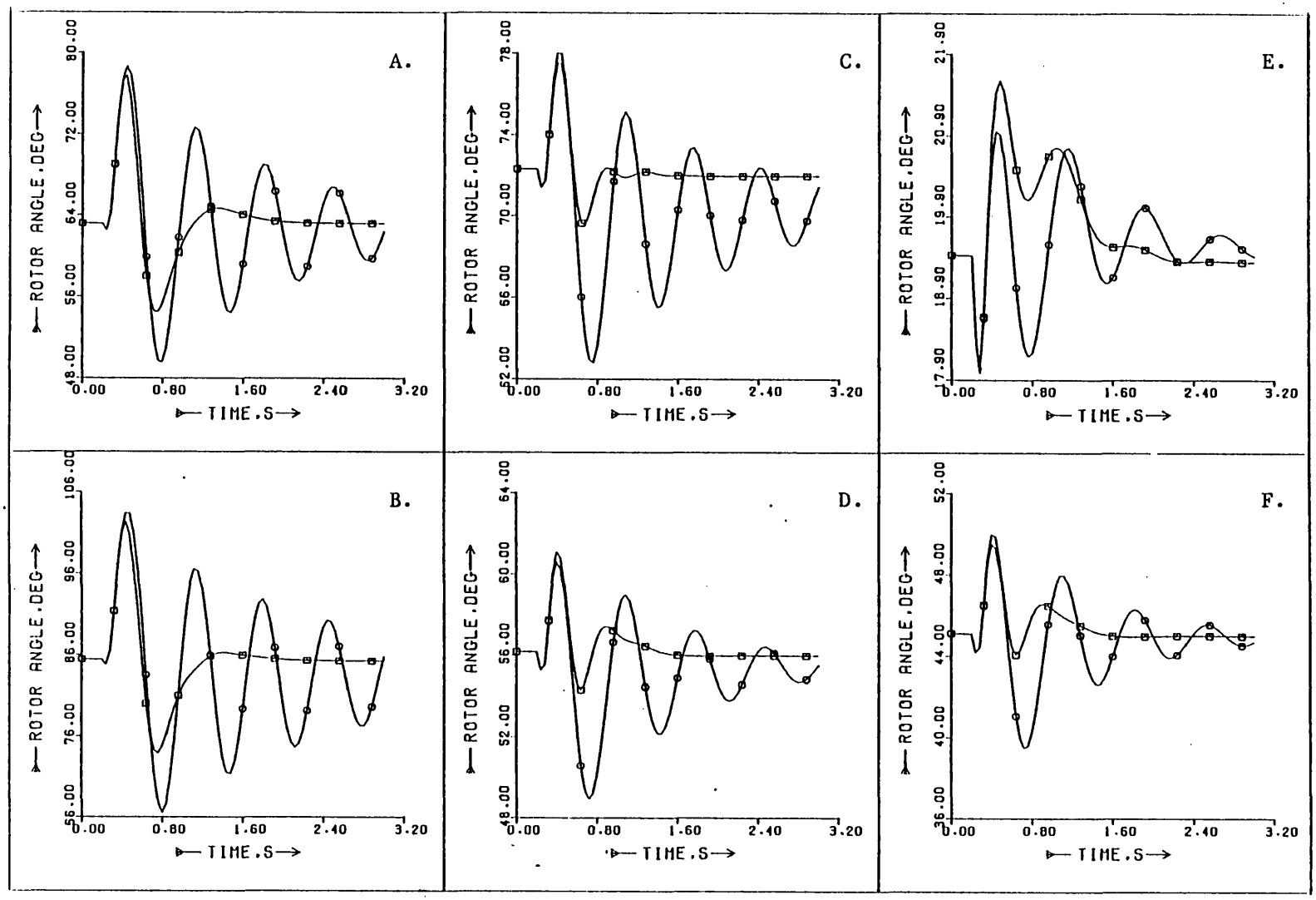

Fig. 4.17: Response of machine simulation □ - with a 12th order cotroller measuring load angle and field voltage o - without supplementary control at operating points:- A: P=-0.8,Q=-0.2; B: P=-0.8,Q=+0.2; C: P=-0.5, Q=0.2; D: P=-0.5,Q=+0.0, E: P=-0.3,Q=-0.7; F: P=-0.5,Q=-0.2.

based on minimisation of a linear quadratic performance index and the Kalman filter, minimising the least-square error of estimated states in the presence of Gaussian white noise, are both problems which can be solved by Riccati equations. Linear gains result for the regulator and filter, which depend on arbitrary choices of weighting matrices best selected by a trial-and-error method.

Specific application of the theory to turbine generator control requires a knowledge of the power system model and parameters, and measurements have to be chosen which are practical to measure, yet also give good information on the whole system. The choice of model order is also important, as higher order models may result in excessive calculation time delays in the controller. The algorithm itself involves a fairly straightforward sequence of matrix multiplications to derive the supplementary control signals. Another advantage of discrete-time controllers of this type over continuous-time controllers is that they apply controls derived from estimates which are predictions of the states at the next time step, rather than estimates of the states at the time of measurement.

Comparison of computer simulations using the micromachine parameters and the 660 MW machine parameters reveals that the behaviour of the two in response to transient disturbances is reasonably close, the main difference being in the damping of rotor oscillations which is slightly worse in the micromachine. A 12^{th} order controller measuring load angle and field voltage gives an improved response to transient disturbances of varying severity, with reduced first swing, good damping in the angle and voltage oscillations and quicker voltage recovery. The response is improved even with controller time steps of up to 85 ms.

A comparison of controllers based on different order models was also made, indicating that an optimally reduced fourth order controller gives results almost as good as the full 12^{th} order controller. 9^{th} and 7^{th} order controllers also give very good, though progressively slightly less well damped responses as the order is reduced.

Alternatives to load angle and field voltage as controller measurements were considered, with rate of change of load angle and field voltage giving the best results of all. Terminal power and field voltage give reasonable results, but not as good a response as with the previous two controllers due to the estimation process giving misleading information during and just after the fault. Controllers based on terminal power and terminal voltage, or valve position and field voltage all give similar results to the power/field voltage controller.

When the supplementary signal is to the AVR only, a possible modification for older plant, damping is still very good but little reduction in the first swing is gained when rotor angle and field voltage are measured. Using the more practical signals of terminal power and terminal voltage in an AVR-only controller seems to give good small-signal stability, but little improvement in the first positive and negative transient swings, in fact worsening the latter slightly.

Finally, robustness studies at different operating points to that used for the controller linearisation revealed that the controller operates successfully at leading and lagging operating points a substantial distance away from the design point, provided the real power setting is not considerably different from the original one.

CHAPTER 5

THE LABORATORY POWER SYSTEM MODEL

5.1 INTRODUCTION

A convenient intermediate step between proving any new computer control scheme theoretically on computer simulations of turbine generators and implementing it on full-size machines is to test it on a micromachine in the laboratory. This will give an insight into the practical difficulties, for example due to noise, transducers and time lags, that may be encountered in an industrial environment, and will require the control algorithm to execute in real time on the on-line computer. Provided the micromachine can be shown to give a realistic scaled-down simulation, this will give more confidence of success and valuable information with regards to a full-size implementation of the control.

The laboratory power system model consists of a 3 kVA micro-alternator driven by a d.c. motor. The alternator output is connected to the laboratory busbar via lumped impedances representing the transmission line. Also associated with the model are circuits to modify various time constants, transducers and fault application equipment. Two computers are interfaced to the model plant, one providing the on-line control and the other recording data from the machine during tests, afterwards plotting out responses with a graphics package. Fig. 5.1 is a schematic diagram of the system.

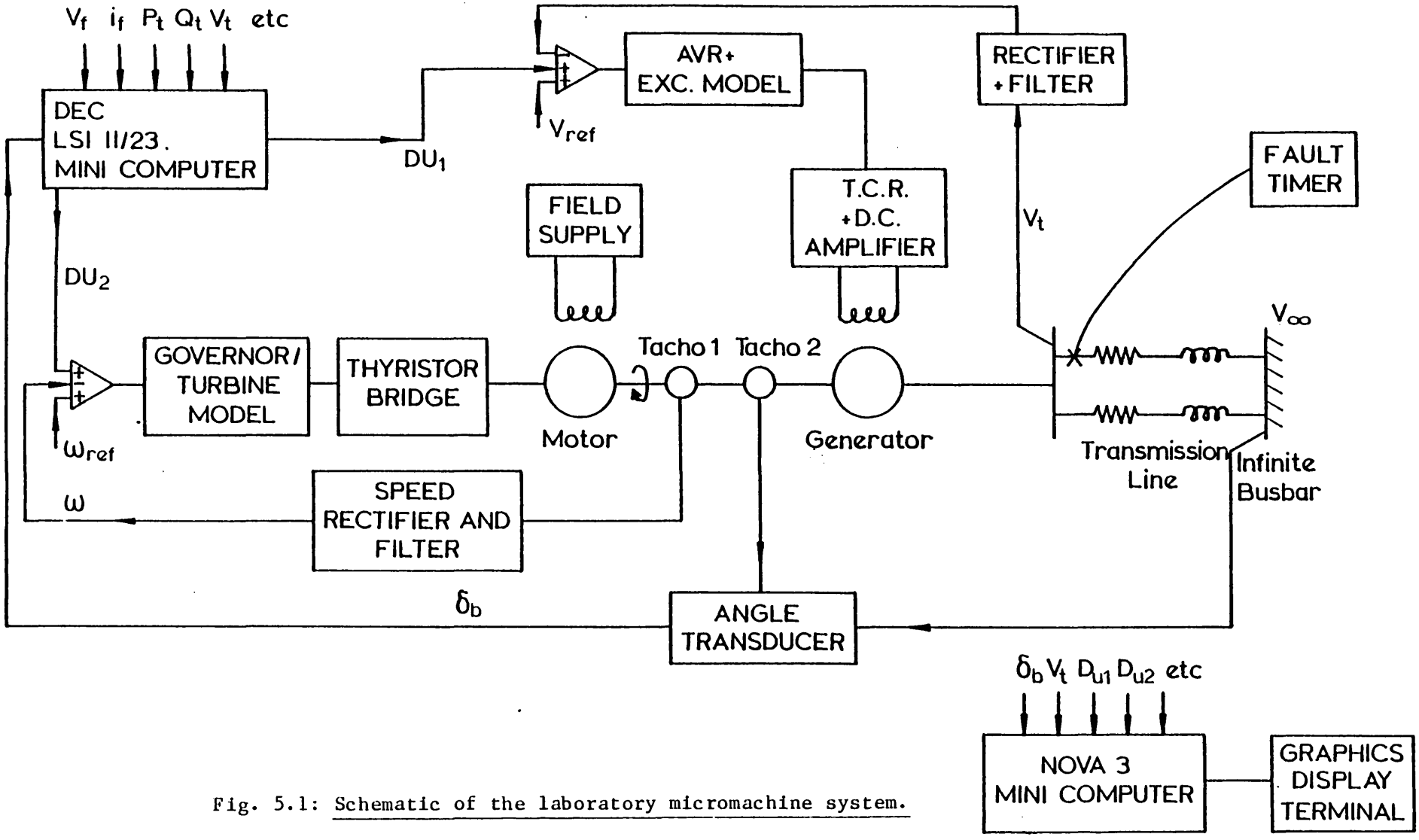

Fig. 5.1: Schematic of the laboratory micromachine system.

5.2 THE MICROALTERNATOR

The microalternator, designed to have similar per-unit parameters to typical turbo-alternators of up to 1000MW rating[117], is actually a six-phase machine but is connected as a three-phase machine throughout this work [see Hanna[118], pp.78-80]. Designed and manufactured by Mawdsley's Ltd., it is a four-pole machine made up with stator No. 3 and rotor No. 5. The rotor winding is in two sections connected here to behave as a conventional field winding with its m.m.f. in the direct axis only [Touri[121], pp.18-20]. There are also shadow field windings which can be used to adjust the field time constant to the same value as that of a larger machine. Details of the time constant regulator [T.C.R.] are in Section 5.4.1. The rotor has solid damper bars and regulation of the damper winding time constants is not possible unless another rotor is used.

The micromachine shaft has provision for bolting annuli on to a flywheel at the motor end. This facilitates changing the inertia constant from 3.0 kWs/kVA upwards in steps of 0.5 kWs/kVA. At present no physical simulation of the distributed inertias coupled by flexible shafts of a real turbine generator is made here, although elsewhere a laboratory system has been constructed to do this for studies of subsynchronous resonance[122,133].

5.3 TURBINE AND GOVERNOR SIMULATION

The prime mover of the turbine generator model is a separately excited 5.57 kW 220Vd.c. motor. A three-phase thyristor bridge[119] provides the d.c. for the motor armature, Fig. 5.2. A constant motor field current

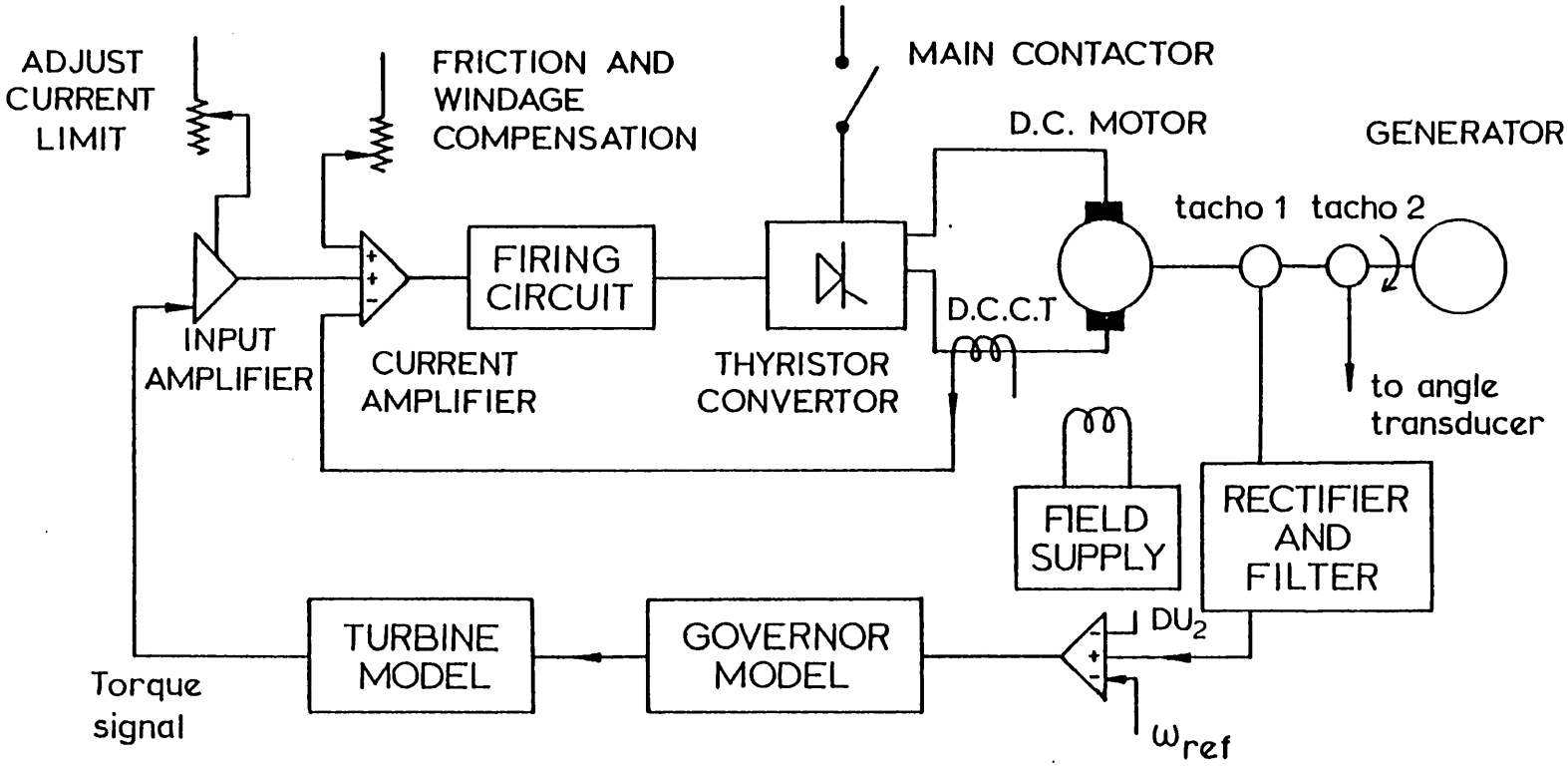

Fig. 5.2: The D.C. motor and controls.

of 4A is supplied via a three-phase diode bridge rectifier. The torque is thus proportional to the armature current, which with feedback from the direct current transformer gives a time constant measured to be approximately 100 msec between changes in the input amplifier signal and torque changes. Also provided with the thyristor unit are friction and windage compensation and current limit protection.

There are two a.c. tachogenerators on the machine shaft: a 50 Hz two-phase permanent-magnet machine providing an input to the rotor angle transducer [Section 5.7.1]; and a 400 Hz single-phase tacho, the output of which is rectified and filtered to supply the speed signal to the governor/turbine model.

5.3.1 Simplified governor/turbine model

The simplified governor/turbine model was designed to simulate practically the representation used in the mathematical models [see Chapter 2, Fig. 2.4] for initial testing of the control scheme, where it is desirable to minimise the number of sources of discrepancy between theoretical and practical simulations. The circuit diagram appears in Appendix J.

5.3.2 Detailed governor/turbine model

For more realistic simulations of the governor and turbine behaviour a more detailed model is needed. In it delays associated with relays, valves, the turbine and reheater stages are all modelled as shown schematically in Fig. 5.3. The different opening and closing velocity limits of the valves are also approximated by using different time constants for positive and negative rates of change. Constants have been chosen to approximately match those of a

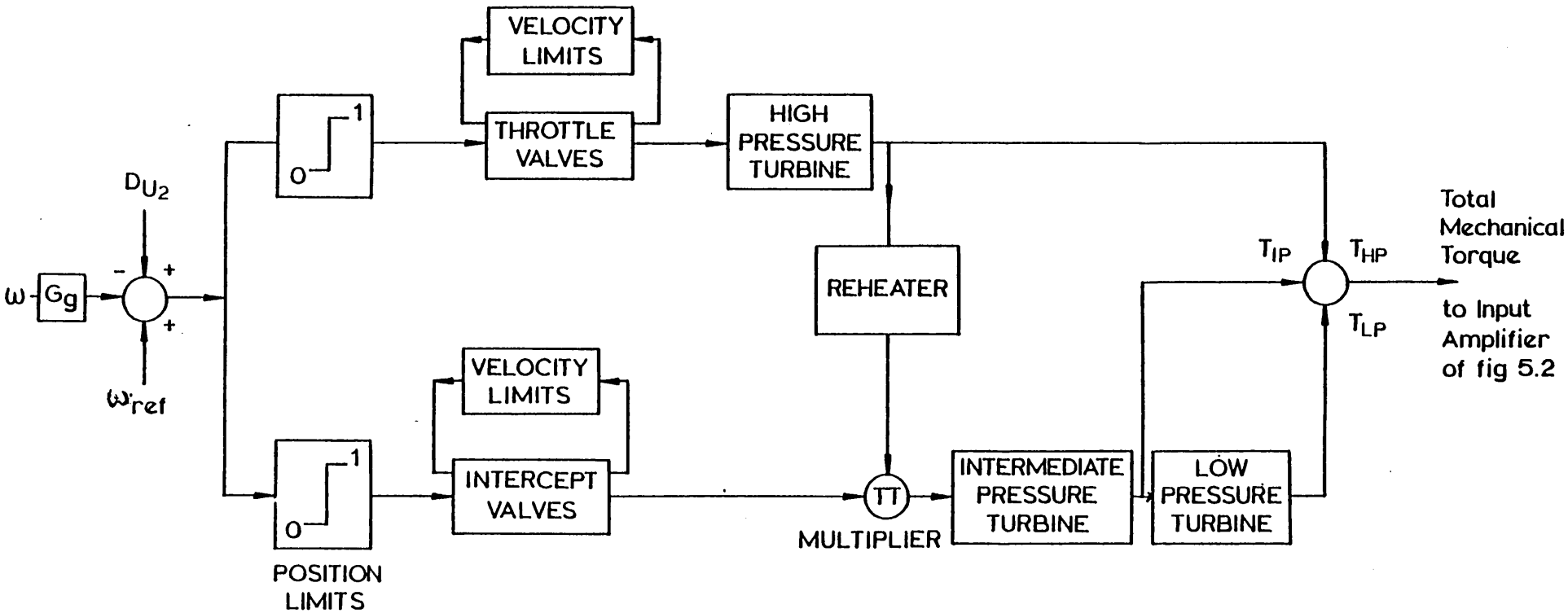

Fig. 5.3: Schematic of the detailed governor/turbine model.

typical electro-hydraulic governing system and 660 MW turbine[120a]. It is assumed that parallel governing is used [i.e., changes in the error signal move the throttle and intercept valves by equal amounts], and that there is no Wattmetric feedback in addition to speed feedback. The circuit of the detailed governor/turbine model is given in Appendix J.

5.4 THE TIME CONSTANT REGULATOR AND EXCITATION SYSTEM

5.4.1 The Time Constant Regulator

The per-unit natural field resistance of the microalternator rotor is much higher than that of the field winding of a large turbo-alternator, so a time constant regulator is used which effectively introduces a negative resistance and hence increases the field time constant. To do this a shadow winding is provided which is wound in the same slots and has the same number of turns as the main rotor winding, hence the same flux links both field and shadow windings.

If a d.c. power amplifier, gain G_1, is used to drive the field and the induced voltage due to the rate of change of rotor flux $\dot{\Psi}$ linking the shadow winding is fed back to the input, together with a voltage drop $K' R_{fb} i_f$ due to the field current through feedback resistor R_{fb}, the system is as shown in Fig. 5.4. With nearly perfect coupling between the field and shadow windings, and assuming the power amplifier time constant to be very small, the amplifier output V_o is given by:

$$V_o = G_1(V_f - \dot{\Psi}_f - K' R_{fb} i_f) \qquad [5.1]$$

but:

$$V_o = \dot{\Psi}_f + (R_f + R_{fb})\, i_f \qquad [5.2]$$

hence:

$$V_f = \{\dot{\Psi}_f + (R_f + R_{fb})\, i_f + G_1[k' R_{fb} i_f + \dot{\Psi}_f]\}G_1 \qquad [5.3]$$

and the effective field resistance is now:

$$V_f / i_f = (R_f + R_{fb} + G_1 k' R_{fb})/G_1 \qquad [5.4]$$

For a large G_1 this approximates to:

$$V_f / i_f \doteq k' R_{fb} \qquad [5.5]$$

For step changes in F_f, i_f changes according to the transient open-circuit time constant T_{do}', which now becomes:

$$T_{do}' = L_{ffd} / k' R_{fb} \qquad [5.6]$$

The bandwidth of the T.C.R. and the gain need to be limited sufficiently to prevent closed-loop instability. The circuit used is due to Touri[121] and is shown in Appendix J.

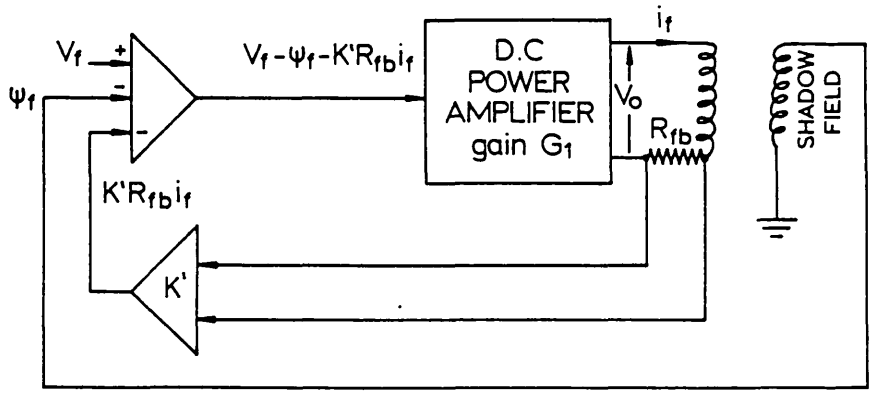

Fig. 5.4 Schematic of the time constant regulator.

5.4.2 The AVR and exciter model

The laboratory micromachine has provision for either manual or automatic field regulation. During manual operation the T.C.R. input is simply supplied with the desired field voltage V_f. With automatic voltage regulation, a three-phase rectifier and filter [with a filter time constant of about 5 ms] provides a d.c. signal proportional to the terminal voltage, which is compared with the reference value and the AVR supplementary signal is added. Delays and limits are modelled electronically to give the same representation as in Chapter 2, Fig. 2.3. Lead-lag compensators can be modelled, but are omitted here and the AVR gain is reduced to about 30 since transient stability is of principal interest. The circuit diagram is in Appendix J.

5.5 TRANSMISSION LINE AND INFINITE BUSBAR

The transmission line is simulated by a bank of inductors, so that a variable impedance may be switched between the generator terminals and infinite busbar. Extra resistance can also be switched in. For initial tests a single series impedance typical of a relatively short tie-line in this country was chosen, but double-circuit and longer lines were also simulated.

The infinite busbar is represented by a 30kVA delta-star transformer, the secondary connected to the departmental 415V mains.

5.6 PARAMETERS OF THE LABORATORY SYSTEM

The microalternator paramaters for the combination of stator and rotor used here have been measured in a series of tests by Menelaou[15] who used, where possible, two different methods to give more certainty of validity. The machine inertia constant H was chosen to be 3.5 by removing all but one of the $\frac{1}{2}$" annuli[117]. Appendix H gives a comparison of the micromachine parameters [including the time constant regulator] with those, calculated at the design stage, of a typical 660 MW machine[120b]. The single-circuit transmission line parameters are those measured with the two smallest inductances of a laboratory unit switched in. Governor/ turbine and AVR gains and time constants are those for the simplified models.

From the table in Appendix H it is apparent that general agreement is very good between the parameters, apart from the discrepancy in the damper winding reactances. Computer simulations comparing both sets of parameters in Section 4.8.1 show that a reasonable similarity between the two responses may be expected.

5.7 TRANSDUCERS AND FAULT APPLICATION EQUIPMENT

5.7.1 Digital Load Angle Transducer

Load angle [also called rotor or power angle] is a somewhat ambiguous term meaning the electrical angle between the generator field m.m.f. and either the infinite busbar or the generator terminals as a rotating reference frame. Here load angle may be taken to mean the former, and terminal load angle

the latter. The method of measurement used here is to determine the phase difference between the infinite bus voltage and the voltage of one of the phases of a four-pole two-phase tacho-generator mounted on the machine shaft.

To make the transducer frequency-independent, Menelaou[15] used a phase-locked loop [P.L.L.] to multiply the mains frequency by a fixed amount, then counted the number of oscillations during the time difference between zero-crossings of the two voltages. This method was tried here but gave unsatisfactory results due to oscillations in the P.L.L. output frequency caused by hunting in the frequency feedback loop.

A different approach was adopted here, using a crystal oscillator to eliminate clock frequency fluctuations but still achieving mains frequency independence by constantly monitoring it. Fig. 5.5 shows the principle of the method. Zero-crossing detectors and logic circuits generate the output shown in Fig. 5.5b. Oscillations at 409.6 KHz are "AND"ed and "NAND"ed with the load angle pulse to give the waveforms in Fig. 5.5c and Fig. 5.5d. Binary counters sum the total number of cycles in each giving N_1 cycles in the load angle pulse and N_2 in the remaining half cycle. N_1 and N_2 can be read into the computer and, using floating point arithmetic:

$$\text{load angle } \delta = \left[\frac{N_1}{N_1 + N_2}\right] . \pi \text{ radians} \qquad [5.7]$$

The clock frequency used gives 12-bit resolution. Circuit diagrams are given in Appendix J. The input voltage waveforms have to be filtered sufficiently to prevent errors occurring in the zero-crossing

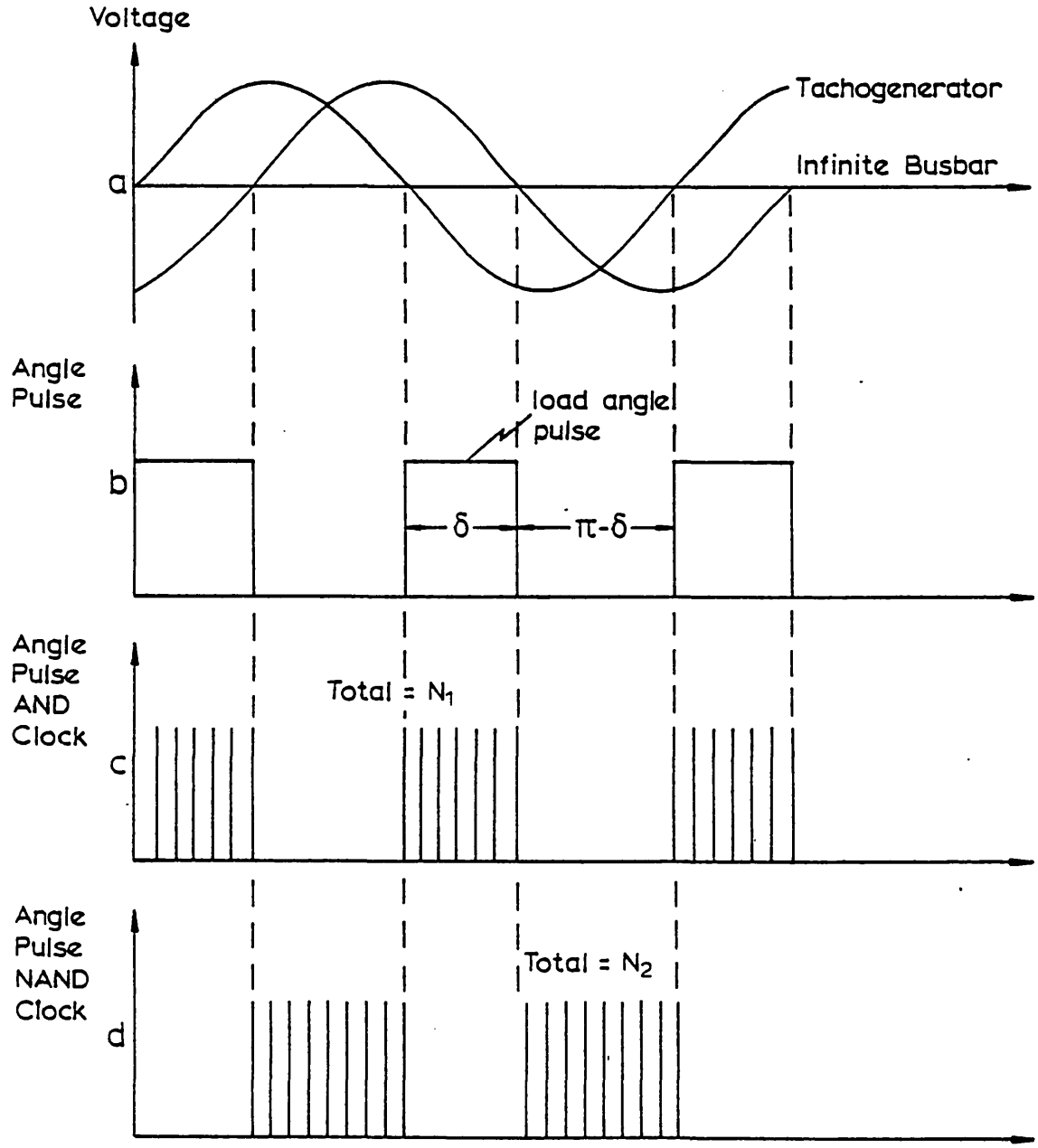

$$\delta = \left(\frac{N_1}{N_1 + N_2}\right)\pi$$

Fig. 5.5: Principle of operation of the load angle transducer.

detection. Accuracy was found to be better than 0.5% when tested by a phase-shifting transformer. Since the transducer output is updated every half-cycle on the basis of measurements taken during this time the delay is 10 ms.

Zero-setting of the angle transducer can be achieved by operating the microalternator with the infinite busbar disconnected on open-circuit, then adjusting the tachogenerator rotor position relative to the generator shaft until an angle of zero is read.

The traditional method of using a stroboscope and a mark on the alternator shaft for measuring rotor angle is a convenient approximate check on the correct operation of the digital angle transducer.

5.7.2 Power and VAr measurement

Power and VAr at the machine terminals are measured by electronic circuits performing analogue multiplications of voltages and currents. These in turn are measured by current transformers [C.T.'s] and capacitor voltage transformers [C.V.T.'s] as described in a generator protection project by Khan[123]. It must be noted that the C.V.T.'s have a very high impedance [1 MΩ] at the output to minimise the phase shift that would otherwise be excessive. All the voltage and current waveforms are then conditioned by matched 6^{th} order Butterworth filters with a cut-off frequency at 450 Hz to filter harmonics above the 9^{th}[123]. The time delays are thus equal for all the line voltages and currents and are about 1.4 millisec.

The conditioned voltage and current waveforms are then input to

the Watt/VAr board where real power is calculated by the two-wattmeter method:-

$$P = V_{RB}I_R \cos\alpha + V_{YB}I_Y \cos\beta \qquad [5.8]$$

where:

$$\alpha = \phi + \pi/6 \qquad \beta = \phi - \pi/6 \qquad [5.9]$$

and cos ϕ is the power factor. The output is then filtered to remove ripple.

Reactive power can be measured by making the following calculation:

$$Q = \sqrt{3}\ V_{YB}I_R \sin\phi \qquad [5.10]$$

However, it was found that ripple could be reduced by calculating Q as follows:

$$A = \frac{\sqrt{3}}{2}(V_{YB}I_R \sin\phi + V_{RB}I_Y \sin\phi) \qquad [5.11]$$

The circuit diagram of the Watt/VAr transducer is given in Appendix J. It was calibrated under steady-state conditions against conventional moving coil wattmeters. By performing load rejection tests, the transient time delay of the transducer was found to be approximately 10 ms for both power and reactive power measurement.

5.7.3 Fault Application Equipment

Faults of variable duration may be applied to the machine using a circuuit breaker sequence control unit designed by Neech[124]. Essentially this is a three-channel unit, each of which may be

programmed to send logical pulses of any desired duration within a 10 sec total cycle time to a circuit breaker interface. Here one channel is used to apply and sustain the fault for the desired duration, and another may be used to remove a line at the same time as the fault if required.

The circuit breakers interfaced to the control unit are energised by a 240v a.c. supply. The operation of the reed relays as originally used in the interface was unsatisfactory due to the contacts frequently sticking and voltage pulses induced at the low voltage side by breaking the energising coil circuit. Replacing each reed relay by an opto-isolated triac circuit given in Appendix J, has proved to give much more reliable and satisfactory performance.

5.8 COMPUTER HARDWARE

The two computers interfaced to the micromachine for on-line control and data monitoring are shown schematically in Fig. 5.6.

5.8.1 On-line control computer

The computer chosen to handle the on-line control requirements was based on the LSI 11/23 microcomputer manufactured by Digital Equipment Corporation[125]. The LSI 11/23 central processing unit [C.P.U.] is at the heart of the system, with 128kBytes of random-access-memory [RAM], a floating point accelerator unit to minimise execution time and DEC-compatible input/output [I/O] boards. The real-time operating system RT-11 runs on the

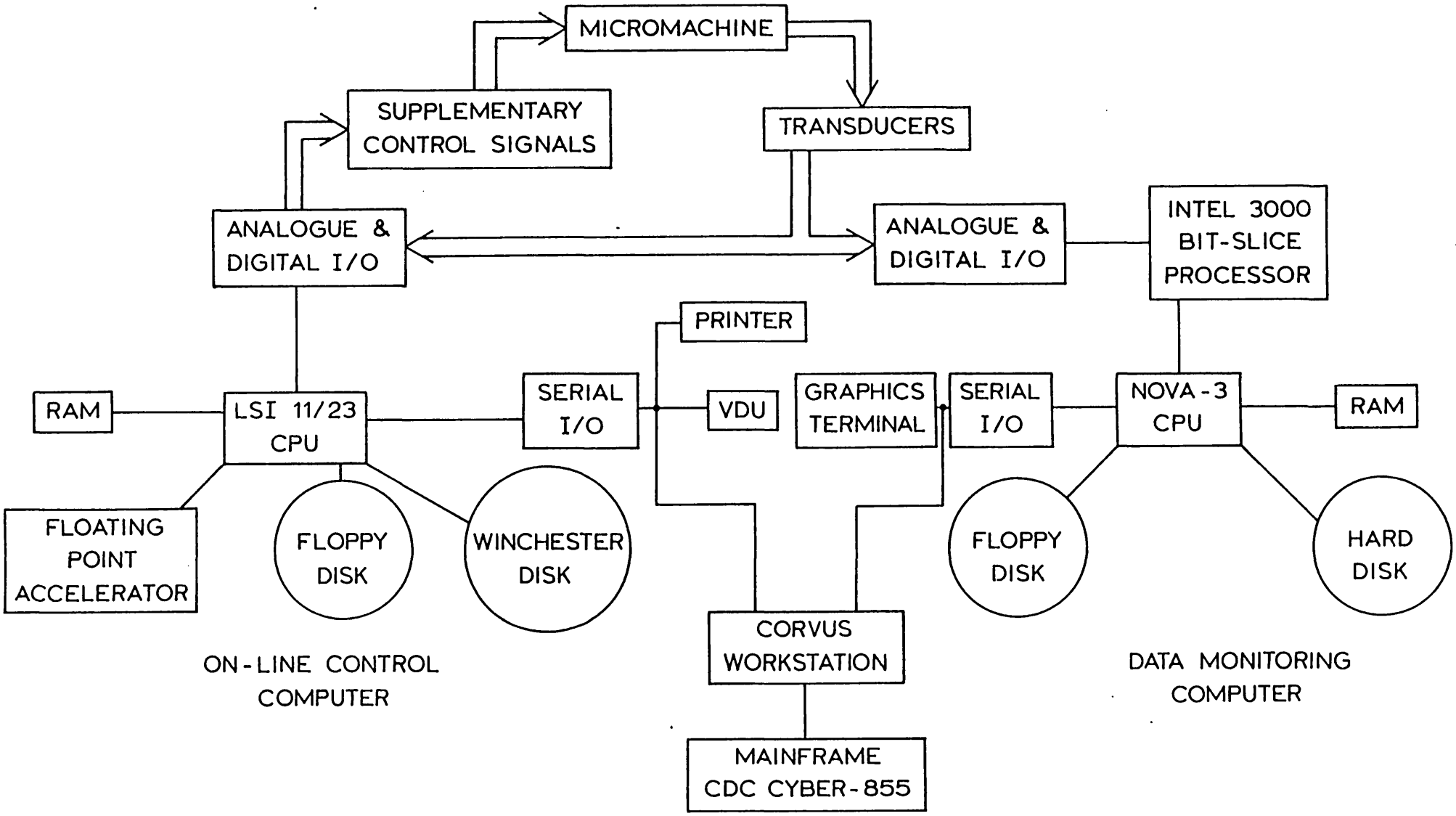

Fig. 5.1: Schematic of the control and data monitoring computers.

computer and mass storage is provided by a 20MByte Winchester disk system and a single flexible disk drive. More detailed specifications of the system are given in Appendix K.

Although at the time of purchase potentially more advanced processors were available, such as the Motorola 68000, the LSI 11/23 was chosen for the following reasons:

a] The extensive software support facilities available for the PDP-11 series of computers is well-known[125], and includes Fortran, Pascal, Macro-11 assembly language, many very good editors and word-processing packages.

b] Software development is possible without the need of an extra support system or emulation facilities which would involve a considerable extra outlay.

c] Tailor-made hardware floating-point multipliers are available which may easily be added to the system, and give overall improvement in speed by a factor of 4 - 6. For microprocessors such as the 68000 much more effort is required to interface floating point units to the CPU.

d] Hardware support is strong for the LSI 11/23 within the Electrical Engineering Department at Imperial College, including spare CPU, memory and I/0 boards and personnel trained in the maintenance of DEC equipment.

e] DEC have the policy of making new, more advanced hardware compatible with older systems [where practicable]. The LSI 11/73 CPU has recently become available and may be used as a direct plug-in replacement to the 11/23. The 11/73 CPU

alone has been found to be about 40% faster than the combined 11/23 CPU and floating point accelerator.

5.8.2 Machine Data Monitoring Computer

It was convenient to use a separate computer for recording data of interest and plotting out results graphically, so as not to disturb the on-line control function of the LSI 11/23 system. A Data General Nova-3 minicomputer served this purpose, with an analogue and digital interface system controlled by on Intel 3000 bit-slice microprocessor, as used by Pavlides[126]. The interface sampling rate is adjustable but here was mostly set to take a total of 300 samples of each variable over a period of 6 sec starting about $\frac{1}{2}$ sec before the fault application. Rotor angle, terminal voltage and the two supplementary signals to the governor and AVR were normally the signals monitored, but as many as 16 8-bit analogue and one 16-bit digital signals may be read into the Nova.

The data read in over the total period may be plotted out using a graphics package based on the Tektronix Plot-10 system[126,127] and a Tektronix-compatible graphics terminal.

5.8.3 Interface to the Mainframe Computer

A means of transmitting information between the LSI 11/23 on-line control computer, the Nova-3 data monitoring computer and the college CDC Cyber-855 mainframe was provided by a Corvus Concept workstation[130]. The Corvus system was used as an intermediate stage when transferring data between any two of the three computers mentioned above via serial data lines [RS-232C standard]. The practical results presented in Chapter 6 consist of data that

has been read and stored by the Nova-3 computer, then plotted graphically by the college mainframe computer after transfer via the Corvus terminal.

Details of interface plug and socket pin connections between the LSI 11/23 and the micromachine, interfacing between the angle transducer and the Nova-3, operating record of the LSI 11/23 etc., are given in a separate report[128].

CHAPTER 6

PRACTICAL IMPLEMENTATION OF THE STATE ESTIMATOR AND OPTIMAL CONTROLLER: TEST RESULTS

6.1 INTRODUCTION

Experimental testing of state estimators and optimal controllers performed previously on a laboratory system similar to that described in Chapter 5[13-15] produced good results but several limitations were acknowledged by the author. One of the most severe was the large time step, between 70 and 170 ms., of the Fortran on-line control program executing on an older-generation Data General Nova-3 minicomputer. The theoretical studies in Section 4.8.3 indicate that much better control may be achieved with an execution time in the order of 10 ms. Another shortcoming in Menelaou's implementation was that the accuracy in the computer/machine interface was limited to 8 bits. It was felt that the range of tests could be extended to look at many different controller configurations operating under a number of different conditions and subjected to various types and severity of fault.

This Chapter describes how the state estimation/optimal control [LQG] algorithm was implemented in assembly language on an LSI 11/23 microcomputer to meet the desired execution time of 10 ms, and its other special features such as digital washout filtering of the input signals. A comparison is made between calculated and measured transient responses of the laboratory power system without supplementary control,

to check the validity of the mathematical modelling and the setting up of the micromachine itself.

Initial tests have been made on controllers designed from 12^{th}, 9^{th}, 7^{th} and optimally reduced 4^{th} order mathematical models measuring load angle and field voltage. Robustness and the performance when subjected to transient disturbances milder or much more severe than the standard 100 ms three-phase fault [including more frequently-met unbalanced faults] are also considered. Controllers measuring more accessible signals than load angle, such as power, speed or terminal voltage, were tested and the influences of noisy measurements and torsionally flexible shafts were looked at. The contribution to dynamic stability and controllers giving a supplementary signal to the AVR loop only were also examined.

6.2 IMPLEMENTATION OF THE CONTROL ALGORITHM

6.2.1 Digital Washout Filtering

Since the controller is designed using a linearised system model, the states, inputs and outputs used in the model are deviations from their steady-state absolute values [Section 2.4]. In the practical implementation steady-state values may, as already mentioned, be obtained by a steady-state phasor diagram calculation at the design operating point and used on-line. However, this would have the drawback that the controller, taking in measurements with reference to constant steady-state values, would interfere with normal operation should it be desired to alter the loading of the machine. It would be better to allow

the reference measurements to alter in accordance with setpoint changes. Furthermore, when there is a change in tieline impedance following a fault, the generator should be allowed to settle to a new operating point as dictated by the conventional governor and AVR settings.

A solution to this problem is the use of washout filtering, where the steady-state or reference value is replaced by the output of a low-pass filter of the measured input signal. Thus the signal used by the controller is the difference between the measured signal and filtered signal. Phung and Gibbard[73] called the filtered signal the "pseudo steady-state" value of the variable, since it is not constant but is allowed to change slowly according to the input signal level. If the low-pass filter time constant is carefully chosen, this will allow the machine to move slowly to new steady-state set-points yet during transients the controller performance is almost identical to that using the true steady-state values.

It was decided to perform the washout filtering digitally with the on-line control computer to enable easy adjustment of the filter coefficients in the software. To keep the number of arithmetic operations to a minimum, the first order low-pass filter algorithm in canonic form was implemented[73,129]:

$$w(k) = a y(k) + b w(k-1) \qquad [6.1]$$

and:

$$y_o(k) = w(k) + w(k-1) \qquad [6.2]$$

starting with initial conditions:

$$w(0) = y(0)/2 \qquad [6.3]$$

where $y(k)$ is the value of the input signal at the k^{th} sampling interval, $y_o(k)$ is the low-pass filter output, and a and b are the filter coefficients, which are chosen such that:

$$a = \omega_{ac}/(1 + \omega_{ac})$$
$$b = (1 - \omega_{ac})/(1 + \omega_{ac}) \qquad [6.4]$$

where ω_{ac} is a frequency given by:

$$A_{ac} = \tan(\omega_{dc}T/2] \qquad [6.5]$$

and ω_{dc} is the desired cut-off frequency and T the sampling rate.

The washout filtering vies the deviation from the "pseudo steady-state" value $y_o(k)$:

$$\Delta y(k) = y(k) - y_o(k) \qquad [6.6]$$

6.2.2 Programming the algorithm on the on-line computer

As stated in Section 6.1, one of the principal aims in the implementation of the state estimation/optimal control algorithm is to achieve a computation time step in the order of 10 msec or better. Early tests were made, before the purchase of the DEC computer system, on other very similar LSI 11/23 computer systems [although they were without floating point hardware multipliers] to see how this aim could be met.

A seventh order estimation/control algorithm programmed in Fortran [for a description of the algorithm see Section 4.6], including washout filtering but not analogue and digital I/O, was found to execute in 70 ms on such a system. The same algorithm

again in Fortran but using scaled 16-bit integer arithmetic throughout instead of floating point, executed on the same system in 25 ms. However, because of the large number of arithmetic operations round-off errors became significant even with scaling and degraded the controller effectiveness on simulations. The conditioning of the matrices in the algorithm could have been improved in an attempt to reduce these errors but would have added more time overheads and increased the complexity, so implementing the algorithm in integer arithmetic was not pursued further.

The approach found to be successful was to program the algorithm in DEC's MACRO-11 assembly language[125b]. Although more time-consuming than programming in Fortran, the lower level language gives more direct control over the computer during execution which reduces time overheads and is in any case necessary for I/O control. The programming procedure was to write a MACRO-11 general-order matrix multiplication routine using floating-point arithmetic, then to program the algorithm of Section 4.6, which is essentially a sequence of matrix multiplications and test it with simulations. This was found to improve the execution time of the seventh order control algorithm to 20 ms.

By specifying a floating point accelerator board when ordering the on-line control computer, the execution time of the seventh order algorithm was further reduced to 5.5 ms. The floating point unit, a co-processor dedicated to execution at high speed of all the floating point instructions in the PDP-11 instruction set, was expensive but enabled the time requirements to be met. The time

overheads of the necessary I/O instructions were later found to be negligible compared with the overall execution time.

A version of the algorithm was written to accept any order A, B and C matrices to implement a controller of one or two outputs and two inputs. This enables a comparison of the execution speeds of algorithms based on four different model orders, as shown in Table 6.1.

Model Order	Execution Time, ms
12	11
9	7.8
7	5.5
4	3.6

Table 6.1: Execution Speeds of Controllers

Thus the execution times for the controllers have been reduced by a factor of more than ten compared with those achieved by Menelaou[13-15], and on-line application of the algorithm with time steps shown theoretically in Chapter 4 to give very good results is possible with this sytem.

Execution of the algorithm on-line is initiated by running a Fortran program which reads in the appropriate gains, calculates steady-state conditions then calls the MACRO-11 on-line control routine which continues to operate until interrupted. With minor modifications state estimators/optimal controllers of any order measuring any desired signals can be tested, with supplementary signals to both or just one of the control loops.

A standard sampling interval of 10 ms has been adopted for all controllers except the 12^{th} order, which was run with its minimum possible interval of 11 ms. For lower order controllers the computer is allowed to idle between the end of one calculation and the start of the next, either by using interrupts synchronised to negative-going edges of the load angle pulse to initiate calculation or by executing dummy software loops a pre-calculated number of times to fill in the remainder of each 10 ms period. The latter method is simpler to program, avoids the possibility of spurious triggering and thus is desirable if, as here, no particular advantage is gained by synchronising the computer to mains frequency.

Appendix L gives a listing of the MACRO-11 assembly language on-line control program.

6.3 COMPARISON OF SIMULATED AND MEASURED RESULTS FOR THE MICROMACHINE WITHOUT SUPPLEMENTARY CONTROL

A comparison between predicted and measured responses determines whether correct modelling techniques are being used and ensures that the apparatus is correctly set up. Fig. 6.1a,b compares predicted and measured terminal voltage and rotor angle responses for an eleventh order nonlinear generator simulation and readings taken from the micromachine for a 100 ms 3-phase fault with full reconnection on fault removal. Clearly the main differences are in the angle response which has a larger backswing on application of the fault and better damping than the theoretical model. However, the first swing amplitude is

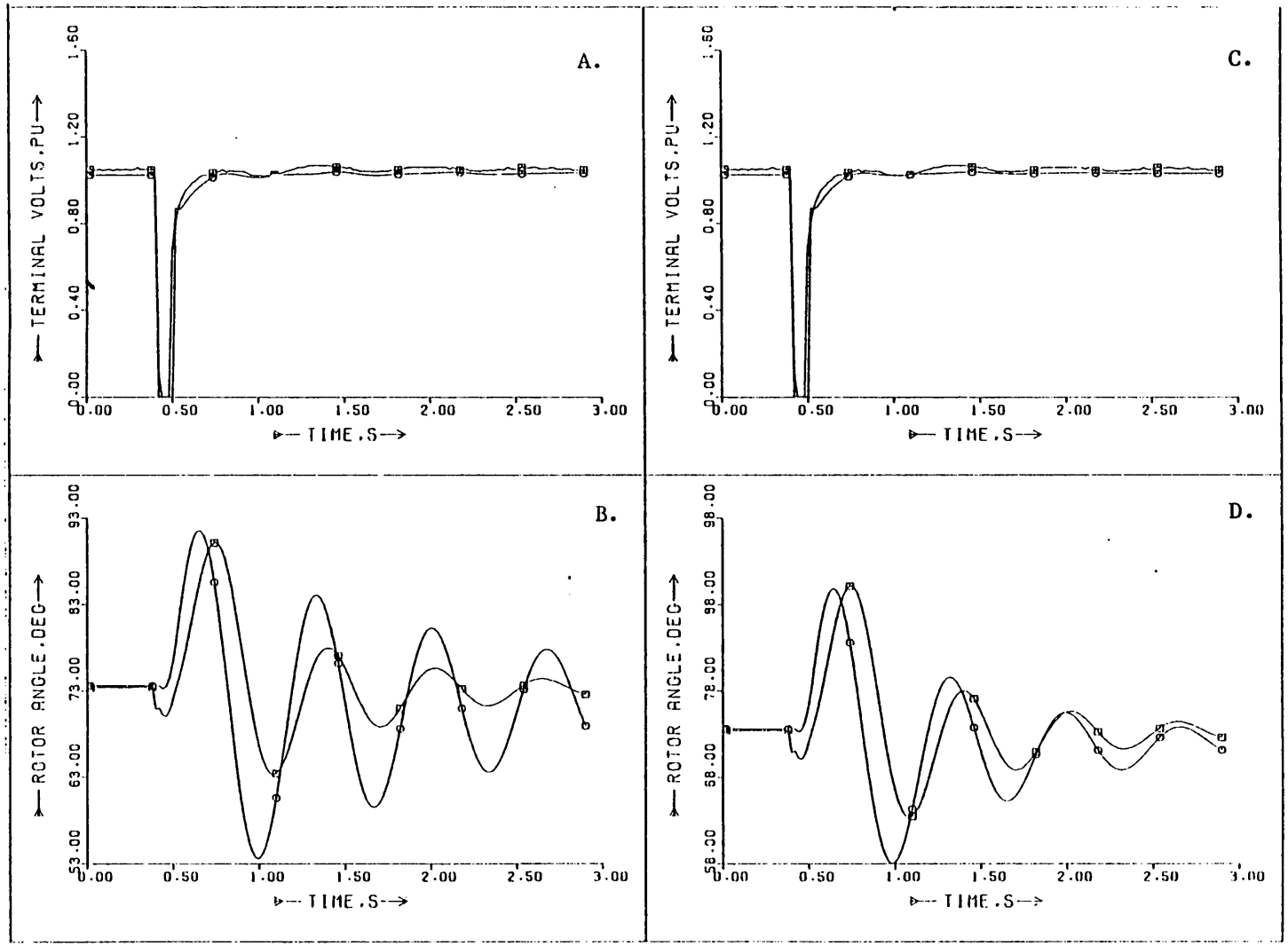

Fig. 6.1: Comparison of o - theoretically predicted and □ - practically measured responses of the micromachine to a 100 ms fault: A,B - Original theoretical model; C,D - Theoretical model with mechanical damping factor k of 0.025.

approximately correct as is the rotor oscillation frequency.

The two possible main causes of the incorrect load angle damping are inaccurate damper winding parameters or greater than prediced mechanical damping of the shaft. The computer model in Fig. 6.1a, b assumes mechanical damping is zero, a justifiable assumption in large machines since friction and windage losses are small compared with the overall machine rating. On the micromachine mechanical losses are compensated for [see Section 5.3], but account only for static friction and low speed losses.

The mechanical damping was measured by running the machine up to synchronous speed under no load, then setting the torque signal from the turbine simulator to zero. The rotor thus decelerated due to the mechanical losses, with compensation, and measuring the time taken to decelerate from 1500 to 1400 or 1300 rpm enabled the damping coefficient to be calculated in the neighbourhood of synchronous speed. By this method the mechanical damping coefficient was calculated to be 0.025 pu.

Including the measured mechanical damping in the computer simulation [Fig. 6.1c,d] makes the angle responses much closer. The predicted backswing is still somewhat less than in the measured response; this is possibly due to the T.C.R. not giving the correct effective rotor resistance during the fault [caused by saturation of the D.C. power amplifier], or incorrect damper winding parameters. However, predicted and measured responses with the modified damping are close enough to give confidence that the system is being reasonably well modelled.

6.4 PRACTICAL TESTS ON STATE ESTIMATORS/OPTIMAL CONTROLLERS MEASURING ROTOR ANGLE AND FIELD VOLTAGE

6.4.1 Three-phase fault of 100 ms duration, standard operating conditions

Fig. 6.2 compares the controlled and uncontrolled measured responses of the micromachine when the operating conditions are as in Appendix H, following a 100 ms short-circuit with full post-fault restoration of the transmission system. The desired nearly dead-beat angle response is achieved when the 12^{th} order controller measuring load angle and field voltage is acting on the machine. The controlled response is similar, even slightly better [with a small second backswing] than that achieved in simulations [Chapter 4, Fig. 4.5], although it must be pointed out that the theoretical simulations did not account for the extra mechanical damping [Section 6.3]. To achieve this response, the weighting matrices were altered from those giving the best theoretical results, with the regulator and filter gains both reduced. Weighting of individual states in relation to one another did not have to be changed, however. For this duration of fault there is virtually no difference between terminal voltage responses with and without control.

6.4.2 Three-phase fault of 450 ms duration, standard operating conditions

Increasing the fault duration, with other conditions the same as in 6.4.1 so that the machine nearly lost synchronism, gave results with and without the same 12^{th} order controller given in Fig. 6.3.

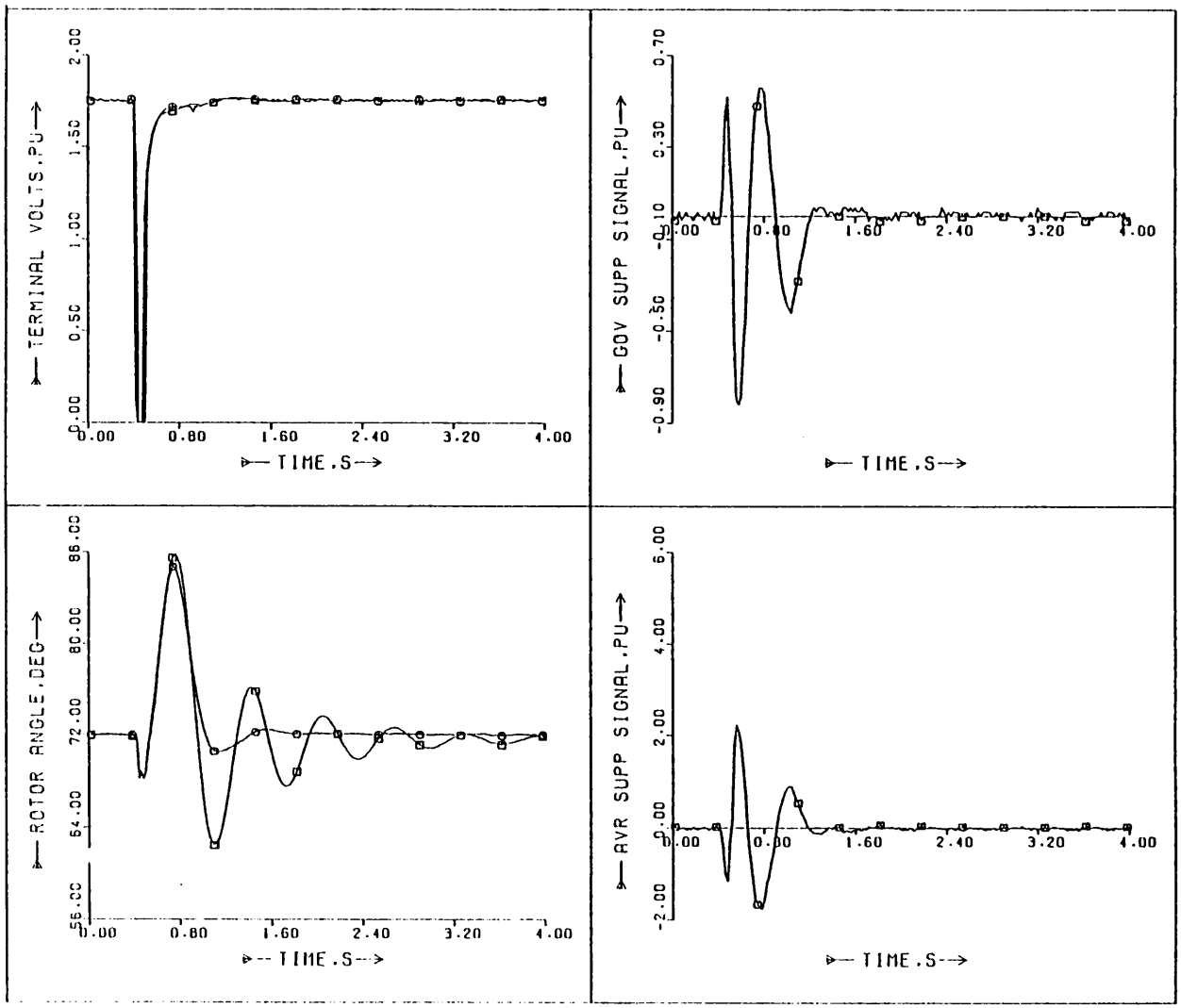

Fig. 6.2: Measured responses o - controlled and □ - without control, to a 100 ms 3-phase fault (standard conditions). 12th order controller measuring load angle and field voltage.

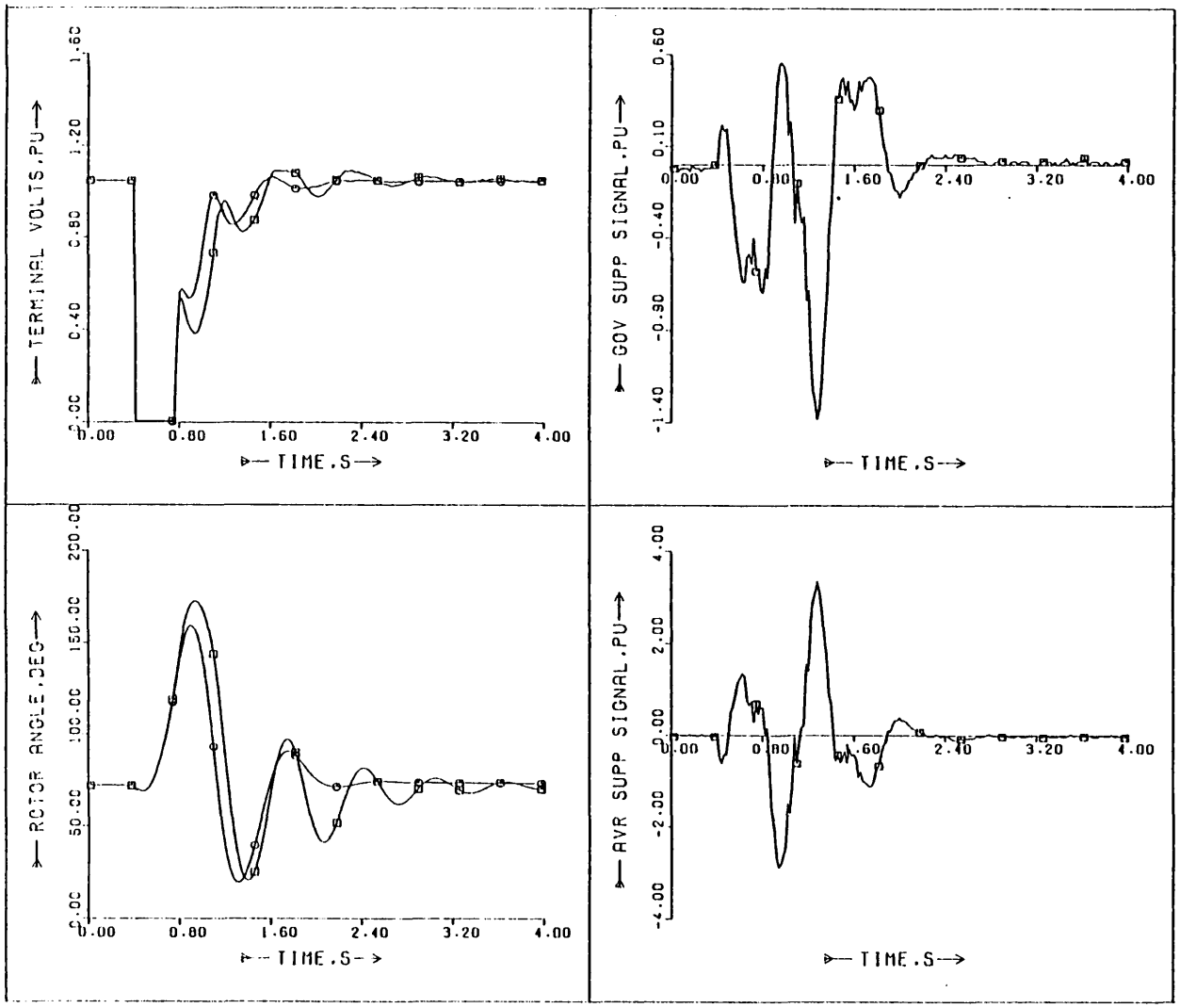

Fig. 6.3: As Fig. 6.2 but with a fault duration of 450 ms. o - controlled and □ - without supplementary control.

The first swing is reduced by about 15°, and the machine returns to steady operation 2 sec after the fault. A considerable improvement in the terminal voltage response can also be seen, with more rapid recovery to the pre-fault value and better damping of oscillations that could propagate to the rest of the system with a large machine.

Increasing the fault duration above this caused the machine to become unstable without supplementary control. With control the machine remained stable for faults of up to 500 ms duration.

6.4.3 Unbalanced line-line fault, standard operating conditions

Unbalanced faults were not simulated theoretically in Chapter 4 but are much more frequently encountered than three-phase faults in power system operation. Fig. 6.4 shows the effect of the 12^{th} order controller when the micromachine is subjected to a 100 ms line-line fault at the terminals. This time the first rotor swing is negative due to the unbalanced conditions. The controller successfully reduces the first and second rotor excursions, then the machine returns to steady operation. Once again there is little difference between the terminal voltage responses.

6.4.4 Loss of one transmission line

For the next tests a second transmission line was connected in parallel to the original one, with a circuit breaker to enable the line to be switched out. The impedance of each line was set to

$$Z_e = 0.031 + j0.56 \text{ p.u.} \qquad [6.7]$$

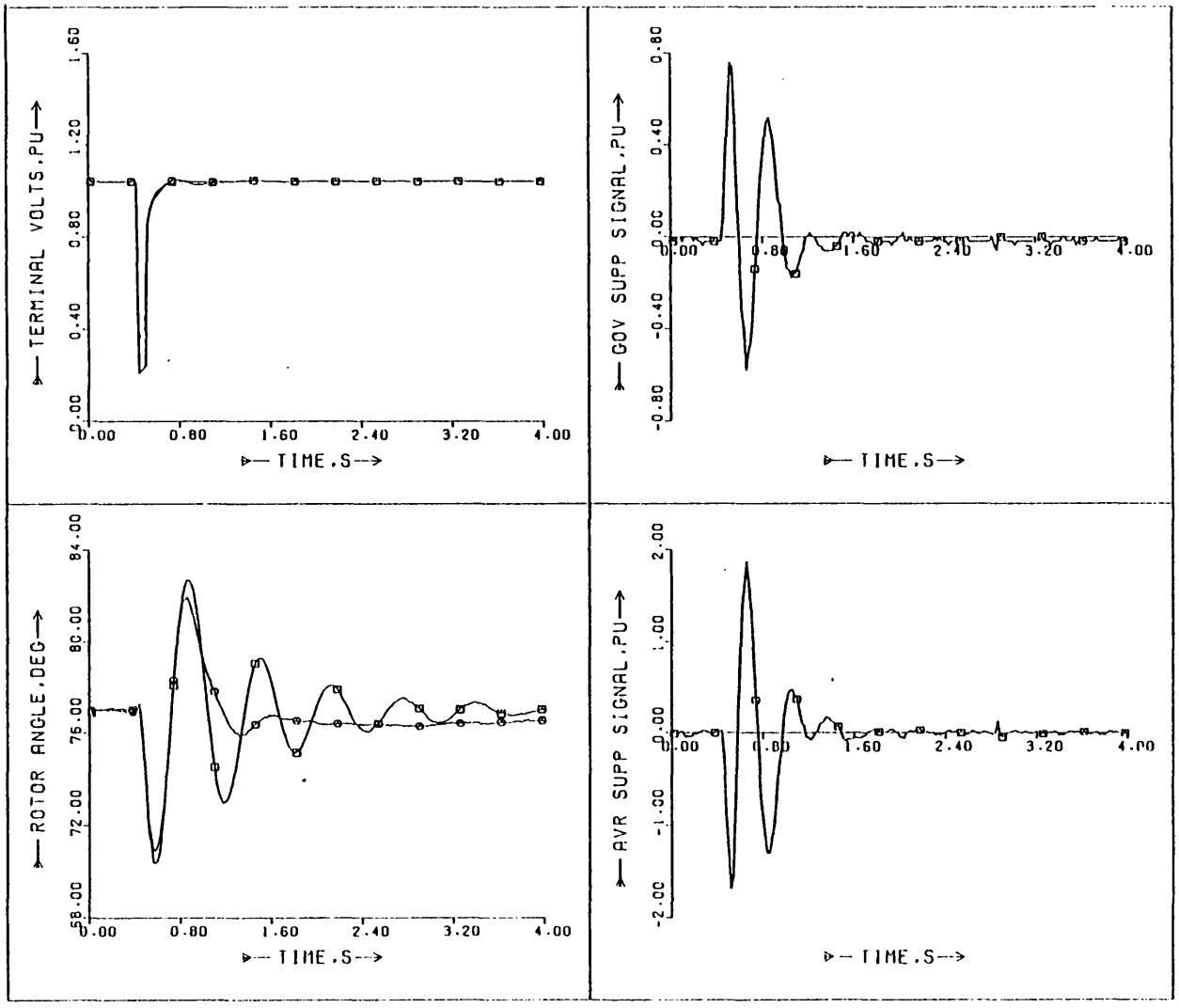

Fig. 6.4: Measured responses o - with and □ - without a 12th order controller measuring load angle and field voltage to a line-line fault of 100 ms.

The response without supplementary control to the switching out of a line, Fig. 6.5, is much more oscillatory than in the previous tests since the high tie-line impedance causes the system to verge on dynamic instability. However, with the controller [designed for the pre-fault operating point and line impedance] the system stabilises to the new angle much more rapidly following the line switching. Note that the jaggedness of the terminal voltage and supplementary signal plots in Fig. 6.5 and some other figures is mainly due to the low resolution [8 bits] of the analogue/digital inputs to the Nova data acquisition system.

6.4.5 Short circuit and loss of a transmission line, conditions as in 6.4.4

A 100 ms three-phase fault was applied to the microalternator, and simultaneously one of the transmission lines was removed giving the results, with and without the 12^{th} order estimator/controller, in Fig. 6.6. As in 6.4.4 the post-fault response without supplementary control is extremely oscillatory. Applying the control reduces the first load angle swing by about 5 degrees and damps oscillations almost to zero 3 seconds after the fault. Oscillations in the terminal voltage are also noticeably reduced.

Note that the modelling here of the fault and loss of line is not completely realistic because the transmission line is actually lost a short time before the fault, instead of on fault removal as would happen in a real system. This is due to practical difficulties with the fault application equipment, and is why the backswing occurs after the angle has started increasing. However, apart from this the response is very similar to that which would be expected for post-fault line removal.

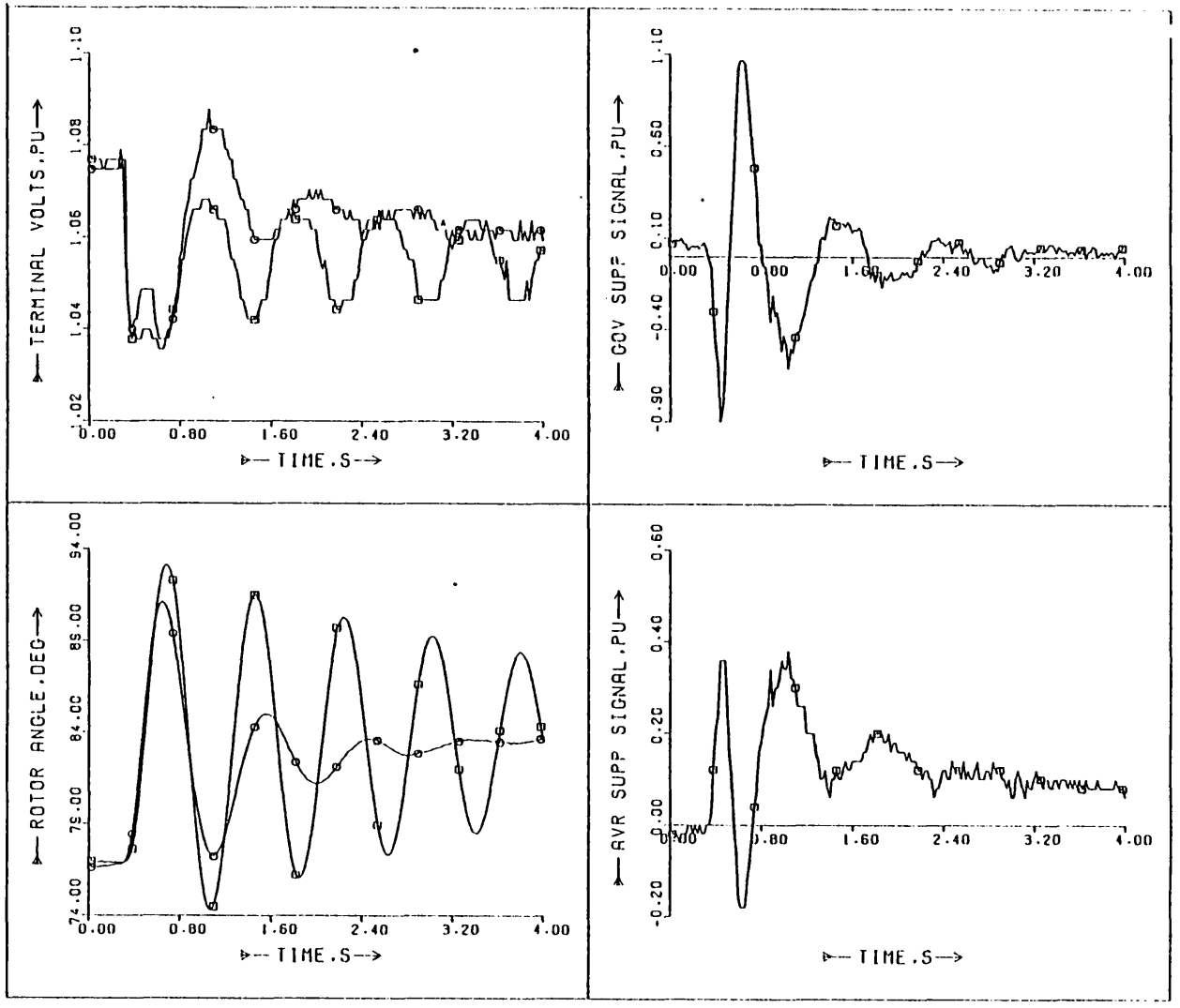

Fig. 6.5: Measured responses to the switching out of a transmission line o - with and □ - without a supplementary 12th order controller measuring load angle and field voltage.

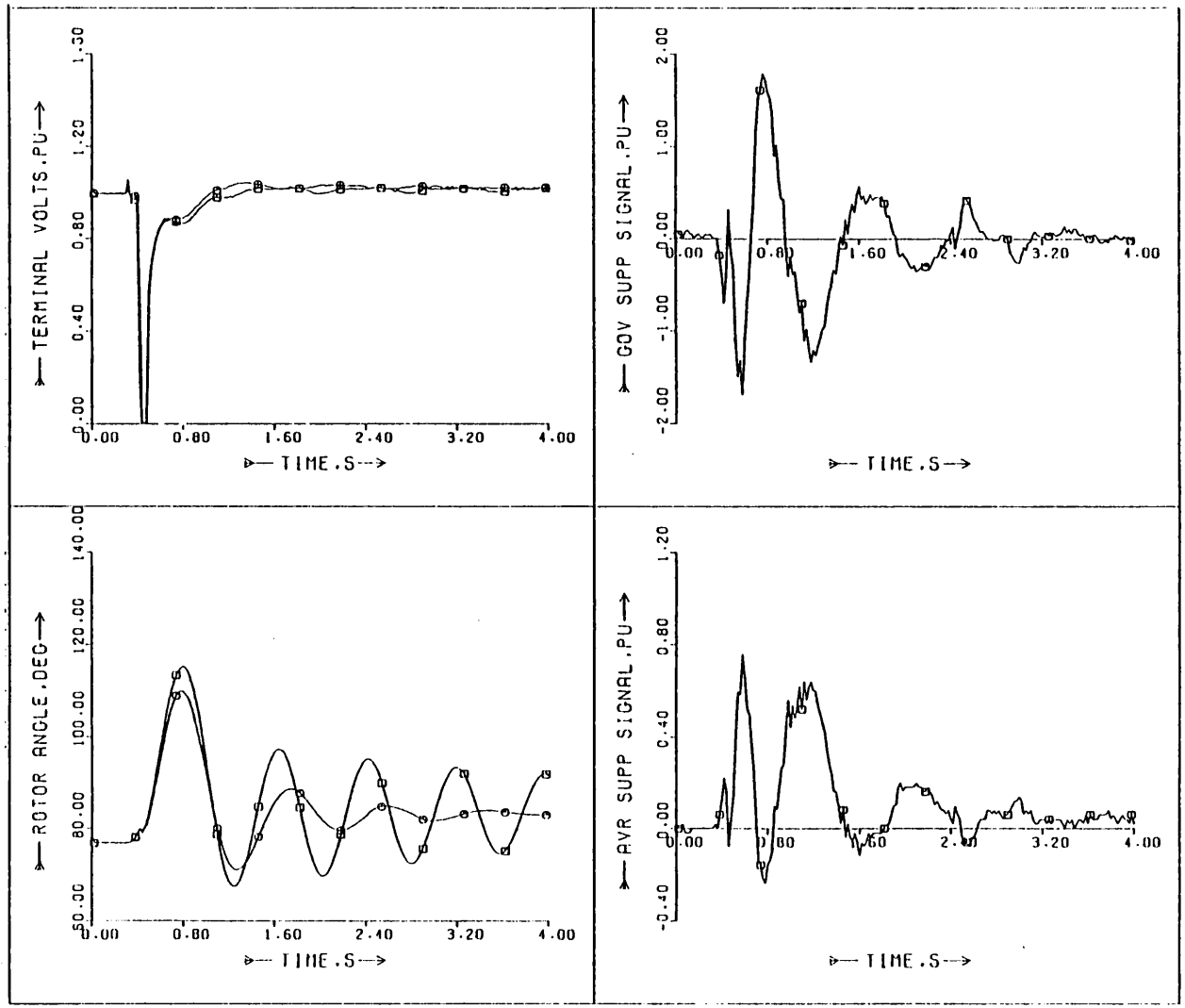

Fig. 6.6: Measured responses to a 100 ms fault and the switching out of a transmission line o - with and □ - without a supplementary 12th order controller.

6.4.6 Effectiveness of the 12th order controller at different operating points

Three-phase faults of 100 ms duration, without loss of a line and with the line impedance given in Appendix H, were applied to the microalternator at six different points over the operation region. The rotor angle responses with and without supplementary control at each of these points are given in Fig. 6.7, where the 12th order controller measures load angle to the busbar and field voltage and has fixed gains calculated at the design point of P = - 0.8, Q = 0.0.

The results are similar to those predicted by computer simulations, the controller working well for leading and lagging power factors at P = - 0.8 and P = - 0.5. At P = - 0.3, Q = 0.0 little improvement is made; the machine is already well behaved at this point without supplementary control. This gives practical verification that a fixed gain state estimator/optimal controller is effective for a wide range of operating points, except with low real power output.

6.4.7 Comparison of different order controllers

In Fig. 6.8 a comparison between LQG controllers designed from 12th, 9th, 7th and optimally reduced 4th order machine models is given, all of which measure rotor angle and field voltage. All the controllers give a considerable improvement over no supplementary control, but it is quite clear that the 12th order estimator/controller gives the best, almost deat-beat response. The 9th and optimally reduced 4th order controllers give similar responses, but the 4th order gives quicker recovery to steady-state conditions.

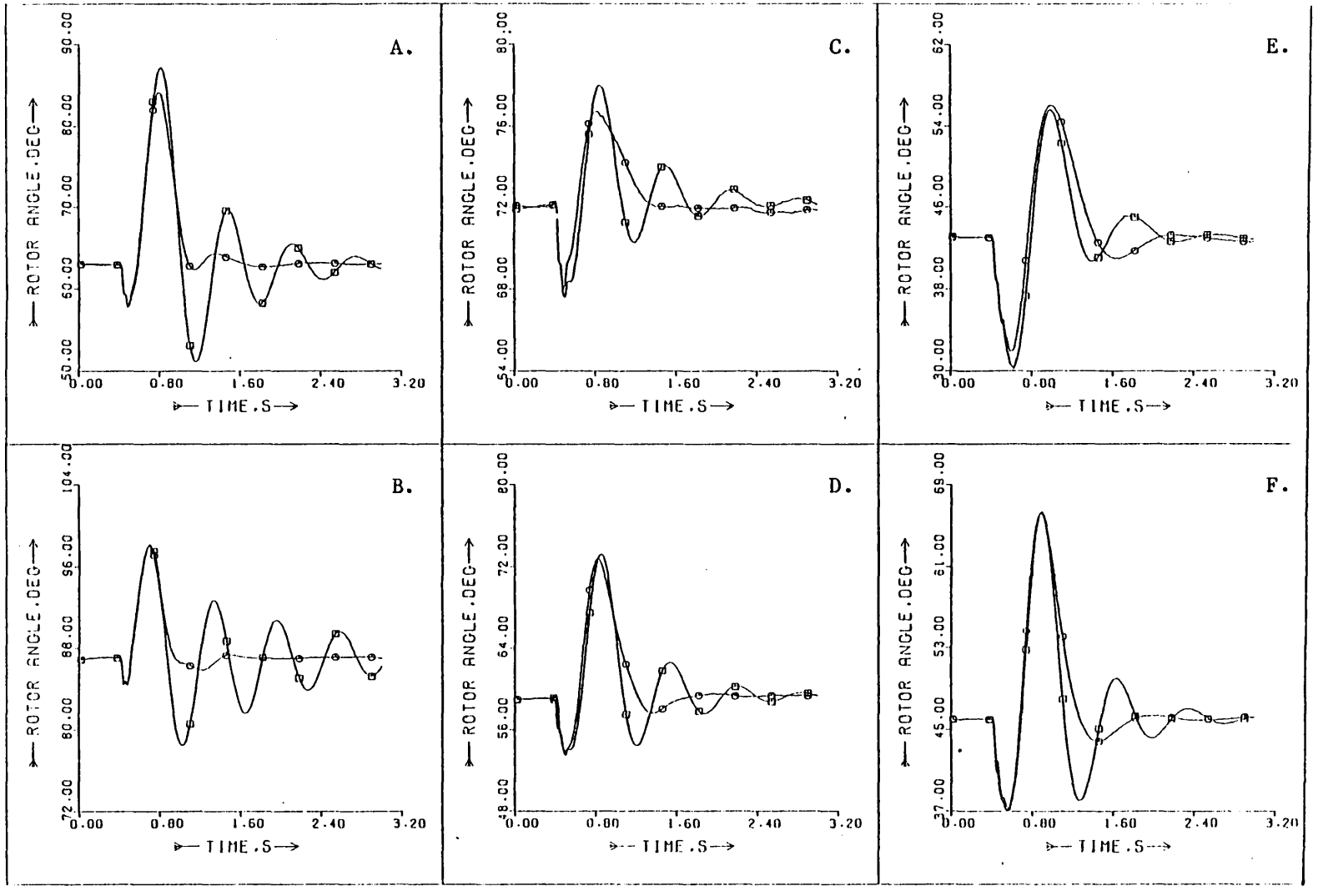

Fig. 6.7: Effectiveness of the 12th order controller designed at P=-0.8,Q=0.0 at different operating points (standard fault). A: P=-0.8,Q=-0.2; B: P=-0.8,Q=+0.2; C: P=-0.5,Q=+0.2; D: P=-0.5,Q=-0.0; E: P=-0.3,Q=0.0; F: P=-0.5,Q=-0.2. o - with and □ - without controller.

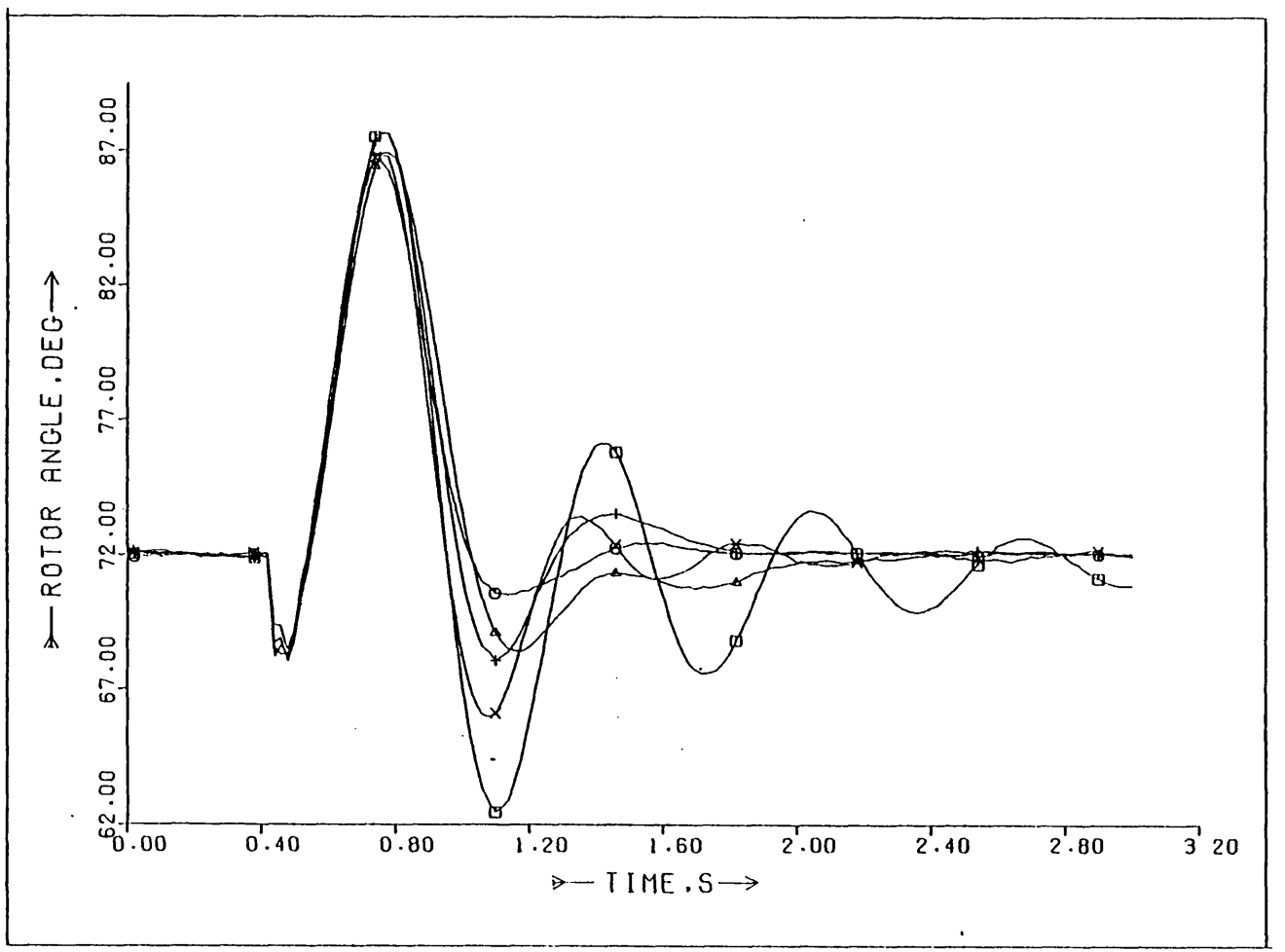

Fig. 6.8: Comparison of measured responses to a 100 ms 3-phase fault. o - 12th order controller; Δ - 9th order controller, X - 7th order controller; + - optimally reduced 4th order controller; □ - no supplementary control.

The response with the 7^{th} order estimator and controller is slightly less-well damped, with no reduction in the first rotor angle swing.

It should be pointed out that each controller was individually tuned on-line to give best results. Fig. 6.8 therefore gives a comparison of the best responses achievable practically with the different orders of estimator/controller.

6.4.8 Effectiveness of the 4^{th} order optimally reduced controller at different operating points

The 4^{th} order optimally reduced controller was tested at six different operating points in the same way as the 12^{th} order controller in Section 6.4.6 to establish whether sensitivity to changes in operating condition is greater than that of higher order models. The results in Fig. 6.9 show that this is not so. Although in general the controller gives a less well damped response compared with Fig. 6.7, the performance is good at all the operating points considered, and is better than that of the 12^{th} order controller at $P = -0.3$, $Q = 0.0$. These discrepancies may be attributed partly to slight differences between the optional regulator and Kalman filter weighting matrices selected to give best results, and partly due to the error in reducing the model order. Generally, though, the optimally reduced 4^{th} order controller seems to perform almost as well as the full 12^{th} order controller away from the design operating point.

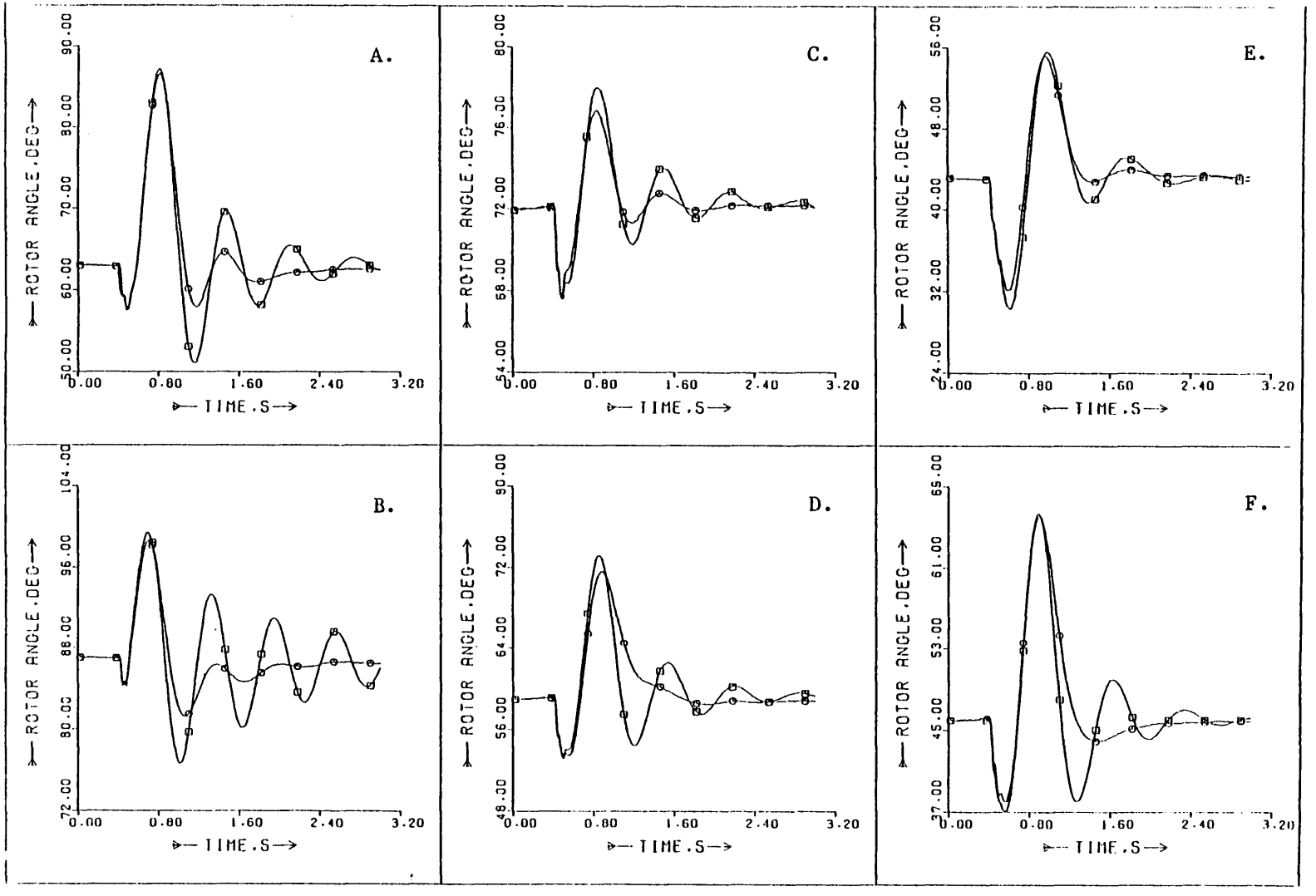

Fig. 6.9: Effectiveness of the optimally reduced 4th order controller designed at P=-0.8,Q=0.0 at different operating points: A: P=-0.8,Q=-0.2; B: P=-0.8,Q=+0.2; C: P=-0.5,Q=+0.2, D: P=-0.5,Q=-0.0; E: P=-0.3,Q=0.0 F: P=-0.5,Q=-0.2 o - with and □ - without controller.

6.5 PRACTICAL TESTS ON STATE ESTIMATORS/OPTIMAL CONTROLLERS MEASURING SIGNALS OTHER THAN ROTOR ANGLE

6.5.1 Rate of change of load angle and field voltage - effect of noise

A simple practical method of determining the rate of change of load angle is by taking the difference between successive samples and dividing by the time interval. This numerical differentiation is ordinarily not a good method of speed measurement and results in a noisy signal, but enables the controller performances with high transducer noise to be investigated.

Fig. 6.10 shows the results when a standard 100 ms three-phase fault is applied to the laboratory system with a 12^{th} order controller measuring V_f and $\dot{\delta}$ by this method. Although not as well damped as when the relatively noise-free rotor angle measurement is used [Fig. 6.2] the response is still very good. Thus noise levels much higher than those likely to be encountered in the field do not badly degrade the controller performance.

6.5.2 Terminal power and field voltage

The response of the laboratory power system to a 100 ms three-phase fault is given in Fig. 6.11, where terminal power and field voltage are used as inputs to a 7^{th} order estimator and controller. Details of the power transducer are given in Section 5.7.2. During the fault itself, the terminal real power falls to zero resulting in large estimation errors, but the net result is a large negative supplementary signal to the governor loop and a positive one to the AVR loop. This gives a very good reduction in the first swing

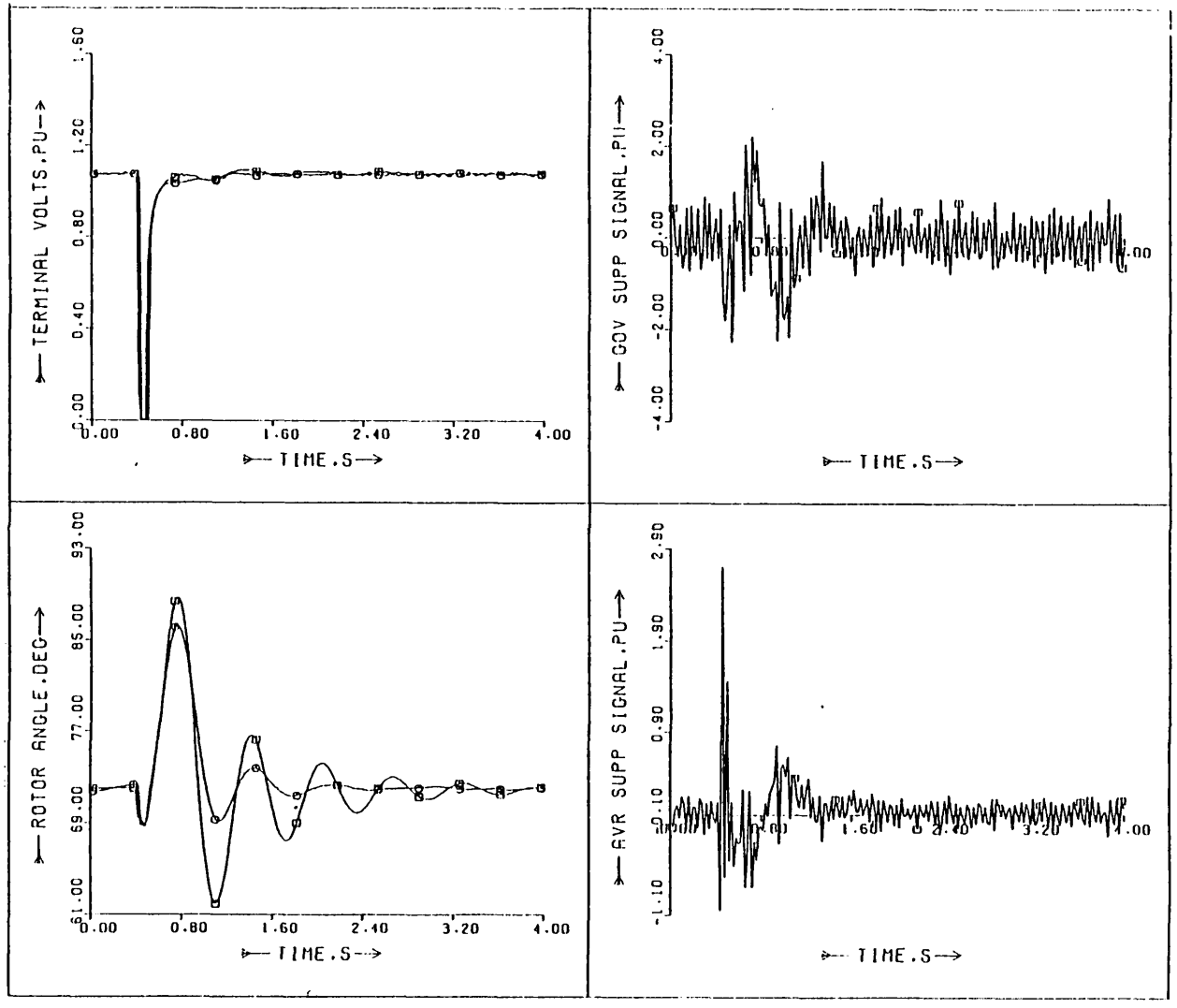

Fig. 6.10: Measured responses to a standard 100 ms fault o - with and □ - without a 12th order controller measuring a noisy rate of change of load angle signal and field voltage.

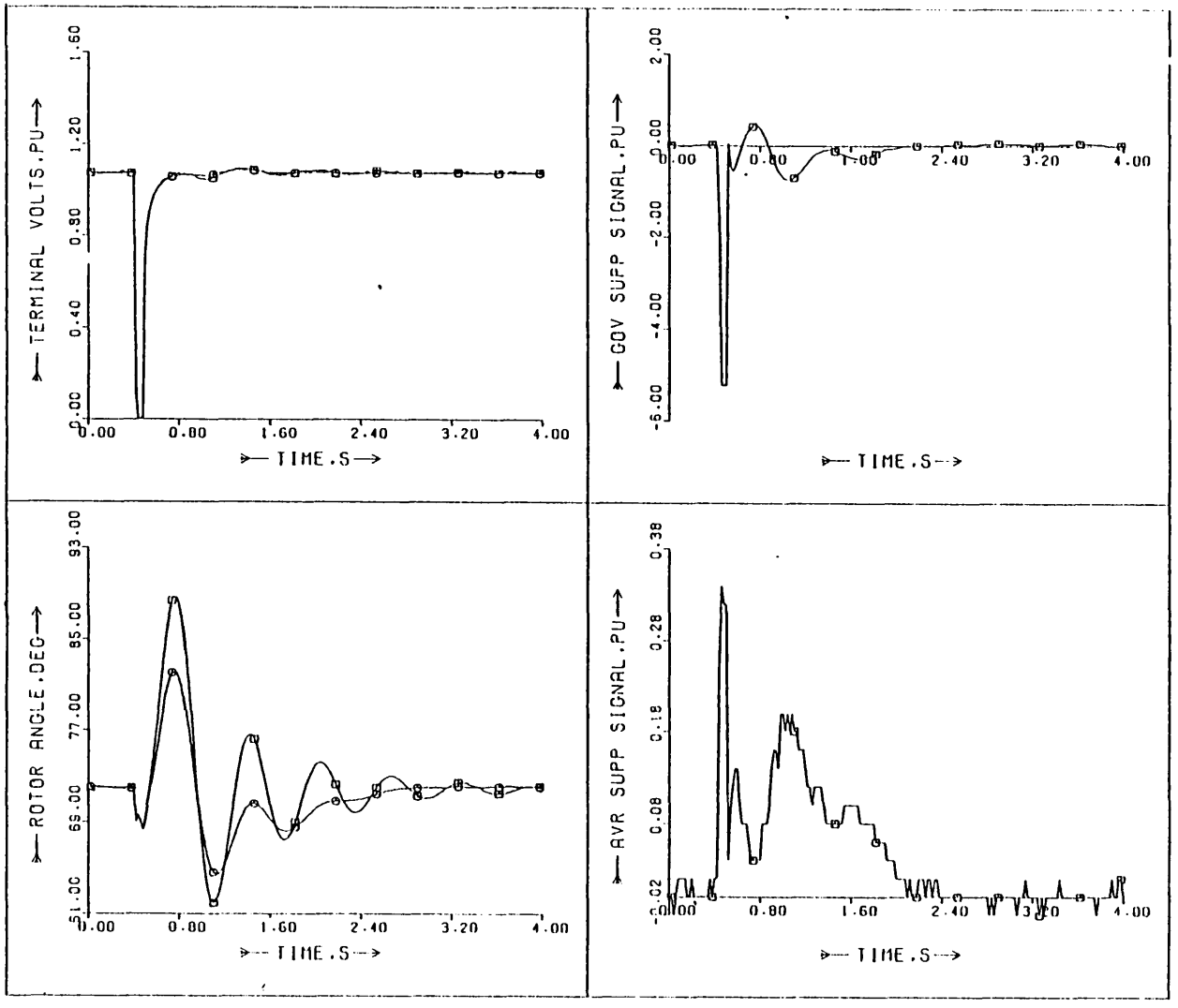

Fig. 6.11: Measured responses to a standard 100 ms fault o - with and □ - without a 7th order controller measuring terminal power and field voltage.

of about 6°, and although the subsequent return to steady-state is slower than when load angle is used, the response is better than predicted in computer simulations [Fig. 4.12]. This is thought to be mainly due to the better natural damping of the micromachine as explained in Section 6.3.

The system response with the same controller to a three-phase fault with loss of one line is given in Fig. 6.12. The first angle reduction of 13° is more than that obtained with controllers measuring rotor angle or its rate of change for the same reasons as above. Despite the change in external reactance the power/field voltage based controller gives good post-fault damping and allows the machine to settle to the new angle. Thus, the extra linearised terms in the output or "C" matrix required when power is measured do not degrade the controller performance badly when changes in tie-line impedance occur.

6.5.3 Terminal power and terminal voltage

Terminal power and terminal voltage, considered by utilities and manufacturers to be convenient stabilising signals [see Section 4.7.2], were used as inputs for a 12^{th} order estimator/controller giving the test results in Fig. 6.13 for a standard 100 ms fault. As with power and field voltage, a good reduction in the first swing [about 5°] is obtained for similar reasons. The response is again slightly better than predicted by simulations with a smaller second negative swing. This controller was found to be more sensitive to the choice of the digital washout filter coefficients than other controllers, and careful tuning was required to give the response in Fig. 6.13. This sensitivity is thought to be the effect

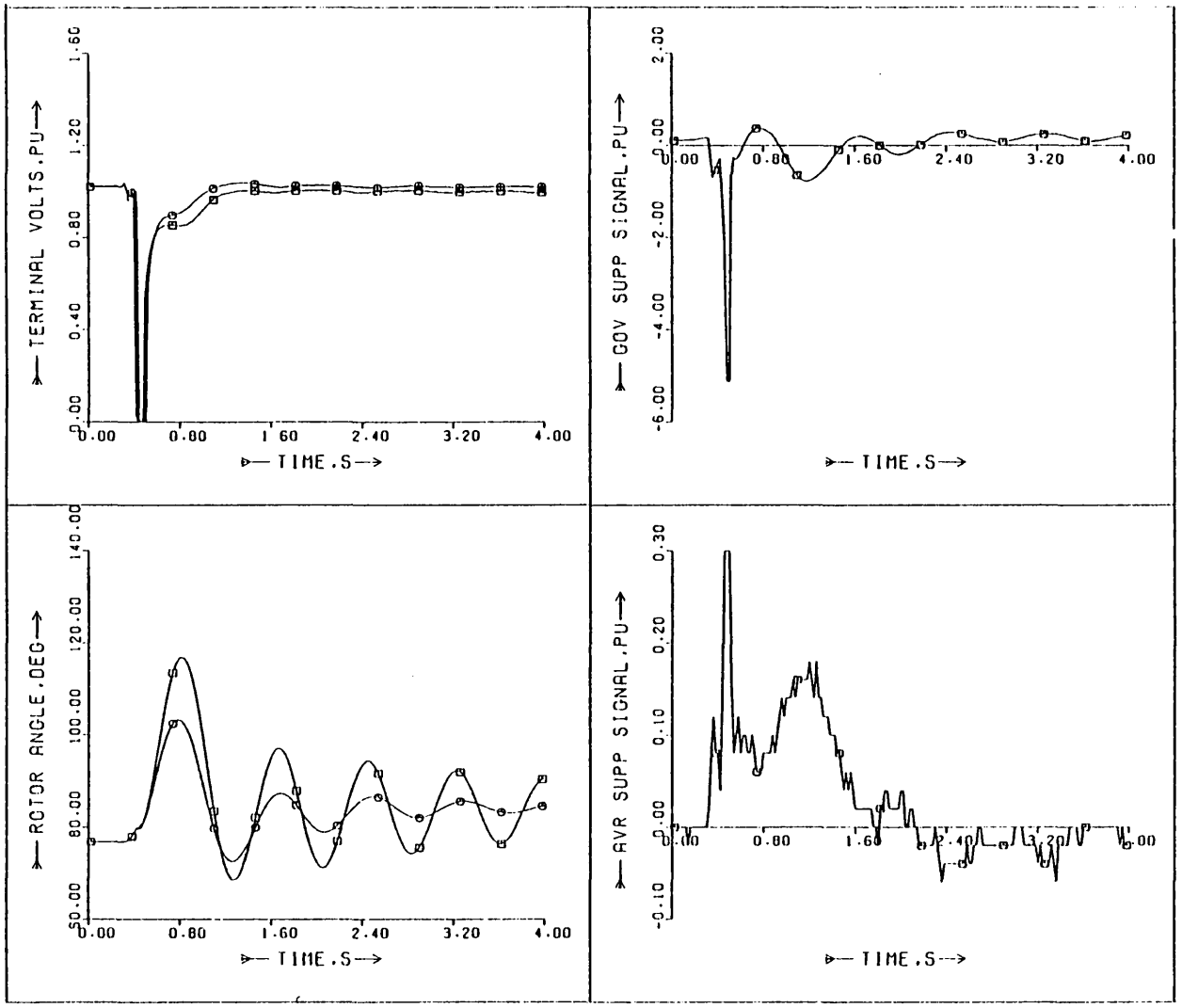

Fig. 6.12: As Fig. 6.11 but with loss of a line after the fault. o - with and □ - without controller.

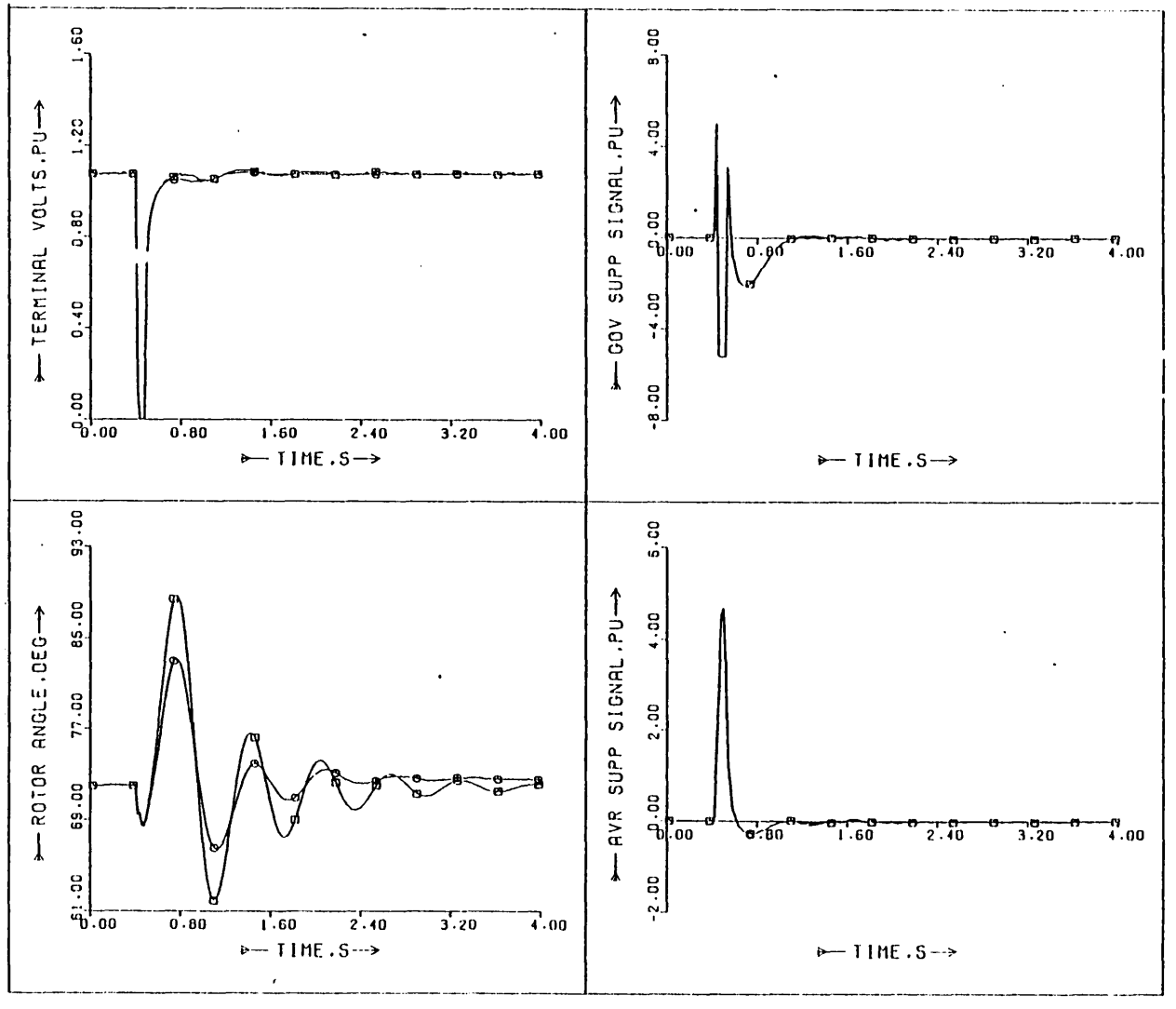

Fig. 6.13: Measured responses to a 100 ms fault o - with and □ - without a 12th order controller measuring terminal power and terminal voltage.

on the low-pass component of the washout filter when power and terminal voltage abruptly decrease to zero during the fault.

6.6 EXPERIMENTAL TESTS ON ESTIMATORS/CONTROLLERS GIVING A SUPPLEMENTARY SIGNAL TO THE AVR ONLY

6.6.1 Controller measuring load angle and field voltage

Fig. 6.14 shows the measured response to a 100 ms three-phase fault when a 12^{th} order controller measuring rotor angle and field voltage is applied, giving a supplementary signal to the voltage regulator only. Little change is made to the first rotor angle swing since supplementary prime-mover control is not available, but thereafter damping is almost as good as with control signals to both inputs. A higher gain is required than that giving the best response with supplementary signals to both control loops. This configuration would seem to make a very good supplementary excitation controller, were it not for the difficulties in measuring load angle on site [Section 4.7.2].

6.6.2 Controller measuring terminal power and terminal voltage

The response of the machine with an excitation-only controller and estimator based on terminal power and terminal voltage to a standard 100 ms fault is given in Fig. 6.15. During the fault the estimator/controller gives a high boost to the field resulting in a slight decrease in the first swing. Damping is not as good as with the previous controller but overall, the performance is very good with better results than predicted theoretically. Once again careful choice of the digital washout filter coefficients was

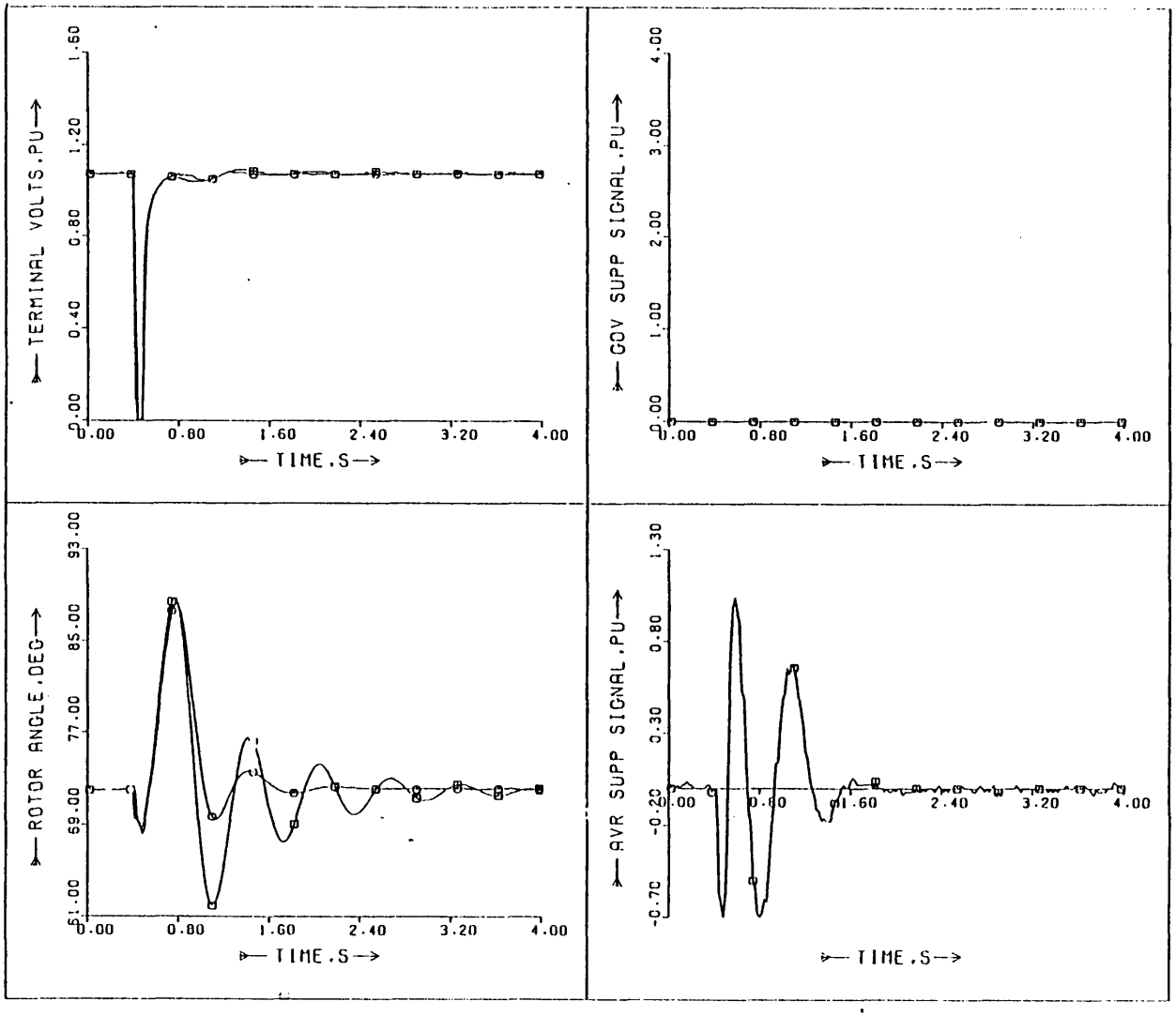

Fig. 6.14: Measured responses to a 100 ms fault o - with and □ - without a 12th order AVR-only controller measuring load angle and field voltage.

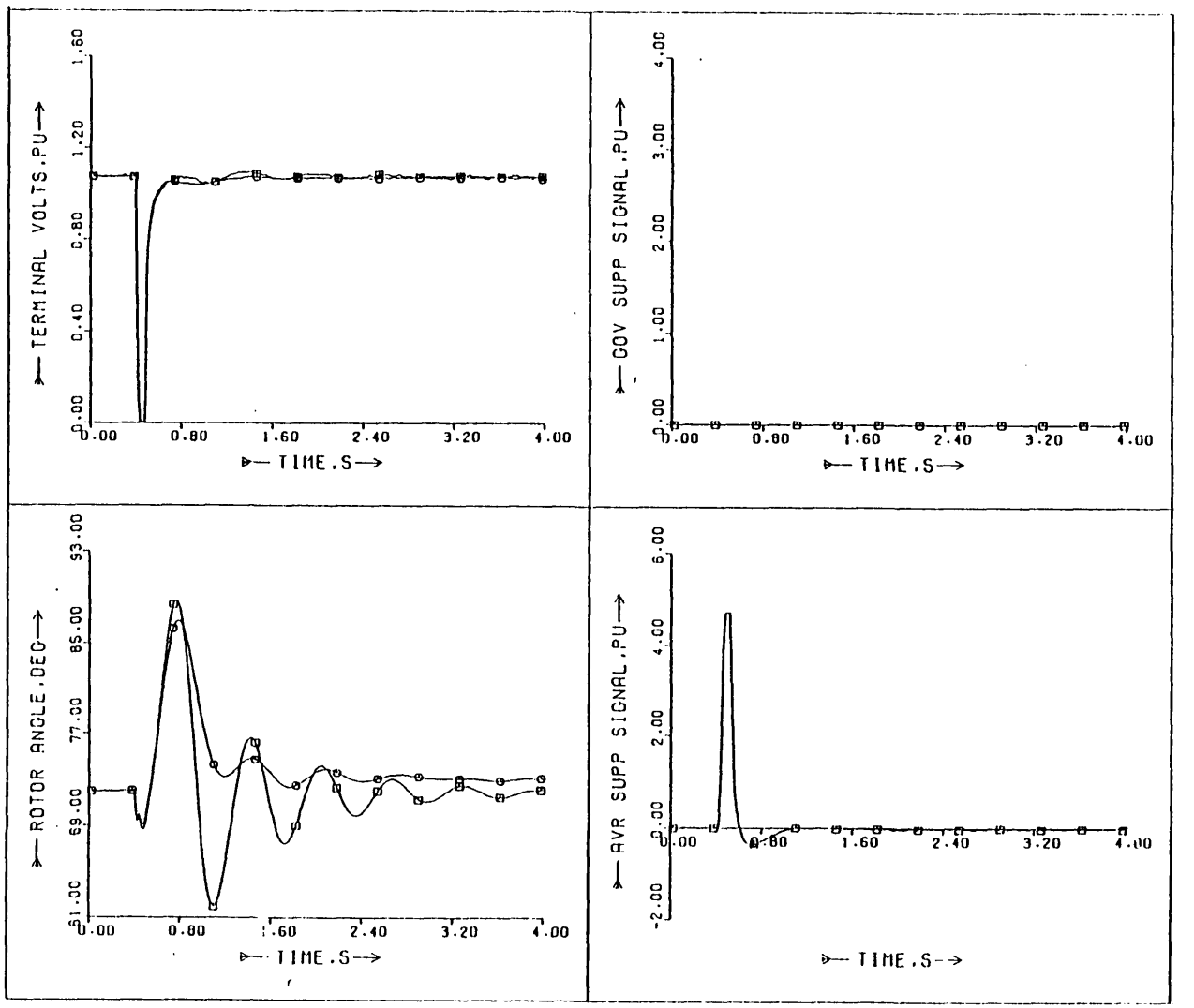

Fig. 6.15: Measured responses to a 100 ms fault o - with and □ - without a 12th order AVR-only controller measuring terminal power and terminal voltage.

essential for good performance.

The results of both this and the previous test show that excitation control gives the main contribution to the damping of rotor oscillations, and prime-mover control can assist with reducing the first swing. With slower governing systems than that considered here the contribution to optimal control possible from the supplementary signal to the governor is likely to be so small that excitation-only controllers would seem to be preferable.

6.7 OTHER RESULTS OF INTEREST

6.7.1 Torsional shaft vibrations

An interesting discovery during the initial part of the experimental work was that sustained torsional oscillations could be excited on the micromachine by the original 9^{th} order controller implementation. The measured signals were load angle and field voltage. The oscillations occurred because the shaft which transmitted drive from the D.C. motor to the alternator incorporated a torque transducer and could not be assumed to be completely rigid. The problem was aggravated at that stage of the project by having a noisy load angle signal and controller output scaling that resulted in very high gains. The oscillations, at a frequency of about 25-30 Hz, disappeared when the torque transducer coupling was replaced by the stiffer conventional shaft.

Fig. 6.16 shows the measured swing curves of the micromachine with the flexible shaft, with and without the 12^{th} order

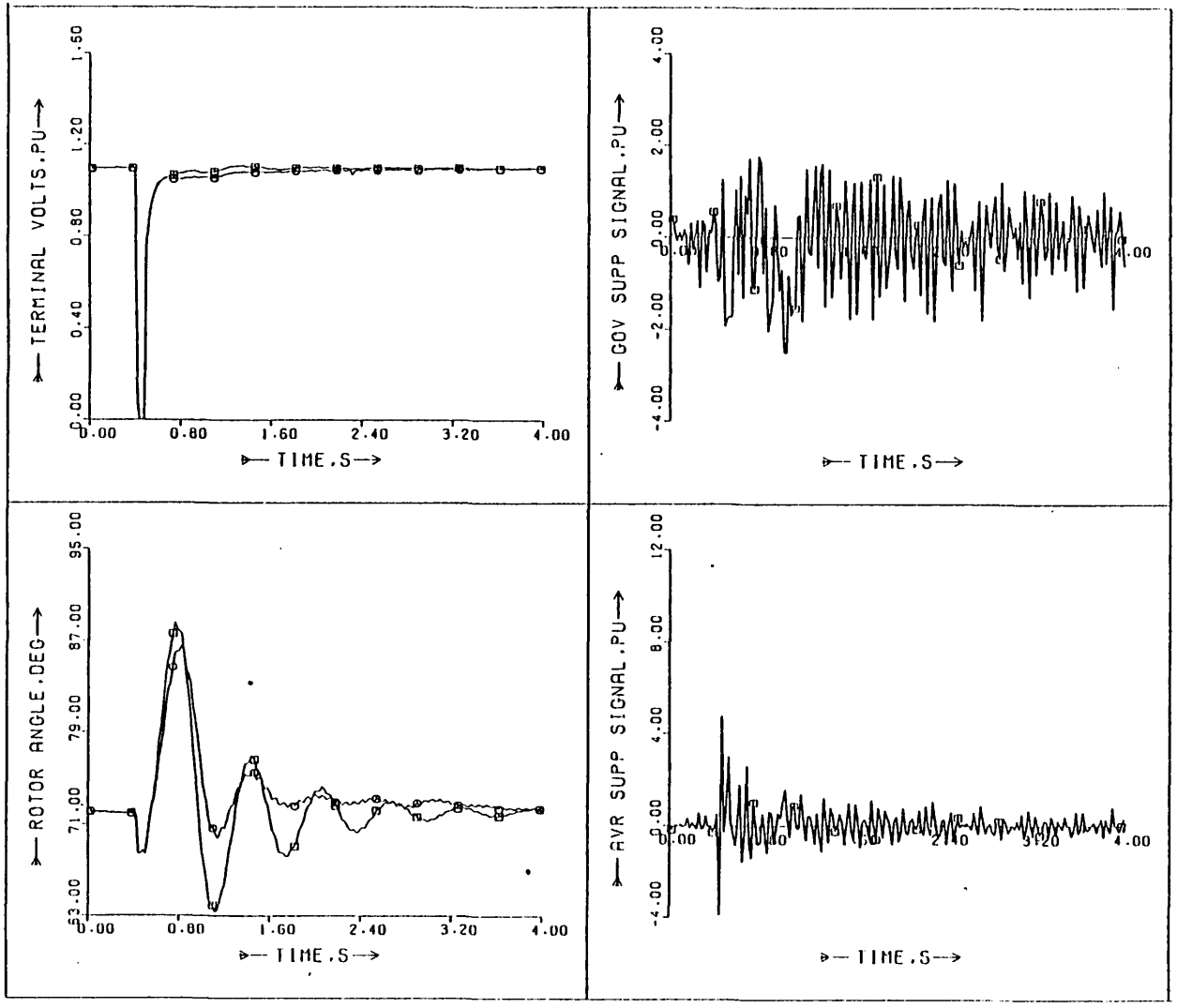

Fig. 6.16: Measured responses of the micromachine with a flexible coupling shaft to a 100 ms fault o - with and □ - without a 12th order controller measuring a noisy rate of change of load angle signal and field voltage.

controller measuring the rate of change of load angle and field voltage. The controller was identical to that used in Section 6.5.1.

From past field experience speed seems to be the worst signal to feed back where torsional oscillations are concerned[35]. The shaft oscillations are clearly visible in the rotor angle measurements [Fig. 6.16] both with and without supplementary control, but the action of the controller in aiding post-fault stabilisation is not degraded significantly when compared with the rigid-shaft system [Fig. 6.10]. Damping of the torsional oscillations does not seem to be very good in either case, but from Fig. 6.16 it is not clear whether the controller is making the situation better or worse.

A better comparison of the average torsional oscillation amplitudes over a period of time may be made by taking a fast Fourier transform [F.F.T., see ref. 131] of the measured angle data. Fig. 6.17 shows F.F.T.'s taken of the rotor angle measurements with the flexible shaft and with:

a] a 12^{th} order controller measuring speed and field voltage;

b] no supplementary control;

c] a 12^{th} order controller measuring load angle and field voltage; and

d] with the rigid shaft and no supplementary control.

256 points for 2.56 sec after the fault were used in all F.F.T.'s taken here with Hanning windowing to enhance amplitude resolution. The dB scale is taken with reference to unit amplitude.

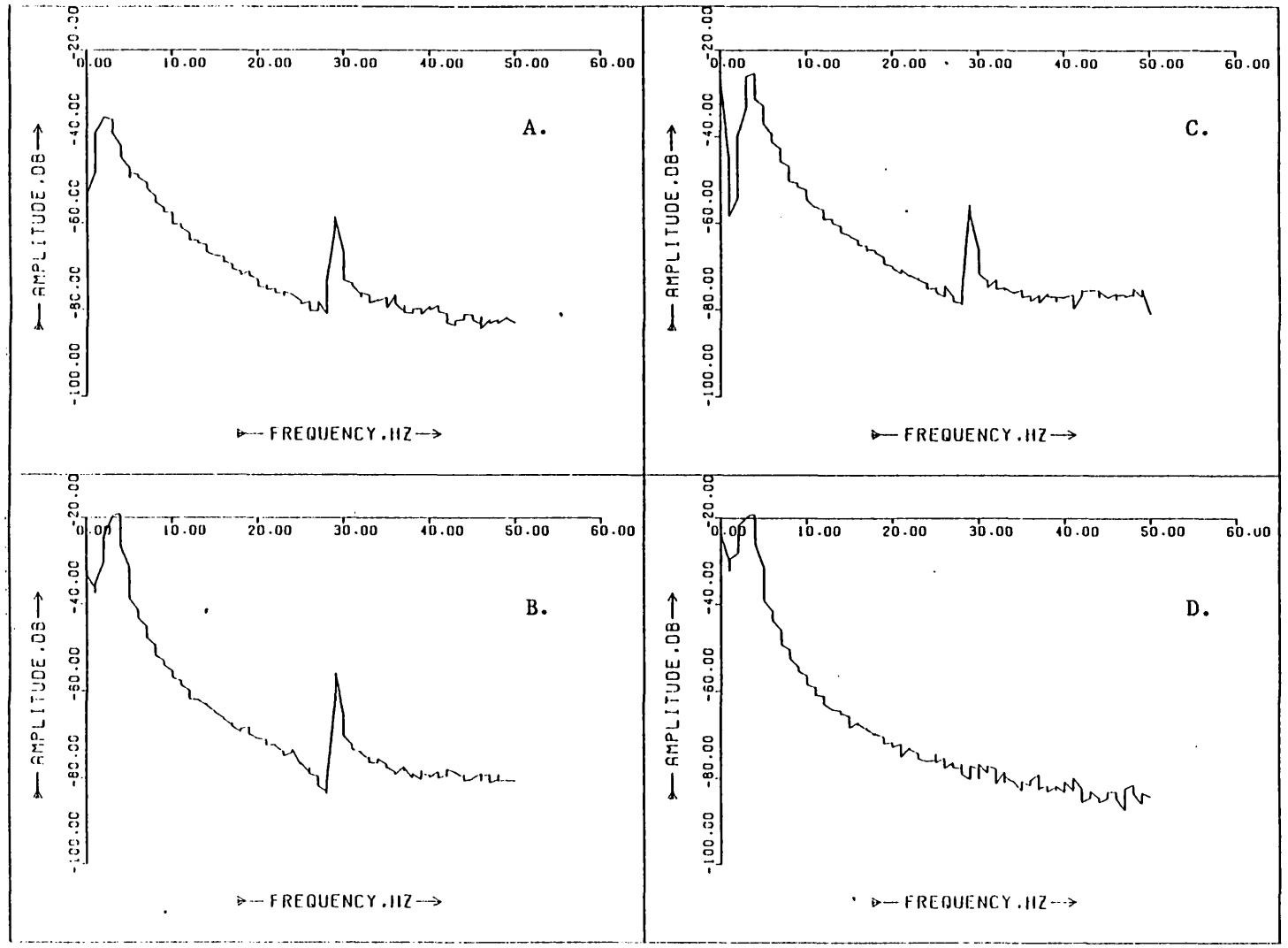

Fig. 6.17: Fast Fourier transforms of micromachine rotor angle with a flexible shaft following a 100 ms 3-phase fault: A: 12th order controller measuring rate of change of load angle and field voltage; B: no supplementary control; C: 12th order controller measuring load angle and field voltage; D: FFT without flexible shaft or controller.

The low frequency peaks in Fig. 6.17a-d are associated with the natural frequency rotor oscillations [2-3 Hz]. In graphs a, b and c a second peak is visible at about 28 Hz which is the torsional oscillation component in the rotor angle measurements, and is absent when the rigid shaft is used [graph d]. Comparing Fig. 6.17a, b and c shows that this peak rises to about - 55 dB in each case, thus the controllers seem to make little difference to the average amplitude of the torsional oscillations during the period considered. Thus at least it may be concluded that the controllers, even where a noisy speed signal is measured, do not worsen torsional oscillations when the correct gains are used. Although this is not a realistic model of the shaft dynamics of a real turbine-generator, a coupling of the appropriate stiffness could be used to simulate the most critical mode of the torsional vibrations present in the full-size machine.

6.7.2 Performance of the controllers when a detailed governor/turbine model is used

All the tests so far described have been performed using a simple two time-constant governor/turbine model [Section 5.3.1]. Here the detailed simulation circuit described in Section 5.3.2 was substituted for the simple model to ascertain how the controller behaved with a more realistic prime-mover model.

A comparison of the rotor angle and terminal voltage behaviour of the micromachine following a 100 ms three-phase fault is given in Fig. 6.18, when either the simple or the detailed turbine simulator is used. There is little difference between the two responses, the main one being the natural frequency of the rotor

oscillations and slightly greater damping with the detailed simulator. The terminal voltage responses were virtually identical. The close agreement between the two sets of results shows that for most purposes the representation of governor and turbine by two appropriately chosen time delays is justified. A minor modification in the simple governor/turbine model to the time constants would make the period of oscillations the same.

The action of a 12^{th} order controller measuring load angle and field voltage on the micromachine following a 100 ms three-phase fault under standard conditions with the detailed governor/turbine model is shown in Fig. 6.19. The controller was identical to that in Section 6.4.1 which was designed using a simple turbine model. Although slightly inferior to the response when the turbine simulation is simplified [Fig. 6.2], the controller is nonetheless very effective in reducing the first load angle excursion and damping system oscillations. This is not a surprising result in view of the similarity in performance between the two turbine/governor simulations, but it does show that valid simplifications of the turbine model can be made in estimator/controller design as well as in modelling.

6.7.3 Contribution of the state estimators/optimal controllers to dynamic stability

When the single transmission line impedance was increased to the value in Eqn. [6.7], and setting P = -0.83, Q = 0.0, the micromachine became dynamically unstable with oscillations growing to about ±20° relative to the mean rotor angle. Fig. 6.20 shows readings of the load angle and terminal voltage when this occurred, with

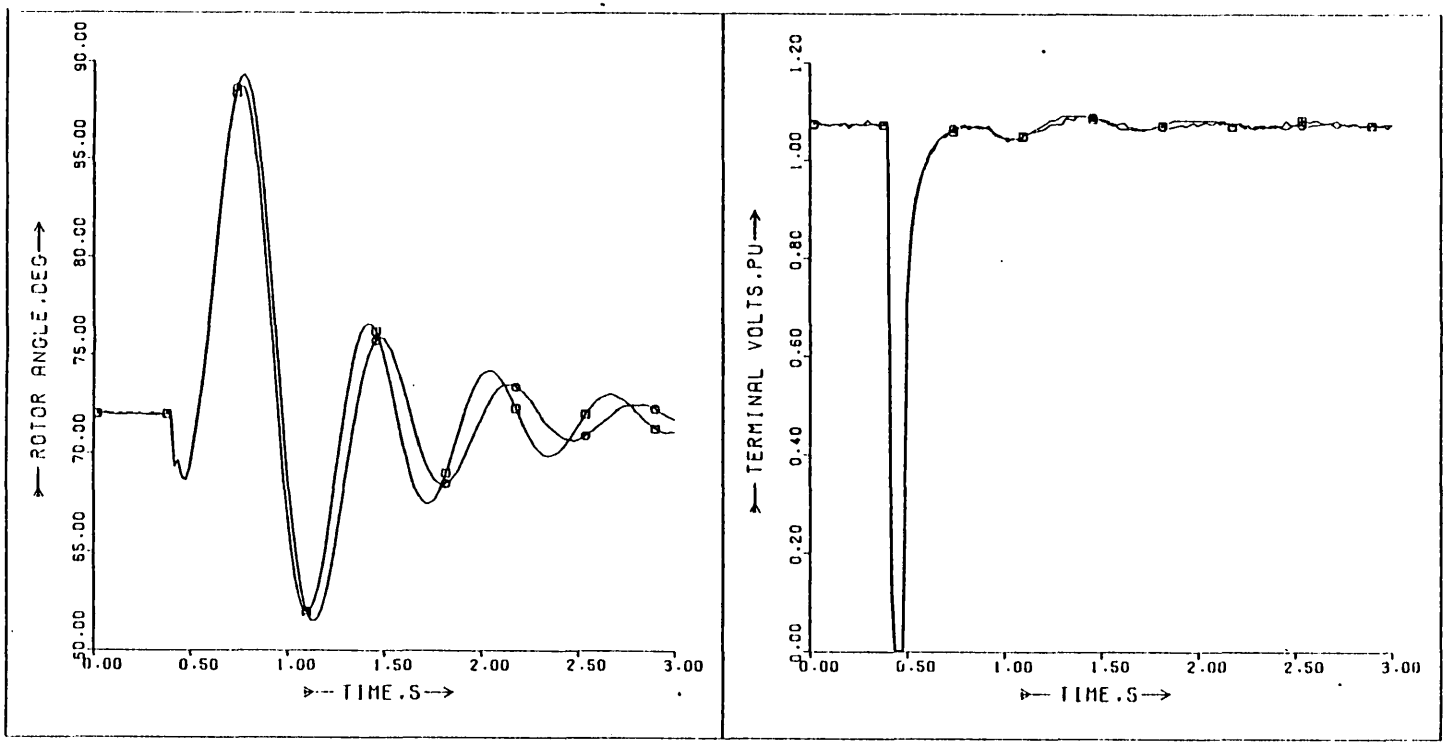

Fig. 6.18: Comparison of measured responses to a 100 ms 3-phase fault with: o - detailed and □ - simple governor/turbine model.

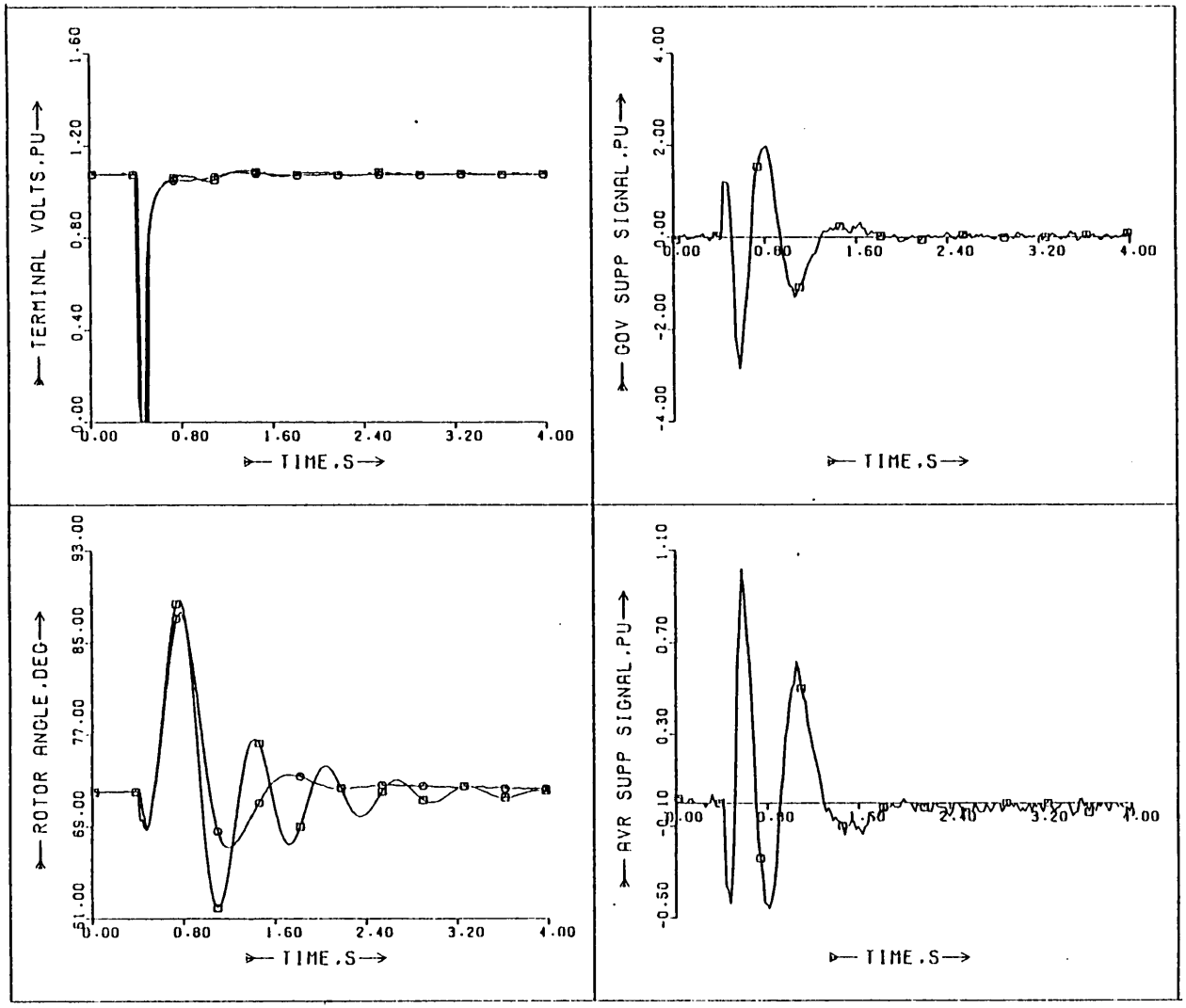

Fig. 6.19: Response of micromachine and detailed governor-turbine model to a 100 ms 3-phase fault o - with and □ - without a 12th order controller measuring load angle and field voltage.

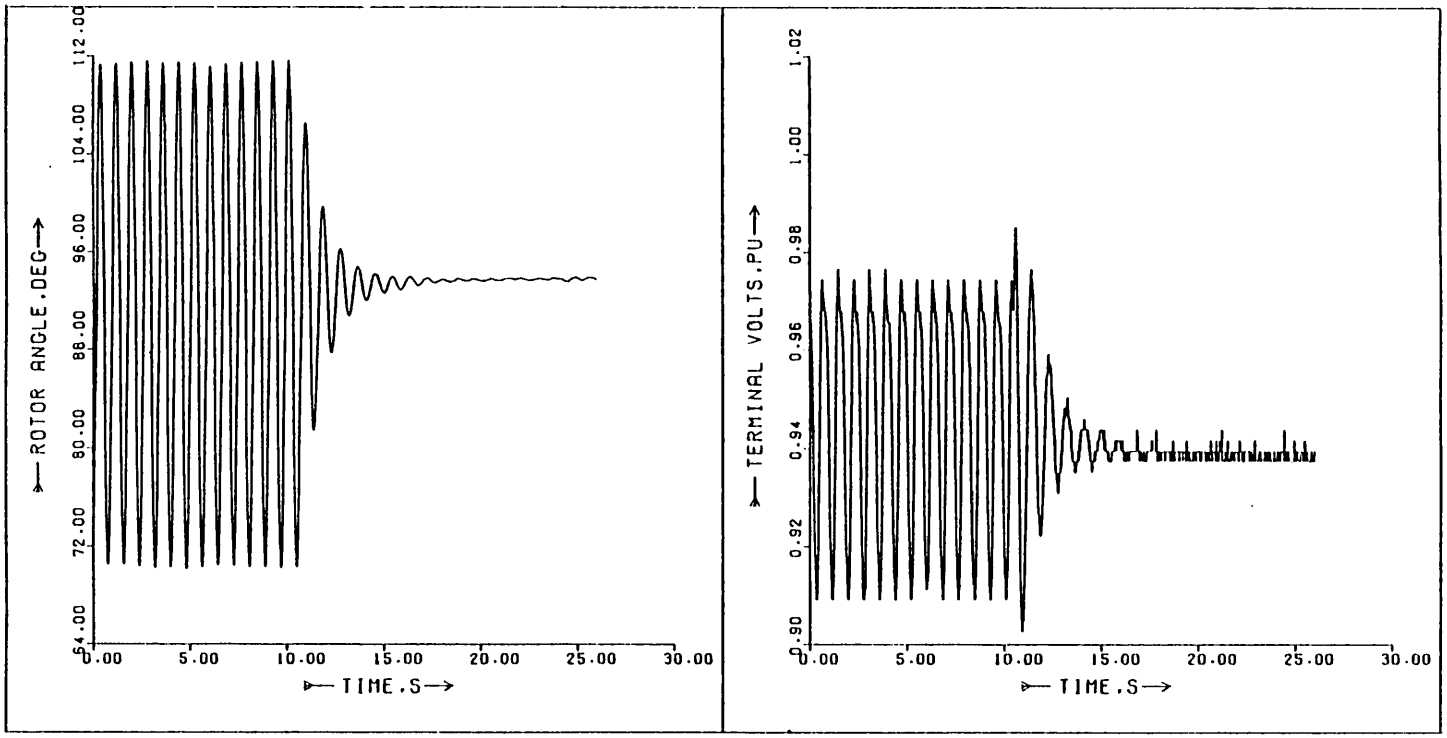

Fig. 6.20: Dynamic instability of the micromachine (P=-0.83,Q=0.0,Ze=0.013+j0.56) and effect of 12th order controller measuring load angle and field voltage switched in after 11 sec.

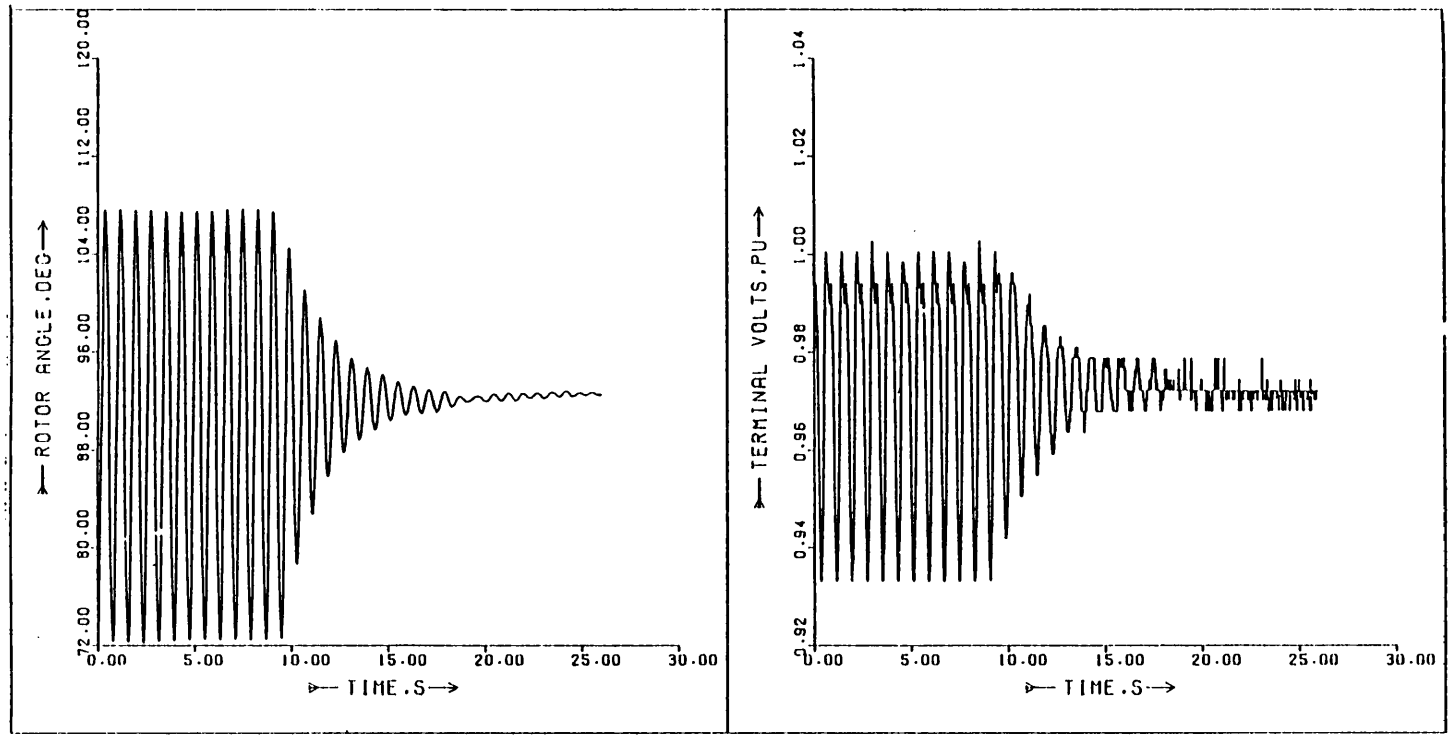

Fig. 6.21: As Fig. 6.20, but with 12th order controller measuring power and terminal voltage switched in after 9.5 sec.

the 12^{th} order controller measuring load angle and field voltage switched in after 11 sec. The controller used the original gains as in Section 6.4.1. The oscillations decay almost completely within 5 sec. Note the slight increase in voltage oscillations immediately after the controller is switched in, but these also are rapidly damped. The poor resolution of the terminal voltage plot is due to the 8-bit analogue/digital interface to the Nova data monitoring computer.

In Fig. 6.21 a 12^{th} order controller measuring power and terminal voltage is switched in after approximately 9 sec. Here the angle oscillations are not so rapidly damped as in Fig. 6.20 and small fluctuations continue. However, both controllers contribute significantly to the dynamic stability of the system.

6.8 CONCLUSIONS

Details of the on-line implementation on a laboratory micromachine of discrete-time state estimators/optimal controllers and the results of a series of tests have been presented here. The estimators/controllers require inputs that are deviations from their steady-state values. Digital washout filtering[73] enables this to be done without assuming constant steady-state conditions. Careful choice of the filter parameters leaves the transient performance of the controller unaffected, but it does not attempt to maintain old operating conditions following load setpoint or line impedance changes.

One of the main drawbacks reported in microcomputer implementations

of many advanced generator control schemes has been the relatively long delay between sampling data from and computing inputs to the laboratory system. Here, using a readily available standard 16-bit microcomputer, programming the algorithm in assembly language and incorporating a hardware floating point multiplier, computation time steps in the order of 10 ms or better have been achieved. These are a factor of 10 better than in previous work on microalternator control by state estimation[13-15], and were shown theoretically to give significantly better control than longer time steps in Section 4.8.3.

The on-line control algorithm has been programmed such that only minor alterations are required to run any order of estimator/controller sampling any two measurements from the machine and giving outputs in the form of supplementary signals to both conventional control loops or to the AVR only. The controller gains are calculated off-line by the solution of Riccati equations as described in Chapter 4, given the system model A, B and C matrices and choices of the optimal regulator and Kalman filter weighting matrices.

A comparison of calculated and measured responses for the micromachine after it has been subjected to a 100 ms three-phase fault revealed two discrepancies: firstly there was a greater than expected angular backswing in the measurements and, secondly, more damping than predicted. Further tests showed that mechanical shaft damping could not be neglected in the micromachine, although it is commonly omitted in simulations of large machines, and including the damping factor in mathematical models reduces the second source of discrepancy. The differences in angular backswing remain and are thought to be either due to amplifier saturation in the time constant regulator circuit during the

fault or incorrect damper winding parameters. Further study is needed on this point and on the adequacy of modelling generally but even so, the agreement achieved confirms that the controllers are based on a reasonably good model of the system.

The first controller tests presented here were carried out with a 12^{th} order estimator/controller measuring load angle and field voltage. As predicted in simulations [Chapter 4] the controller was very effective in damping oscillations in the rotor angle and in reducing the first swing for a 100 ms fault clearance time. For a 450 ms fault the improvement in terminal voltage recovery was also evident. This 12^{th} order controller also performed well for unbalanced faults, the switching out of a transmission line or three-phase faults followed by loss of line.

Experimental comparison of different orders of controller shows a degradation in performance as the model is simplified. However, a controller derived from an optimally reduced 4^{th} order model [obtained by the Hankel-norm method described in Chapter 3] gives a response on a par with that of the 9^{th} order conventionally reduced model. Tests at several different operating points showed that the 12^{th} and 4^{th} order controllers both give a substantial control improvement over conventional loops even well away from the nominal operating point. Thus the complications associated with look-up tables that have been used for lower order state-feedback controllers[71-75] appear to be avoidable here.

More readily accessible generator measurements than load angle to the infinite busbar have been used as a basis for estimation and control. Speed [rate of change of load angle] gave the best theoretical results in

Chapter 4 and here a noisy speed signal with field voltage in a 12^{th} order controller also gave good practical results. The use of terminal power and field voltage, or terminal power and terminal voltage as inputs led to better first-swing reduction than with other controllers. This is due to the high amplitude supplementary signals generated when the controller input signals change abruptly by a large amount during the fault. Damping, however, was not as good as could be achieved with load angle or speed based controllers.

Consideration of controllers giving a supplementary signal to the AVR loop only showed that the main contribution to damping is through the field control, but little change in the first swing magnitude may be expected without supplementary prime-mover control. Thus for older, slower responding speed regulating systems with slower steam valves, or turbines without intercept valves, the additional stability improvement by supplementary governor loop control compared with AVR-only control is likely to be minimal and therefore not worth the expense of modification.

Torsional oscillations due to a flexible motor-alternator coupling shaft were unexpectedly encountered during early tests on the control policy. The problem was aggravated by much higher than necessary gains in the supplementary controller. Later analysis using fast Fourier transform techniques revealed an oscillatory component at 28 Hz not present when a rigid shaft replaced the flexible one. When correct controller gains were used, it appeared that speed or angle and field voltage measuring controllers neither improved nor worsened the torsional oscillations.

A minor degradation of the controller performance is detectable when a detailed governor/turbine simulator is used. Brief dynamic stability studies showed that the estimator/controller prevented the micro-alternator from hunting when attempting to send a high real power through a simulated long transmission line.

CHAPTER 7

CONCLUSIONS

7.1 GENERAL CONCLUSIONS

Turbine-generator stability may be improved by estimating the state-variables of a mathematical model of the machine on a microcomputer, then optimally feeding them back to the plant. Here it has been shown both theoretically and practically that this method of control can substantially increase stability margins following disturbances and rapidly damp system oscillations as compared to conventional governors and AVR's. Inputs to the controller can be any convenient measurements from the generator and outputs are in the form of supplementary signals to one or both existing control loop reference points. This makes the scheme flexible, cost-effective and readily applicable to both new and existing plant.

There are many reasons for attempting to improve generator stability. Apart from the physical damage that may result from loss of synchronism, it is desirable to prevent oscillations spreading throughout the system. Improvement of individual generator stability should make overall system operation more flexible and economic. Furthermore, microcomputers capable of handling complex control algorithms are continuing to come down in price.

Of the many different approaches to generator stability improvement, only self-tuning regulators require no a priori model of the system. These need

low-level noise injections to perform on-line system identification, however, and generally such algorithms have been found to be time-consuming. Linear optimal regulators require a plant model linearised about a nominal operating point, and the approach is to minimise a performance index consisting of weighted deviations of the model states and inputs from their desired steady-state values. With optimal state-feedback controllers, however, there are the conflicting requirements that on the one hand a detailed model is desirable for best control and, on the other, the states of such a model may be physically difficult or even impossible to measure. Hence most practical optimal generator control schemes reported have applied an optimal regulator based on a crude model of only three or four states.

The scheme adopted here involves the estimation of the generator states from any convenient measurements taken from the machine. This may be accomplished by a Kalman filter, based on a discrete-time linearised model of the system, which gives best least-squares estimates of all the system states, given the measurements and assuming white noise. The constraint that the model must consist of measurable states is thus removed, and the highest order representation that executes within the desired time on-line may be selected. Any number of measurements from one upwards may be taken, and they do not have to be state variables.

A nonlinear turbine-generator mathematical model may be constructed with states accounting for the mechanical subsystem, the control loops and the electrical subsystem. Either currents or fluxes may be used as electrical state-variables; they give equivalent representations and both have been considered here. It is concluded that currents are advantageous for simplicity in deriving the linearised output or C-matrix which describes

the mathematical relationship between state-variables and measurements. Both the Kalman filter and the optimal regulator require a linear system model obtained by linearising the generator equations about an operating point. The linearised continuous-time model is then transformed to the discrete-time domain to suit the sampled-data nature of the micro-computer control system.

Recent advances in linear systems theory have shown how a linear model may have its number of state-variables reduced with very little error resulting in input/output properties. The technique, known as optimal Hankel-norm model reduction, is potentially very useful in this type of application where the storage and computation speed requirements of the on-line control computer may be relaxed with very little detriment to the performance. Thus a cheaper computer may be used, or if the algorithm is to be part of a global control/supervisory system more time and storage may be allowed for other functions. To reduce the model order, firstly the system model is balanced, i.e., transformed so that inputs and outputs are equally weighted with respect to the individual states. It is important to realise that the states in a balanced model are generally not physically measurable, but are a transformation of the original states. Truncating a balanced realisation of an n^{th} order system to k states, where $1 \leqslant k < n$, gives a reduced order model which is optimal in the sense that it gives the best relationship between past inputs and future outputs as an approximation to that of the full model. The frequency response error for any reduced-order model is easily calculated from data computed when balancing the system [the Hankel singular-values]. This enables the order of the reduced model to be selected such that very little error is introduced.

The theoretical work of Vaahedi[11,12] on continuous-time state estimation and optimal control of turbine-generators has been extended to the discrete-time case, more suited to the sampled-data control system. Solution of the linear-quadratic optimal control and optimal estimation problems lead to two Riccati equations which can readily be solved to give the estimator and controller gains. The gains are affected by arbitrarily-selected weighting matrices, which generally have to be chosen by trial-and-error, although certain guidelines are given.

Nonlinear simulations established initially that the response of the micro-machine following a transient is predicted to be reasonably close, as far as per-unit quantities are concerned, to that of a 660 MW turbine-generator. Further off-line tests showed that a 12^{th} order controller measuring load angle and field voltage gave much improved transient performance over conventional control loops for varying severities of disturbance. For controller time steps of up to 85 ms, the predicted improvement in performance was good. Shorter time steps gave progressively better responses until those of less than 10 ms, when very little further improvement was predicted.

Testing of the control algorithm in real time in a practical environment was carried out on a laboratory power system model consisting of a 3kVA microalternator driven by a d.c. motor. Analogue circuits simulated turbine/governor and AVR/exciter systems, and effectively modified the field time constant to a realistic figure. An analogue Watt-VAr transducer and an accurate digital load angle transducer were also constructed. Faults of any desired duration or line switching could be initiated by a sequence control unit. The laboratory system was a scaled-down model of a typical 660 MW turbine-generator feeding a

stiff busbar.

Two separate computers were interfaced to the model plant, one a DEC LSI 11/23 microcomputer to provide on-line control and the other a Nova-3 minicomputer to record data from the machine and plot it out using a graphics package. Communication between these two computers and the college mainframe was enabled by a Corvus Concept workstation.

The time step in the order of 10 ms predicted to give best results was met on the DEC on-line control computer by programming the algorithm in assembly language and using a floating point hardware multiplier unit. The time steps achieved are a factor of more than 10 faster than in a previous implementation of a similar strategy[13-15]. This enabled higher orders of turbine generator estimators/controllers to be investigated than has previously been documented. Digital washout filtering was adopted in the implementation and proved to be a good way for the controller to allow the machine to make a smooth transition to new setpoints and to successfully handle changes in tie-line impedance.

Comparison of simulated and measured transient responses of the micro-machine showed a good agreement, apart from a greater than predicted initial angular backswing, once the not insignificant mechanical damping was accounted for in the simulation. Response of the machine to a 100 ms three-phase fault with a 12^{th} order controller measuring load angle and field voltage was very good, even slightly better than predicted with an almost dead-beat angular swing curve. This controller also worked well for other types and severity of fault, including line-switching and unbalanced faults.

Both practical and theoretical comparisons of different orders of controller all measuring load angle and field voltage, and with similar time-steps, show that the performance deteriorates slightly as the model is simplified. However, an optimally reduced 4^{th} order controller [derived from a model obtained by applying the Hankel-norm reduction method to a 12^{th} order model] gives performance on a par with that of a 9^{th} order conventionally reduced controller. Both 12^{th} and optimally reduced 4^{th} order controllers work well at operating points considerably different from the nominal, except at low real power output. Thus the complications of look-up tables appear to be avoidable with this type of controller.

It is recognised that load angle is generally not convenient to measure in a real system due to practical difficulties and the problem of which part of the system to consider as infinite. Terminal output power, voltage, current and speed are more easily available. Speed deviation [rate of change of load angle] with field voltage gave the best theoretical results of the signals considered and an intentionally noisy speed signal also gave good practical results demonstrating the immunity of the algorithm to high noise levels.

Speed is, however, regarded as undesirable to use in supplementary stabiliser schemes due to torsional shaft oscillations that have been caused in the past by feeding speed in addition to voltage into the AVR. Power seems to be more desirable in this respect, and controllers measuring power and field voltage or power and terminal voltage were designed and tested. Since power is not a state variable in the models, linearised terms are required in the output matrix. This results in greater estimation errors, particularly during the fault, than with other measurements

such as load angle or speed deviation. As a consequence the first-swing reduction is greater but the time taken for the system to settle to steady-state is longer, and the overall stability improvement is less than with controllers measuring load angle or speed.

Controllers providing only the AVR with a supplementary signal gave a response almost as good as that with signals to both loops, except there was little first-swing reduction. It appears that AVR only control would be a suitable supplementary stabilising scheme for older plant or hydro sets, where control of the mechanical input power is relatively slow. This is because in such circumstances supplementary control to the mechanical loop as well is likely to provide even less benefit than with the model here.

The surprising detection of torsional shaft oscillations due to a flexible coupling on the micromachine gave the opportunity for brief tests to see how they interacted with the controllers. Only a slight degradation in performance was apparent. Fast-Fourier transform analysis showed a peak at about 28 Hz absent when the flexible coupling was replaced by a rigid one. Controllers measuring rotor angle or speed and field voltage seemed to make little difference to the average amplitude and decay time of the torsional oscillations.

Practical tests showed that the use of a simplified governor/turbine model to replace a detailed simulator on the micromachine has little bearing on the results. The estimator/controller was also shown to prevent the microalternator from hunting when sending a high active power through a high impedance transmission line.

The experimental results have shown that real-time implementation of an advanced generator control scheme based on state estimation and optimal feedback is feasible. The controller considerably improved both transient and dynamic stability, is effective with two measurements chosen for convenience and can be implemented with little modification to the existing generator control system.

7.2 RECOMMENDATIONS FOR FUTURE RESEARCH

a] The theoretical and practical results of this work at present cannot be directly compared with those of other control schemes in the literature due to the different conditions and apparatus used. Comparison of state estimation and optimal control with other schemes, for example self-tuning regulators, optimal aiming strategies, controllers designed by pole assignment and frequency-response methods is possible on the existing laboratory system. Conditions can be carefully controlled and the results would be valuable.

b] Before accepting an advanced generator control scheme such as that studied here, utilities need to be confident that the controller shall under no circumstances excite torsional shaft oscillations. As a first step in investigating this the flexible coupling mentioned in Section 6.7 can be replaced by another giving a natural torsional frequency typical of the most important mode in a large turbine-generator [at 5 -15 Hz]. The mathematical model may be modified to include shaft dynamics[132], and modes of vibration may be weighted and if possible damped by the estimator/controller. A

laboratory system modelling all the torsional modes has been constructed by Limebeer[122,133]; a similar system could be built here to test the control scheme.

Independently controlling the input power distribution along the shaft is possible by controlling the turbine main throttle and intercept valves separately. Consequently further damping of torsional oscillations may be achieved if the valves can respond rapidly enough.

c] Multimachine studies need to be carried out to predict how an estimator/controller affects overall system steady-state and transient stability. The simulated contribution of a controller to the damping of inter-area oscillations such as those which occurred between England and Scotland[18] would also be of interest.

d] For linear discrete time 9^{th} order generator models, the control microcomputer simulated 10 ms of real time and performed estimation and control calculations in 7.8 ms. Nonlinear simulations using Runge-Kutta or Kutta-Merson integration routines would take considerably longer but with suitable software streamlining and a faster microcomputer, real-time modelling should be possible. A real-time generator simulator would be considerably less expensive than a micromachine, in many ways more versatile and very useful for testing control schemes, operator training, etc.

e] Controllers having several inputs may have advantages in terms of reliability [if a transducer fails] and quality of estimation over those with just two, and are worthy of investigation.

f] The application of optimal Hankel-norm model reduction to high-order linear multimachine power system models could be a very good way of reducing the computer time and storage requirements of these simulations, at the same time retaining more information than conventional methods of reduction.

g] Optimal Hankel-norm reduction could also be applied to simplify complex AVR/exciter and governor/turbine linear subsystems of a nonlinear generator model thus reducing its order. This may turn out to be better than standard methods of reducing these sub-systems. However, for deriving reduced-order linearised generator models it is theoretically better to start with a full-order model of the generator and its control subsystems.

h] One discrepancy between theoretical and practical results was the greater than expected initial angular backswing measured on the micromachine following a three-phase fault. Theoretical and practical investigations are required to trace the source of this discrepancy. Transient test data from a full-size modern machine would also be useful to ascertain the quality of modelling in simulations both on the computer and in the laboratory.

i] The use of a tie-line impedance estimator in the controller was looked at theoretically by Vaahedi[11,12]. On-line recalculation of the transition matrices, controller and estimator gains every time the tie-line impedance changes does not seem feasible since it would be too time-consuming, so a look-up table at different impedances would be required. Theoretically a three-dimensional look-up table with different gains at different values of power,

Var and tie-line impedance should give best results, but storage requirements, particularly with higher order models, would be very large. Therefore whether the benefits of having such a look-up table as compared with a fixed-gain controller outweigh the disadvantages should be carefully assessed.

j] Another possible use of the state estimator is in monitoring difficult-to-access signals such as torques, fluxes or field quantities in brushless machines, or in filtering noisy measurements. Practical tests could be carried out on the microalternator to compare estimates with measured values thus assessing the accuracy of estimation.

APPENDIX A

VOLTAGE REGULATOR GAINS

The voltage input V_e to the exciter, determined by the AVR amplifier gains, in the steady-state [with no supplementary signal] is:

$$V_e = G_a(V_r - V_t) \qquad [A.1]$$

The exciter can be regarded as an amplifier, gain G_e, so that in the steady-state:

$$V_f = G_e V_e \qquad [A.2]$$

The generator may also be regarded as an amplifier, since, neglecting saturation, its output voltage on no-load is proportional to the field voltage:

$$V_t = K_2 V_f \qquad [A.3]$$

But Adkins and Harley[16] show that, on open circuit

$$V_t = \frac{x_{md} i_f}{\sqrt{2}} \qquad [A.4]$$

So: $$V_t = \frac{x_{md} V_f}{\sqrt{2} R_f} \qquad [A.5]$$

Therefore:

$$K_2 = \frac{x_{md}}{\sqrt{2} R_f} \qquad [A.6]$$

is the generator gain expressed in per-unit values.

From equations [A.1 - A.3]:

$$V_t = G_a G_e K_2 (V_{ref} - V_t) \qquad [A.7]$$

and the relationship between AVR amplifier gain G_a, exciter gain G_e and overall AVR gain K_a is:

$$G_a G_e = \frac{K_a \sqrt{2} R_f}{x_{md}} \qquad [A.8]$$

AVR's are normally designed with a K_a of about 200 in the steady-state. During transients a lead-lag compensator reduces K_a effectively to about 30 for 1 Hz oscillations.

APPENDIX B

GENERATOR MODEL BASED ON FLUX EQUATIONS

B.1 VECTORS

$$\left[I_d\right] = \begin{bmatrix} i_d \\ i_f \\ i_{kd} \end{bmatrix}, \left[\Psi_d\right] = \begin{bmatrix} \Psi_d \\ \Psi_f \\ \Psi_{kd} \end{bmatrix}, \left[I_q\right] = \begin{bmatrix} i_q \\ i_{kq} \end{bmatrix}, \left[\Psi_q\right] = \begin{bmatrix} \Psi_q \\ \Psi_{kq} \end{bmatrix} \quad [B.1]$$

B.2 MATRICES

$$\left[X_{gd}\right] = \begin{bmatrix} x_{md} + x_a & x_{md} & x_{md} \\ x_{md} & x_{md} + x_f & x_{md} \\ x_{md} & x_{md} & x_{md} + x_{kd} \end{bmatrix} . \quad [B.2]$$

$$\left[X_{gq}\right] = \begin{bmatrix} x_{mq} + x_a & x_{mq} \\ x_{mq} & x_{mq} + x_{kq} \end{bmatrix} \quad [B.3]$$

$$\left[Y_{gd}\right] = \left[X_{gd}\right]^{-1} \quad [B.4]$$

$$\left[Y_{gq}\right] = \left[X_{gq}\right]^{-1} \quad [B.5]$$

$$\left[R_{gd}\right] = \begin{bmatrix} R_a & 0 & 0 \\ 0 & R_f & 0 \\ 0 & 0 & R_{kd} \end{bmatrix} \quad [B.6]$$

$$\left[R_{gq}\right] = \begin{bmatrix} R_a & 0 \\ 0 & R_{kq} \end{bmatrix} \quad [B.7]$$

B.3 ELEVENTH ORDER NONLINEAR MODEL

Nonzero elements of the matrix A_n:

$A_n(1,2) = 1$
$A_n(2,2) = -k/J$
$A_n(2,11) = -1/J$
$A_n(3,3) = Z_1(1,1)$
$A_n(3,4) = Z_1(1,2)$
$A_n(3,5) = Z_1(1,3)$
$A_n(3,6) = -\omega_o$
$A_n(4,3) = Z_1(2,1)$
$A_n(4,4) = Z_1(2,2)$
$A_n(4,5) = Z_1(2,3)$
$A_n(4,9) = \omega_o$
$A_n(5,3) = Z_1(3,1)$
$A_n(5,4) = Z_1(3,2)$
$A_n(5,5) = Z_1(3,3)$
$A_n(6,3) = \omega_o$
$A_n(6,6) = Z_2(1,1)$
$A_n(6,7) = Z_2(1,2)$
$A_n(7,6) = Z_2(2,1)$
$A_n(7,7) = Z_2(2,2)$
$A_n(8,8) = -1/T_a$
$A_n(9,8) = -G_e/T_e$
$A_n(9,9) = -1/T_e$
$A_n(10,2) = G_g/T_v$
$A_n(10,10) = -1/T_v$
$A_n(11,10) = 1/T_s$
$A_n(11,11) = -1/T_s$

Where: $$\left[Z_1\right] = \omega_o . \left[R_{gd}\right] \cdot \left[Y_{gd}\right] \qquad [B.8]$$

$$\left[Z_2\right] = \omega_o . \left[R_{gq}\right] \cdot \left[Y_{gq}\right] \qquad [B.9]$$

$$J = 2H/\omega_o \qquad [B.10]$$

Nonzero elements of the vector F_n:

$$F_n(2) = M_e/J$$
$$F_n(3) = \omega_o V_{bd} + \dot{\delta}\, \omega_o \Psi_q$$
$$F_n(6) = \omega_o V_{bq} + \dot{\delta}\, \omega_o \Psi_d$$
$$F_n(8) = -G_a V_t/T_a$$

where:

$$M_e = 0.5\Big(\left[Y_{gq}(1,1) - Y_{gd}(1,1)\right] \omega_o \Psi_d \omega_o \Psi_q + Y_{gq}(1,2)\, \omega_o \Psi_d \omega_o \Psi_{kq}$$
$$- Y_{gd}(1,2) \omega_o \Psi_q \omega_o \Psi_f - Y_{gd}(1,3)\, \omega_o \Psi_q \omega_o \Psi_{kd}\Big) \qquad [B.11]$$

$$V_{bd} = V_{mb} \sin \delta \qquad [B.12]$$

$$V_{bq} = V_{mb} \cos \delta \qquad [B.13]$$

The rms terminal voltage V_t is given by:

$$V_t = 0.5(V_{td}^2 + V_{tq}^2)^{\frac{1}{2}} \qquad [B.14]$$

where:

$$V_{td} = V_{bd} - R_{eq}\, i_d - i_d\, X_{eq}/\omega_o - (\omega_o - \dot{\delta})\, i_q\, X_{eq}/\omega_o \qquad [B.15]$$

$$V_{tq} = V_{bq} - R_{eq}\, i_q - i_q\, X_{eq}/\omega_o + (\omega_o - \dot{\delta})\, i_d\, X_{eq}/\omega_o \qquad [B.16]$$

$$R_{eq} = R_t + R_e \qquad [B.17]$$

$$X_{eq} = X_t + X_e \qquad [B.18]$$

The vector F_n is re-calculated at each stage of the Kutta-Merson integration process [see Appendix F].

Nonzero elements of the matrix B_n:

$$B_n(8,1) = G_a/T_a$$

$$B_n(10,2) = 1/T_v$$

B.4 NINTH ORDER NONLINEAR MODEL

In this model $\omega_o \Psi_d$ and $\omega_o \Psi_q$ are assumed to be constant during each time step, then at the end re-calculated as follows:

$$\omega_o \Psi_d = - \frac{(h_1 Z_2(1,1) + h_2 (\omega_o - \dot{\delta})}{h_3} \qquad [B.19]$$

$$\omega_o \Psi_q = \frac{h_1(\omega_o - \dot{\delta}) - h_2 Z_1(1,1)}{h_3} \qquad [B.20]$$

where:

$$h_1 = \omega_o V_{bd} + Z_1(1,2)\, \omega_o \Psi_f + Z_1(1,3)\, \omega_o \Psi_{kd} \qquad [B.21]$$

$$h_2 = \omega_o V_{bq} + Z_2(1,2)\, \omega_o \Psi_{kq} \qquad [B.22]$$

$$h_3 = Z_1(1,1)\, Z_2(1,1) + (\omega_o - \dot{\delta})^2 \qquad [B.23]$$

Thus the 3^{rd} and 6^{th} states of the eleventh order model may be omitted reducing it to ninth order.

APPENDIX C

GENERATOR MODEL BASED ON CURRENT EQUATIONS

C.1 VECTORS

$$[I] = [i_d, i_f, i_{kd}, i_q, i_{kq_1}, i_{kq_2}]^T \qquad [C.1]$$

$$[V] = [v_d, v_f, 0, v_q, 0, 0]^T \qquad [C.2]$$

C.2 MATRICES

$$[R] = \text{diag.}\,[R_a, R_f, R_{kd}, R_a, R_{kq_1}, R_{kq_2}] \qquad [C.3]$$

$$[G] = \left[\begin{array}{ccc|ccc} & & & (L_{mq}+L_a) & L_{mq} & L_{mq} \\ & 0 & & 0 & 0 & 0 \\ & & & 0 & 0 & 0 \\ \hline -(L_{md}+L_a) & L_{md} & -L_{md} & & & \\ 0 & 0 & 0 & & 0 & \\ 0 & 0 & 0 & & & \end{array}\right] \qquad [C.4]$$

$$[L] = \left[\begin{array}{ccc|ccc} (L_{md}+L_a) & L_{md} & L_{md} & & & \\ L_{md} & L_{ffd} & L_{md} & & 0 & \\ L_{md} & L_{md} & L_{kkd} & & & \\ \hline & & & (L_{mq}+L_a) & L_{mq} & L_{mq} \\ & 0 & & L_{mq} & L_{kkq_1} & L_{mq} \\ & & & L_{mq} & L_{mq} & L_{kkq_2} \end{array}\right] \qquad [C.5]$$

where:

$$L_{md} = X_{md}/\omega_o \quad [C.6]$$

$$L_{mq} = X_{mq}/\omega_o \quad [C.7]$$

$$L_{ffd} = L_{md} + X_f/\omega_o \quad [C.8]$$

$$L_{kkd} = L_{md} + X_{kd}/\omega_o \quad [C.9]$$

$$L_{kkq1} = L_{mq} + X_{kq1}/\omega_o \quad [C.10]$$

$$L_{kkq2} = L_{mq} + X_{kq2}/\omega_o \quad [C.11]$$

C.3 SIMPLE SEVENTH ORDER MACHINE MODEL

C.3.1 Damping Coefficient Calculation

The mechanical damping coefficient k_{mech} for higher order models is normally negligible [although it is not for the micromachine - see Section 6.3]. In the simplified representation electrical damping is included in k, calculated by the following formula[2]:

$$ad = (x_d' + x_e) / (x_d'' + x_e)\, T_{do}'' \quad [C.12]$$

$$aq = (x_q + x_e) / (x_q'' + x_e)\, T_{qo}'' \quad [C.13]$$

$$a = V_t^2 (x_d' - x_d'') / (x_d' + x_e)(x_d'' + x_e)\, ad \quad [C.14]$$

$$b = V_t^2 (x_q - x_q'') / (x_q + x_e)(x_q'' + x_e)\, aq \quad [C.15]$$

$$k = k_{mech} + 0.5(a + b) \quad [C.16]$$

C.3.2 Simple machine model equations

Neglecting $\dot{\Psi}_{d'}$ $\dot{\Psi}_{q'}$ $\dot{\Psi}_{kd'}$ $\dot{\Psi}_{kq'}$ the machine equations[16] can be summarised as follows, taking the infinite busbar as the machine terminals:

$$V_{bd} = \omega_o \Psi_q + R_{ae}\, i_d \qquad [C.17]$$

$$V_{bq} = -\omega_o \Psi_d + R_{ae}\, i_q \qquad [C.18]$$

$$V_f = R_f\, i_f + (x_{md}\, \dot{i}_d + (x_{md} + x_f)\, \dot{i}f) / \omega_o \qquad [C.19]$$

$$\omega_o \Psi_d = (x_{ae} + x_{md})\, i_d + x_{md}\, i_f \qquad [C.20]$$

$$\omega_o \Psi_q = (x_{ae} + x_{mq})\, i_q \qquad [C.21]$$

By eliminating Ψ_d and Ψ_q, i_d and i_q are obtained as:

$$i_d = a_1 V_{bd} + a_2 V_{bq} + a_3 i_f \qquad [C.22]$$

$$i_q = b_1 V_{bd} + b_2 V_{bq} + b_3 i_f \qquad [C.23]$$

where:

$$a_1 = \frac{R_{ae}}{Z^2}, \quad a_2 = \frac{-X_{qe}}{Z^2}, \quad a_3 = \frac{-X_{qe} X_{md}}{Z^2}$$

$$b_1 = \frac{X_{de}}{Z^2}, \quad b_2 = \frac{R_{ae}}{Z^2}, \quad b_3 = \frac{X_{md} R_{ae}}{Z^2} \qquad [C.25]$$

where:

$$R_{ae} = R_a + R_t + R_e \qquad [C.26]$$

$$X_{ae} = X_a + X_t + X_e \qquad [C.27]$$

$$X_{de} = X_d + X_t + X_e \qquad [C.28]$$

$$X_{qe} = X_q + X_t + X_e \qquad [C.29]$$

$$Z^2 = R_{ae}^{\,2} + X_{de} X_{qe} \qquad [C.30]$$

Substituting for i_d and i_q in Eqn. [C.19] gives:

$$\dot{i}_f = D_1 V_f + D_2 V_{mb}\, \dot{\delta} \sin \delta + D_3 V_{mb}\, \dot{\delta} \cos \delta + D_4 i_f \qquad [C.31]$$

where:

$$D_1 = \omega_o / \alpha \qquad [C.32]$$

$$D_2 = - \frac{X_{qe} X_{md}}{Z_f^3} \qquad [C.33]$$

$$D_3 = - \frac{X_{md} R_{ae}}{Z_f^3} \qquad [C.34]$$

$$D_4 = - \omega_o R_f / \alpha \qquad [C.35]$$

$$Z_f^3 = Z^2 (X_{md} + X_f) - X_{md}^2 X_{qe} \qquad [C.36]$$

$$\alpha = Z_f^3 / Z^2 \qquad [C.37]$$

Electrical torque is obtained by substituting the above values of current and fluxes in Eqn. [2.17] as:

$$M_e = C_1 \sin^2\delta + C_2 \cos^2\delta + C_3 i_f^2 + C_4 \sin\delta \cos\delta + C_5 i_f \sin\delta + C_6 i_f \cos\delta \qquad [C.38]$$

where:

$$C_1 = \frac{1}{2} (X_d - X_q) R_{ae} X_{de} V_{mb}^2 / Z^4 \qquad [C.39]$$

$$C_2 = - \frac{1}{2} (X_d - X_q) R_{ae} X_{qe} V_{mb}^2 / Z^4 \qquad [C.40]$$

$$C_3 = \frac{1}{2} X_{md}^2 R_{ae} (X_q^2 + R_{ae}^2) / Z^4 \qquad [C.41]$$

$$C_4 = \frac{1}{2} V_{mb}^2 (X_d - X_q)(R_{ae}^2 - X_{de} X_{qe}) / Z^4 \qquad [C.42]$$

$$C_5 = \frac{1}{2Z^4} (X_d - X_q)(R_{ae}^2 - X_{de} X_{qe}) X_{md} V_{mb} + \frac{1}{2Z^2} X_{md} X_{de} V_{mb} \qquad [C.43]$$

$$C_6 = \frac{1}{Z^2} R_{ae} X_{md} V_{mb} \left[- \frac{1}{Z^2} (x_d - x_q) x_{qe} + \frac{1}{2} \right] \qquad [C.44]$$

The terminal voltage components for the simple 7^{th} order model are:

$$V_{td} = X_q i_q + R_a i_d \quad [C.45]$$

$$V_{tq} = - X_d i_d - X_{md} i_f + R_a i_q \quad [C.46]$$

Substituting for i_d and i_q from Eqns. [C.22 - 23] gives:

$$V_{td} = e_1 \sin \delta + e_2 \cos \delta + e_3 i_f \quad [C.47]$$

$$V_{tq} = f_1 \sin \delta + f_2 \cos \delta + f_3 i_f \quad [C.48]$$

where:

$$e_1 = V_{mb} (X_q b_1 + R_a a_1) \quad [C.49]$$

$$e_2 = V_{mb} (X_q b_2 + R_a a_2) \quad [C.50]$$

$$e_3 = (X_q b_3 + R_a a_3) \quad [C.51]$$

$$f_1 = V_{mb} (- X_d a_1 + R_a b_1) \quad [C.52]$$

$$f_2 = V_{mb} (- X_d a_2 + R_a b_2) \quad [C.53]$$

$$f_3 = (- X_d a_3 + R_a b_3 - X_{md}) \quad [C.54]$$

APPENDIX D

LINEARISED SYSTEM REPRESENTATION

In deriving linearised models, the objective is to evaluate the A_L and B_L matrices of:

$$\Delta\dot{x} = A_L \Delta x + B_L \Delta u \qquad [D.1]$$

where:

$$\Delta x = \left[\Delta x_1, \Delta x_2, \ldots \Delta x_n\right]^T \qquad [D.2]$$

and:

$$\Delta u = \left[\Delta V_r + du_1, \Delta Y_o + du_2\right]^T \qquad [D.3]$$

D.1 TERMINAL VOLTAGE LINEARISATION

In all the linearised models, a linearised terminal voltage expression is derived using the transmission line model equations [2.26 -.27], repeated here:-

$$V_{td} = V_{bd} - R_{eq} i_d - (x_{eq} \dot{i}_d + \omega i_q x_{eq}) / \omega_o \qquad [2.26]$$

$$V_{tq} = V_{bq} - R_{eq} i_q - (x_{eq} \dot{i}_q - \omega i_d x_{eq}) / \omega_o \qquad [2.27]$$

We know that:

$$\Delta V_t = \frac{\partial V_t}{\partial V_{td}} \Delta V_{td} + \frac{\partial V_t}{\partial V_{tq}} \Delta V_{tq} \qquad [D.4]$$

and

$$V_t = \frac{1}{2}\sqrt{V_{td}^2 + V_{tq}^2} \qquad [D.5]$$

hence:

$$\frac{\partial V_t}{\partial V_{td}} = \frac{V_{td}}{2V_t}, \quad \frac{\partial V_t}{\partial V_{tq}} = \frac{V_{tq}}{2V_t} \qquad [D.6]$$

Linearising [2.26] and [2.27] gives:

$$\Delta V_{td} = \Delta V_{bd} - R_{eq}\Delta i_d - x_{eq}\Delta i_d / \omega_o \qquad [D.7]$$

$$- \Delta\omega\, i_q\, x_{eq} / \omega_o - \omega\Delta i_q\, x_{eq} / \omega_o$$

$$\Delta V_{tq} = \Delta V_{bq} - R_{eq}\Delta i_q - x_{eq}p\Delta i_q / \omega_o \qquad [D.8]$$

$$+ \Delta\omega i_d\, x_{eq} / \omega_o + \omega\Delta i_d\, x_{eq} / \omega_o$$

where:

$$\Delta V_{bd} = \frac{\partial V_{bd}}{\partial\delta}\,\Delta\delta = \frac{\partial}{\partial\delta}\,(V_{mb}\sin\delta)\,\Delta\delta$$

$$= V_{mb}\cos\delta\,\Delta\delta \qquad [D.9]$$

$$\Delta V_{bq} = \frac{\partial V_{bq}}{\partial\delta}\,\Delta\delta = \frac{\partial}{\partial\delta}\,(V_{mb}\cos\delta)\Delta\delta$$

$$= - V_{mb}\sin\delta\Delta\delta \qquad [D.10]$$

Equations [D.7] and [D.8] can be used directly in a linear model if currents are the generator state variables, and can be transformed if fluxes are the state variables.

Linearisation of the electrical torque expression and other non-linearities is by straightforward partial differentiation with respect to each state variable.

D.2 TWELFTH ORDER LINEAR MODEL

Inverting the inductance matrix [L] gives the following susceptance matrix [B]:

$$[L]^{-1} = [B] = \left[\begin{array}{ccc|ccc} B_{11} & B_{12} & B_{13} & & & \\ B_{21} & B_{22} & B_{23} & & 0 & \\ B_{31} & B_{32} & B_{33} & & & \\ \hline & & & B_{44} & B_{45} & B_{46} \\ & 0 & & B_{54} & B_{55} & B_{56} \\ & & & B_{64} & B_{65} & B_{66} \end{array}\right] \qquad [D.11]$$

The linear system matrix A_L is calculated to be the following [non-zero elements]:

$A_L(1,2) = 1$

$A_L(2,2) = - k / J + M_T / (\omega_o J)$

$A_L(2,3) = - \omega_o i_q (L_d - L_q) / 2J$

$A_L(2,4) = - \omega_o L_{md} i_q / 2J$

$A_L(2,5) = - \omega_o L_{md} i_q / 2J$

$A_L(2,6) = - \omega_o (L_d i_d + L_{md} i_f - L_q i_d) / 2J$

$A_L(2,7) = \omega_o L_{mq} i_d / 2J$

$A_L(2,8) = \omega_o L_{mq} i_d / 2J$

$A_L(2,9) = - 1/J$

$A_L(3,1) = - B_{11} V_{bq}$

$A_L(3,2) = - B_{11} L_q i_q$

$A_L(3,3) = - B_{11} (R_a + R_t + R_e)$

$A_L(3,4) = - B_{12} R_F$

$A_L(3,5) = - B_{13} R_{kd}$

$A_L(3,6) = - B_{11} \omega_o L_q$

$A_L(3,7) = - B_{11} \omega_o L_{mq}$

$A_L(3,8) = - B_{11} \omega_o L_{mq}$

$A_L(3,10) = B_{12}$

$A_L(4,1) = - B_{12} V_{bq}$

$A_L(4,2) = - B_{12} L_q i_q$

$A_L(4,3) = - B_{12} (R_a + R_t + R_e)$

$A_L(4,4) = - B_{22} R_f$

$A_L(4,5) = - B_{23} R_{kd}$

$A_L(4,6) = - B_{12} \omega_o L_q$

$A_L(4,7) = - B_{12} \omega_o L_{mq}$

$A_L(4,8) = - B_{12} \omega_o L_{mq}$

$A_L(4,10) = B_{22}$

$A_L(5,1) = - B_{13} V_{bq}$

$A_L(5,2) = - B_{13} L_q i_q$

$A_L(5,3) = - B_{13} (R_a + R_t + R_e)$

$A_L(5,4) = - B_{23} R_f$

$A_L(5,5) = - B_{33} R_{kd}$

$A_L(5,6) = - B_{13} \omega_o L_q$

$A_L(5,7) = - B_{13} \omega_o L_{mq}$

$A_L(5,8) = - B_{13} \omega_o L_{mq}$

$A_L(5,10) = B_{23}$

$A_L(6,1) = B_{44} V_{bd}$

$A_L(6,2) = B_{44} (L_d i_d + L_{md} i_f)$

$A_L(6,3) = B_{44} \omega_o L_d$

$A_L(6,4) = B_{44} \omega_o L_{md}$

$A_L(6,5) = B_{44} \omega_o L_{md}$

$$A_L(6,6) = -B_{44}\ (R_a + R_t + R_e)$$

$$A_L(6,7) = -B_{45}\ R_{kq1}$$

$$A_L(6,8) = -B_{46}\ R_{kq2}$$

$$A_L(7,1) = B_{45}\ V_{bd}$$

$$A_L(7,2) = B_{45}\ (L_d i_d + L_{md} i_f)$$

$$A_L(7,3) = B_{45}\ \omega_o L_d$$

$$A_L(7,4) = B_{45}\ \omega_o L_{md}$$

$$A_L(7,5) = B_{45}\ \omega_o L_{md}$$

$$A_L(7,6) = -B_{45}\ (R_a + R_t + R_e)$$

$$A_L(7,7) = -B_{55}\ R_{kq1}$$

$$A_L(7,8) = -B_{56}\ R_{kq2}$$

$$A_L(8,1) = B_{46}\ V_{bd}$$

$$A_L(8,2) = B_{46}\ (L_d i_d + L_{md} i_f)$$

$$A_L(8,3) = B_{46}\ \omega_o L_d$$

$$A_L(8,4) = B_{46}\ \omega_o L_{md}$$

$$A_L(8,5) = B_{46}\ \omega_o L_{md}$$

$$A_L(8,6) = -B_{46}\ (R_a + R_t + R_e)$$

$$A_L(8,7) = -B_{56}\ R_{kq1}$$

$$A_L(8,8) = -B_{66}\ R_{kq2}$$

$$A_L(9,9) = -1 / T_s$$

$$A_L(9,12) = 1 / T_s$$

$$A_L(10,10) = -1 / T_e$$

$$A_L(10,11) = G_e / T_e$$

$$A_L(11,1) = K_v\ (V_{tq} V_{bd} - V_{td} V_{bq})$$

$$A_L(11,2) = K_v\ (V_{tq} L_t i_d - V_{td} L_t i_q)$$

$$A_L(11,3) = K_v \left(V_{tq}(x_t + x_e) - V_{td}(R_t + R_e)\right)$$

$$A_L(11,6) = -K_v \left(V_{td}\ (x_t + x_e) + V_{tq}\ (R_t + R_e)\right)$$

$$A_L(11,11) = -1 / T_a$$

$$A_L(12,2) = G_g / T_v$$

$$A_L(12,12) = -1 / T_v$$

where: $L_d = L_{md} + L_a$

$K_v = - G_a / (T_a 2V_t)$

$L_t = (x_t + x_e) / \omega_o$

$L_q = L_{mq} + L_a$

The non-zero B_L control matrix elements are:

$$B_L(11,1) = G_a / T_a$$

$$B_L(12,2) = 1 / T_v$$

D.3 NINTH ORDER LINEAR MODEL

Equations [B 19 - 23] are used to find the partial derivatives with respect to δ of $\omega_o \Psi_d$ and $\omega_o \Psi_q$:

$$\frac{\partial}{\partial\delta}(\omega_o \Psi_d) = V_{mb}\,\omega_o(\omega_o \sin\delta - Z_2(1,1)\cos\delta) / Z_1(1,1)\,Z_2(1,1) \qquad [D.12]$$

$$\frac{\partial}{\partial\delta}(\omega_o \Psi_q) = V_{mb}\,\omega_o(\omega_o \cos\delta + Z_1(1,1)\cos\delta) / Z_1(1,1)\,Z_2(1,1) \qquad [D.13]$$

The matrix A_L becomes:

$A_L(2,1) = 1$

$A_L(2,1) = \omega_o V_{mb}\Big(M_3(\omega_o \sin\delta - Z_2(1,1)\cos\delta) + M_6\big(\omega_o \cos\delta\, Z_1(1,1)\sin\delta\big)\Big) / ZZZ.J$

$A_L(2,2) = - k/J$

$A_L(2,3) = \Big(- M_3 Z_1(1,2)Z_2(1,1) + M_6\,\omega_o Z_1(1,2) + M_4.ZZZ\Big) / ZZZ.J$

$A_L(2,4) = \Big(- M_3 Z_1(1,3)Z_2(1,1) + M_6\,\omega_o Z_1(1,3) + M_5.ZZZ\Big) / ZZZ.J$

$A_L(2,5) = \Big(- M_3\,\omega_o Z_2(1,2) - M_6 Z_1(1,1)\,Z_2(1,2) + M_7.ZZZ\Big) / ZZZ.J$

$A_L(2,9) = - 1/J$

$A_L(3,1) = Z_1(2,1)\,V_{mb}\omega_o(\omega_o \sin\delta - Z_2(1,1)\cos\delta) / ZZZ$

$$A_L(3,3) = - Z_1(2,1)\, Z_1(1,2)\, Z_2(1,1) / ZZZ + Z_1(2,2)$$

$$A_L(3,4) = - Z_1(2,1)\, Z_1(1,3)\, Z_2(1,1) / ZZZ + Z_1(2,3)$$

$$A_L(3,5) = - \omega_o Z_1(2,1)\, Z_2(1,2) / ZZZ$$

$$A_L(3,7) = \omega_o$$

$$A_L(4,1) = Z_1(3,1)\, V_{mb}\, \omega_o \left(\omega_o \sin\delta - Z_2(1,1) \cos\delta\right) / ZZZ$$

$$A_L(4,3) = - Z_1(3,1)\, Z_1(1,2)\, Z_2(1,1) / ZZZ + Z_1(3,2)$$

$$A_L(4,4) = - Z_1(3,1)\, Z_1(1,3)\, Z_2(1,1) / ZZZ + Z_1(3,3)$$

$$A_L(4,5) = - \omega_o\, Z_1(3,1)\, Z_2(1,2) / ZZZ$$

$$A_L(5,1) = Z_2(2,1)\, V_{mb}\, \omega_o \left(\omega_o \cos\delta + Z_1(1,1) \sin\delta\right) / ZZZ$$

$$A_L(5,3) \quad Z_2(2,1)\, \omega_o Z_1(1,2) / ZZZ$$

$$A_L(5,4) = Z_2(2,1)\, \omega_o Z_1(1,3) / ZZZ$$

$$A_L(5,5) = - Z_2(2,1)\, Z_2(1,2)\, Z_1(1,1) / ZZZ + Z_2(2,2)$$

$$A_L(6.1) = - G_a\, \omega_o\, V_{mb} \left(V_3 (\omega_o \sin\delta - Z_2(1,1) \cos\delta) + V_6 (\omega_o \cos\delta + Z_1(1,1) \sin\delta) + V_1 ZZZ / \omega_o V_{mb}\right) / ZZZ.T_a$$

$$A_L(6,2) = - V_2\, G_a / T_a$$

$$A_L(6,3) = - G_a \left(- V_3 Z_1(1,2)\, Z_2(1,1) + V_6 \omega_o Z(1,2) + V_4 ZZZ\right) / T_a\, ZZZ$$

$$A_L(6,4) = - G_a \left(- V_3 Z_1(1,3)\, Z_2(1,1) + V_6\, \omega_o Z_1(1,3) + V_5 ZZZ\right) / T_a\, ZZZ$$

$$A_L(6,5) = - G_a \left(- V_3 \omega_o\, Z_2(1,2) - V_6 Z_1(1,1)\, Z_2(1,2) + V_7 ZZZ\right) / T_a\, ZZZ$$

$$A_L(6,6) = - 1 / T_a$$

$$A_L(6,7) = - G_e / T_e$$

$$A_L(7,7) = - 1 / T_e$$

$$A_L(8,2) = G_g / T_v$$

$$A_L(8,8) = - 1 / T_v$$

$$A_L(9,8) = 1 / T_s$$

$$A_L(9,9) = - 1 / T_s$$

$$B_L(6,1) = G_a / T_a$$

$$B_L(8,2) = 1 / T_v$$

where:

$$V_1 = V_{mb} (V_{td} \cos\delta - V_{tq} \sin\delta) / 2.V_t$$

$$V_2 = X_{eq} (V_{td} i_q - V_{tq} . i_d) / 2 \omega_o V_t$$

$$V_3 = Y_{gd}(1,1) (X_{eq} V_{tq} - R_{eq} V_{td}) / 2.V_t$$

$$V_4 = Y_{gd}(1,2) (X_{eq} V_{tq} - R_{eq} V_{td}) / 2.V_t$$

$$V_5 = Y_{gd}(1,3) (X_{eq} V_{tq} - R_{eq} V_{td}) / 2.V_t$$

$$V_6 = Y_{gq}(1,1) (- X_{eq} V_d - R_{eq} V_q) / 2.V_t$$

$$V_7 = Y_{gq}(1,2) (- X_{eq} V_d - R_{eq} V_q) / 2.V_t$$

and:

$$M_3 = 0.5 \omega_o \Psi_d \left(Y_{gq}(1,1) - Y_{gd}(1,1)\right) + \omega_o \Psi_{kq} Y_{gq}(1,2)$$

$$M_4 = 0.5 \; Y_{gd}(1,2) \omega_o \Psi_q$$

$$M_5 = - 0.5 \; Y_{gd}(1,3) \omega_o \Psi_q$$

$$M_6 = 0.5 \left(\omega_o \Psi_d (Y_{gq}(1,1) - Y_{gd}(1,1)\right) - Y_{gd}(1,2) \omega_o \Psi_f - Y_{gd}(1,3) \omega_o \Psi_{kd}$$

$$M_7 = 0.5 \; Y_{gq}(1,2) \omega_o \Psi_d$$

$$ZZZ = Z_1(1,1) \; Z_2(1,1) + \omega_o^2$$

$$R_{eq} = R_e + R_t$$

$$X_{eq} = X_e + X_t$$

D.4 SEVENTH ORDER LINEAR MODEL

$$A_L(1,2) = 1$$

$$A_L(2,1) = (2 C_1 \sin\delta \cos\delta - 2 C_2 \sin\delta \cos\delta + C_4 \cos 2\delta + C_5 i_f \cos\delta - C_6 i_f \sin\delta) / J$$

$$A_L(2,2) = - \frac{k}{J}$$

$$A_L(2,3) = (2C_3 i_f + C_5 \sin\delta + C_6 \cos\delta) / J$$

$$A_L(2,7) = - \frac{1}{J}$$

$$A_L(3,2) = V_{mb}(D_2 \sin\delta + D_3 \cos\delta)$$

$$A_L(3,3) = D_4$$

$$A_L(3,5) = D_1$$

$$A_L(4,1) = - G_a V_{td}(e_1 \cos\delta - e_2 \sin\delta) + V_{tq}(f_1 \cos\delta - f_2 \sin\delta) / 2.V_t.T_a$$

$$A_L(4,3) = - G_a(V_d e_3 + V_q f_3) / 2.V_t.T_a$$

$$A_L(4,4) = - 1 / T_a$$

$$A_L(5,4) = - G_e / T_e$$

$$A_L(5,5) = - 1 / T_e$$

$$A_L(6,2) = G_g / T_v$$

$$A_L(6,6) = - 1 / T_v$$

$$A_L(7,6) = 1 / T_s$$

$$A_L(7,7) = - 1 / T_s$$

$$B_L(4,1) = G_a / T_a$$

$$B_L(6,2) = 1 / T_v$$

Expressions for $C_1 \ldots C_6$, $D_1 \ldots D_4$, $e_1 \ldots e_3$, and $f_1 \ldots f_3$, are evaluated in Appendix C, Part 3.2.

APPENDIX E

"STEADY-STATE" PHASOR DIAGRAM CALCULATION

The calculation of the machine steady-state operating condition is based on the following information being supplied:

a] Voltage, power and reactive power at the machine terminals;

b] Parameters of the synchronous generator and transmission line.

From the information a phasor diagram can be used to calculate current components, busbar voltage and load angle to both terminals and infinite busbar, Fig. E.1, and hence steady-state values of all state variables can be found.

$$\phi = \arctan (Q/P) \qquad [E.1]$$

$$I_{mt} = 2\sqrt{P^2 + Q^2} / V_{mt} \qquad [E.2]$$

From the phasor diagram, the terminal load angle δ_t is given by:

$$\tan \delta_t = \frac{NR}{ON} \qquad [E.3]$$

Where RS is perpendicular to the current phasor, and RN is the perpendicular on OT produced.

Therefore: $$\tan \delta_t = \frac{X_q I_{mt} \cos \phi - R_a I_{mt} \sin \phi}{V_{mt} - R_a I_{mt} \cos \phi - X_q I_{mt} \sin \phi} \qquad [E.4]$$

$$= \frac{X_q \cos \phi - R_a \sin \phi}{V_{mt}/I_{mt} - R_a \cos \phi - X_q \sin \phi} \qquad [E.5]$$

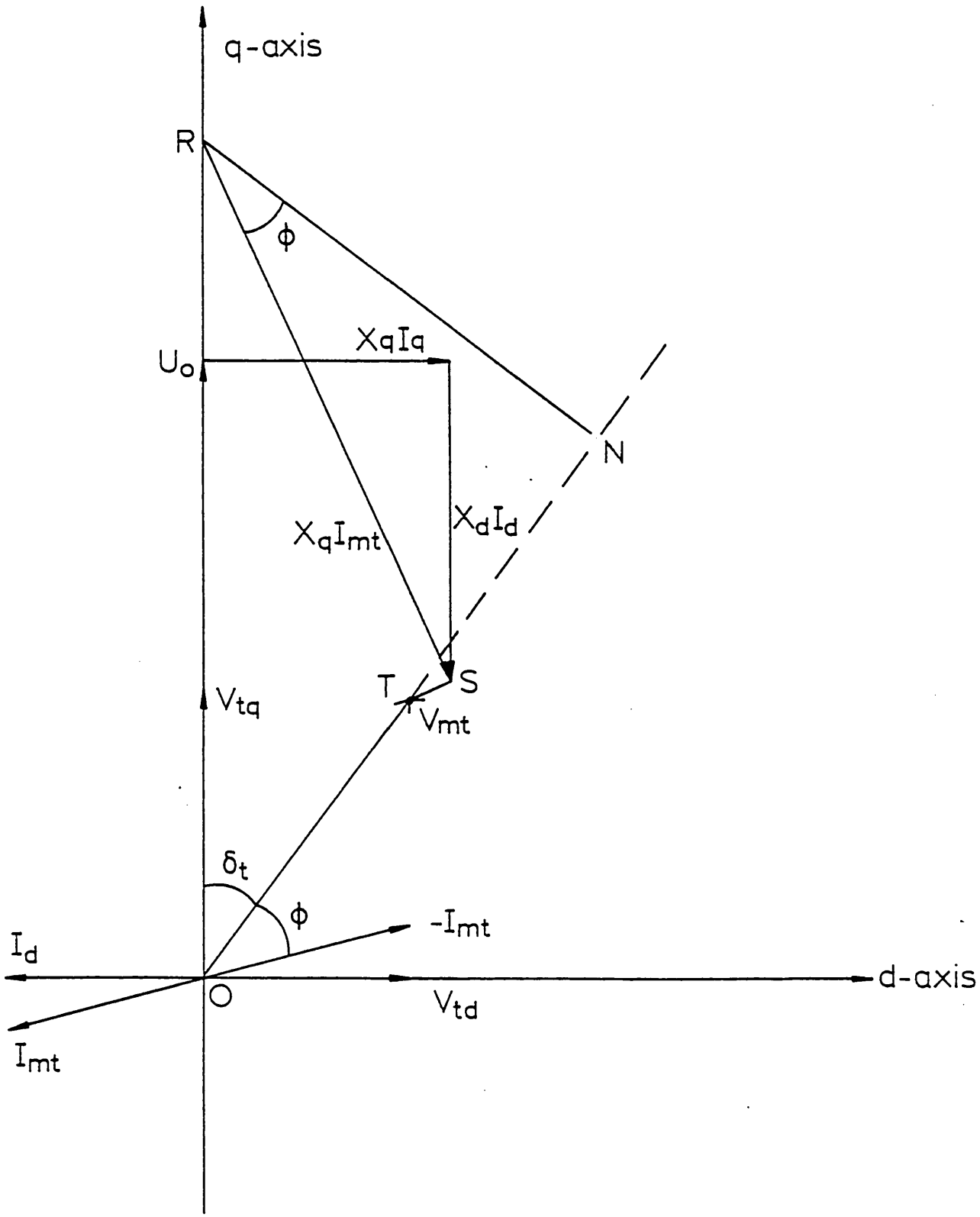

Fig. E.1: Synchronous machine phasor diagram

From δ_t we can calculate axis components of voltages and currents:

$$V_{td} = V_{mt} \sin \delta_t \quad [E.6]$$

$$V_{tq} = V_{mt} \cos \delta_t \quad [E.7]$$

$$I_d = I_{mt} \sin (\delta_t - \phi) \quad [E.8]$$

$$I_q = I_{mt} \cos (\delta_t - \phi) \quad [E.9]$$

From the transmission line equations [2.26 - .27] in the steady state we can calculate the busbar voltage and load angle to the infinite busbar:

$$V_{bd} = V_{td} + (R_t + R_e) I_d + (X_t + X_e) I_q \quad [E.10]$$

$$V_{bq} = V_{tq} + (R_t + R_e) I_q - (X_t + X_e) I_d \quad [E.11]$$

$$\delta_b = \arctan (V_{bd}/V_{bq}) \quad [E.12]$$

Field current and voltage can be derived from flux equations:

$$\omega_o \Psi_d = R_a I_q - V_{bq} \quad [E.13]$$

$$I_f = (\omega_o \Psi_d - X_d I_d) / X_{md} \quad [E.14]$$

$$V_f = I_f R_f \quad [E.15]$$

hence: $$V_e = - V_f / G_e \quad [E.16]$$

Electrical torque is given by Eqn. [2.17]:

$$M_e = 0.5 \omega_o (\Psi_d I_q - \Psi_q I_d) \quad [2.17]$$

where: $$\omega_o \Psi_q = I_q . X_q \quad [E.17]$$

It is easy to show that, omitting constant mechanical losses:

$$Y_o = A_p = M_t = M_e \qquad [E.18]$$

is the steady state.

For models based on currents as state-variables, damper currents are zero in steady-state.

Damper fluxes are given by:

$$\omega_o \Psi_{kd} = (I_d + V_f/R_f) X_{md} \qquad [E.19]$$

$$\omega_o \Psi_{kq} = X_{mq} I_q \qquad [E.20]$$

APPENDIX F

INTEGRATION METHOD

The Kutta-Merson numerical integration method calculates the vector $y_f = y(x_o + h)$ at the end of the integration step, length h, for the set of differential equations:

$$\frac{dy}{dx} = f(x, y) \qquad [F.1]$$

The routine calculates five intermediate values of y ($y_1 \ldots y_5$)

$$y_1 = y_o + \frac{1}{3} hf(x_o, y_o) \qquad [F.2]$$

$$y_2 = y_o + \frac{1}{6} hf(x_o, y_o) + \frac{1}{6} hf(x_o + \frac{1}{3} h, y_1) \qquad [F.3]$$

$$y_3 = y_o + \frac{1}{8} hf(x_o, y_o) + \frac{3}{8} hf(x_o + \frac{1}{3} h, y_2) \qquad [F.4]$$

$$y_4 = y_o + \frac{1}{2} hf(x_o, y_o) - \frac{3}{2} hf(x_o + \frac{1}{3} h, y_2) + 2hf(x_o + \frac{1}{2} h, y_3) \qquad [F.5]$$

$$y_5 = y_o + \frac{1}{6} hf(x_o, y_o) + \frac{2}{3} hf(x_o + \frac{1}{2} h, y_3) + \frac{1}{6} hf(x_o + h, y_4) \qquad [F.6]$$

and $$y_f = \frac{1}{5}(y_4 - y_5)$$

APPENDIX G

METHODS OF SOLVING THE DISCRETE-TIME RICCATI EQUATION

Optimal Regulator Discrete-time Riccati Equation:

$$A^T P_R A - A^T P_R B (R_R + B^T P_R B)^{-1} B^T P_R A + Q_R - P_R = 0 \qquad [G.1]$$

Regulator gain F:

$$F = (R_R + B^T P_R B)^{-1} B^T P_R A \qquad [G.2]$$

Kalman Filter Discrete-time Riccati Equation:

$$A P_F A^T - A P_F C^T (R_F + C P_F C^T)^{-1} C P_F A^T + Q_F - P_F = 0 \qquad [G.3]$$

Filter Gain K:

$$K = A P_F C^T (R_F + C P_F C^T)^{-1}. \qquad [G.4]$$

An equivalence between the two sets of Riccati equations can be demonstrated by making the following transformations:

Regulator	Filter
A	A^T
B	C^T
C	B^T
Q_R	Q_F
R_R	R_F
F	K^T

The three methods of solving the discrete-time Riccati equation are:

a] The Recursive Method;

b] The eigenvalue/eigenvector method;

c] The real Schur method.

G.1 RECURSIVE METHOD[58,72,92]

The recursive form of the regulator Riccati equation is as follows:

$$P_R(n) = A^T P_R(n+1)\,[I + BR_R B^T P_R(n+1)]^{-1}\,A + Q_R \qquad [G.5]$$

We start by making an initial symmetric positive definite guess for the solution $P_R(0)$. This is necessary because the regulator Riccati equation has many solutions, but only one giving closed loop stability which is shown in Kuo[92] to be symmetric positive definite. For the infinite time optimal control problem applied to linear time - invariant discrete-time systems, as $n \to -\infty$ $P_R(n)$ becomes a constant matrix, i.e.,

$$\lim_{n \to -\infty} P_R(n) = P_R$$

so equation [G.5] becomes:

$$P_R = A^T P_R\,[I + BR_R B^T P_R]^{-1}\,A + Q_R \qquad [G.6]$$

Using the identity (proved, for example in Kailath[116])

$$[I + BR_R B^T P_R]^{-1} = I - B\,[R_R + B^T P_R B]^{-1}\,B^T P_R \qquad [G.7]$$

it is easily shown that equations [G.6] and [G.1] are equivalent.

Having chosen an initial guess $P_R(0)$, the backward recursive equation [G.5] is repeatedly solved until the difference between $P_R(k)$ and $P_R(k-1)$ is within the required tolerances.

The speed of this method obviously depends on the initial choice $P_R(0)$, but in general it is fairly slow, particularly for higher order systems, due to the matrix inversion required at every step. Also there are possible numerical problems in converging to a final solution in some instances.

G.2 EIGENVALUE-EIGENVECTOR METHOD

In this method we form the 'Simplectic' matrix S, which is the discrete-time equivalent of the Hamiltonian of continuous-time systems:

$$S = \left[\begin{array}{c|c} A + BR_R^{-1} B^T A^{-1} Q_R & - B R_R^{-1} B^T A^{-T} \\ \hline -A^{-T} Q_R & A^{-T} \end{array}\right] \qquad [G.8]$$

A property of all Simplectic matrices is that the eigenvalues occur in reciprocal pairs, i.e., if λ_i is an eigenvalue, then so is $1 / \lambda_i$. This property may be used to test that the Simplectic matrix has been properly formed.

The eigenvalues and corresponding eigenvectors of S are found, and we select the eigenvectors of S corresponding to eigenvalues lying within the unit circle [since this is a condition for closed-loop stability] and form:

$$W = \begin{bmatrix} W_{11} \\ W_{21} \end{bmatrix} \qquad [G.9]$$

W is a 2n x n matrix of eigenvectors corresponding to eigenvalues of S lying within the unit circle.

The Riccati equation solution is then given by:

$$P_R = W_{21} W_{11}^{-1} \qquad [G.10]$$

This method is generally much quicker than the recursive method, its efficiency dependent largely on the eigenvalue-eigenvector routine. There is the possibility of this routine giving difficulties for large, ill-conditioned Simplectic matrices.

G.3 SCHUR METHOD[115]

The Simplectic matrix is decomposed into the real Schur form:

$$\left[\begin{array}{c|c} A + BR_R^{-1}B^T A^{-T} Q_R & -BR_R^{-1}B^T A^{-T} \\ \hline -A^{-T}Q_R & A^{-T} \end{array}\right] \begin{bmatrix} W_{11} & W_{12} \\ W_{21} & W_{22} \end{bmatrix} = \begin{bmatrix} W_{11} & W_{12} \\ W_{21} & W_{22} \end{bmatrix} \begin{bmatrix} T_1 & T_3 \\ & T_2 \end{bmatrix} \qquad [G.11]$$

where $\begin{bmatrix} T_1 & T_3 \\ & T_2 \end{bmatrix}$ is the upper triangular real Schur form of the Simplectic matrix.

The Riccati solution P_R is obtained from the transformation matrix W:

$$P_R = W_{21} W_{11}^{-1}$$

As before in the eigenvalue-eigenvector method, the Schur form used in the solution has to be such that the eigenvalues within the unit circle are all in T_1.

We can show that this method gives a solution to the Riccati equation by the following:

From the (1,1) block in [G.11] -

$$(A + BR_R^{-1} B^T A^{-T} Q_R) W_{11} - BR_R^{-1} B^T A^{-T} W_{21} = W_{11} T_1 \qquad [G.12]$$

Premultiplying by $P_R = W_{21} W_{11}^{-1}$

$$P_R(A + B R_R^{-1} B^T A^{-T} Q_R) W_{11} - PBR_R^{-1} B^T A^{-T} W_{21} = W_{21} T_1 \qquad [G.13]$$

From the (2,1) block in [G.11] -

$$- A^{-T} Q_R W_{11} + A^{-T} W_{21} = W_{21} T_1 \qquad [G.14]$$

Combining [G.13] and [G.14] -

$$P_R(A + BR_R^{-1} B^T A^{-T} Q_R) W_{11} - P_R BR_R^{-1} B^T A^{-T} W_{21} + A^{-T} Q_R W_{11} - A^{-T} W_{21} = 0 \qquad [G.15]$$

Premultiplying by A^T and postmultiplying by W_{11}^{-1} gives -

$$A^T P_R A - P_R - A^T P_R BR_R^{-1} B^T A^{-T} P_R + (I + A^T P_R BR_R^{-1} B^T A^{-T}) Q_R = 0 \qquad [G.16]$$

Using the matrix identity[116] -

$$(K + LMN)^{-1} = K^{-1} - K^{-1}L(NK^{-1}L + M^{-1})^{-1} NK^{-1} \qquad [G.17]$$

on $(I + A^T P_R B\, R_R^{-1} B^T A^{-T})$ with $K = I$, $L = A^T P_R B$, $M = R^{-1}$, $N = B^T A^{-T}$ changes [G.16] to -

$$A^T P_R A - P_R - A^T P_R B R_R^{-1} B^T A^{-T} P_R +$$

$$[I - A^T P_R B(B^T P_R B + R_R)^{-1} B^T A^{-T}]^{-1} Q_R = 0 \qquad [G.18]$$

Premultiplying by $[I - A^T P_R B(B^T P_R B + R)^{-1} B^T A^{-T}]$:

$$A^T P_R A - A^T P_R B\, R_R^{-1} B^T A^{-T} P_R - P_R - A^T P_R B(R_R + B^T P_R B)^{-1} B^T P_R A$$

$$+ A^T P_R B(B^T P_R B + R_R)^{-1} B^T A^{-T} P_R$$

$$+ A^T P_R B(B^T P_R B + R_R)^{-1} B^T P_R B R_R^{-1} B^T A^{-T} P_R + Q = 0 \qquad [G.19]$$

which simplifies to the Riccati equation [G.1].

$$A^T P_R A - A^T P_R B(R_R + B^T P_R B)^{-1} B^T P_R A - P + Q = 0$$

G.4 COMPUTATION TIMES

For a 9^{th} order discrete-time generator model, solution of the Riccati equation using a CDC Cyber 720 took 24 seconds for the recursive method, 2.7 seconds for the eigenvalue/eigenvector method, and 5.6 seconds for the Schur method.

APPENDIX H

660 MW AND MICROMACHINE PARAMETERS: STEADY-STATE CONDITIONS

H.1 PARAMETERS

	660 MW unit	Micromachine with TCR
D Axis mutual reactance X_{md}	1.959	2.274 p.u.
Q Axis mutual reactance X_{mq}	1.899	2.145 p.u.
Armature resistance R_a	0.00234	0.00528 p.u.
Armature leakage reactance X_a	0.179	0.149 p.u.
Field resistance R_f	0.00112	0.00116 p.u.
Field leakage reactance X_f	0.159	0.16 p.u.
D. Axis transient reactance X_d'	0.344	0.297 p.u.
D. Axis subtransient reactance X_d''	0.229	0.205 p.u.
Q. Axis subtransient reactance X_q''	0.205	0.285 p.u.
Time constants T_d'	0.910	0.821 S
T_d''	0.0417	0.0292 S
T_{do}'	5.66	6.27 S
T_{do}''	0.0626	0.0424 S
D Axis damper resistance R_{kd}	0.01012	0.0179 p.u.
D Axis damper reactance X_{kd}	0.052	0.09 p.u.
Q1 Axis damper resistance R_{kq1}	0.01012	0.0179 p.u.
Q1 Axis damper reactance X_{kq1}	0.026	0.146 p.u.
Q2 Axis damper resistance R_{kq2}	0.01012	0.0179 p.u.
Q2 Axis damper reactance X_{kq2}	0.026	0.146 p.u.
Transmission line resistance R_e	0.06	0.06 p.u.
Transmission line reactance X_e	0.25	0.25 p.u.
Generator transformer resistance R_T	0.0	0.0 p.u.
Generator transformer reactance X_T	0.0	0.0 p.u.
Inertia Constant H	3.77	3.5 S
Time Constants: AVR T_a	0.01	0.01 S
Exciter T_e	0.01	0.01 S
Valves T_v	0.1	0.1 S
Steam T_s	0.3	0.3 S

		660 MW unit	Micromachine with TCR
Gains:	AVR G_a	0.001	0.001
	Exciter G_e	5.56	5.56
	Governor G_g	0.0796	0.0796
Base values:	line voltage	23500	200 V
	line current	9361	8.67 A
	kVA	776000	3 kVA
	field voltage	209030	1188.5 V
	field current	1856.2	1.262 A

H.2 'STANDARD' STEADY-STATE TEST CONDITIONS

H.2.1 Standard conditions in Chapter 4:

$P_t = -0.8$

$Q_t = 0.0$

$V_t = 1.00$

$I_t = 0.8$

$V_b = 0.9727$

Micromachine		660 MW Unit	
δ_b =	-73.18°	δ_b =	-70.79°
V_f =	$-1.5745.\ 10^{-3}$	V_f =	$-1.6026.\ 10^{-3}$
i_f =	-1.3573	I_f =	-1.4309
i_d =	0.9925	i_d =	0.9690
i_q =	-0.5431	i_1 =	-0.5840
V_d =	-1.2406	V_d =	-1.2113
V_q =	0.6789	V_a =	0.7300

H.2.2 **Standard conditions in Chapter 6** (Micromachine only)

P_t = -0.8

Q_t = 0.0

V_t = 1.025

I_t = 0.7805

V_b = 0.9974

δ_b = -71.39°

V_f = $-1.5528.\ 10^{-3}$

i_f = $-1.3386.\ 10^{-3}$

i_d = 0.957

i_q = -0.55

V_d = -1.2568

V_q = 0.7224

- Steady-state values of other variables of interest can be calculated by the formulae in Appendix E.

APPENDIX I

OUTPUT MATRICES

1.1 INTRODUCTION

The output or "C" matrix relates measurements taken from the system y(k) to the system states x(k) by:

$$y(k) = C\,x(k) \qquad [I.1]$$

Thus if the measured variables are state variables then the C matrix contains unity elements, for example if the measured variables are rotor angle and field voltage in a 12^{th} order model, the C matrix is:

$$C = \begin{bmatrix} 1 & 0 & 0 & 0 & 0 & 0 & 0 & 0 & 0 & 0 & 0 & 0 \\ 0 & 0 & 0 & 0 & 0 & 0 & 0 & 0 & 0 & 1 & 0 & 0 \end{bmatrix} \qquad [I.2]$$

I.2 LINEARISED OUTPUT MATRICES

Variables mentioned in Chapter 4 as being desirable measurements to take but requiring linearised output matrices are terminal load angle δ_t, power P_t, Var Q_t, current i_t and voltage V_t.

In terms of d and q axis voltages and currents, they may be expressed as follows:

$$P_t = \frac{1}{2}(V_{td}\, i_d + V_{tq}\, i_q) \qquad [I.3]$$

$$Q_t = \frac{1}{2}(V_{td}\, i_q - V_{tq}\, i_d) \qquad [I.4]$$

$$V_t = \left(\frac{1}{2}(V_{td}^2 + V_{tq}^2)\right)^{\frac{1}{2}} \quad [I.5]$$

$$i_t = \left(\frac{1}{2}(i_d^2 + i_q^2)\right)^{\frac{1}{2}} \quad [I.6]$$

$$\delta_t = \text{Arctan}\,(V_{td}/V_{tq}) \quad [I.7]$$

Linearising for small disturbances gives:

$$\Delta P_t = \frac{1}{2}(\Delta V_{td}\, i_{do} + \Delta V_{tq}\, i_{qo} + \Delta i_d\, V_{tdo} + \Delta i_q\, V_{tqo}) \quad [I.8]$$

$$\Delta Q_t = \frac{1}{2}(\Delta V_{td}\, i_{qo} - \Delta V_{tq}\, i_{do} + \Delta i_q\, V_{tdo} - \Delta i_d\, V_{tqo}) \quad [I.9]$$

$$\Delta V_t = (V_{tdo}\, \Delta V_{td} + V_{tqo}\, \Delta V_{tq}) / 2V_{to} \quad [I.10]$$

$$\Delta i_t = (i_{do}\, \Delta i_d + i_{qo}\, \Delta i_q) / 2i_{to} \quad [I.11]$$

$$\Delta \delta_t = \left(\frac{1}{1 + \tan^2\delta_{to}}\right)\left(\frac{\Delta V_{td}}{V_{tqo}} - \frac{V_{tdo}\, \Delta V_{tq}}{V_{tqo}^2}\right) \quad [I.12]$$

Where the subscript o indicates values of the variables at the steady-state operating point about which linearisation is made, and ΔV_{td}, ΔV_{tq}, Δi_d and Δi_q can be expressed as linear functions of the machine state-variables [see Section 2.2.3, Appendices B and C].

APPENDIX J

DIAGRAMS OF CIRCUITS USED IN THE LABORATORY POWER SYSTEM

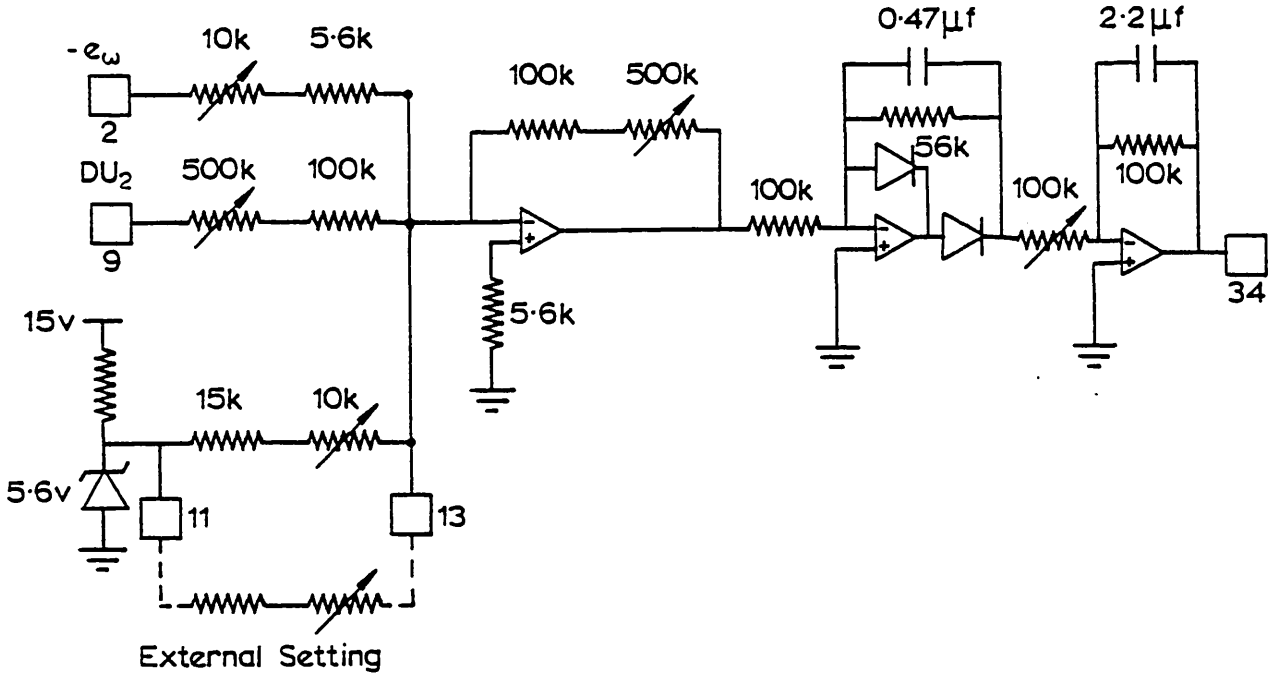

J.1 SIMPLE GOVERNOR/TURBINE MODEL

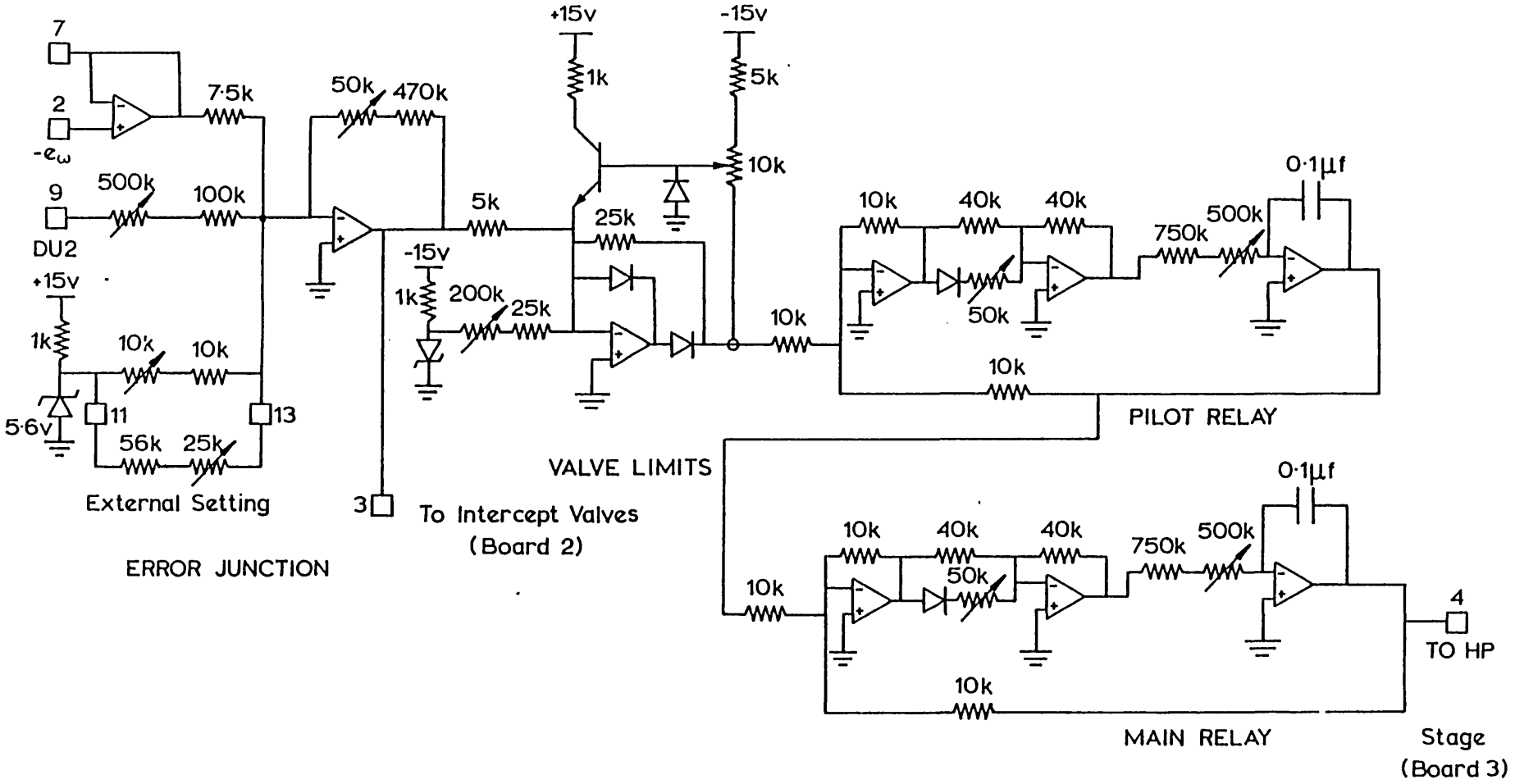

J.2.1 DETAILED GOVERNOR/TURBINE MODEL - GOVERNOR AND THROTTLE VALVE SYSTEM [BOARD 1].

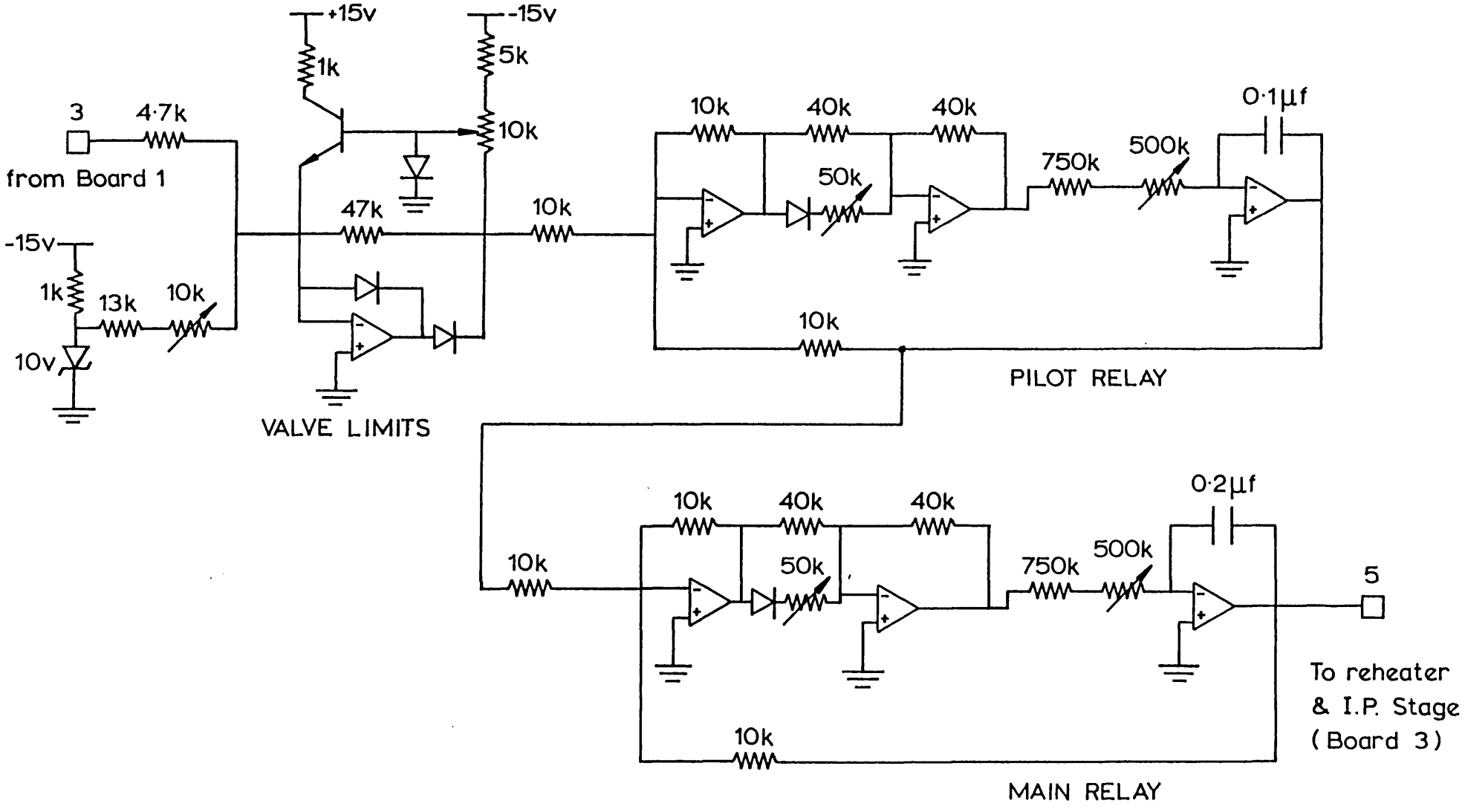

J.2.2 DETAILED GOVERNOR/TURBINE MODEL - INTERCEPT VALVE SYSTEM [BOARD 2].

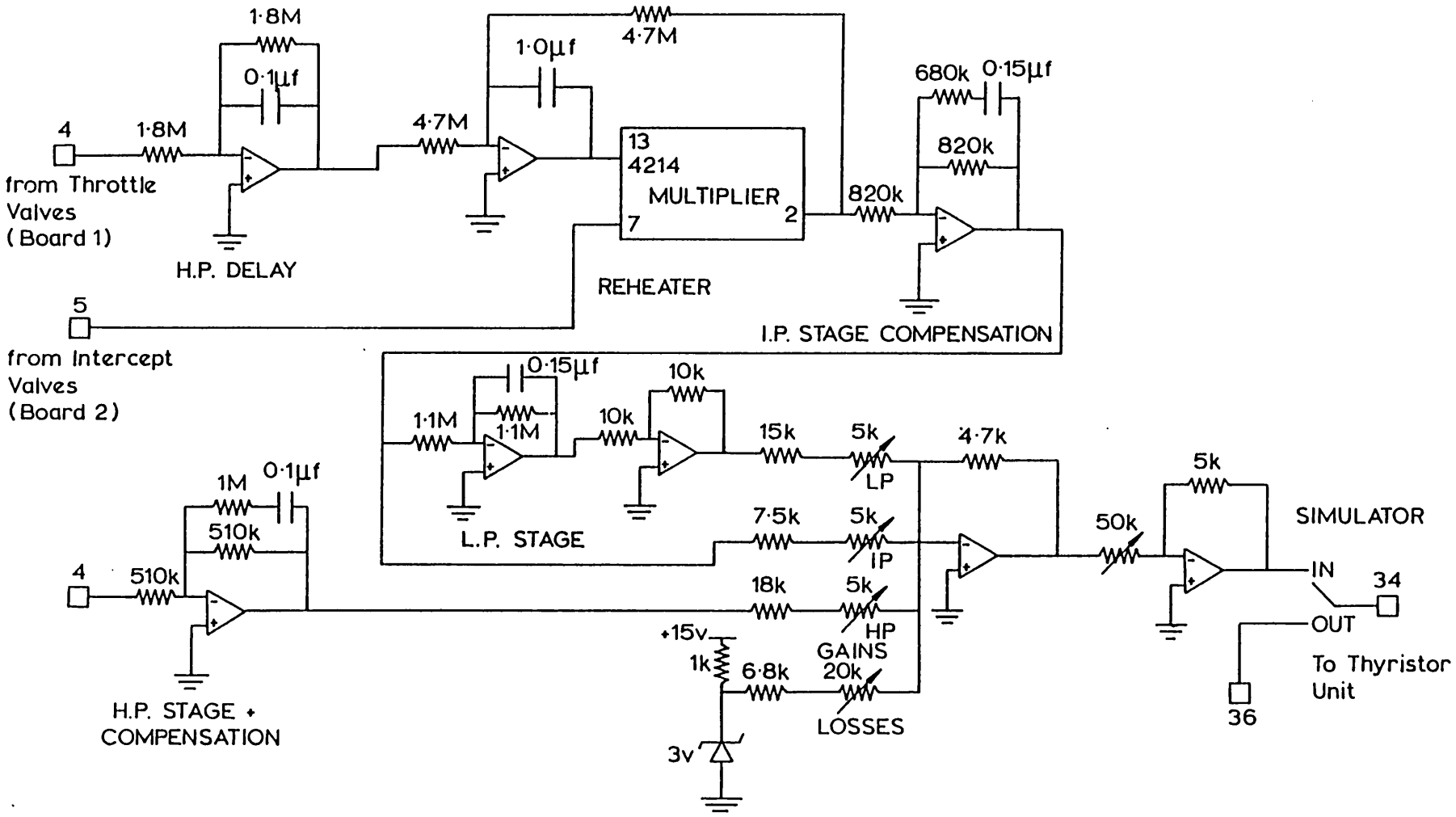

J.2.3 DETAILED GOVERNOR/TURBINE MODEL - REHEATER AND TURBINE MODELS [BOARD 3].

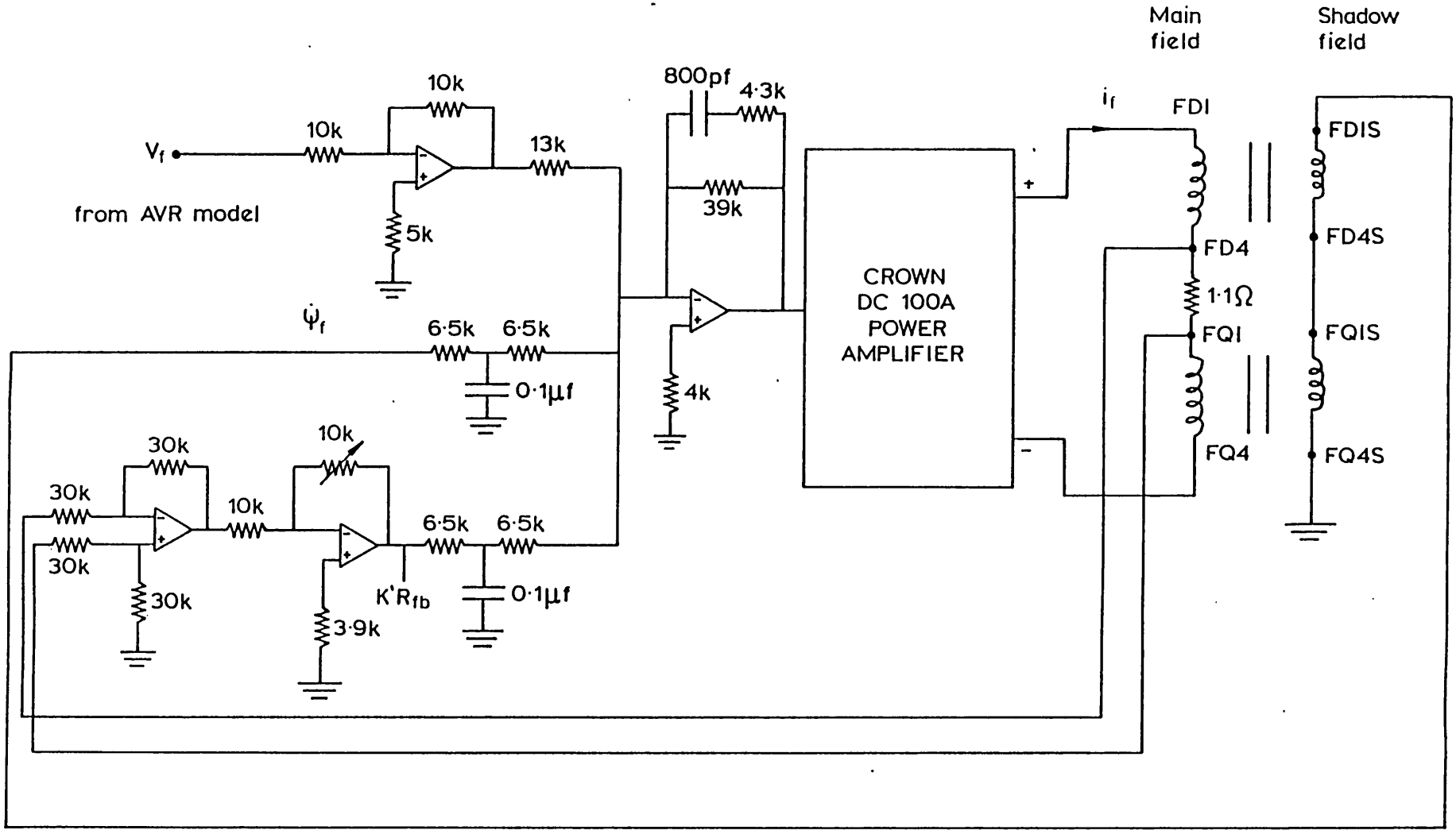

J.3 THE TIME CONSTANT REGULATOR CIRCUIT.

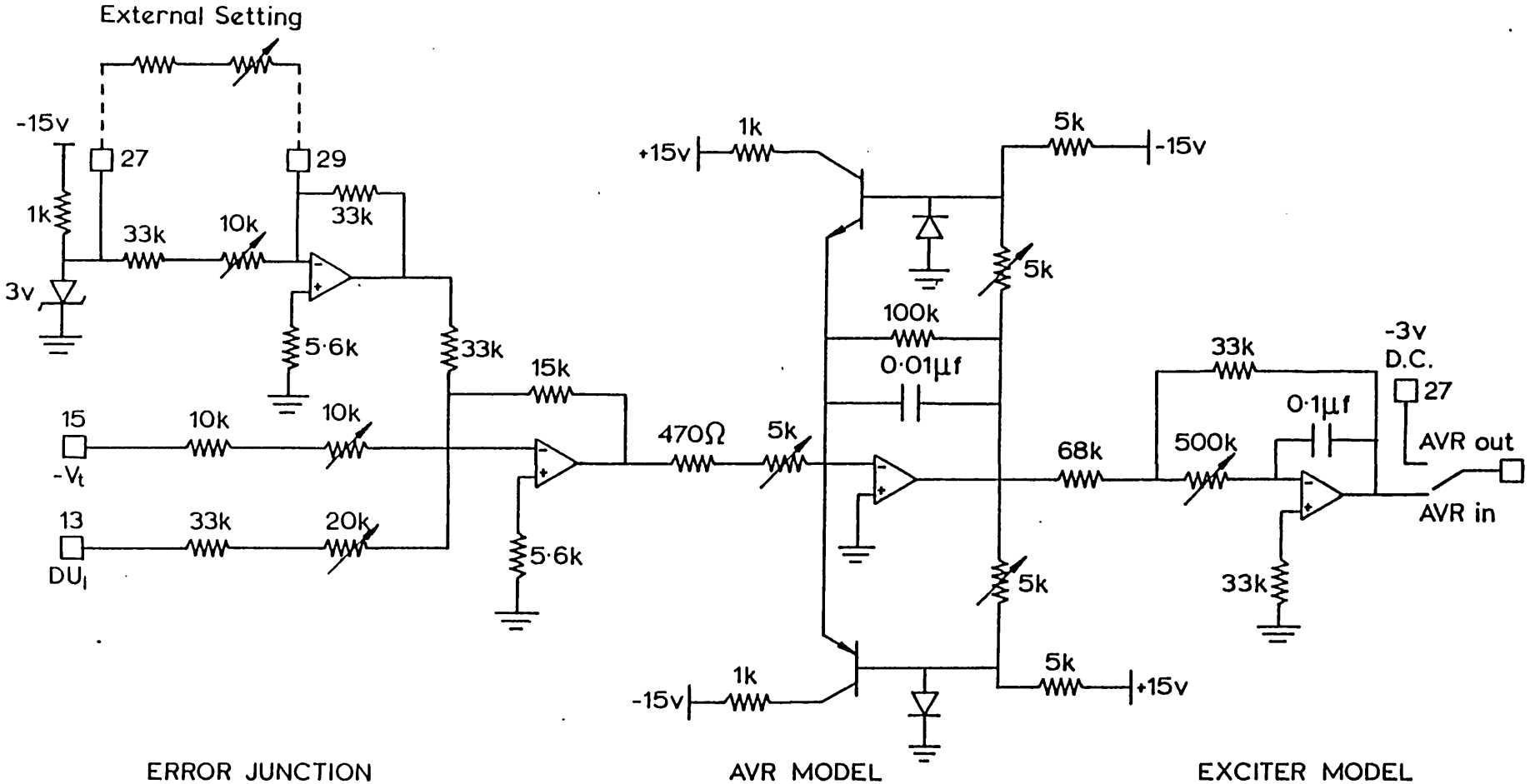

J.4 AVR AND EXCITER MODEL.

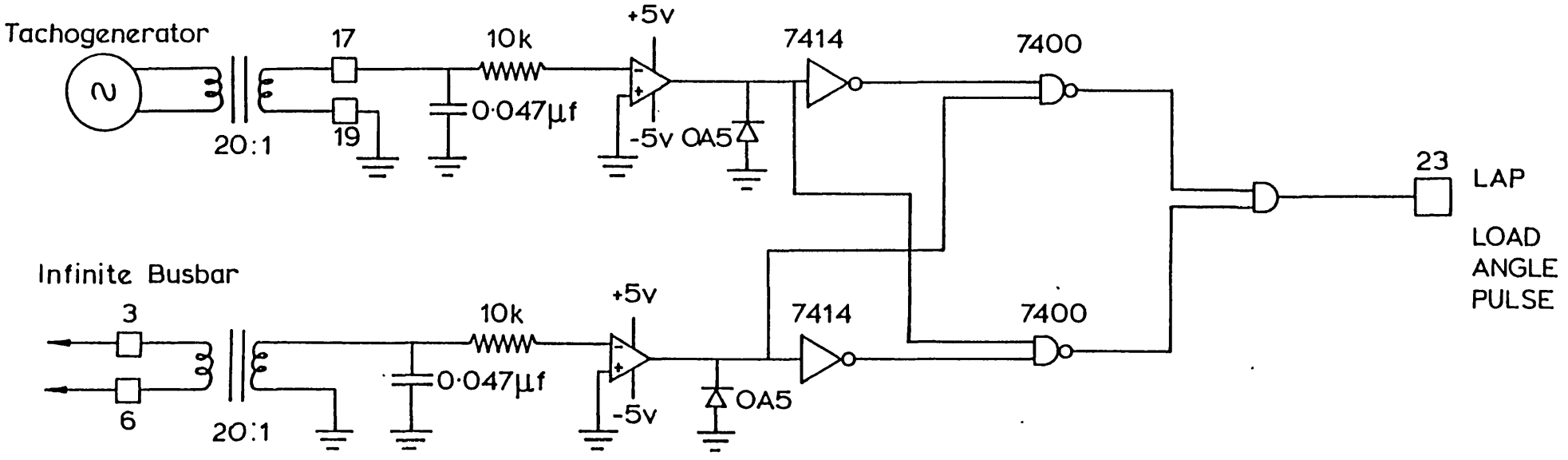

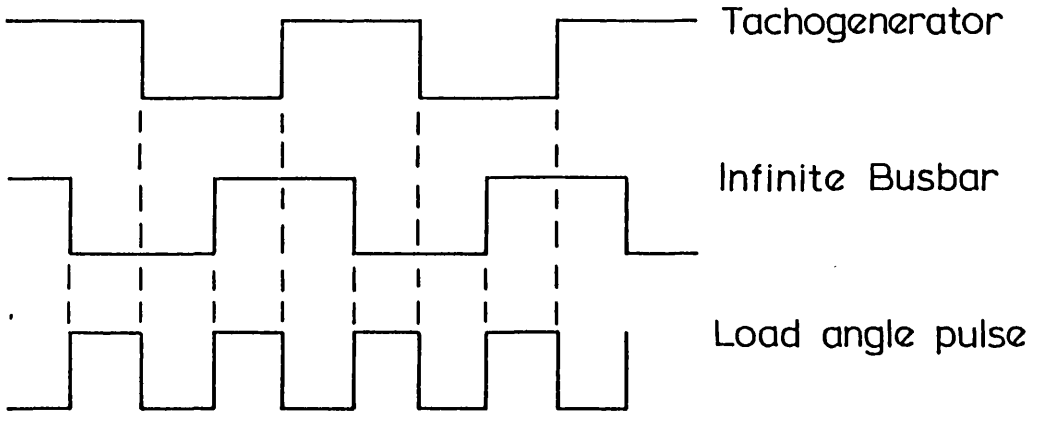

J.5.1 LOAD ANGLE TRANSDUCER - PULSE CIRCUIT.

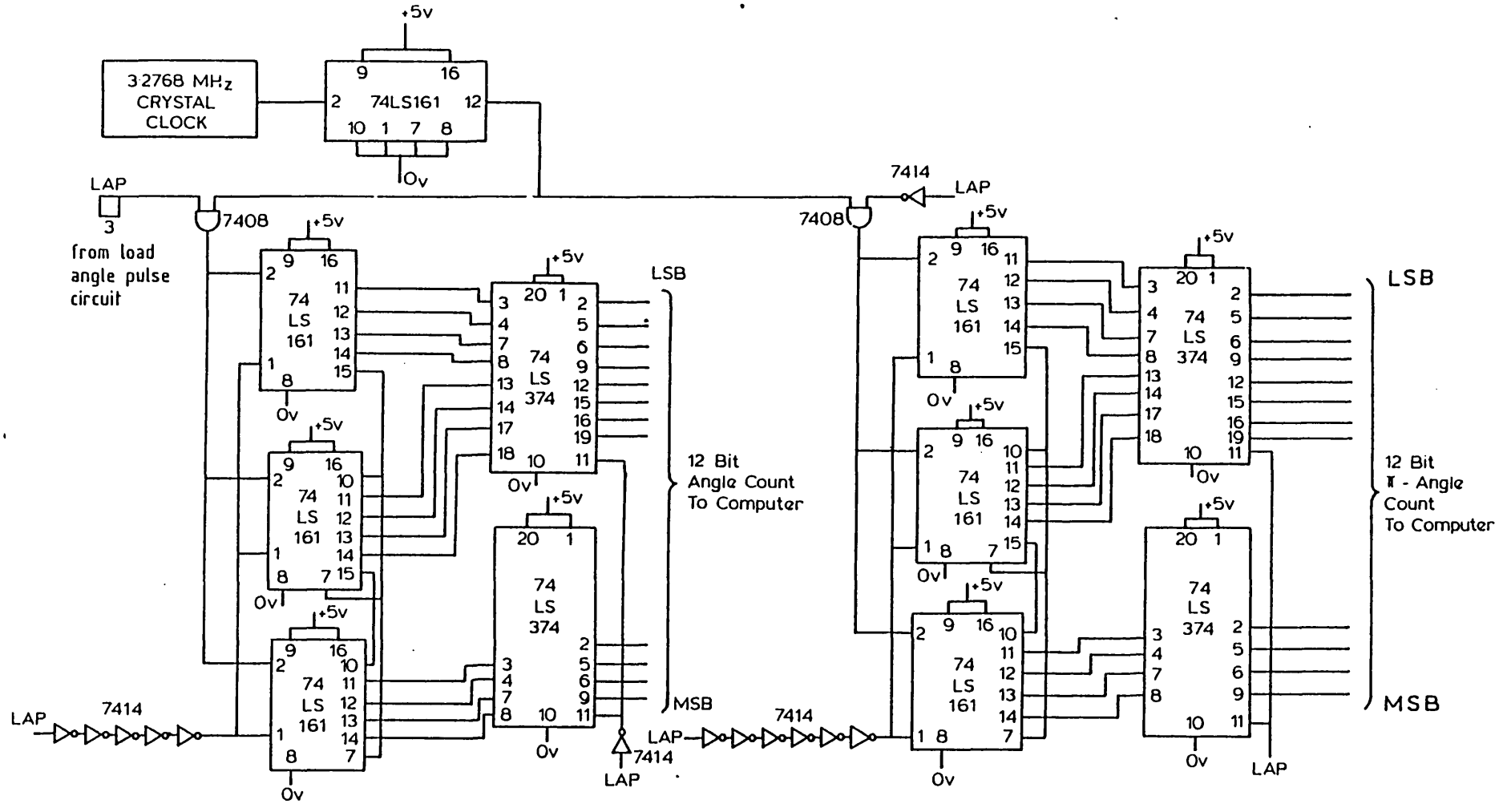

J.5.2 LOAD ANGLE TRANSDUCER - COUNTER AND LATCH CIRCUIT.

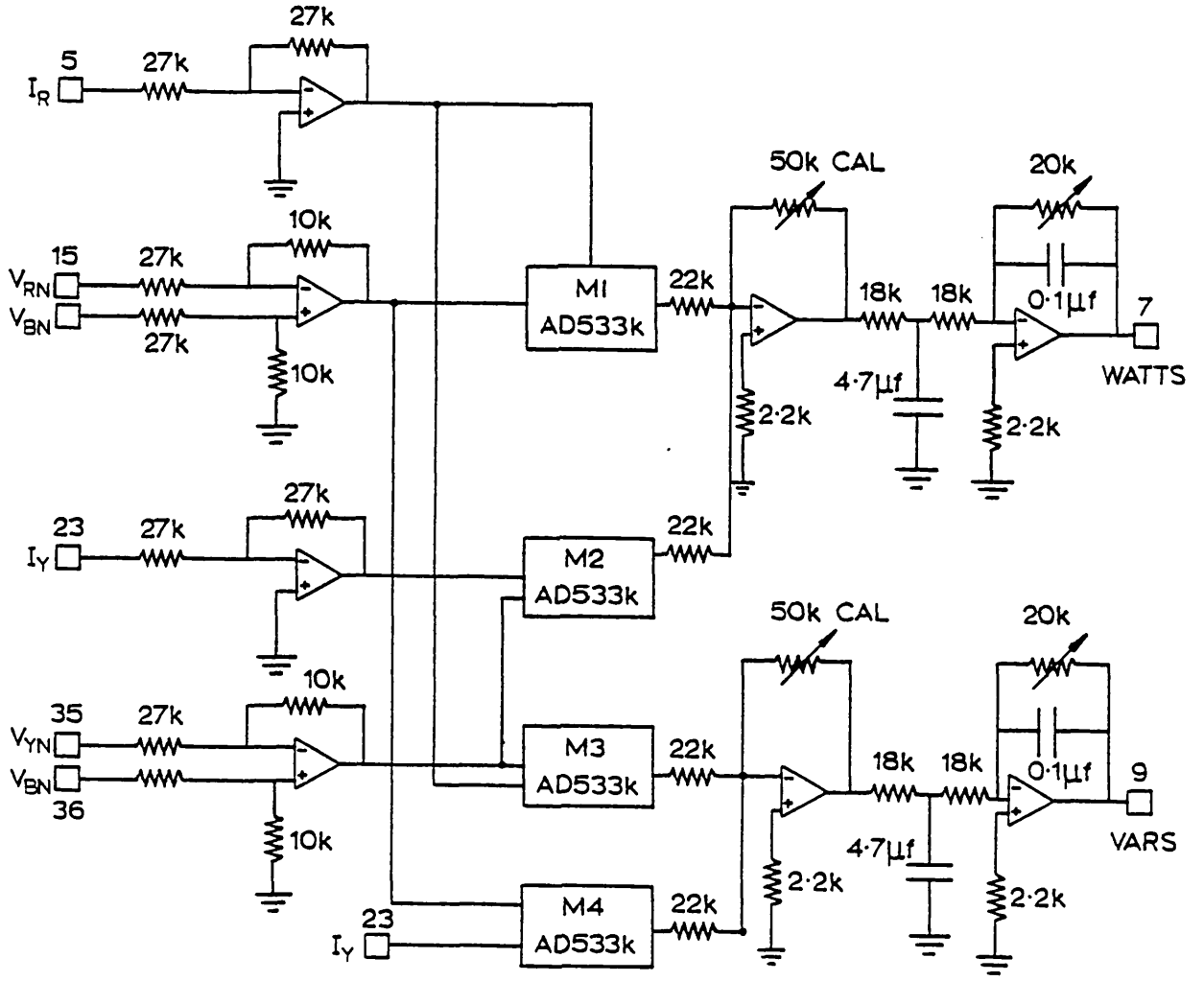

J.6 WATT-VAR TRANSDUCER

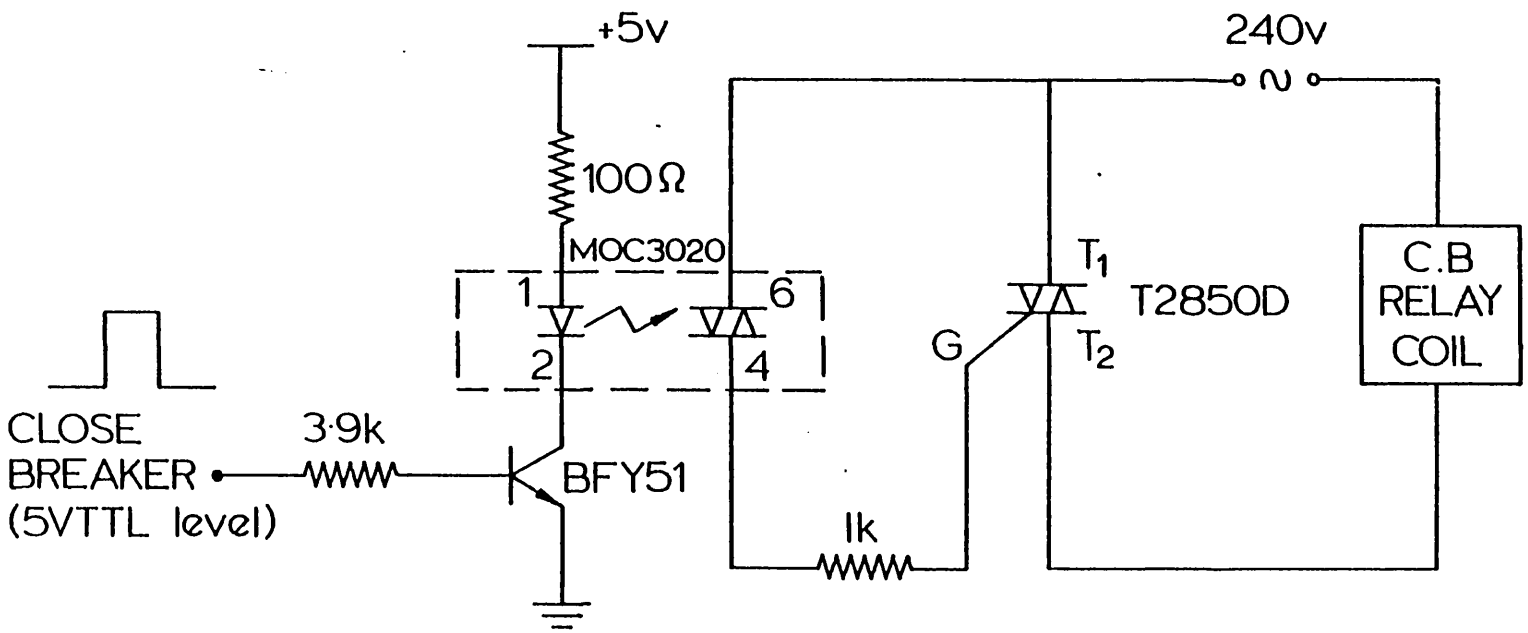

J.7 OPTO-ISOLATED CIRCUIT BREAKER INTERFACE

APPENDIX K

THE DEC LSI 11/23 ON-LINE CONTROL COMPUTER SYSTEM

CPU:	KDF 11-AA [DEC]
Floating Point Processor:	FPF 11-A [DEC]
RAM:	128k Byte MSC 4804 [Monolithic Systems Corp.]
Parallel I/O:	4 channels x 16 bits DRV 11-J [DEC]
Analogue I/O:	8 different A/D channels, 2 D/A AXV 11-C [DEC]
Serial I/O:	4 channels Model 304 [Grant Technology Systems]
Enclosure and Backplane:	SA-H 105 [Arrow Computer Systems]
Floppy Disk Drive:	Single $8\frac{1}{2}$" double-sided YD-180 [YE-data]
Floppy Disk Controller:	RXV-21 [General Robotics Corp.]
Winchester Disk:	20M Byte $5\frac{1}{4}$" RMS-500 [Rotating Memory Systems]
Winchester Disk Controller:	DQ614 [Dilog Corp.]
VDU:	3100 [Cobar]
Operating system:	RT-11 [DEC]

APPENDIX L

THE ON-LINE CONTROL PROGRAM

There follows a listing of the MACRO-11 assembly language general-order on-line control program. The measured variables are load angle and field voltage, but only minor modifications to I/O statements are required to read in other variables [see Ref. 128]. The routine is called from a FORTRAN initialisation program, which reads in all required gain and transition matrices, sets up workspaces and calculates steady-state conditions. The calling procedure is as follows:

```
CALL OLCOGN(VFSCAL, A, B, V1A, DVF, DSCALE,
VV1A, DY1, YPKM, DYE, GKT, WK, NN, PP, CORR,
YKM, IWK, FBT, DU, U1SCAL, U2SCAL, HBT,
YK1, TPHIT, YK2, CT)
```

Where the arguments are explained in the documentation accompanying the listing.

```
.TY OLCOGN.MAC
        .TITLE OLCOGN
        .GLOBL OLCOGN
        .GLOBL FPMULT
;
;  ASSEMBLY LANGUAGE OPTIMAL CONTROL ROUTINE
;  GENERAL KALMAN FILTER/OPTIMAL CONTROLLER MEASURING ANY INPUTS
;  Y1 AND Y2 VIA THE C MATRIX. PERFORMS DIGITAL WASHOUT FILTERING
;  CALCULATES ESTIMATES & FEEDS BACK SUPPLEMENTARY SIGNALS
;  DU1 AND DU2
;  GENERAL VERSION FOR A,B AND C MATRICES OF ANY ORDER
;
;  WRITTEN APRIL 1983 BY A.D.NOBLE
;  MODIFIED FOR INTERFACING TO MACHINE SEPT 1983
;  MODIFIED FOR DRV11-J 16-FEB-84
;  GENERAL VERSION WRITTEN 9-MAR-84
;
;  VERSION FOR MEASURING 2 INPUTS FROM DRV11-J -  ANGLE AND
;  REMAINING HALF CYCLE. PERFORMS CHECKSUM FOR BAD DATA
;  REJECTION.
;  DATA READY SIGNAL IS AI/O 8 (WIRE 47 ON J1) TO DRV11-J
;  CAN BE USED EITHER INTERRUPT-FREE OR INTERRUPT-DRIVEN.
;
        AC0=%0                  ;FLOATING POINT ACCUMULATORS
        AC1=%1
        AC2=%2
        AC3=%3
        AC4=%4
        AC5=%5
        CSRA    =164160         ;DRV11J:CONTROL/STATUS REG A
        CSRB    =164164         ;       DITTO B
        CSRC    =164170         ;       DITTO C
        CSRD    =164174         ;       DITTO D
        DBRC    =164172         ;       INPUT PORT C
        DBRD    =164176         ;       INPUT PORT D
        AXVCSR  =170400         ;AXV11C:CONTROL/STATUS REGISTER
        ADC     =170402         ;       A/D INPUT
        DAC1    =170404         ;       D/A OUTPUT 1
        DAC2    =170406         ;       D/A OUTPUT 2
        KBS     =177560         ;KEYBOARD:CONTROL/STATUS REG
        KBB     =KBS+2

        .ASECT
        .       =400
        RDINT
        340

        .PSECT

        .MCALL  .EXIT
;
;  NO OF ARGUMENTS:27 INCLUDING ARGUMENT COUNT
;  ARGUMENTS Y2SCALE,A,B,V1,DY2,Y1SCALE,VV1,DY1,
;  YPK,DYE,GKT,WK,NSTATE,NIPOP,CORR,YK
;  WK1,(-)FBT,DU,U1SCALE,U2SCALE,HBT,YK1,PHIT,YK2,CT
```

```
;  A,B:FILTER CONSTANTS V1,VV1:FILTER VARIABLES
;  YPK:CURRENT ESTIMATES DYE: ESTIMATED INPUTS
;  GKT: KALMAN MATRIX(TRANSPOSED WRT
;  NORMAL CONVENTION) WK:WORKSPACE(4 WORDS)
;  NSTATE:NO.OF STATES  NIPOP:NO.OF INPUTS/OUTPUTS OF SYSTEM
;  CORR:CORRECTIVE TRACKING TERM YK:ESTIMATE OF STATES AT NEXT T.STEP
;  WK1:WORKSPACE(6 WORDS) FBT:FEEDBACK MATRIX(TRANSPOSED WRTNC)
;  DU:SUPPLEMENTARY CONTROL SIGNALS   U1SCALE,U2SCALE: OUTPUT SCALE
;  FACTORS FOR DU1 AND DU2  HBT:INPUT TRANSITION MATRIX
;  YK1:PART OF YK DUE TO INPUTS PHIT:STATE TRANSITION MATRIX
;  YK2:PART OF YK DUE TO STATES
;  CT: OUTPUT MATRIX OF SYSTEM TRANSPOSED
;
OLCOGN: TST     (R5)+           ; SKIP ARGT COUNT ARG1
        SETF                    ; SET TO SINGLE PRECISION F.P.MODE
        MOV     R5,@#ARG1       ; STORE LOC OF FIRST ARGUMENT
        BIC     #100,@#KBS      ; DISABLE KEYBOARD INTERRUPTS
        MOV     #1000,@#CSRA    ; ENABLE DRV11-J INTERRUPTS
        MOV     #CSRC,R0        ; R0 POINTS TO CSRC
        CLR     (R0)            ; RESET GROUP 2 CONTROLLER
        MOVB    #340,(R0)       ; PRESELECT VECTOR ADDRESS MEMORY
                                ; (IRQ LEVEL 6)
        MOVB    #100,@#CSRD     ; LOAD VECTOR OF 400 ( VECTOR=CSRD BYTE
                                ; SHIFTED 2 BITS TO RIGHT )
        MOVB    #241,@#CSRA     ; ARM GROUP 1 WITH MASTER MASK BIT
                                ; THIS WILL ENABLE GROUP 2
        MOVB    #241,(R0)       ; ARM GROUP 2 WITH MASTER MASK BIT
        MOVB    #300,(R0)       ; PRESELECT ACR FOR WRITING
        MOVB    #1,@#CSRD       ; AUTO-CLEAR OPTION ON BIT 6
        MOVB    #50,(R0)        ; CLEAR GROUP 1 IMR BIT 6

AGAIN:
;       WAIT                    ; DISABLE IF INTERRUPTS NOT USED
        MOV     @#ARG1,R5
        LDF     @(R5)+,AC1      ; Y2SCALE TO AC1 ARG2
;
;  READ IN Y2
;
        MOV     #1,@#AXVCSR     ; START A/D OF Y2
ADCON:  CMP     @#AXVCSR,#200   ; CONVERSION DONE ?
        BNE     ADCON
        MOV     @#ADC,R4        ; YES - PUT IN R4
        SUB     #3777,R4        ; CONVERT FROM OFFSET BINARY
;       MOV     #-500.,R4       ; CONSTANT VALUE OF Y2 FOR TEST PURPOSES
        LDCIF   R4,AC0
        MULF    AC1,AC0         ; SCALE & RESULT TO R0
        LDF     @(R5)+,AC1      ; A TO AC1 ARG3
        LDF     @(R5)+,AC2      ; B TO AC2 ARG4
        LDF     @(R5),AC3       ; V1 TO AC3 ARG5
        STF     AC3,AC4         ; AND AC4
        STF     AC0,AC5         ; Y2 TO AC5
;
;  FILTERING OF Y2
;
        MULF    AC1,AC0         ; A*Y2 TO AC0
        MULF    AC2,AC3         ; B*V1 TO AC3
        ADDF    AC0,AC3         ; V2=A*Y2+B*V1
        STF     AC3,@(R5)+      ; V2 REPLACES V1
```

```
        ADDF    AC4,AC3         ; V2+V1=Y20 TO AC3
        LDF     AC5,AC0         ; Y2 TO AC0
        SUBF    AC3,AC0         ; DY2 TO AC0
        MOV     R5,@#TEMP1      ; STORE ARGT POINTER
        STF     AC0,@(R5)+      ; DY2 TO ARGT LIST ARG6
;
;  READ IN DELTA(Y1)
;
        LDF     @(R5)+,AC3      ; Y1 SCALE FACTOR TO AC3 ARG7
        MOV     @#DBRC,R4       ; DELTA TO R4
        BIC     #170000,R4      ; MASK FIRST 4 BITS
        MOV     #1740.,R4       ; CONSTANT READING FOR TEST PURPOSES
        MOV     @#DBRD,R3       ; 180-DELTA TO R3
        BIC     #170000,R3      ; MASK FIRST 4 BITS
        ADD     R4,R3           ; CHECKSUM ERROR TEST:
        CMP     R3,#3950.       ; SUM MUST BE CLOSE TO 4096.
        BLE     3$              ; IF NOT REJECT DATA
        CMP     R3,#5150.
        BGE     3$
3$:     LDCIF   R4,AC0          ; CALCULATE  ANGLE*SCALE
        MULF    AC3,AC0         ; & RESULT TO AC0
        LDF     @(R5),AC3       ; VV1 TO AC3 ARG8
        STF     AC3,AC4         ; AND AC4
        STF     AC0,AC5         ; Y1 TO AC5
;
;  FILTERING OF DELTA(Y1)
;
        MULF    AC1,AC0         ; A*Y1 TO AC0
        MULF    AC2,AC3         ; B*VV1 TO AC3
        ADDF    AC0,AC3         ; VV2=A*Y1+B*VV1
        STF     AC3,@(R5)+      ; VV2 REPLACES VV1
        ADDF    AC4,AC3         ; VV2+VV1=Y10 TO AC3
        LDF     AC5,AC0         ; Y1 TO AC0
        SUBF    AC3,AC0         ; DY1 TO AC0
        STF     AC0,@(R5)+      ; DY1 TO ARGT LIST ARG9
        MOV     @#TEMP1,R4      ; DY2 ADDR TO R4
        LDF     @(R4),AC1       ; DY2 TO AC1
;
;  KALMAN ESTIMATION
;
        MOV     (R5)+,@#YPK     ; ADDR OF YPK TO @#YPK ARG10
        MOV     (R5)+,@#TEMP7   ; ADDR OF DYE TO @#TEMP7 ARG11
        MOV     @#TEMP7,R0      ; ADDR OF DYE TO R0
        SUBF    (R0)+,AC0       ; DY1-DYE(1) TO AC0
        SUBF    (R0)+,AC1       ; DY2-DYE(2) TO AC1
        TST     (R5)+           ; SKIP GK ADDRESS ARG12
        MOV     (R5)+,R4        ; ADDRESS OF WK TO R4 ARG13
        STF     AC0,(R4)+       ; STORE DY1-DYE(1)
        STF     AC1,(R4)        ; IN WK
        MOV     R5,@#TEMP2      ; STORE ARGT POINTER
        SUB     #6,R5           ; SET ARGT POINTER TO CORRECT LOCATION
        JSR     PC,FPMULT       ; CALCULATE CORR=FB*(DY(MEAS)-DY(ESTIMATED))
        MOV     @#TEMP2,R5      ; RETRIEVE ARGT POINTER
        MOV     (R5),@#NIPOP    ; STORE POINTER TO NIPOP
        TST     (R5)+           ; SKIP NIPOP ARG14
        MOV     (R5),@#NSTATE   ; STORE POINTER TO NSTATE
```

```
        MOV     @(R5)+,R0       ; NSTATE TO R0 ARG15
        MOV     (R5)+,R1        ; ADDR OF CORR TO R1 ARG16
        MOV     (R5)+,R2        ; ADDR OF YK TO R2 ARG17
        MOV     R2,@#TEMP6      ; ADDR OF YK TO TEMP6
        MOV     @#YPK,R3        ; ADDR OF YPK TO R3
1$:     LDF     (R1)+,AC0       ; CORR(I) TO AC0
        ADDF    (R2)+,AC0       ; CORR(I)+YK(I) TO AC0
        STF     AC0,(R3)+       ; STORE NEW YPK(I)
        SOB     R0,1$           ; DO P TIMES
;
;  CALCULATION OF SUPPLEMENTARY FEEDBACK SIGNALS DU
;  DU(2) TO GOV. LOOP DU(1)TO AVR LOOP
;
        MOV     (R5)+,R0        ; ADDR OF WK1 TO R0 ARG18
        MOV     R0,@#TEMP4      ; ADDR OF WK1 TO TEMP4
        TST     (R0)+           ; ARGT. COUNT SPACE
        MOV     (R5)+,(R0)+     ; ADDR OF FB POINTED TO BY R0 ARG19
        MOV     @#YPK,(R0)+     ; ADDR OF YPK TO LIST
        MOV     @#NSTATE,(R0)+  ; N=NSTATE
        MOV     @#NIPOP,(R0)+   ; P=NIPOP
        MOV     (R5),@#TEMP5    ; ADDR OF DU TO TEMP5
        MOV     (R5)+,(R0)      ; ADDR OF DU TO LIST ARG20
        MOV     R5,@#TEMP2      ; STORE R5 .
        SUB     #12,R0          ; SET R0 POINTER BACK TO ARGT COUNT
        MOV     R0,R5           ;
        JSR     PC,FPMULT       ; CALCULATE DU=-FB*YPK
        MOV     @#TEMP5,R0      ; ADDR OF DU TO R0
        MOV     @#TEMP2,R5      ; RETRIEVE R5
;
;  DU OUTPUT FOR FEEDBACK TO PLANT FOR OPTIMAL CONTROL
;
        LDF     @(R5)+,AC0      ; U1SCALE TO AC0 FOR O/P OF DU(1) TO D/A ARG21
        MULF    (R0)+,AC0       ; DU(1)*SCALING FACTOR
        STCFI   AC0,R1          ; CONVERT TO INTEGER & STORE IN R1
        ADD     #3777,R1        ; CONVERT TO OFFSET BINARY NOTATION
        MOV     R1,@#DAC1       ; OUTPUT TO DAC CHANNEL 1
        LDF     @(R5)+,AC0      ; U2SCALE TO AC0 ARG22
        MULF    (R0),AC0        ; DU(2)*SCALING FACTOR
        STCFI   AC0,R1          ; CONVERT TO INTEGER & STORE IN R1
        ADD     #3777,R1        ; CONVERT TO OFFSET BINARY
        MOV     R1,@#DAC2       ; O/P TO DAC CH 2
        MOV     @#TEMP4,R0      ; WK1 ADDR TO R0
        TST     (R0)+           ; ARGT COUNT SPACE
        MOV     (R5)+,(R0)+     ; ADDR OF HB TO LIST ARG23
;
;       OUTPUT TO DAC FINISHED
;
        MOV     @#TEMP5,(R0)+   ; ADDR OF DU TO LIST
        MOV     @#NIPOP,(R0)+   ; N=NIPOP
        MOV     @#NSTATE,(R0)+  ; P=NSTATE
        MOV     (R5),@#TEMP5    ; ADDR OF YK1 TO TEMP5
        MOV     (R5)+,(R0)      ; ADDR OF YK1 TO LIST ARG24
        MOV     R5,@#TEMP2      ; STORE R5      .
        SUB     #12,R0          ; SET R0 POINTER BACK TO ARGT COUNT
        MOV     R0,R5           ;
        JSR     PC,FPMULT       ; CALCULATE YK1=HB*DU
        MOV     @#TEMP2,R5      ; RETRIEVE R5
```

```
;
;   ESTIMATE STATES AT BEGINNING OF NEXT TIME STEP
;
        MOV     @#TEMP4,R0      ; WK1 ADDR TO R0
        TST     (R0)+           ; ARGT COUNT SPACE
        MOV     (R5)+,(R0)+     ; ADDR OF PHI TO LIST ARG25
        MOV     @#YPK,(R0)+     ; ADDR OF YPK TO LIST
        MOV     @#NSTATE,(R0)+  ; N=NSTATE
        MOV     @#NSTATE,(R0)+  ; P=NSTATE
        MOV     (R5),@#TEMP1    ; ADDR OF YK2 TO TEMP1
        MOV     (R5)+,(R0)      ; ADDR OF YK2 TO LIST  ARG26
        MOV     R5,@#TEMP2      ; STORE R5
        SUB     #12,R0          ; SET R0 POINTER BACK TO ARGT COUNT
        MOV     R0,R5           ;
        JSR     PC,FPMULT       ; CALCULATE YK2=PHI*YPK
        MOV     @#NSTATE,R1     ; SET COUNTER VARIABLE
        MOV     (R1),R0
        MOV     @#TEMP5,R1      ; ADDR OF YK1 TO R1
        MOV     @#TEMP1,R2      ; ADDR OF YK2 TO R2
        MOV     @#TEMP6,R3      ; ADDR OF YK TO R3
2$:     LDF     (R1)+,AC0       ; YK1(I) TO AC0
        ADDF    (R2)+,AC0       ; YK1(I)+YK2(I) TO AC0
        STF     AC0,(R3)+       ; STORE NEW YK(I)
        SOB     R0,2$           ; DO NSTATE TIMES
;
;    ESTIMATE NEXT INPUTS
;    DYE=C*YPK
;
        MOV     @#TEMP2,R5      ; RETREIVE R5
        MOV     @#TEMP4,R0      ; WK1 TO R0
        TST     (R0)+           ; ARGT COUNT SPACE
        MOV     (R5)+,(R0)+     ; ADDR OF C POINTED TO BY R0 ARG27
        MOV     @#YPK,(R0)+     ; ADDR OF YPK TO LIST
        MOV     @#NSTATE,(R0)+  ; N=NSTATE
        MOV     @#NIPOP,(R0)+   ; P=NIPOP
        MOV     @#TEMP7,(R0)    ; ADDR OF DYE TO LIST
        MOV     R5,@#TEMP2      ; STORE R5
        SUB     #12,R0          ; SET R0 POINTER BACK TO R0
        MOV     R0,R5           ;
        JSR     PC,FPMULT       ; CALCULATE DYE=C*YPK
        MOV     @#TEMP2,R5      ;
;
;   REPEAT EXECUTION OF ALGORITHM UNTIL INTERRUPTED FROM KEYBOARD
;
        TSTB    @#KBS           ; TEST FOR KEY PRESSED
        BPL     4$              ; NO- CONTINUE
        TSTB    @#KBB           ; YES- CLEAN UP & RETURN TO RT11
        BIS     #100,@#KBS      ; RE-ENABLE KEYBOARD INTERRUPT
        CLR     @#CSRA          ; DISABLE DRV11-J INTERRUPTS
        CLR     @#CSRC
        .EXIT                   ; RETURN TO RT11 OPERATING SYSTEM
4$:
        CLR     @#CSRA          ; DISABLE INTERRUPTS
        RTS     PC
;       JMP     AGAIN           ; REPEAT
```

```
;
RDINT:  RTI
;
        RTS     PC
ARG1:   .BLKW
TEMP1:  .BLKW
TEMP2:  .BLKW
YPK:    .BLKW
TEMP4:  .BLKW
TEMP5:  .BLKW
TEMP6:  .BLKW
TEMP7:  .BLKW
NSTATE: .BLKW
NIPOP:  .BLKW
        .END
```

```
.TY FPMULT.MAC
        .TITLE FPMULT
        .GLOBL FPMULT
        AC0=%0
        AC1=%1
        AC2=%2
;
;  ROUTINE TO MULTIPLY A MATRIX OF P ROWS AND N COLUMNS
;  (ALPHA) BY A (P*1) ARRAY (BETA) - RESULT GAMMA
;  ARGUMENTS ALPHA,BETA,N,P,GAMMA
;  FLOATING POINT DATA REPRESENTATION
;
FPMULT: TST     (R5)+
.       SETF                    ;;SET TO SINGLE PRECISION F.PT.
        MOV     (R5)+,R0        ;;R0 HAS ADDRESS OF ALPHA
        MOV     (R5)+,R1        ;,R1 HAS ADDRESS OF BETA
        MOV     R1,@#BETA1      ;;STORE ADDRESS OF BETA(1)
        MOV     @(R5)+,R2       ;;R2 HAS N
        MOV     @(R5)+,R3       ;;R3 HAS P
        MOV     (R5),R4         ;,R4 HAS ADDR OF GAMMA
        MOV     R2,R5           ;;ORDER OF SYSTEM N TO R5
        CLRF    AC2             ;;CLEAR F.PT. ACCUMULATOR FOR RESULT
1$:     LDF     (R0)+,AC0       ;;PUT ALPHA(I,J) IN AC0
        LDF     (R1)+,AC1       ;;PUT BETA(J) IN AC1
        MULF    AC1,AC0         ;;MULTIPLY:RESULT TO AC0
        ADDF    AC0,AC2         ;;ADD TO AC2
        SOB     R2,1$           ;;DO N TIMES
        MOV     R5,R2           ;;RESET J
        STF     AC2,(R4)+       ;;STORE GAMMA(I)
        DEC     R3
        BEQ     RETURN          ;;RETURN WHEN DONE
        MOV     @#BETA1,R1      ;;RESET POINTER TO BETA(1)
        CLRF    AC2             ;;CLEAR F.P.ACC. FOR NEXT RESULT
        BR      1$
RETURN: RTS     PC
BETA1:  .BLKW   1
        .END
```

REFERENCES

1. WEEDY, B.M. "Electric Power Systems", John Wiley and Sons, London, 1979.

2. CRARY, S.B. "Power System Stability", John Wiley and Sons, New York, 1955.

3. JOYCE, J.S., KULIG, T., and LAMBRECHT, D. "Torsional fatique of turbine generator shafts caused by different electrical system faults and switching operations", IEEE Vol. PAS-97, No. 5, pp. 1965-1977, 1978.

4. HAMMONS, T.J. "Effects of Three-Phase System faults and faulty synchronisation on the mechanical stressing of large turbine generators", Revue Generale Electrique, 86(7-8), p.558, 1977.

5. CANAY, I.M., ROHRER, H.J. and SCHNIRKEL, K.E. "Effect of electrical disturbances, grid recovery voltage and generator inertia on maximisation of mechanical torques in large turbo-generator sets", IEEE Vol. PAS-99, No. 4, pp. 1357-1370, 1980.

6. GIBSON, P.F., JACK, A.G., and PETTY, D.J. "Comparison of fatigue life expenditure of turbine generator shafts due to torsional oscillations produced by various types of fault" IEE Power Division Colloquium on torsional oscillations in motors and generators, Digest No. 1982/20, pp. 5/1 - 5/8, 1982.

7. HAM, P.A.L. "Electronics in the control of turbine generators", Electronics and Power, pp. 365-369, 1978.

8. FENWICK, D.R. and WRIGHT, W.F. "Review of trends in excitation systems and possible future developments", Proc. IEE, Vol. 123, No. 5, pp.413-420, 1976.

9. BLAND, C.H., and HAM, P.A.L. "Some applications of microprocessors in the improvement of turbine-generator plant", IEE North Eastern Centre Symposium on microcomputer applications in power engineering, pp. 5/1-5/7, 1982.

10. SCHLEIF, F.R., HUNKINS, H.D., MARTIN, G.E., and HATTAN, E.C. "Exitation control to improve powerline stability", IEEE, vol. PAS-87, No. 6, pp.1426-1434, 1968.

11. VAAHEDI, E., and MACDONALD, D.C. "Optimal Generator control using a dynamic estimator", Paper No. A79044-9 presented at IEEE PES Winter Meeting, New York, 1979.

12. VAAHEDI, E. "Optimal control of power system generations using self-tuning state estimators", Ph.D. Thesis, University of London, 1979.

13. MENELAOU, M.C., and MACDONALD, D.C. "Supplementary signals to improve generator transient stability, on-line application to a generator", IEEE Trans., Vol. PAS-101, pp. 3543-3550, 1982.

14. MENELAOU, M.C., and MACDONALD, D.C. "Generator transient stability improvements with digitally derived supplementary signals" Proc. 16th UPEC, Sheffield, 1981.

19. MENELAOU, M.C. "Digital Control for turbine generators", Ph.D. Thesis, University of London, 1981.

16. ADKINS, B., and HARLEY, R.G. "The general theory of a.c. machines. Applications to practical problems", Chapman and Hall, London 1975.

17. LARSEN, E.V., SWANN, D.A. "Applying Power System Stabilisers. Part 1: General concepts. Part II: Performance objectives and tuning concepts. Part III: Practical considerations", IEEE, Vol. PAS-100, No. 6, pp. 3017-3045, 1981.

18. FAIRNEY, W., MYLES, A., WHITELEGG, T.M., and MURRAY, N.S. "Low frequency oscillations on the 275 KV interconnections between England and Scotland", CIGRE, Paper 31-08, Vol. 11, Paris, 1982.

19. MACLAREN, R.G.B., and TOAL, J.A. "Design and commissioning of power system stabiliers in the SSEB network", Proc 19th UPEC, Dundee, 1984.

20. ALIYU, U.O., EL-ABIAD, A.H. "A local control strategy for power systems in transient emergency state. Part I: Functional Design. Part II: Implementation and test results by simulation", Papers No. 82-WM-161-8 and 82-WM-162-6 presented at IEEE winter power meeting, New York, 1982.

21. KIMBARK, E.W. "Improvement of power system stability by switched series capacitors", IEEE, vol. PAS-85, pp.180-188, 1966.

22. SMITH, O.J.M. "Power system transient control by capacitor switching" IEEE, Vol. PAS-88, pp.28-35, 1969

23. PARK, R.H. "The design and use of braking resistors", IEEE paper no. 69C-12 published in IEEE Resources Roundup, Phoenix, Arizona, 1969.

24. FRIEDLANDER, E., YOUNG, D.J. "A.C. saturated reactors for power stability", Electrical Review, p.88, January 1965.

25. VENIKOV, V.A., STROEV, V.A., TAWFIK, M.A.H. "Optimal control of electrical power systems containing controlled reactors", IEEE, Vol. PAS-100, No. 9, 1981.

26. HUMPAGE, W.D., STOTT, B., "Effect of autoreclosing circuit breakers on transient stability in e.h.v. transmission systems". Proc. IEE vol. 111, pp. 1287-1298, 1964.

27. FAIRNEY, W., and HENSER, P.B. "Torsional oscillations in large generator shaft systems". IEE Power Division Colloquium on "Torsional oscillations in motors and generators", Digest No. 1982/20, pp. 3/1 - 3/13, 1982.

28. SOPER, J.A., and FAGG, A.R. "Divided winding rotor synchronous generator", Proc. IEE, Vol. 116, p.113, 1969.

29. HARLEY, R.G., and ADKINS, B. "Stability of synchronous machine with a divided-winding rotor", Proc. IEE, Vol. 117, p. 933, 1970.

30. WANGER, W. "Stability of parallel operation for high power transmission over long distances with alternating current", Brown Boveri Review, pp. 275-279, 1946.

31. EASTON, V., FITZPATRICK, J.A., and PARTON, K.C. "The performance of continuously acting voltage regulators with additional angle control", CIGRE, paper 308, part III, 1960.

32. SHIER, R.M., and BLYTHE, A.L. "Field tests of dynamic stability using a stabilising signal and computer program verification", IEEE, Vol. PAS-87, No. 2, pp. 315-322, 1968.

33. DANDENO, P.L., KARAS, A.N., McCLYMONT, K.R., and WATSON, W. "Effect of high-speed rectifier excitation signals on generator stability limits", IEEE, Vol. PAS-87, No. 1, pp. 190-201, 1968.

34. DEMELLO, F.P., and CONCORDIA, C. "Concepts of synchronous machine stability as affected by excitation control", IEEE, Vol. PAS-88, No. 4, pp. 316-329, 1969.

35. WATSON, W., and COULTES, M.E. "Static Exciter stabilising signals on large generators: Mechanical problems", IEEE, Vol. PAS-92, No. 1, pp. 204-212, 1973.

36. WALKER, D.M., BOWLER, C.E.J., JACKSON, R.L., and HODGES, D.A. "Results of SSR tests at Mohave", IEEE, Vol. PAS-94, No. 5, pp. 1878 - 1889, 1975.

37. HALL, M.C., and HODGES, D.A. "Experience with 500KV subsynchronous resonance and resulting turbine generator shaft damage at Mohave generating station", paper no. A76-40153 presented at IEEE PES winter meeting, New York, 1976.

38. LAWSON, R.A., SWANN, D.A., and WRIGHT, G.F. "Minimisation of power system stabiliser torsional interaction on large steam turbine generators", IEEE, Vol. PAS-97, No. 1, pp. 183-190, 1978.

39. RAINA, V.M., WILSON, W.J., and ANDERSON, J.H. "The control of rotor torsional oscillations by supplementary exciter stabilisation", paper no. A76-457-2 presented at IEEE PES summer meeting, Portland, Oregon, 1976.

40. DEMELLO, F.P., HANNETT, L.N., and UNDRILL, J.M. "Practical approaches to supplementary stabilising from accelerating power" IEEE, Vol. PAS-97, No. 5, pp. 1515-1522, 1978.

41. BAYNE, J.P., LEE, D.C., and WATSON, W. "A power system stabiliser for thermal units based on derivation of accelerating power", IEEE, Vol. PAS-96, No. 6, pp. 1777-1783, 1977.

42. UENOSONO, C., OKADA, T., MATSUKI, J., YAMADA, M., YOKOKAWA, S., and MORIYASU, S. "Development and testing of an automatic stability prediction and control [ASPAC] for a synchonous generator by air-gap flux", IEEE, Vol. PAS-101, No. 3, pp. 719-725, 1982.

43. MAXWELL, J.C. "On Governors". Proceedings of the Royal Society, 16, p. 270, 1868.

44. DINELEY, J.L., and KENNEDY, M.W. "Influence of governors on power system stability", Proc. IEE, Vol. 111, No. 1, pp. 98-106, 1964.

45. COLES, H.E. "Effects of prime-mover governing and voltage regulation on turboalternator performance", Proc. IEE, Vol. 112, No. 7, pp. 1395-1405, 1965.

46. CUSHING, E.W., DRECHSLER, G.E., KILLGOAR, W.P., MARSHALL, H.G., and STEWART, H.R. "Fast valving as an aid to power system transient stability and prompt resynchronisation and rapid reload after full load rejection", IEEE Vol. PAS-91, pp. 1624-1636, 1971.

47. WOODALL, J.R. and VANDERGRIFT, J. "Fast intercept valving aids unit stability". Electrical World, July 13, 1970.

48. JONES, G.A. "Transient stability of a synchronous generator under conditions of bang-bang excitation scheduling", IEEE Vol. PAS-84, pp. 114-121, 1965.

49. SMITH, O.J.M. "Optimal transient removal in a power system", IEEE Vol. PAS-84, pp. 361-374, 1965.

50. RAJAGOPALAN, A., and HARIHARAN, M.V. "Bang-bang excitation control", IEEE Vol. PAS-92, pp. 703-711, 1973.

51. MUSAAZI, M.K. "On-line generator control", M.Sc. Thesis, University of London, 1977.

52. BARNARD, R.D. "An optimal-aim control strategy for nonlinear regulator systems", IEEE, Vol. AC-20, No. 2, pp. 200-208, 1975.

53. MEISEL, J., SEN, A., LEQUARRE, J., and GILLES, M. "Emergency operating state control on bulk interconnected power systems", Final report on U.S. Dept. of Energy contract No. E(49-18)-2074, Wayne State University, Detroit, Michigan, pp.16-28, 1979.

54. PAVLIDES, S.A. "Digital possibilities for supplementary controls". Paper presented at conference on "Synchronous machines in Power Systems", Imperial College, March-April 1981.

55. NICHOLSON, H. "Integrated control of a nonlinear turbogenerator model under fault conditions", Proc. IEE, Vol. 116, No. 6, pp. 834-844, 1967.

56. IYER, S.N., and CORY, B.J. "Optimisation of turbo generator transient performance by differential dynamic programming", IEEE, Vol. PAS-90, pp. 2149-2157, 1971.

57. MUKHOPADHYAY, B.K., and MALIK, O.P. "Optimal control of synchronous machine excitation by quasilinearisation techniques", Proc. IEE, Vol. 119, pp. 91-98, 1972.

58. ATHANS, M., and FALB, P.L. "Optimal Control", McGraw Hill, New York, 1966.

59. ANDERSON, J.H. "The control of a synchronous machine using optimal control theory", Proc. IEEE, Vol. 59, No. 1, pp. 25-35, 1970.

60. YU, Y.N., VONGSURIYA, K., and WEDMAN, L.N. "Application of an optimal control theory to a power system", IEEE, Vol. PAS-89, No. 1, pp. 55-62, 1970.

61. DAVISON, E.J. and RAU, N.S. "The optimal output feedback of a synchronous machine", IEEE, Vol. PAS-90, pp. 2123-2133, 1971.

62. RAMAMOORTY, M., and ARUMUGAM, M. "Design of optimal regulators for synchronous machines", paper no. 71TP 586-PWR presented at IEEE summer power meeting, 1971.

63. QUINTANA, V.H., ZOHDY, M.A., and ANDERSON, J.H. "On the design of output feedback excitation controllers of synchronous machines", IEEE, Vol. PAS-95, pp. 954-961, 1976.

64. YU, Y.N., and MOUSSA, H.A.M. "Optimal power system stabilisation through excitation and/or governor control", IEEE Vol. PAS-90, pp. 1166-1173, 1971.

65. EVANS, F.J., NGO, Y.H., and OUTHRED, H.R. "The on-line digital and optimal control of generator excitation systems", CIGRE, paper 32-05, Vol. 1] Paris, 1972.

66. MOYA, O.E.O., and CORY, B.J. "On-line control of generator transient stability by minicomputer", Proc. IEE, Vol. 124, pp. 252-258, 1977.

67. ELMETWALLY, M.M., RAO, N.D., and MALIK, O.P. "Experimental results on the implementation of an optimal control for synchronous machines", IEEE, Vol. PAS-94, No. 4, pp.1192-1199, 1975.

68. DANIELS, A.R., DAVIS, D.H., and PAL, M.K. "Linear and nonlinear optimisation of power system performance", IEEE, Vol. PAS-94, No. 3, pp.810-818, 1975.

69. PULLMAN, R.T., and HOGG, B.W. "Discrete state-space controller for a turbogenerator", Proc. IEE, Vol. 126, No. 1, pp. 87-92, 1979.

70. NEWTON, M.E., and HOGG, B.W. "Optimal control of a microalternator", IEEE, Vol. PAS-95, pp. 1821-33, 1976.

71. BARTLETT, J.P., GIBBARD, M.J.. and WOODWARD, J.L. "Performance of a 5 kVA synchronous generator with an optimal excitation regulator", Proc. IEE, Vol. 120, No. 10, pp. 1250-56, 1973.

72. LIMEBEER, D.J., HARLEY, R.G., and NATTRASS, H.L. "Agile computer control of a turbogenerator", Proc. IEE, Vol. 26, No. 5, pp. 385-392, 1979.

73. PHUNG, V.A., and GIBBARD, M.J. "Practical implementation on a 5 kVA synchronous generator of an adaptive excitation controller strategy for a wide range of operating conditions", Proc. IEE, Vol. 125, No. 10, pp. 1009-1014, 1978.

74. BONANOMI, P., GUTH, G., BLASER, F., GLAVITSCH, H. "Concept of a practical adaptive regulator for excitation control", paper no. A79 453-2 presented at IEEE PES summer meeting, Vancouver, 1979.

75. CRAVEN, R., and GLAVITSCH, H. "Large disturbance performance of an adapted linear excitation control system", paper no. A79 452-4 presented at IEEE PES summer meeting, Vancouver, 1979.

76. KALMAN, R.E., and BUCY, R.S. "New results in linear filtering and prediction theory", Journal of Basic Engineering, Trans ASME, ser. D, no. 83, pp.95-108, 1961.

77. OKONGWU, E.H., WILSON, W.J., and ANDERSON, J.H. "Optimal state feedback control of a microalternator using an observer", IEEE Vol. PAS-87, No. 2, pp. 594-602, 1978.

78. LUENBERGER, D.G. "An introduction to observers", IEEE, Vol. AC-16, pp. 596-602, 1971.

79. ASTROM, K.J., and WITTENMARK, B. "On self-tuning regulators", Automatica, pp. 185-199, 1973.

80. CLARKE, D.W., and GAWTHROP, P.J. "Self-tuning control", Proc. IEE, Vol. 126, pp. 633-640, 1979.

81. LEDWICH, G. "Adaptive excitation control", Proc. IEE, Vol. 126, pp. 249-253, 1979.

82. MALIK, O.P., HOPE, G.S., and SHEIRAH, M.A.H. "Self-tuning voltage and speed regulators for a generating unit", IEEE/ASME/ASCE Joint power engineering conference, Dallas, Texas, paper A78 810-4 1978.

83. GHOSH, A., LEDWICH, G., MALIK, O.P., and HOPE, G.S. "Power system stabiliser based on adaptive control techniques", paper no. 84WM 018-8, presented at IEEE winter power meeting, Jan.-Feb. 1984.

84. SHARAF, S.M., HOGG, B.W., ABDALLAH, O.H., EL-SAYED, M.L. "Adaptive control of a turbogenerator", Proc. 19th Universities Power Engineering Conference, paper 7.1, Dundee, 1984

85. ROSENBROCK, H.H. "Computer-aided control system design", Academic Press, 1974.

86. MACFARLANE, A.G.J. "Characteristic loci technique in multivariable control system design", Proc. IEE, Vol. 118, 1971.

87. HUGHES, F.M., and HAMDAN, A.M.A. "Design of turboalternator excitation controllers using multivariable frequency-response methods", Proc. IEE, Vol. 123. pp.901-905, 1976.

88. AHSON, S.I., HOGG, B.W., and PULLMAN, R.T. "Integrated control system for turbogenerator designed by Inverse Nyquist array method", IEEE, Vol. PAS-98, No. 2, pp.543-553, 1979.

89. CHAN, S.M., and ATHANS, M. "Applications of robustness theory to power system models", IEEE trans. on Automatic Control, Vol. AC-29, No. 1, pp.2-8, 1984.

90. MOORE, B.C. "Principal component analysis in linear systems: controllability, observability and model reduction", IEEE, Trans. on Auto. Control, Vol. AC-26, pp.17-37, 1981.

91. PERNEBO, L., and SILVERMAN, L.M. "Model reduction via balanced state-space representation", IEEE, Trans. on Auto. Control, Vol. AC-27, pp. 382-387, 1982.

92. KUO, B.C. "Digital control systems", Holt, Rinehart and Winston, Inc., New York, 1980.

93. LIMEBEER, D.J., and LAHOUD, M.A. "Optimal reduced order synchronous machine models", Paper submitted to IEE for publication, 1984.

94. PARK, R.H. "Two-reaction theory of synchronous machines", Trans. AIEE, 48, p.716, 1929.

95. KRON, G. "Tensors for circuits", Dover Publications, New York, 1959.

96. HUMPAGE, W.D., SMITH, J.R., and ROGERS, G.J. "Application of dynamic optimisation to synchronous generator excitation controllers", Proc, IEE, Vol. 120, pp. 87-93, 1973.

97. HARLEY, R.G., and ADKINS, B. "Calculation of the angular back swing following a short circuit of a loaded alternator", Proc. IEE, Vol. 117, p.377, 1970.

98. DEVOTTA, J.B.X. "The optimal control of a synchronous machine with a divided winding rotor", Ph.D. Thesis, University of London, 1972.

99. SILVERMAN, L.M. "Approximation of linear systems", Internal Report, Dept. of Elec. Eng., University of Southern California, Los Angeles, 1980.

100. GLOVER, K. "All optimal Hankel-norm approximations of linear multi-variable systems and their L-infinity error bounds", Int. J. Control, Vol. 39, pp.1115-1193, 1984.

101. IEEE COMMITTEE REPORT: "Excitation system models for power system stability studies", IEEE, Vol. PAS-100, pp. 494-509, 1981.

102. SHACKSHAFT, G. "General-purpose turbo-alternator model", Proc. IEE, Vol. 110, pp. 703-713, 1963

103. SCHWARTZ, R.J., and FRIEDLAND, B. "Linear Systems", McGraw Hill, New York, 1965.

104. FENWICK, P.J. "Modelling of AVR and Governors - Part II: AVRs", Synchronous machines in power systems conference, Imperial College, London, March-April 1981.

105. CHANA, G.S., and DANIELS, A.R. "Turbogenerator Excitation Control Incorporating nonlinear state feedback", Proc. IEE, Vol. 125, No. 11. pp. 1245-1246, 1978.

106. MAYNE, D.Q., and SAHBA, M. "A modified Newton method for solving inequalities in a finite number of iterations", paper to be published in Journal of Optimisation Theory and Applications, 1983.

107. SAHBA, M. "Optimal control of power system generators incorporating nonlinear state feedback", Proc. IEE, Vol. 130, part D, No. 6, p. 345, 1983.

108. KANNIAH, J., MALIK, O.P., and HOPE, G.S. "Excitation control of synchronous generators using adaptive regulators. Part I: Theory and simulation results. Part II: Implementation and test results". IEEE Trans. Vol. PAS-103, No. 5, pp. 897-910, 1984.

109. DANIELS, A.R., LEE, Y.B., and PAL, M.K. "Nonlinear power-system optimisation using dynamic sensitivity analysis", Proc. IEE, Vol. 123, No. 4, pp. 365-370, 1976.

110. GILL, P.E., and MURRAY, W. "Quasi-Newton methods for unconstrained optimisation", J. Inst. Math. Appl., No. 9, pp. 91-108, 1972.

111. LAUB, A.J. "Computation of 'balancing' transformations", paper FA 8-E, JACC, San Fransisco, Ca., 1980.

112. BOZIC, S.M. "Digital and Kalman Filtering", Edward Arnold, 1979.

113. KWAKERNAAK, H., and SIVAN, R. "Linear optimal control systems", John Wiley and Sons, New York, 1972.

114. ANDERSON, B.D.O., and MOORE, J.B. "Linear Optimal Control", Prentice-Hall, New Jersey, 1971.

115. LAUB, A.J. "A Schur method for solving algebraic Riccati equations", IEEE, Vol. AC-24, pp. 913-921, 1979.

116. KAILATH, T. "Linear Systems", Prentice-Hall, Englewood Cliffs, N.J., 1980.

117. MAWDSLEY'S LIMITED. "Operating and Maintenance manual for the Mawdsley micro synchronous generator set", Specification no. 103/R13, Mawdsley's Ltd., Dursley, Glos., 1980.

118. HANNA, R.A. "The six-phase two-circuit synchronous generator and its associated transformer", Ph.D. Thesis, University of London, 1978.

119. MAWDSLEY'S LIMITED. "Commissioning and maintenance manual for the Matador thyristor drive, no. DSU 7851", Mawdsley's Ltd., Dursley, Glos., 1977.

120. NEI PARSONS LIMITED. a] "Models of governor and AVR systems", R & M report No. 241A [confidential], Newcastle upon Tyne, 1974. b] Private correspondence, 1981.

121. TOURI, M.O. "Regulation of the time constants of a laboratory micro-machine", M.Sc. Thesis, University of London, 1977.

122. LIMEBEER, D.J.N. "Analysis and control of a.c. rotating machines in the presence of series capacitor compensated networks", Ph.D. Thesis, University of Natal, Durban, 1980.

123. KHAN, K.R. "Digital Generator Protection", Ph.D. Thesis, University of London, 1984.

124. NEECH, K. "Circuit Breaker Sequence Control [point-on-wave switching] unit", 3rd year project report, Imperial College, 1977.

125. DIGITAL EQUIPMENT CORPORATION. a] "Microcomputers and Memories". b] "PDP-11 Software Handbook". c] "PDP-11 Architecture Handbook". d] "PDP-11 Microcomputer interfaces Handbook". Digital Equipment Corp., Marlboro, Massachusetts, 1983.

126. PAVLIDES, S.A. "The Nova 3 minicomputer and Intel 3000 bit-slice data acquisition system", Power Systems Report in preparation, Imperial College, 1984.

127. TEKTRONIX, INC. "PLOT-10 Terminal Control System", Manual No. 070-224-00, Tektronix, Inc. 1983.

128. NOBLE, A.D. "LSI 11/23 system log book 1983-84 and micromachine interface". Power systems report in preparation, Imperial College, 1984.

129. GOLD, B., and RADER, C. "Digital Processing of Signals", McGraw-Hill, New York, 1969.

130. CORVUS SYSTEMS, "Personal Workstation User Guide - The Corvus Concept", Corvus Systems, San Jose, Ca., 1983.

131. BRIGHAM, E.O. "The fast-Fourier Transform", Prentice-Hall, Englewood Cliffs, New Jersey, 1974.

132. IEEE SSR Task Force "First Benchmark model for computer simulation of subsynchronous resonance", IEEE, Vol. PAS-96, pp.1565-1571, 1977.

133. LIMEBEER, D.J.N., HARLEY, R.G., LAHOUD, M.A., and NATTRASS, H.L. "Laboratory measurements of subsynchronous resonance", Proc. IFAC symposium on Automatic Control in Generation, Distribution and Protection, Pretoria, 1980.

134. ADAMJAN, V.M., AROV, D.Z., and KREIN, M.G. "Analytic properties of Schmidt pairs for a Hankel operator and the generalised Schur-Takagi problem", Math. USSR Sbornik, Vol. 15, No. 1, pp. 31-73.

135. NOBLE, A.D., and MACDONALD, D.C. "On-line control of generator transients by microcomputer using optimal control and state estimation", Proc. 19th UPEC, Dundee, 1984.

136. VAAHEDI, E., NOBLE, A.D., and MACDONALD, D.C. "Power system stability improvement by optimal control", Proc. 8th Power System Computation Conference, Helsinki, 1984.